

NEURAL AND MECHANICAL RESPONSES
TO ELECTRIC STIMULATION OF THE CAT'S INNER EAR

by

Edwin Charles Moxon

S. B. , Massachusetts Institute of Technology
(1965)

S. M. , Massachusetts Institute of Technology
(1967)

SUBMITTED IN PARTIAL FULFILLMENT OF THE
REQUIREMENTS FOR THE DEGREE OF
DOCTOR OF PHILOSOPHY

at the

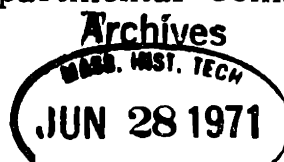
MASSACHUSETTS INSTITUTE OF TECHNOLOGY

June, 1971

Signature of Author -----
Department of Electrical Engineering, May 17, 1971

Certified by -----
Thesis Supervisor

Accepted by -----
Chairman, Departmental Committee on Graduate Students



NEURAL AND MECHANICAL RESPONSES TO
ELECTRIC STIMULATION OF THE CAT'S INNER EAR

by

EDWIN CHARLES MOXON

Submitted to the Department of Electrical Engineering on May 17, 1971 in partial fulfillment of the requirements for the Degree of Doctor of Philosophy

ABSTRACT

Responses of fibers in the cat's auditory nerve were recorded with a micropipette when the inner ear was stimulated electrically, and response characteristics were compared with characteristics of response to acoustic stimuli. For both pulse and sinusoidal current waveforms, two separate types of response were identified. In one type of response, analogous electric and acoustic stimulus waveforms appear to be transformed into similar patterns of nerve-fiber discharge; the other response type shows distinctive characteristics which are not found for simple acoustic stimuli. The nerve-fiber response characteristics suggest that the former response type is mediated by a cochlear electromechanical phenomenon, while the latter type can be attributed to direct depolarization of nerve membrane by the electric stimuli. The existence of the hypothesized electrical-to-mechanical transduction was verified by detecting motion of the round-window membrane which accompanied electric stimulation of the cochlea; measurements indicated that round-window volume velocity was proportional to stimulus current. This electromechanical phenomenon was shown to be essentially independent of known mechanical-to-electrical cochlear transduction phenomena. Origins of the observed mechanical and neural responses are considered and correlations between the physiological results and human psychophysical observations are discussed.

THESIS SUPERVISOR: William T. Peake
TITLE: Associate Professor of Electrical Engineering

ACKNOWLEDGMENT

During the course of the thesis work, personal support was provided principally by a training grant (#5 T01 GM01555-04 BEN) from the National Institutes of Health. The author is indebted to Professor William M. Siebert of the Communications Biophysics Group of the Research Laboratory of Electronics, M. I. T., for his part in making this traineeship available.

The suggestions and assistance of several people have helped form the course and facilitate the execution of this research. Professor William T. Peake, as thesis supervisor, was ready with fresh ideas at key times, and his many recommendations regarding the preparation of the thesis manuscript have been invaluable. Dr. Nelson Y. S. Kiang supplied much helpful instruction and needed direction. Professors Thomas F. Weiss and James R. Melcher served as readers for the thesis, and their interest and comments are appreciated. Special thanks are due Professor Stephen K. Burns for support in many forms, some directly related to this thesis.

The experimental work was conducted in the Eaton-Peabody Laboratory of the Massachusetts Eye and Ear Infirmary and owes much to the contributions of many EPL staff members. While it would be difficult to enumerate all of the ways they helped, several individuals deserve special mention. Miss Betsy Marr assisted with surgery, as well as with collecting and analyzing experimental data.

Mrs. Arianna Morino furnished the histology required in some experiments. Miss Helen Yin and Mr. Thomas Wilson participated during many long hours of experimentation, and Mrs. Shelley Guinan, Miss Barbara Norris, and Mrs. Janet Miller contributed to other aspects of the project. Some of the data presented are from a series of experiments conducted jointly with Dr. Robert A. Levine, while other of the results were obtained in collaboration with Steven C. Chamberlain and Dr. Michael L. Wiederhold. Miss Diane Demont prepared most of the final figures, contributing willingly of her time and talent.

Finally there is my wife Susan, who worked on this project in several capacities. As a colleague in the laboratory, she provided the surgical preparation for many experiments, and her careful treatment of quantities of data has entered into many of the experimental results. Most recently, although she has had to tolerate and cope with an original manuscript and numerous revisions which were not always legible, she has done an excellent job of preparing the final copy of this thesis.

TABLE OF CONTENTS

Title Page	1
Abstract	2
Acknowledgment	3
Table of Contents	5
List of Figures	9
I. INTRODUCTION	14
II. BACKGROUND	18
2.1 Anatomy and Physiology of the Peripheral Auditory System.	18
2.1.1 Acoustic characteristics of the head and external ear.	18
2.1.2 Transmission characteristics of the middle ear	23
2.1.3 Description of the inner ear and auditory nerve	25
2.1.4 Cochlear mechanics	29
2.1.5 Cochlear electrophysiology.	31
2.1.6 Auditory-nerve electrophysiology	35
2.2 Action of Electric Stimuli on the Peripheral Auditory System	38
2.2.1 Electric stimulation of human subjects	38
2.2.2 Electric stimulation of experimental animals	46
2.3 Outline of Thesis Research	49

III.	EXPERIMENTAL METHODS	54
	3.1 Animals and Preparation	54
	3.2 Configuration of Stimulating Electrodes	55
	3.3 Methods for Recording Auditory-Nerve Response	58
	3.4 Methods for Recording the Mechanical Response of the Cochlea	65
	3.5 Characterization of Sinusoidal Signals	75
IV.	AUDITORY-NERVE-FIBER RESPONSES TO ELECTRIC STIMULATION OF THE COCHLEA	79
	4.1 Characteristics of Responses to Analogous Electric and Acoustic Stimulus Waveforms	79
	4.1.1 Shock and click	79
	4.1.2 Bursts of sinusoidal current and tone	89
	4.1.3 Maintained sinusoidal current and tone	102
	4.1.4 Simultaneous bursts of sinusoidal current and tone	114
	4.1.5 Equivalence of sinusoidal acoustic and electric stimuli based on Class I nerve- fiber response	118
	4.2 Experimental Investigations of Origins of Responses	130
	4.2.1 Responses to electric and acoustic stimuli in cochleas modified at the sensory cell stage.	131
	4.2.2 Effects of constraints on mechanical variables at the input terminals of the cochlea on responses to sinusoidal current and tone	140
	4.2.3 Influence of stimulating electrodes on response to sinusoidal current	146
	4.3 Summary	147

V.	MECHANICAL RESPONSES OF THE COCHLEA TO SINUSOIDAL ACOUSTIC AND ELECTRIC STIMULI	149
5.1	Effect of Measuring System on the Function of the Normal Cochlea	149
5.2	Signals Recorded in the Absence of Stimuli	152
5.3	Responses of the Normal Cochlea	158
5.3.1	Waveform of microphone output	158
5.3.2	Response to acoustic stimuli	161
5.3.3	Response to electric stimuli	168
5.3.4	Equivalence of sinusoidal acoustic and electric stimuli based on round-window motion	174
5.4	Responses in Modified Preparations	178
5.4.1	Response of the normal cochlea to modified stimulus current distribution	178
5.4.2	Post-mortem responses	179
5.4.3	Responses in hair-cell-deficient cochleas	188
5.4.4	Role of electrodes in production of response	196
5.5	Summary	200
VI.	DISCUSSION	202
6.1	Origins of Neural Responses	202
6.1.1	Class II response to sinusoid and α -component of response to shock	202
6.1.2	Class I response to sinusoid and β -component of response to shock.	203

6.2	Origin of Mechanical Response to Electric Stimuli . . .	206
6.2.1	Comparison of neural and mechanical stimulus equivalence data	206
6.2.2	Properties of response pertinent to mechanisms of electromechanical transduction	211
6.2.3	A simple description of mechanical response . .	213
6.3	Relationship of Experimental Results to Human Perception	221
6.3.1	Correlation of physiological and psychophysical results	221
6.3.2	Communication possibilities	226

APPENDICES

I.	Characteristics of the Electric Stimulus Circuit	230
II.	Characteristics of the Probe-Tube System	237
III.	Spurious Effects of Electric Stimuli	244
IV.	Intracochlear Voltage Developed by Electric Stimuli	249
	REFERENCES	252
	BIOGRAPHICAL NOTE	264

LIST OF FIGURES

Figure 2.1	Schematic drawing of the macroscopic anatomy of the peripheral auditory system	19
Figure 2.2	Block diagram representing the normal operation of the peripheral auditory system	21
Figure 2.3	Diagram of a cross section of the cochlear duct.	27
Figure 2.4	PST histograms of firings of single auditory-nerve fibers in response to shocks and clicks	50
Figure 3.1	Photographs of the temporal bone of the cat indicating the placement of stimulating electrodes	56
Figure 3.2	Block diagram of stimulus-generation and response-recording equipment used for studying response of single auditory-nerve fibers	59
Figure 3.3	Block diagram of stimulus-generation and response-recording equipment used for detecting motion of the round-window membrane.	67
Figure 3.4	Cross-sectional drawing of the probe tube, coupler, and probe microphone	70
Figure 4.1	PST histograms of fiber response to clicks and shocks at three levels	81
Figure 4.2	PST histograms of fiber response to shocks of opposite polarity	84
Figure 4.3	Threshold for α -component of response to shock plotted against f_c for 19 fibers from 2 cats	87
Figure 4.4	Tuning curves for sinusoidal electric and acoustic stimuli for 9 fibers from one cat	90
Figure 4.5	Composite plots of tuning curves for electric stimuli for two cats	93

Figure 4.6	Histograms of fiber response to bursts of sinusoidal acoustic and electric stimuli (tone bursts and current bursts)	96
Figure 4.7	Histograms of response to tone bursts and of Class I and Class II response to bursts of sinusoidal current.	99
Figure 4.8	Time course of Class I and Class II discharge rate in response to maintained sinusoidal electric current.	103
Figure 4.9	Photographs of the discharges from which data of figure 4.8 were computed	106
Figure 4.10	Histograms of response pattern of a low- f_c fiber to three levels of tone and sinusoidal current.	109
Figure 4.11	Discharge rate plotted against level of acoustic and electric stimuli	112
Figure 4.12	Histograms of fiber response to simultaneous bursts of sinusoidal electric and acoustic stimuli	116
Figure 4.13	Plots of tone threshold at f_c and current threshold at f_{ce} for fibers from each of two cats.	120
Figure 4.14	The magnitude of the ratio of equivalent stimuli $ Q_f^t $ based on fiber threshold for tone at f_c and threshold for current at f_{ce}	122
Figure 4.15	The complex stimulus equivalence ratio Q_f^c based on cancellation of nerve-fiber response	126
Figure 4.16	Angle of Q_f^c based on cancellation of nerve-fiber response at frequencies other than f_{ce}	128
Figure 4.17	Histograms of fiber response to shocks and clicks modified by activation of the COCB	132
Figure 4.18	PST histograms of fiber response to bursts of tone and sinusoidal current modified by activation of the COCB.	134

Figure 4.19	PST histograms of response to shock for a fiber in a kanamycin-treated cat and a fiber in an untreated cat	138
Figure 4.20	Tuning curves for sinusoidal electric stimuli in a cat with stapes embedded in dental cement	141
Figure 4.21	Effect of interruption of the ossicular chain on tone threshold at f_c , current threshold at f_{ce} , and magnitude of the ratio of equivalent stimuli $ Q_f^t $	144
Figure 5.1	Round-window potential E_{rw} measured before and after sealing probe-microphone system over the round window	150
Figure 5.2	Ratio of round-window potentials measured before and after sealing probe-microphone system over the round window	153
Figure 5.3	Microphone pressure waveform recorded in the absence of controlled stimuli	156
Figure 5.4	Averaged probe-microphone pressure waveform and current waveform in response to 2 kHz electric stimulus	159
Figure 5.5	Output voltage of the probe-microphone amplifier under different recording conditions	162
Figure 5.6	Sound pressure developed at the probe microphone in response to acoustic stimulus in four experiments	165
Figure 5.7	Sound pressure at the probe microphone in response to four levels of sinusoidal electric stimulus	169
Figure 5.8	Sound pressure developed at probe microphone in response to sinusoidal electric stimuli in 3 cats	172
Figure 5.9	Stimulus equivalence ratio Q_m based on measurements of the motion of the round-window membrane.	176

Figure 5.10	Probe-microphone response to tone and current and round-window voltage response to tone during transition from ante- to post-mortem values	181
Figure 5.11	Time course of endocochlear potential and of probe-microphone response to 5 kHz current recorded during asphyxia	183
Figure 5.12	The transfer function (sound pressure at probe microphone)/(electrode current) measured before and after death	186
Figure 5.13	Stimulus equivalence ratio Q_m in a cat having extensive ototoxically-induced hair-cell deficiency	189
Figure 5.14	Schematic representation of hair-cell degeneration in the cochlea of the kanamycin-treated cat from which data of figure 5.13 were obtained	191
Figure 5.15	Round-window potential E_{RW} in response to tone in the same kanamycin-treated cat from which data of figure 5.13 were obtained	194
Figure 5.16	The ratio (sound pressure at probe microphone)/(electrode current) recorded from a saline-filled cochlea	198
Figure 6.1	Comparison of the stimulus equivalence ratios Q_m and Q_f	207
Figure 6.2	Ratio of equivalent stimuli from mechanical measurements expressed as U_{st}/I_e	214
Figure 6.3	Dependent-source model of the acoustic terminal behavior of the electrically-stimulated cochlea	217
Figure 6.4	Idealized subdivision of the stimulus plane based on response characteristics of the entire auditory nerve	222
Figure A1.1	Electrical characteristics of a typical stimulating electrode pair	231

Figure A1.2	Magnitude of electrode current at constant attenuator setting plotted against time throughout the course of an experiment	233
Figure A2.1	Pressure transfer function of probe-microphone system	238
Figure A3.1	Histograms of response of a low- f_c fiber to click and shock in a cat with intact middle-ear muscles	247

CHAPTER I.

INTRODUCTION

At the beginning of the 19th century, Volta (1800) described sensations that resulted from application of electric current to various sense organs, including the ear. Since that time, a number of "hearing sensations" evoked by electric stimuli have been reported. Many of these hearing sensations can be classified according to the scheme of Jones, Stevens, and Lurie (1940), who described three separate subjective phenomena resulting from electric stimulation of the peripheral auditory system.

One subjective phenomenon was explained in terms of an electrostatic mechanism in which forces of electric origin were developed on the tympanic membrane (eardrum). The proposed transducer accounted for what had been described as a "square-law" sensation, in which a sinusoidal electric stimulus was perceived as a tone of twice the frequency. This phenomenon was not observed when electric stimuli were applied directly to the inner ear (cochlea) of subjects whose tympanic membranes had been surgically removed. On the basis of the sensations experienced by these subjects, however, the other two phenomena, which involved the cochlea and auditory nerve, were identified.

One of these was a phenomenon attributed to direct electric

excitation of auditory-nerve fibers by the applied currents. The associated sensation was complex; it did not correspond to a simple sound and was described as a noise which had a buzzing character.

The remaining phenomenon was described as resulting from action of electric stimuli on elements within the inner ear. The associated subjective phenomenon was a simple one: when the cochlea was stimulated with sinusoidal current, subjects reported a sensation of tone of the same frequency as the electric stimulus. No physiological basis for this phenomenon was clearly indicated, although the authors suggested that it might reflect properties of the sensory cells in the organ of hearing.

Although some further investigations of the two subjective phenomena associated with electric stimulation of the human cochlea and auditory nerve have been conducted, few comparable experiments have been performed using experimental animals to investigate the physiological basis for these subjective effects, and none has directly investigated the basis of the "linear-law" phenomenon attributed to mechanisms of the cochlea.

The present study is an investigation of the physiological effects of electric stimuli on the inner ear and auditory nerve of an experimental animal, the cat. The purpose of this study is to describe the basic ways in which electric stimulation can affect the electrical and electromechanical systems of the cochlea.

For this purpose, the discharges of single auditory-nerve fibers (the output signals of the cochlea) were recorded when the cochlea was stimulated electrically, and the electrically-evoked responses were compared with responses to sound.

These experiments show two distinct kinds of auditory-nerve-fiber response which appear to be physiological correlates of the two subjective phenomena associated with electric stimulation of the human cochlea. In one type of response, distinctive discharge characteristics are found which do not resemble the response to simple acoustic stimuli, and this response type is the apparent correlate of the sensation described as noise. Characteristics of this response indicate that it is the result of direct excitation of nerve fibers, the mechanism which had been proposed on the basis of subjective characteristics.

In the other type of response, nerve-fiber discharge characteristics resemble the characteristics observed in response to a tone; this response type is the apparent correlate of the "linear-law" subjective phenomenon. On the basis of the observed characteristics, it appears that this nerve-fiber response is produced by mechanical signals which occur in the cochlea in response to electric stimuli.

This hypothesis was verified experimentally by detecting motion of the round-window membrane produced in response to electric stimuli. Properties of this mechanical response were determined

and possible mechanisms underlying it were investigated.

According to the experimental results, this electromechanical effect appears to be the basis for the "linear-law" perception of electric stimuli by humans. However, the evidence shows that this effect can exist independently of other, normal sensory processes of the inner ear, and that therefore it is not a phenomenon intimately related to the specialized mechanisms of the organ of hearing.

CHAPTER II.

BACKGROUND2.1 Anatomy and Physiology of the Peripheral Auditory System.

A schematized representation of the anatomy of the mammalian peripheral auditory system is shown in figure 2.1. A block diagram representing stages of signal processing and variables of interest is shown in figure 2.2. Variables defined in the block diagram are also indicated in figure 2.1.

2.1.1 Acoustic characteristics of the head and external ear.

The presence of the head in an acoustic medium places constraints on the acoustic signals in that medium. The effects of the head and auricle (pinna) have been characterized by relating the sound pressure developed at the entrance of the external ear canal to the sound pressure which would exist at a remote point in an incident progressive sound field. In the block diagram, the incident free-field sound pressure is indicated as $p_{ff}(t)$, and the sound pressure near the tragus at the external canal entrance is indicated as $p_t(t)$; the first stage in the diagram represents the transformation of p_{ff} to p_t .

The sound pressure at the tragus is transmitted through the external canal and sound pressure $p_d(t)$ is developed on the tympanic membrane; the tympanic membrane may be considered an input port

Figure 2.1

Schematic drawing of the macroscopic anatomy of the peripheral auditory system.

Major anatomical features are indicated. In this two-dimensional representation the cochlea is shown uncoiled. (From Békésy and Rosenblith, 1951.) Signal variables have been superimposed on the original drawing:

- p_t , sound pressure at the tragus
- p_d , sound pressure at the tympanic membrane (drum membrane)
- x_s , linear displacement of the stapes footplate
- $y_m(z)$, transverse linear displacement of the basilar membrane, a function of longitudinal position z .

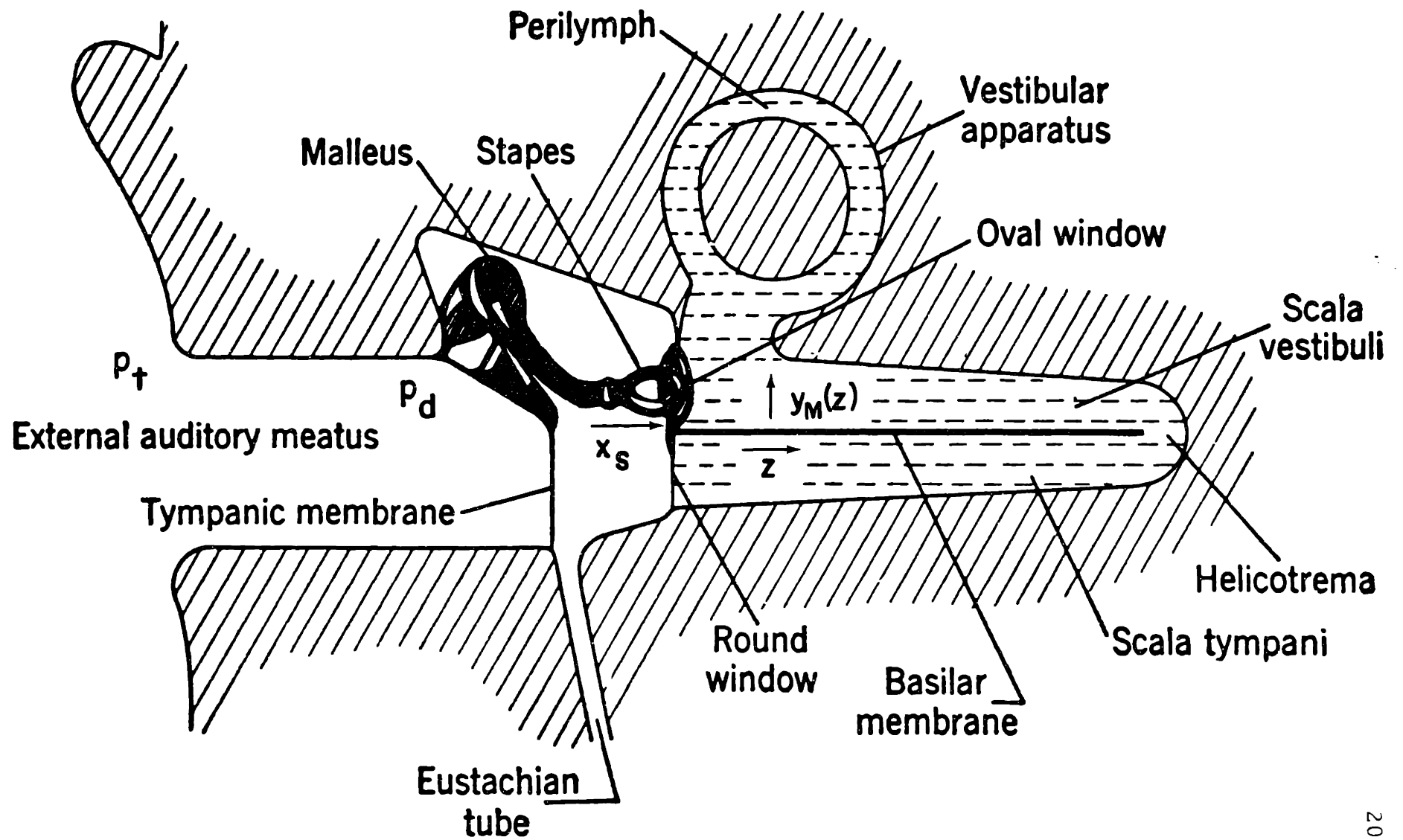


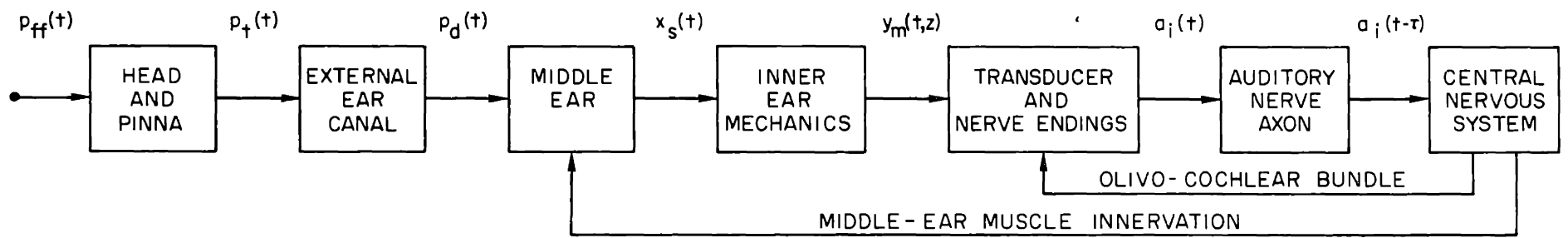
Figure 2.2

Block diagram representing the normal operation of the peripheral auditory system.

Major stages of signal processing are indicated. Indicated variables:

- $p_{ff}(t)$, sound pressure in the free field;
- $p_t(t)$, sound pressure at the tragus;
- $p_d(t)$, sound pressure at the drum membrane;
- $x_s(t)$, linear displacement of the stapes footplate;
- $y_m(t, z)$, transverse linear displacement of the basilar membrane, a function of longitudinal position z ;
- $a_i(t)$, action potential generated in the i th nerve fiber at the site of impulse initiation;
- $a_i(t - \tau_i)$, action potential in the i th nerve fiber, delivered to the central nervous system, delayed by conduction time τ_i .

Pathway from the central nervous system to the middle ear represents the innervation of middle-ear muscles. Pathway from the central nervous system to the transducer and nerve endings represents the olivo-cochlear bundle (OCB) of efferent nerve fibers which end on the hair cells and afferent nerve endings in the organ of Corti.



of the middle ear, with $p_d(t)$ as a middle-ear input signal. The second stage in the block diagram represents the transformation of p_t to p_d .

Transfer functions describing these transformations have been determined experimentally. In man the ratio P_t/P_{ff} has been determined by Wiener (1947) and by Shaw (1966), and the ratio P_d/P_t has been described by Wiener and Ross (1946) and Shaw and Teranishi (1968). For the cat, these functions have been described by Wiener, Pfeiffer, and Backus (1966). In general these transfer functions describe linear low-pass acoustic systems. For frequencies greater than a few kHz, both P_t/P_{ff} and P_d/P_t depend on frequency, and in addition P_t/P_{ff} depends on the orientation of the head in the sound field.

2.1.2 Transmission characteristics of the middle ear.

In the experiments described in this thesis, the acoustic stimuli are usually expressed in terms of the sound pressure measured close to the tympanic membrane, and the transformation characteristics of the head and external canal are not involved. However, sound stimuli do pass through the middle ear to reach the cochlea and are affected by middle-ear transformation characteristics.

The function of the middle ear is to couple acoustic signals at the tympanic membrane to the inner ear. Suspended in the middle ear cavity are three small bones, or ossicles. One ossicle, the malleus,

is connected to the tympanic membrane and to the second ossicle, the incus. The incus is connected to the third ossicle, the stapes, which makes contact with the cochlear fluid through the oval window, an opening in the bony shell of the cochlea. The indicated middle-ear output signal is the displacement of the footplate of the stapes, $x_s(t)$.

Connected to the ossicles are two muscles, which can exert forces on the malleus (the tensor tympani muscle) or on the stapes (the stapedius muscle) to alter the transmission characteristics of the middle ear. The tensor tympani innervation is derived from the trigeminal nerve and the stapedius innervation from the facial nerve.

A middle-ear transfer-function, X_s/P_d , has been determined for the anesthetized cat by Guinan and Peake (1967). Using optical measurement techniques, they found that, with the bulla open and the bony septum separating bulla and tympanic cavities removed, the transfer function exhibits low-pass characteristics. Transfer function magnitude diminishes between 1 and 9 kHz with a slope of about 6 dB/octave and appears to fall more rapidly from 9 to 12 kHz (the highest frequency investigated). The middle ear acts as an acoustic transformer due to lever action of the ossicles and due to the ratio of tympanic membrane area to the area of the stapes footplate. Békésy (1960, pp. 95-104) has described the pressure gain of the middle ear of human cadavers to be 20 to 25 dB below 2 kHz, and in the cat, this ratio may be as high as 35 dB (Wever and Lawrence, 1954). In the anesthetized

cat, the middle ear has been found to operate linearly for input sound pressures up to 130 dB re 0.0002 dynes/cm² rms (130 dB SPL)(Guinan and Peake, 1967).

A number of authors have described the contraction of middle-ear muscles as resulting in a reduction of the signal transmission through the middle ear [see Wever and Lawrence (1954)]. The normal role of the muscles in hearing is not well understood. It has been proposed that the reflexive response of the muscles to high-level sound stimuli protects sensitive inner ear structures from possible damage. Evidently in the barbiturate-anesthetized cat the middle-ear muscles are relaxed (Dallos, 1970).

2.1.3 Description of the inner ear and auditory nerve.

As a whole, the physical mechanisms of signal processing within the cochlea are not understood, although experimental data exist on many aspects of cochlear function. In the external and middle ears, there is little doubt that the signals of interest are mechanical. In some essential processes of the cochlea, however, it is not known whether signals of interest exist as mechanical, electrical, chemical, or other physical quantities. The following sections contain a short summary of the known mechanical and electrical functions of the cochlea.

The cochlea of the cat is a spiral chamber of three turns within the temporal bone. Over most of its length this chamber is divided

into three spiral, fluid-filled compartments by the cochlear partition. In the schematic drawing of figure 2.1 the cochlea is shown uncoiled.

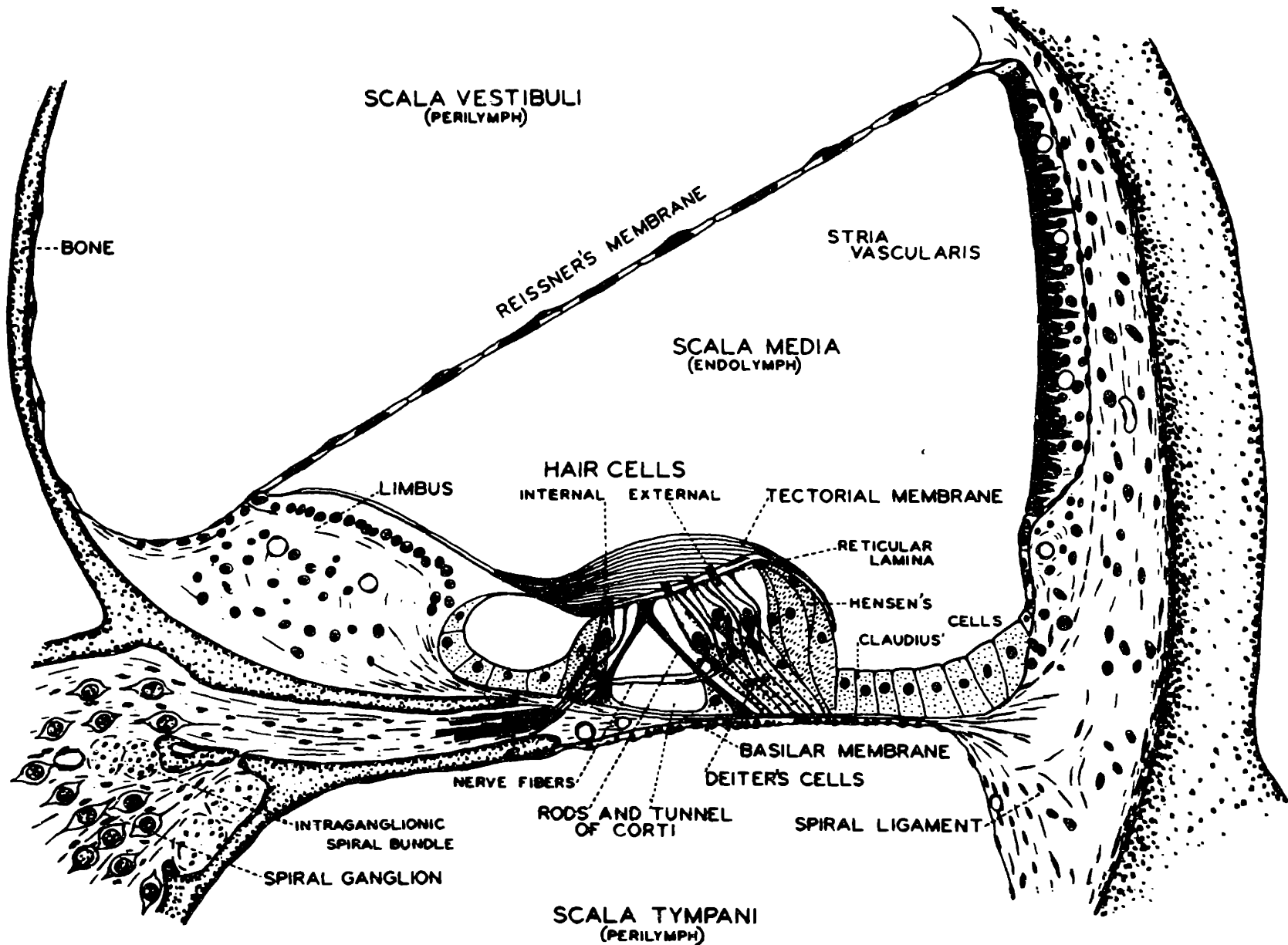
A drawing of a cross-section of the compartments of the cochlea is shown in figure 2.3. (The plane of this section is perpendicular to the plane of the schematic drawing of figure 2.1.) In this cross-section, the cochlear partition is triangularly shaped, bounded on two sides by membranes and the third by bone. Scala vestibuli is separated from scala media by Reissner's membrane, and scala tympani is separated from scala media by the basilar membrane. The fluid contained within scala media is endolymph; scala vestibuli and scala tympani contain perilymph. At the very apex of the cochlea, the cochlear partition ends and scala vestibuli and scala tympani are connected through an opening, the helicotrema. At the base of the cochlea the oval window, containing the footplate of the stapes, opens into the scala vestibuli, and the round window, covered by an elastic membrane, opens into scala tympani. The basilar membrane supports the sensory organ of hearing, the organ of Corti.

The organ of Corti contains the hair cells (believed to be the sensory cells), supporting cells, and the peripheral terminations of the afferent fibers of the auditory nerve. Fine hairs protrude from the hair cells and contact the tectorial membrane (Kimura, 1966). The hair cells are arranged in rows along the basilar membrane. One row of inner hair cells lies between the tunnel of Corti and the axis of the

Figure 2.3

Diagram of a cross section of the cochlear duct.

Drawing shows the important anatomical features of the organ of Corti and the three cochlear scalae.
(From Davis and Associates, 1953.)



cochlear spiral; the hair cells lying on the other side of the tunnel are called the outer hair cells, which in the cat are arranged in three rows. The fibers of the auditory nerve form synapses on the bases of the hair cells. The nerve fibers are unmyelinated in the organ of Corti, becoming myelinated as they exit through the habenula perforata.

The cell bodies of the auditory-nerve neurons form the spiral ganglion, which is situated in a spiral canal in the temporal bone. The myelinated central processes of the auditory-nerve fibers extend into the central nervous system and form synapses with the cells of the cochlear nucleus. The auditory nerve of the cat contains about 50,000 afferent fibers, whose diameters range from 2 to 5 μm (Gacek and Rasmussen, 1961).

An efferent system of nerve fibers from the central nervous system, the olivo-cochlear bundle (OCB), forms a neural feedback path to the peripheral auditory system. OCB fibers which originate in the contralateral half of the brainstem and cross the midline to the ipsilateral cochlea are referred to as the crossed component of the OCB (COCB). Efferent fibers enter the cochlea and end on the bases of the hair cells and on the fine, unmyelinated terminals of the afferent auditory-nerve fibers (Smith, 1961; Spoendlin and Gacek, 1963).

2.1.4 Cochlear mechanics.

The displacement of the stapes footplate in the oval window

moves the perilymph in scala vestibuli, which in turn causes the cochlear partition to move. In figures 2.1 and 2.2 the displacement of the cochlear partition at a point z along the length of the cochlea is indicated as $y_m(z)$. The displacement of apical portions of the cochlear partition for a sinusoidal stapes displacement was observed directly by Békésy in studies reported in the early 1940s (Békésy, 1960, pp. 446-469, 500-510). More recently, motion of the basilar membrane at the basal end of the cochlea has been measured using the velocity-sensitive Mössbauer effect (Johnstone, Taylor, and Boyle, 1970; Rhode, 1970). These studies indicate that, for constant stapes displacement, the displacement of a point along the partition is maximum at some frequency, that is, the transfer function $Y_m(z)/X_s$ exhibits band-pass characteristics. The frequency-selective filtering which is performed by the mechanical system of the cochlea evidently contributes to the ability of the auditory system to discriminate tones of different frequencies. Békésy (1960, pp. 460-469) has indicated that cochlear mechanics at this level may be represented as a distributed, linear system. Models for the motion of the cochlear partition have been proposed which show band-pass frequency responses (e. g. Zwislocki, 1948; Wansdronk, 1962).

There are no measurements of the normal motion of smaller cochlear structures within the partition, such as the motion of hair cells relative to the tectorial membrane surrounding the hairs. This motion has been inferred from other evidence, however, and the pos-

sibility that shearing motion of the hairs is the mechanical output which excites the sensory hair cells has been advanced (Békésy, 1960, pp. 672-684, 703-710).

2.1.5 Cochlear electrophysiology.

One essential function of the cochlea is to transduce mechanical signals, particularly the motion of the basilar membrane, into action potentials in auditory-nerve fibers. This function of the cochlea is indicated by the stage labeled transducer in figure 2.2. Although the mechanism of the transducer is not understood, electric phenomena thought to be associated with the cochlear transducer have been extensively studied. The electric signals measured are usually voltages, recorded by electrodes placed somewhere in the peripheral auditory system, usually on or in the cochlea. These voltages, or cochlear potentials, can be grouped into four classes; constant potentials, microphonic potentials, summing potentials, and compound action potentials originating in the nerve.

The latter of these, the compound action potential, is apparently the extracellularly-recorded response of synchronously discharging auditory-nerve fibers, and can be recorded with electrodes in or on the surface of the cochlea and auditory nerve. The all-or-none action potentials of the myelinated central processes of single auditory-nerve fibers can be recorded by suitable microelectrodes. The extracellu-

larly-recorded neural responses do not provide information on cochlear function distinct from that available in single auditory-nerve fibers [see Kiang (1965)]. Some characteristics of single-fiber action potentials are described in the next section; properties of extracellularly-recorded action potentials are not discussed here.

A constant potential difference of 80 to 100 millivolts, the endocochlear potential (EP), can be measured between the endolymph of scala media and the perilymph of scala vestibuli or scala tympani, scala media being the more positive (Békésy, 1960, pp. 647-654). In addition, there is evidence that cells in the organ of Corti exhibit negative, resting potentials such as those found in other cells (Békésy, 1960; Lawrence, 1965). These constant potentials exist in the absence of any auditory stimulus; they are apparently maintained by metabolic activity [see Davis (1957)].

In response to an acoustic input to the cochlea, time-varying voltages are readily found anywhere in the vicinity of the cochlea, and particularly in the cochlear fluids.

One component of these voltage changes, the cochlear microphonic potential (CM), is so named because the observed voltage waveform is similar to the waveshape of the acoustic stimulus. For tone stimuli, CM appears to be linearly related to the mechanical input to the cochlea over a wide dynamic range, although the relationship departs from linearity at high signal levels. The CM, then, is an

indication that a linear mechano-electrical transduction process occurs in the cochlea. However, the role, if any, of this process in the chain of events which leads to production of spike signals in the auditory nerve, and therefore any relation it may have to hearing, has not been demonstrated. The arguments which have been advanced to implicate the microphonic phenomenon in the hearing process are summarized by Wever (1966) and discussed by Davis (1957, 1960).

Although a stage for production of CM is not explicitly indicated in the block diagram of figure 2.2, within the depicted framework, CM might be associated with the stage labeled transducer.

The source of CM is known to be associated with the organ of Corti [see Stevens and Davis (1938)], and on the basis of experimental observations, CM is thought to be generated by the hair cells. Experiments designed to correlate intra-cochlear voltages with the anatomical location of recording microelectrodes have recently been performed, but detailed electrophysiological results have not been associated with structures as small as cells (Sohmer, Peake, and Weiss, 1971). Some data concerning receptor potentials of hair cells in another mechano-receptor, the amphibian lateral-line organ, have recently been reported (Harris, Frishkopf, and Flock, 1970). However, the effects of mechanical stimuli on the membrane potentials of hair cells or nerve endings have not been studied in detail in any preparation.

Mechanisms by which mechanical signals are transduced into

CM have been considered by several authors. An electric circuit model of the hair cell which accounts for several properties of CM was developed by Davis [see Davis (1965)] and later modified by Wiederhold (1967) to account for the effect of the OCB on CM and nerve activity. Békésy (1960, pp. 636-647) concluded from an energy consideration that the microphonic does not result from a passive transformation of mechanical energy, but is produced by an active process. At present the mechanism underlying the microphonic action of the cochlea is not known and is a subject of active research.

The other cochlear potentials that can be identified as response to an acoustic stimulus are the positive and negative summing potentials, SP_+ and SP_- (Davis et al., 1958), and an additional slow potential which may be related to these (Kiang and Peake, 1960). These potentials appear as maintained shifts of the baseline potential (sometimes called dc shifts) during stimulation with suitable tones. The possibility that these potentials reflect a process which excites neural activity has been advanced (Davis et al., 1958) and is based on arguments similar to those made for the microphonic. As with CM, the origin of the summing potential is not well understood.

Electrically-generated activity in the crossed component of the efferent olivo-cochlear bundle (COCB) has a demonstrable effect on CM (Fex, 1959; Desmedt, 1962; Wiederhold and Peake, 1966). Although it is known that action potentials in the efferent COCB fibers can occur

in response to sound (Fex, 1962), the normal operation of the central portion of this physiological feedback system, and therefore its role in normal hearing processes, is largely unknown. The OCB is often presumed to be inactive in the barbiturate-anesthetized animal.

2.1.6 Auditory-nerve electrophysiology.

Auditory-nerve fibers conduct all-or-none neural impulses from the cochlea to the brain. In figure 2.2, the action potentials (spikes) generated in the nerve fibers are represented by the set of $a_i(t)$; the action potentials delivered to the central nervous system are shown delayed by conduction time τ_i . The responses of auditory-nerve fibers to several types of acoustic stimuli have been systematically studied by Kiang (1965, 1968). Some of the descriptions of responses to tonal and click stimuli are pertinent to the present investigation.

All fibers show randomly distributed discharges in the absence of any controlled acoustic stimulus. The rate of these spontaneous firings varies from fiber to fiber, ranging from less than 0.1 to over 100 per second.

The response to tone is a function of both frequency (f) and level. The threshold of just-detectable response exhibits a minimum at a particular frequency which is a characteristic of the fiber (characteristic frequency, f_c or CF), and rises sharply for $f > f_c$ and $f < f_c$. A plot of threshold against frequency is called the tuning curve, and the area of

the stimulus plane above the tuning curve is called the response area. Tuning curves show frequency selectivity which can be compared with the mechanical band-pass characteristics of the cochlear partition.

As tone level is raised from low- to supra-threshold values, fiber discharge rates generally increase. The relation between rate of firing of a fiber (number of spikes per second) and the level of a stimulus tone is often termed the intensity function of the fiber, although the stimulus is usually specified in terms of the magnitude of a quantity such as sound pressure, rather than actual sound intensity (power). In general the rate rises from the spontaneous firing rate to a maximum rate as stimulus level is raised 20 to 40 dB above the threshold value. Intensity functions have frequently been found to be monotonic, high stimulus levels producing a saturated maximum average firing rate (usually < 200 spikes per second). Recent evidence shows that when intensity functions are measured using sufficiently fine steps of stimulus level, exception to monotonicity is often found (Kiang et al., 1969). The nature of the exception is that a sharp minimum in the intensity function occurs at some stimulus frequencies. When intensity functions are measured at 5 or 10 dB level increments, the sharp minimum is usually not apparent.

The effect of electrically-generated efferent activity of the COCB on afferent fiber response to tones has been described as a shift of the intensity function along the stimulus-level axis, reducing fiber sensi-

tivity by as much as 20 dB (Wiederhold, 1970).

For click stimuli, fibers of f_c below about 5 kHz show several preferred times of firing which are simply related to f_c ; intervals between preferred firing times are equal to $1/f_c$ (Kiang, 1965; Gray, 1966). It is possible that both the value of f_c and the firing times for click stimuli are determined by the dynamics of the cochlear partition, with click response reflecting an oscillatory mechanical impulse response [see Weiss (1966)].

For low-frequency tones, discharges tend to occur in synchrony with individual cycles of the stimulus. A preferred phase of firing can be detected for stimulus frequencies below about 5 kHz and interspike-interval distributions show peaks at the period of the stimulus. For tone frequencies > 5 kHz, the average distribution of spikes appears to be uniform throughout a period of the stimulus. With continuous tones at these stimulus frequencies (and for spontaneous activity), distributions of interspike intervals are comparable to the distribution of inter-event times in a Poisson process; a notable exception is that the nerve-fiber discharge shows far fewer very short (< 10 msec) intervals than would be predicted by Poisson statistics.

At present much is known about the output signals of the cochlea (the discharges of the auditory nerve) that occur in response to a variety of acoustic stimuli, but the signal-processing stages within the cochlea are not as readily available for study, and understanding of

the internal mechanisms of the cochlea is incomplete. No comprehensive model of the operation of intermediate stages has been devised which accounts even qualitatively for properties of auditory-nerve-fiber response to simple stimuli (e. g. Weiss, 1966; Gray, 1966; Lynn and Sayers, 1970).

2.2 Action of Electric Stimuli on the Peripheral Auditory System.

2.2.1 Electric stimulation of human subjects.

It has long been known that sensation can result from electric excitation of sense organs. Volta (1800) observed that by connecting a battery of his voltaic cells to his own head, he could perceive visual, gustatory, and auditory sensations. The investigations which followed this discovery throughout the 19th and early 20th centuries are mainly of historical interest and have little significance for the present investigation. Simmons (1966) and Flottorp (1953) have recently reviewed the auditory effects of electric current that were reported in the literature of this period.

In the early 20th century a number of reports of electrically-induced hearing sensations appeared in the scientific literature. The observation that signals from a radio could be heard without the use of a loudspeaker or earphone led one worker to patent a device which purportedly permitted deaf persons to listen to radio broadcasts (Eichhorn, 1930). Other contemporary reports described new methods

of hearing based on electric stimulation of the ear (Perwitzchsky, 1930; Jellinek and Scheiber, 1930) which were thought to be promising for restoring auditory communication to the deaf.

Later in the 1930's, more systematic investigations of the action of electric stimuli on the human peripheral auditory system were undertaken. The following is a brief review of these and more recent human and animal studies which form the background for the present investigation.

Some of the recent experimentation has been directed toward development of electric prosthetic devices for restoring useful hearing to the deaf through stimulation of the auditory nerve. In patients without functional cochleas, however, stimuli applied directly to the cochlea or auditory nerve have proven disappointingly poor for conventional auditory communication. Simple stimuli are perceived as complex sounds, and intelligibility of electric analogs of speech waveforms applied directly to the nerve has been poor (Djourno and Eyriès, 1957; Zöllner and Keidel, 1963; Doyle et al., 1963; Doyle et al., 1964; Simmons et al., 1964; Simmons et al., 1965; Simmons, 1966; Michelson, 1970)

Subjects with normal hearing have been found to experience several kinds of auditory sensation when stimulated electrically in the vicinity of the ear. In one type of experiment, subjects have been stimulated with high-frequency signals that are modulated at audio

frequencies. Evidently there are at least two mechanisms that can be responsible for perception of such stimuli. One mechanism is associated with radiation in the microwave region such as is found near radar transmitters (Frey, 1961, 1962, 1963; Ingalls, 1964). Although there seems to be some uncertainty as to whether subjects with peripheral deafness experience auditory sensations in microwave fields, Frey (1962) has suggested that a central-nervous-system effect does exist. This effect can be distinguished from another kind of effect, which is believed to occur in the peripheral auditory system.

An electromechanical mechanism which accounts for auditory perception of electric stimuli has been described by several authors (Kahler and Ruf, 1931; Meyer, 1931; Chocolle, 1950; Sommer and von Gierke, 1964; Harvey and Hamilton, 1965; Tuhy, 1967). They have proposed that when an electric field is developed at the surface of the body, electrostatic forces are developed which produce perceptible vibration under certain circumstances. This mechanism has been incorporated into models of the effects observed when an electrode insulated with a thin layer of dielectric is placed against the skin of the head and another contact is made through an electrode on another part of the body [see Tuhy (1967)]. When an electric signal is supplied to the electrodes, a potential difference, and thus a stress of electric origin, is developed between the conducting surface of the insulated electrode and the tissue beneath it. As modeled, the force produced

is essentially proportional to the square of the applied voltage. If the applied voltage is a modulated carrier of the form

$$v(t) = V_o \left(1 + s_m(t) \right) \cos \omega_c t$$

the resulting stress is proportional to

$$\frac{V_o^2}{2} \left[1 + 2s_m + s_m^2 + \left(1 + 2s_m + s_m^2 \right) \cos 2\omega_c t \right]$$

This force contains components proportional to the first and second powers of the modulating signal s_m and other components which for sufficiently large ω_c are inaudible. Because the skin and tissue are not rigid, they would move under the influence of the force. Tuhy (1967) observed that the electrode-tissue system generated a significant airborne acoustic signal. Harvey and Hamilton (1965) considered the possibility that subjects perceive an acoustic signal that is transmitted to the cochlea by bone conduction. Whatever the sound transmission path, the intelligible perception evidently results from the acoustic signal generated by the electric stimulus. It has been suggested that a modulated carrier waveform applied in this way is transmitted to the inside of the head, where it stimulates neurons directly to produce readily-intelligible auditory perception [see Einhorn (1967)]; however, the available evidence does not support this hypothesis.

Stevens and Jones (1939) described the results of other perceptual experiments in which electric stimuli were introduced through an

electrode contacting fluid in the external-ear canal. Sinusoidal currents introduced in this way were often perceived as a tone of twice the stimulus frequency. When a direct bias voltage was added to the sinusoidal stimulus, the perceived pitch changed to correspond to a tone at the fundamental rather than second harmonic of the applied sinusoid. To account for this result, Stevens and Jones proposed an electrostatic transducer in which the eardrum membrane effectively formed one plate of a capacitor, and the surface of the promontory, situated across the middle-ear cavity, formed the other effective plate. The force developed between the effective surfaces is again proportional to the square of the potential difference between them; the effect of a bias voltage is to introduce a linear term in the transduction. The force of electric origin exerted on the tympanic membrane is equivalent to a force exerted by an incident sound pressure and is perceived in the same way.

Forces of electric origin exerted on the skin or eardrum membrane may be responsible for many of the reports in the literature of electrically-evoked auditory sensation found in subjects with intact auditory apparatus, although at the time this possibility may either have gone unrecognized or may have been discounted (Eichhorn, 1930; Fromm, Nylén, and Zotterman, 1935; Craik, Rawdon-Smith, and Sturdy, 1937; Hallpike and Hartridge, 1937; Stevens, 1937; Fiori-Ratti and Manfredi, 1951; Puharich and Lawrence, 1964; Einhorn, 1967).

The electrically-evoked auditory sensations described above have no particularly significant relation to processes of the cochlea, since they are responses to signals generated either central to or peripheral to the cochlear transducer. However, an additional sensation can be identified both by subjects with normal hearing and by subjects lacking tympanic membrane and ossicles. Production of this sensation appears to require that the cochlea be functional.

It should be emphasized that a mixture of sensations was often reported by normal subjects when alternating current was delivered with electrodes in direct contact with the ear. Jones, Stevens, and Lurie (1940) identified three types of sensation in normal subjects, and proposed a separate origin of each type. One of these was the square-law, electrostatic mechanism associated with the tympanic membrane, which had been identified previously (Stevens and Jones, 1937). Sensation characteristics associated with this square-law mechanism were absent in patients whose middle-ear structures had been surgically removed, even though cochlear function was maintained.

The two remaining sensation types occurred when currents were delivered directly to the cochlea. Of these sensations, one was attributed to currents acting directly on auditory-nerve fibers. The complexity of this type of sensation seems to be similar to that reported in the more recent investigations in which electric stimuli have been

applied directly to the nerve (see page 39).

The other sensation type was described as following a linear law (as distinguished from the square-law effect of peripheral electrostatic transducers). This sensation occurred only in subjects who possessed a functioning cochlea, and although the authors were not able to specify a particular mechanism underlying this sensation, they did conclude that electric stimuli had an effect within the cochlea itself.

Other workers have also found an effect localized to the cochleas of patients without middle-ear structures, and the cochlear origin of the effect was shown in other control experiments (Volokhov and Gersuni, 1934; Andreev, Gersuni, and Volokhov, 1935; Gersuni and Volokhov, 1937; Andreev, Arapova, and Gersuni, 1938). However, in some of their characterizations of electrically-induced auditory sensations these authors seem to have presumed that this one effect predominated, and thus their observation of an apparent square-law (second harmonic) response in normally-hearing subjects was presumed to be a cochlear effect (Arapova, Gersuni, and Volokhov, 1937; Arapova and Gersuni, 1938). It was suggested, with some reservations, that the effect could result from electromechanical action within the cochlea (Volokhov and Gersuni, 1934; Gersuni and Volokhov, 1936; Arapova and Gersuni, 1938) or possibly from immediate action on receptor elements (Arapova et al., 1937; Andreev et al., 1938).

More recently, Wallner (1956) concluded that electric stimuli affected the auditory system peripheral to the auditory nerve, but in this case the author may have been observing the effects of peripheral electrostatic transduction as well as a cochlear effect. Salomon and Starr (1963) elicited auditory sensations from a patient when both direct and alternating currents were applied directly to the cochlea, apparently reflecting an effect of the electric stimuli on the cochlea itself.

The possibility that an electric stimulus might affect the cochlea had been recognized earlier (Perwitzchsky, 1930; Hallpike and Hart-ridge, 1937). Two alternative mechanisms were hypothesized to account for experimental observations. On the basis of the subjective response to abrupt phase changes in sinusoidal stimuli, some authors believed that both an electric stimulus and an acoustic stimulus were subject to the same resonant, band-pass filtering (Hallpike and Hart-ridge, 1937; Bárány, 1937; Kellaway, 1944, 1946). They hypothesized a mechanism by which an electric signal would first be transformed into a mechanical one in the cochlea, and then analyzed by the mechanical system of the cochlea in the usual way, although it was acknowledged that either mechanical or electrical resonance would account for the experimental observations. Earlier workers had a priori conceived of the electric current as exciting electrically-tuned sensory cells directly (Fromm, Nylén, and Zotterman, 1935), but this possibility

was specifically rejected by Kellaway (1946).

Some authors have rejected the idea that an electric stimulus has any significant effect on the cochlea itself (Flottorp, 1953; Chocolle, 1954). Instead, it was proposed that in most, if not all cases, the observed effects might be due to transducer mechanisms associated with the particular electrodes used or with the soft tissue lining the middle ear.

At present there is insufficient evidence in the literature to specify the origin or the mechanism underlying linear-law perception of electric stimuli by human subjects. One result of the present study is the demonstration of a "linear-law" physiological phenomenon associated with electric stimulation of the cochlea.

2.2.2 Electric stimulation of experimental animals.

The perceptual studies of human subjects described in the preceding section have indicated possible effects of electric stimuli on the cochlea and auditory nerve. Few comparable electric stimulation experiments have been conducted on the inner ear of experimental animals, and none has been designed as a further investigation of the effects found in humans. The types of experiment which have been performed are discussed briefly in this section.

Effects of electric stimuli on the cochlea and auditory nerve have been studied by monitoring neural activity at some station of the

auditory system and comparing response to acoustic and electric stimuli, recording either gross neural potentials (Kiang and Peake, 1958; Peake, Teas, and Capranica, 1962; Agin and Lowy, 1962; Simmons and Glatke, 1970), or single-unit discharge (Clark, 1969).

Some experimenters have observed gross responses of the brain to direct electric stimulation of portions of the auditory nerve, the purpose being to study the projections of the peripheral auditory system on the central nervous system (Woolsey and Walzl, 1942; Tunturi, 1944, 1945, 1946; Marty and Thomas, 1963; Kayser and Libouban, 1963).

Direct electric stimulation of the nerve has also been used to establish and study activity in the efferent system (Fex, 1962; Pfalz, 1966; Pfalz and Pirsig, 1966). In these investigations, the electric stimuli were intended to bypass some of the signal-processing stages which influence response to acoustic stimuli. None of these studies revealed response characteristics which could be a correlate of the two perceptual effects observed for electric stimulation of the cochleas of human subjects. In some of these experiments, intentional destruction of the cochlea or the placement of the stimulating electrodes evidently precluded this possibility; in others, the recorded neural potentials may not have been sufficiently sensitive to differences in individual neuron discharge which might be associated with different types of sensation.

Some experimenters have excited the intact cochlea with cur-

rent, usually d. c. , to determine resistances of intracochlear fluids and membranes (e. g. Békésy, 1960, pp. 654-672; Misrahy et al. , 1958; Johnstone et al. , 1966). In these experiments, however, no direct effect of the electric stimuli on the sensory function of the cochlea was reported.

Other workers have reported effects of electric currents on the operation of the cochlea. Tasaki and Fernandez (1952) observed that the gross cochlear potentials evoked by acoustic stimuli were modified when a direct bias current was injected into the cochlear scalae. More recently, Konishi et al. (1970) and Teas et al. (1970) observed that acoustically-evoked response of single auditory-nerve fibers was modified when the cochlea was simultaneously stimulated with direct or low-frequency (< 30 Hz) sinusoidal current. The direct and slowly-varying current waveforms used in these experiments are not analogous to audible acoustic stimuli, and the results are not directly comparable to the effects of alternating currents found in human subjects. The reported effects of direct currents may be a correlate of the perceptions reported by Salomon and Starr (1963) or even by Volta (1800).

Although it has not been apparent in the studies described above, the possibility that electric stimuli can have multiple effects on the cochlea of experimental animals has been indicated by other experimental evidence. In one recent study, responses of single fibers of the cat's auditory nerve were recorded when pulses of current (shocks)

were delivered to the cochlea (Moxon, 1967, 1968), and temporal patterns of discharge were described. Figure 2.4 shows an example of these results. The figure shows post-stimulus-time (PST) histograms of the response found in auditory-nerve fibers when 100 μ sec rectangular current pulses were applied to the cochlea. It was suggested that the large peak occurring at about 1/2 msec in the histograms in (A), (B), and (C) resulted from the direct action of electric current on auditory-nerve fibers. The peaks appearing between 2 and 6 msec in the histogram in (C) are similar to the peaks found in response to acoustic clicks in the same fiber [histogram (D)]. As indicated in section 2.1.6, the time patterns of click response may be due to an oscillatory impulse response in the mechanical system of the cochlea; consequently, the shock response in part (C) of the figure was tentatively explained by hypothesizing that the electric stimulus was actually transduced into a mechanical stimulus, and the resulting motion excited the sensory cells in much the same way as a click. Whether or not the actual mechanisms are as proposed, it appears that this shock response implies two excitation processes, possibly those responsible for the two sensations experienced by human subjects.

2.3 Outline of Thesis Research.

According to these results, when suitable response quantities

Figure 2.4

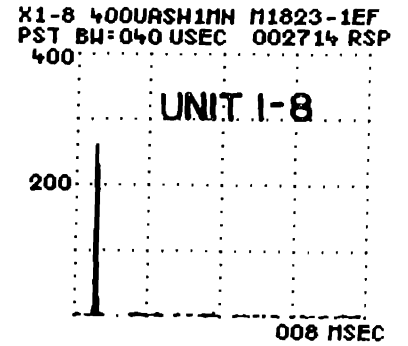
PST histograms of firings of single auditory-nerve fibers in response to shocks and clicks.

In (A), shocks were applied across the organ of Corti in the basal turn, with electrodes in scala media and scala tympani. In (B), shocks were applied with electrodes introduced into the nerve through the bony modiolus. In (C), shocks were applied to electrodes on the surface of the cochlea, one placed near the round window, the other placed near the apex. Shocks 100 μ sec. In (A) scala tympani negative, in (C) round window negative. In (D), response to clicks is shown for the same fiber whose response to shocks is shown in (C). Click amplitude, -50 dB re 100 V peak into 1" condenser earphone. (From Moxon, 1968.)

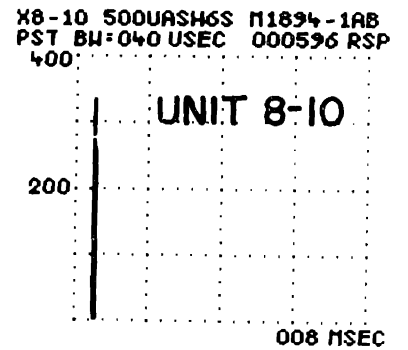
ELECTRIC STIMULATION

ELECTRODE LOCATION SHOCK LEVEL

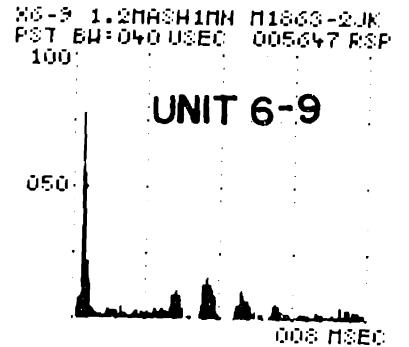
A SCALA MEDIA -
 SCALA TYMPANI 0.4 ma



B IN
 MODIOLUS 0.5 ma



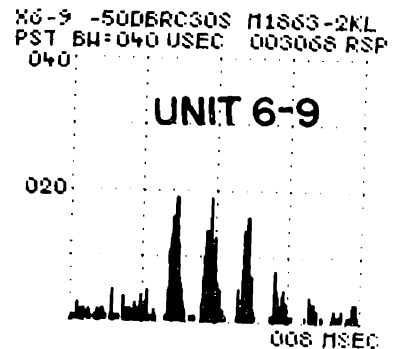
C SURFACE OF
 COCHLEA 1.2 ma



ACOUSTIC STIMULATION

STIMULUS STIMULUS LEVEL

D RAREFACTION - 50dB
 CLICK



are measured, two components of response to electric stimulation of the cochlea are found in the auditory nerve of the cat. It is possible that the similarity of auditory-nerve-fiber response to shock and click found in this experimental animal can be attributed to the physiological mechanism which accounts for tonal sensations found when the human cochlea is stimulated with sinusoidal electric current.

The present study is a further investigation of the effects of electric stimuli suggested by these results. As outlined in the introduction, the objectives of this study were

- 1) to describe effects of electric stimuli on the response of auditory-nerve fibers
- and
- 2) to test hypotheses concerning the origin of these responses.

To investigate the role of various cochlear elements and processes in the production of nerve-fiber response, discharge characteristics were studied when the operation of various signal-processing stages was experimentally modified. The general characteristics of auditory-nerve-fiber responses are described in the first chapter of experimental results (Chapter IV).

The origins of nerve-fiber responses were further explored in another set of experiments. Some characteristics of nerve-fiber response suggest that a mechanical signal occurs in the inner ear in response to electric stimuli. Consequently, response of the cochlea was investigated using a mechanical detector to measure motion of

the round-window membrane. To explore possible mechanisms underlying this phenomenon, mechanical response was studied in normal cochleas and in cochleas whose normal mechano-electrical transduction characteristics had been altered. The mechanical response of the cochlea is described in the second chapter of experimental results (Chapter V).

Finally, the experimental data allow some conclusions to be drawn regarding the origin of nerve-fiber response and the origin of mechanical response to electric excitation of the cochlea. These conclusions are presented in the final chapter (Chapter VI) along with a discussion of other implications of the data obtained in this study.

CHAPTER III.

EXPERIMENTAL METHODS

The basic experimental techniques and equipment for generating acoustic stimuli and recording the response of auditory-nerve fibers are those described by Kiang (1965). Modifications and additions were introduced for the study of the neural and mechanical responses to electric stimuli. The following includes a brief description of the important basic experimental methods, along with a more complete description of the methods peculiar to this study.

3.1 Animals and Preparation.

For all experiments adult cats were anesthetized with an intraperitoneal injection of Dial (75 mg/kg) and the bulla opened and the bony septum removed. The external auditory meatus was cut to permit the installation of the acoustic stimulus system. In most experiments the tendons of the middle-ear muscles were cut. To provide access to the auditory nerve, the posterior fossa of the skull was opened and the cerebellum gently retracted to expose the auditory nerve as it emerges from the internal auditory meatus. When COCB stimuli were used, the cerebellum was removed to expose the floor of the IVth ventricle.

In some cats a program of intramuscular injections of an ototoxic antibiotic was used to produce degeneration of hair cells. The drug

used was kanamycin, a member of the streptomycin family. The effects of kanamycin on the organ of Corti have recently been summarized by Kohonen (1965) and by Engström et al. (1966). Drug doses ranged from 200 to 250 mg/kg per day for from 6 to 12 days. Physiological recordings were made 19 to 163 days after the last drug injection. To determine the condition of the hair cells, the cochleas were fixed with osmium, dissected, and examined with a phase contrast microscope (Engström et al., 1966). The damage to each row of hair cells was assessed and estimates of the degree of degeneration were plotted as a function of position along the basilar membrane (Kiang, Moxon, and Levine, 1970).

3.2 Configuration of Stimulating Electrodes.

In most experiments, electric stimuli to the cochlea were delivered through wire electrodes placed in a standard position on the surface of the cochlea. A photograph of electrodes in place on a cat skull is shown in figure 3.1. One electrode makes contact near the edge of the round-window membrane; the other electrode is placed on the soft periosteal tissue on the surface of the cochlear capsule between the round window and the apex. Sometimes when the cochlea was sufficiently moist, the cotton around the round-window electrode was omitted and the wire made contact through a small quantity of liquid suspended between the wire and the tissue. In some experiments the electrodes

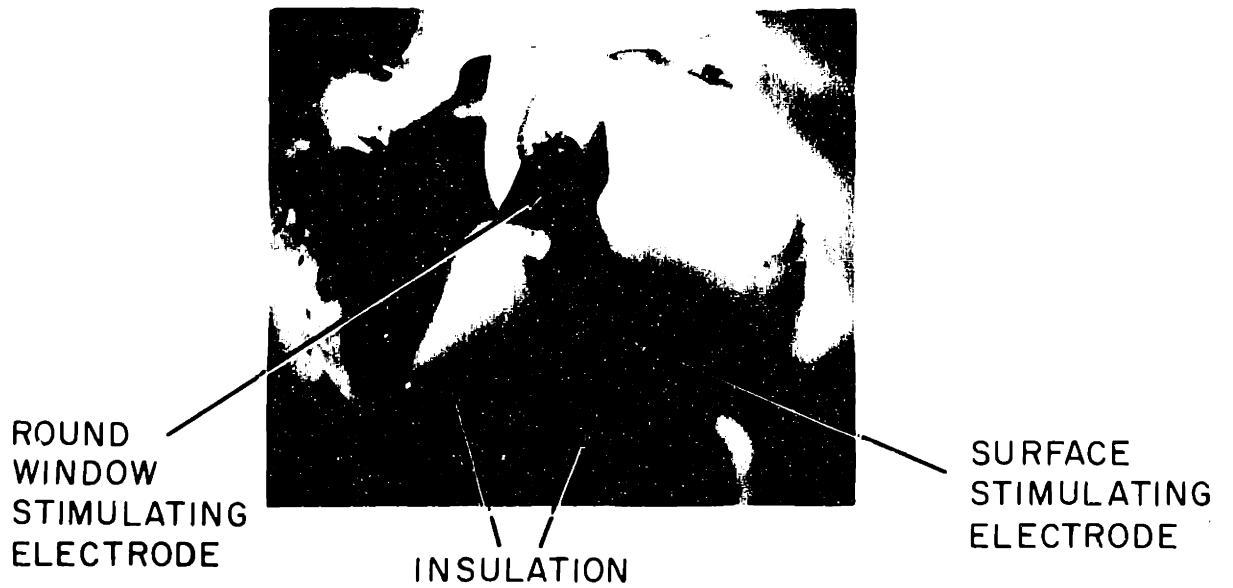
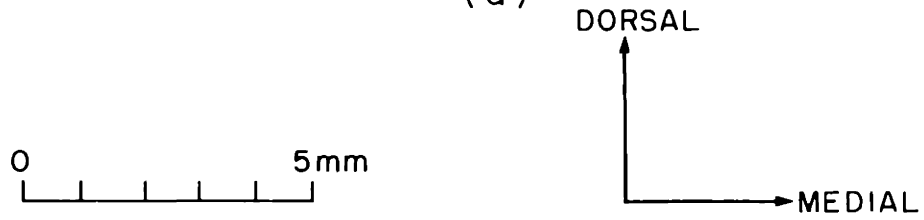
Figure 3.1

Photographs of the temporal bone of the cat indicating the placement of stimulating electrodes.

The skull of a cat was photographed through the opening in the bulla made to provide access to the cochlea during the experiment. View is from posterior looking anteriorly. The bony septum separating the bulla cavity from the middle-ear cavity has been removed. In (a), pertinent anatomical features are indicated. In (b), the electrodes are shown in place. The round-window stimulating electrode has a tuft of cotton moistened with saline solution (0.9% NaCl) which rests on the rim of bone below the round window. In the experiment, the other electrode contacts the moist periotum on the surface of the cochlear capsule. Electrodes shown are #20 stainless-steel wire.



(a)



(b)

used were made from pieces of 1-cm-diameter glass tubing about 5 cm long, bent and drawn to a 1 mm diameter and plugged with cotton at the end. The tubing was filled with 0.9% NaCl and stainless-steel wires were used to make electric contact with the electrolyte. These electrodes were arranged to contact the cochlea at the standard positions.

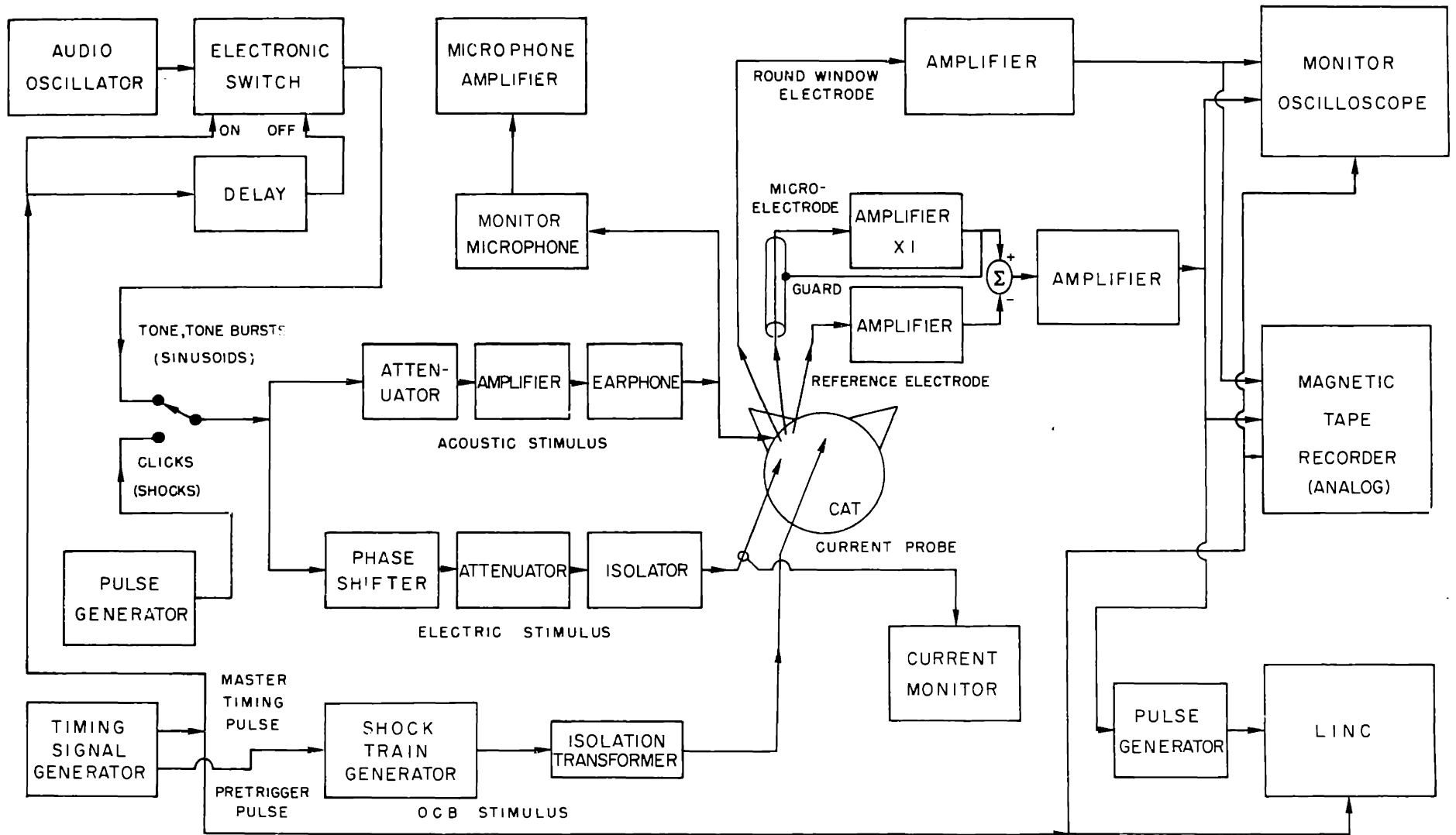
3.3 Methods for Recording Auditory-Nerve Response.

To record the action potentials of single auditory-nerve fibers, the animal was fitted to a head-holder which held the skull rigidly and the preparation was placed in a sound-isolated chamber. The apparatus used is shown in the block diagram of figure 3.2. Acoustic stimuli were generated using either a 1-inch or 1/2-inch capacitor earphone (Brüel & Kjær #4132 or 4134 microphone cartridge) in a closed acoustic system sealed into the external meatus. A calibrated probe tube and 1/4-inch condenser microphone (Brüel & Kjær #4136) monitored the sound pressure developed near the tympanic membrane. Clicks were produced by 100 μ sec rectangular voltage pulses delivered to the earphone. Continuous tones and tone bursts were derived from a sinusoidal oscillator (General Radio 1310) gated by an electronic switch (Grason-Stadler #829). Repetition rates for clicks and bursts were usually 10/sec, and burst duration was set to be 25 to 50 msec with a rise-fall time of 2.5 msec. The signals were passed through a variable attenuator (Hewlett-Packard 350A) to an earphone-driver amplifier.

Figure 3.2

Block diagram of stimulus-generation and response-recording equipment used for studying response of single auditory-nerve fibers.

The equipment shown in approximately the left half of the diagram is stimulus-generation apparatus; response-recording and processing stages are represented on the right. Optional provision for shifting phase of sinusoidal electric stimulus and provision for activating the olivocochlear bundle were included only when required.



Using the probe-tube calibration and monitor-microphone output obtained at constant attenuator setting, attenuator settings could be converted to sound-pressure levels. When required, phase of tympanic-membrane sound pressure was also obtained from monitor-microphone output by correcting for the phase characteristics of the probe tube and microphone.

Current was supplied to the stimulating electrodes through one of two systems. For delivering rectangular pulses of current (shocks), a high-output-impedance, optically-coupled stimulus isolator was used. Isolation of the stimulus prevented net flow of stimulus current through other electrical contacts to the preparation, and reduced stimulus artifact in the records of auditory-nerve activity. The high-impedance feature helped maintain constant electrode current and reduce effects of polarization which might have occurred at the electrode metal-liquid interface due to the non-zero dc component of the stimulus pulses. Amplitude and duration of the stimulus current pulse were adjusted by the controls on the pulse generator supplying the signal to the isolator. Pulse polarity was reversed by switching the output of the isolator. The polarity convention adopted was to call current into the round-window electrode positive.

Sinusoidal stimuli were coupled to the electrodes by means of a wide-band audio transformer (UTC A-20). Sinusoidal current, either continuous or in bursts, was obtained by connecting the transformer

through an attenuator to the same sources used to generate tones and tone bursts. A phase shifter and meter (Acton Laboratories 329B with type C plug-in) could be included in order to vary and measure relative phase between electric and acoustic stimuli.

For all electric stimuli, round-window-electrode terminal current was monitored with an inductively-coupled calibrated current probe (Tektronix type 131). Current pulse amplitude was measured directly with an oscilloscope. For sinusoidal stimuli, current-probe output was measured as a function of frequency at constant setting of the stimulus attenuator. By applying the current-probe calibration, current level at other attenuator settings could be calculated. The phase of electrode current was also determined by a similar procedure. The voltage applied to the electrodes was considered an unsatisfactory measure of stimulus delivered to the cochlea because of uncertainty of the voltage difference across the electrode-tissue interface. For this reason current was routinely measured and used to characterize the stimulus.

Electric stimulation distinct from that applied to the cochlea was used in some auditory-nerve experiments to excite the efferent COCB fibers. The techniques have been described by Wiederhold and Kiang (1970). A pair of electrodes was introduced into the COCB just below the surface of the floor of the IVth ventricle, which had been surgically exposed. A bipolar (doublet) stimulus waveform (100 μ sec positive

pulse followed by a 100 μ sec negative pulse) was coupled to the electrodes through an isolation transformer. Stimuli were delivered in trains of 32 doublets, individual doublets separated by 2.5 msec. Clicks or shocks to the cochlea were presented at 2/sec, and alternate stimuli were preceded by the train of COCB stimuli (the last doublet of the train preceded the stimulus by 10 msec). For bursts of tone or sinusoidal current the alternating paradigm was not used; bursts were presented at 10/sec and COCB stimuli accompanied each successive burst. The doublet amplitude was adjusted either to give maximum amplitude reduction of gross neural response to click (N_1), or to just below the level which excited motor systems and caused the animal to twitch.

A wire electrode which made contact with the surface of the cochlea near the round window was used to record gross electric responses. The signals from this electrode were amplified and observed on an oscilloscope to monitor the general condition of the cochlea and auditory nerve.

Drawn glass capillaries of tip diameter in the vicinity of 1 μ m or less were filled with electrolyte (2 molar KCl) for use as microelectrodes. The microelectrode was advanced into the nerve by means of a micro-manipulator operated remotely from outside the chamber. The voltage between the grounded head-holder and the microelectrode was amplified by a unity-voltage-gain, high-input-impedance amplifier

(Instrumentation Laboratory PICO-metric amplifier). The lead wire connecting the electrode to the amplifier was guarded. A reference electrode of stainless-steel wire placed near the auditory nerve recorded approximately the same artifact waveform resulting from the electric stimuli as did the microelectrode. The signals from the microelectrode and the reference electrode were subtracted in a differential amplifier to reduce the electric artifact present in the record of auditory-nerve potentials. Sometimes the signal from the differential amplifier was low-pass filtered (at a few kHz) to further reduce artifact resulting from both shocks and high-frequency sinusoidal stimuli; spike signals were usually high-pass filtered (at a few hundred Hz) to reduce low-frequency fluctuations of the baseline.

The spike signals were displayed on an oscilloscope and reproduced through a loudspeaker. Nerve-fiber discharges could be detected visually and audibly by the experimenter. A pragmatic threshold of nerve-fiber response for a given stimulus was defined to be the lowest stimulus level at which a pattern of response synchronized with the stimulus could be detected using both audio and visual cues. The output of the microelectrode channel and a signal derived from the stimulus were recorded on magnetic tape to allow subsequent processing.

Quantitative analysis of the response pattern of nerve fibers was performed on-line or from magnetic tape using a computer (LINC) to compile post-stimulus-time (PST) and interval histograms. PST histo-

grams show the relationship between spike discharge times and time of stimulus, while interval histograms show the distribution of interspike intervals (Gerstein and Kiang, 1960). The amplified microelectrode signal was used to trigger a pulse generator and the output of the pulse generator signified the occurrence of a spike to the computer. The computer was also supplied a signal indicating the time of occurrence of a stimulus. When the COCB was stimulated on alternate click or shock presentations, two simultaneous PST histograms were computed, one from responses to the stimuli which were preceded by COCB excitation, the other from responses to the stimuli which were not [see Wiederhold (1970)].

Another type of histogram was computed to show the time course of discharge rate. The number of spikes in a 500 msec interval was counted, divided by the length of the interval, and the resulting rate plotted for successive intervals.

Histograms compiled by the computer were observed on a cathode-ray tube display. When a permanent record was desired, the display was photographed. Actual spike waveforms were photographed for the purpose of illustration from an oscilloscope display of data recorded on magnetic tape.

3.4 Methods for Recording the Mechanical Response of the Cochlea.

The basic system used to record mechanical response of the coch-

lea is outlined in the block diagram of figure 3.3. For investigating frequency-dependence of response to sinusoidal stimuli, the automated stimulus-generation and response-recording system described by Weiss et al. (1969) was used. Sinusoids were generated by a programmable oscillator (Wavetek model 157). For 120 discrete frequencies distributed logarithmically between 20 Hz and 20 kHz, calibration of the acoustic system was obtained and stored in the controlling computer (PDP-8). On command an operating system swept frequency through the 120 steps, at each frequency setting the oscillator output to achieve constant level of a selected stimulus variable (e. g. constant sound-pressure level at the tympanic membrane). To obtain fixed-frequency stimuli, a manually-controlled oscillator and attenuator were substituted for the programmed oscillator.

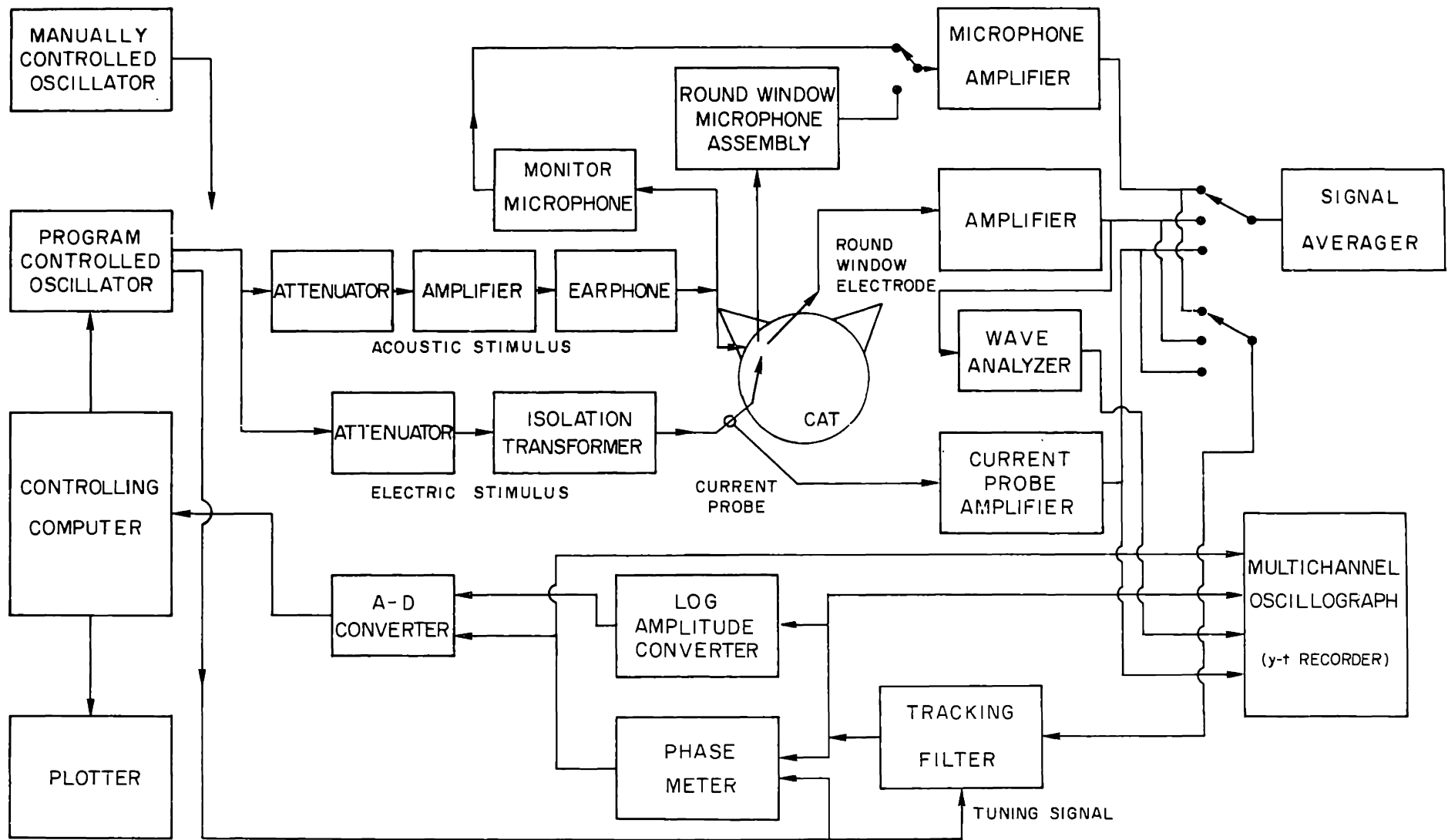
Sinusoidal stimuli generated by the computer-controlled oscillator were delivered to earphone and stimulating-electrode systems which were essentially the same as described in the preceding section, and stimulus variables were monitored in the same way. Because of the physical arrangement of the mechanical detector over the round window, a smaller round-window stimulating electrode (#30 stainless-steel wire) was used in these experiments. In some experiments a stimulating electrode was introduced into the cochlear scalae through the round-window membrane.

The mechanical response of the round-window membrane was

Figure 3.3

Block diagram of stimulus-generation and response-recording equipment used for detecting motion of the round-window membrane.

Basic elements of the automated stimulus-generation and response-recording system (Weiss et al. , 1969) are indicated. Tracking filter extracted fundamental component of essentially sinusoidal response waveforms and improved signal-to-noise ratio. Response waveforms could be averaged to observe waveshape with improved signal-to-noise ratio.



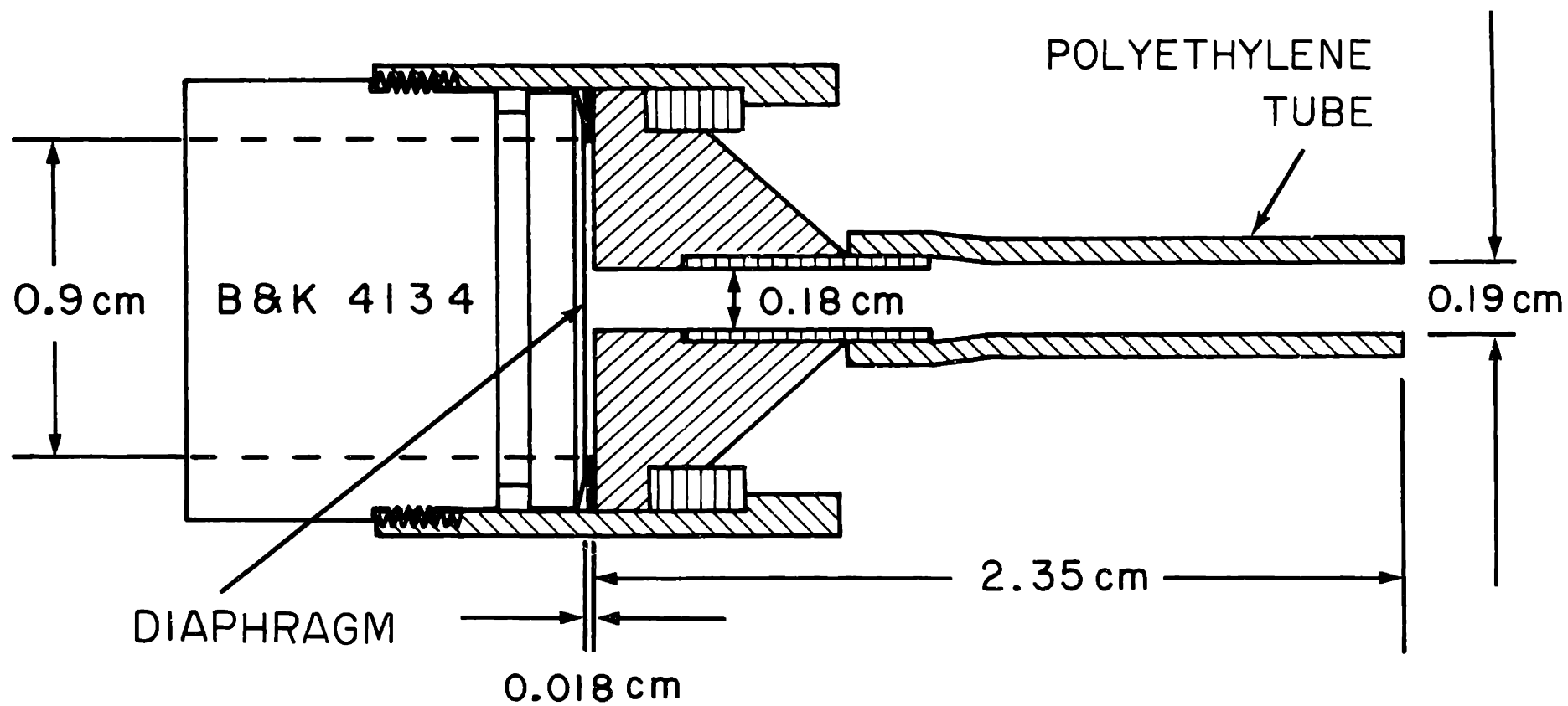
detected using a 1/2-inch microphone (Brüel & Kjaer #4134), coupler, and a plastic probe tube which could be positioned over the round window to form a closed acoustic system. A diagram of this system is shown in figure 3.4. The microphone output voltage was amplified by a Brüel & Kjaer #2604 microphone amplifier. The frequency dependence of the microphone pressure response was calibrated with an electrostatic actuator. The magnitude of pressure response was essentially flat to 10 kHz, and down 3 dB at 20 kHz. Using a calibrated pressure source, the absolute mid-band sensitivity of the microphone was measured and typically was -60 dB re 1 V/ μ bar, which implies a 1 μ V output voltage at 14 dB SPL. These calibrations were used to convert microphone output voltage to pressure at the diaphragm. Since the microphone system was principally used to determine the ratio of round-window-membrane motion for acoustic and electric stimuli, knowledge of the acoustic characteristics of the tube was in general not necessary. Some further characteristics of the microphone system are discussed in Appendix II.

In this type of experiment the animal was placed in an adjustable head-holder and positioned to allow access to the cochlea and round window. To facilitate sealing of the microphone and tube over the round window, the periosteum surrounding the round window was scraped from the bone, and the surface was swabbed with cotton and allowed to dry. The wire stimulating electrode and an electrode for

Figure 3.4

Cross-sectional drawing of the probe tube, coupler,
and probe microphone.

A Brüel & Kjær type 4134 1/2-inch capacitor microphone cartridge is coupled to the polyethylene probe tube. The dimensions shown describe the volume of air in the system. Total air volume, 0.075 cm^3 . Equivalent microphone volume calculated from absolute pressure sensitivity and from manufacturer's specifications, approximately 0.0033 cm^3 .



monitoring surface cochlear potentials were placed close to the round-window membrane, and a ridge of cement (Grip, L. D. Caulk Co.) was then built up around the round window and roughly shaped to fit the open end of the tube. (The round-window electrodes were embedded in the cement ridge.) The tube and microphone assembly was then placed in position and a small quantity of petrolatum applied to the joint between the tube and cement ridge, completing the acoustic seal. In some experiments a notch was left in the ridge to allow an electrode to be advanced into the cochlear scalae through the round window. In such a case, the electrode was positioned before the tube was installed, and a drop of petrolatum was used around the electrode, allowing it to move while maintaining an acoustic seal. A microelectrode was sometimes introduced into the cochlea to measure the direct endocochlear potential (Sohmer, Peake, and Weiss, 1971). Sometimes, as indicated above, a stimulus electrode was introduced in this way.

The effects that the procedure of scraping and cementing the bone had on the electrical properties of the surface of the cochlea were not investigated directly. The removal of the moist soft tissue around the round window might be expected to increase the electric impedance of the surface and cause a larger percentage of electrode current to flow into the cochlea. However, when other conditions were comparable, electrode impedances in other cochleas fell within the range of variability of those found in the scraped and cemented cochleas, suggesting

that in both cases the major component of current flowed into the cochlea.

Care was taken to insure that the microphone system and the electric stimulating system shared no common connections that could couple stimulus signals to the electric output of the microphone system. In particular, it was necessary to insulate the metal microphone case from the animal's ground system inside the experimental chamber. When the probe tube was occluded with a small quantity of water or petrolatum, it was verified that the signals recorded at the output of the microphone amplifier were due to the acoustic output of the cochlea.

The signals of interest in this type of experiment were all responses to sinusoidal electric and acoustic stimuli, and came from three

sources:

- 1) Gross round-window electrode
- 2) Probe microphone system
- 3) Current probe connected to stimulating electrodes.

The first two signals were usually accompanied by a high noise level, and some processing was usually used to facilitate measurement of response characteristics. Signal waveshape at a single frequency was determined by averaging repetitive responses to improve the signal-to-noise ratio [see Clark (1961)]. A computer (PDP-8) was used on-line to calculate the average and the result was displayed on a cathode-ray tube. The display was usually photographed to obtain a permanent record of the data.

When the response waveform was essentially a sinusoid of the

same frequency as the stimulus, the response-recording features of the system described by Weiss et al. (1969) were used to characterize complex amplitude of a response in terms of its magnitude and angle. The magnitude and angle of response were measured as a function of frequency using the computer-controlled stepped-frequency stimulus source described above. To extract signals from the noise, response waveforms were filtered by an electrically-tuned band-pass filter (3 dB width = 2 Hz) [Spectral Dynamics model SD101A Dynamic Analyzer (tracking filter)]. Tracking-filter output was connected to a log converter (Spectral Dynamics SD112-1), which produced a dc level proportional to the logarithm of signal magnitude. A phase meter (Acton Laboratories #329B) produced a dc output proportional to phase lag of tracking-filter output relative to oscillator voltage. The dc levels proportional to response magnitude and phase were measured and stored in digital form in a computer (PDP-8) as stimulus frequency was stepped from 20 Hz to 20 kHz. The data were plotted during the experiment and stored in digital form on magnetic computer tape. The digitized characteristics could subsequently be manipulated in the computer to form products and ratios of desired quantities.

In some experiments, it was of interest to observe the way several response quantities changed with time. In this case a constant stimulus frequency was selected and a relay which switched between acoustic and electric stimulus every 10 seconds could be included. The

variables of interest were plotted on a multi-channel ink-writing oscillograph (Brush Mark 200). Typically the variables plotted were a combination of:

- 1) Magnitude and angle of filtered probe-microphone response
 - 2) Stimulus current magnitude
 - 3) Magnitude of filtered round-window recording-electrode response
- and
- 4) Endocochlear potential.

The filtering of the probe-microphone output was performed by the tracking filter; filtering of the signal from the round-window recording electrode was performed by the narrow-band (3 Hz) filter of a conventional wave analyzer (Hewlett-Packard 302A) connected to the oscillograph.

In some experiments recording continued while asphyxia was established by clamping the tracheal cannula or while the animal was sacrificed by injection of 1 to 2 cc of anesthetic into or around the heart.

3.5 Characterization of Sinusoidal Signals.

This section describes the methods of specifying sinusoidal signals used in this study. Some elementary discussion is included for completeness and clarity.

A signal of the form

$$s(t) = \text{Re} \left\{ S(f) e^{j2\pi ft} \right\}$$

has usually been conveniently characterized in terms of its complex

amplitude S , a function of frequency. This complex amplitude has been expressed in terms of its magnitude $|S|$ and its angle in degrees $\angle S$, so that

$$S = |S| e^{j \frac{2\pi \angle S}{360}}$$

For quantities such as voltage, current, pressure, and velocity, magnitudes (levels) have been expressed in dB as

$$20 \log_{10} \left(\frac{|S|}{|S_{\text{ref}}|} \right)$$

where $|S_{\text{ref}}|$ is a reference level. Reference levels are usually given in terms of rms (effective) values

$$|S_{\text{ref}}|_{\text{rms}} = \frac{1}{\sqrt{2}} |S_{\text{ref}}|$$

Thus, for example, specification of a current magnitude ($|I|$) as -20 dB re 0.7 mA rms means that the current $i(t)$ had an rms value of 0.07 mA, or a peak value $|I|$ of 0.1 mA.

By convention, the level of a gated sinusoid, such as a stimulus tone burst, has been defined as the level attained by the sinusoid during the gated period. Thus the level of a tone burst is the same as the level of the corresponding pure tone.

Signal phases have been specified with respect to a reference signal such as a stimulus variable. In measurements of phase angles in the sinusoidal steady state, there is always an ambiguity of an

integral multiple of 360° . All phase data presented below have been plotted within an arbitrary 360° range. One consequence of this procedure is that data which would describe a smooth phase curve on a scale extending over several multiples of 360° contain discontinuities when plotted within 360° .

According to the above definition, a positive angle represents a lead, and a negative angle a lag. Note that according to the convention for plotting, $0^\circ = 360^\circ$, $+180^\circ = -180^\circ$, and $+90^\circ = -270^\circ$.

Products (and ratios) of complex amplitudes were formed by adding (subtracting) their magnitudes in dB and angles in degrees; resulting magnitudes are specified in dB referred to the product (ratio) of the constituent reference levels. For example, when a sound pressure at +20 dB re $0.0002 \text{ dynes/cm}^2 \text{ rms}$ and of a given phase is divided by a current at -10 dB re 0.7 mA rms lagging the pressure by 90° (-90° phase), the quotient magnitude is +30 dB re $\frac{0.0002 \text{ dynes/cm}^2}{0.7 \text{ mA}}$ and the quotient angle is $+90^\circ$. When ratios of two quantities measured in the same units are formed, the magnitude of the ratio is expressed in dB, with no reference specified.

EXPERIMENTAL

RESULTS

CHAPTER IV.

Auditory-Nerve-Fiber Responses to Electric Stimulation of the Cochlea

CHAPTER V.

Mechanical Responses of the Cochlea to Sinusoidal Acoustic and Electric Stimuli

CHAPTER IV.

AUDITORY-NERVE-FIBER RESPONSES TO
ELECTRIC STIMULATION OF THE COCHLEA

In the results presented in this chapter, the interaction of electric stimuli with the electrical and electromechanical systems of the cochlea and auditory nerve is described in terms of the response of auditory-nerve fibers. The first major division of the chapter is a description of the characteristics of response to simple electric-stimulus waveforms, including short rectangular pulses (shocks) and continuous and interrupted sinusoids. The second subdivision of the chapter describes experiments which bear on the problem of the origins of the observed responses.

4.1 Characteristics of Responses to Analogous Electric and Acoustic Stimulus Waveforms.4.1.1 Shock and click.

The background material of Chapter II (figure 2.4) showed an example of nerve-fiber response to shock. The fiber in the example exhibited several preferred firing times (several peaks in the PST histogram), including a prominent peak at short latency (≈ 0.5 msec) and other, smaller peaks which bore a resemblance to the click response of the fiber. The purpose of this section is to describe some further characteristics of patterns of nerve-fiber response to shocks.

Figure 4.1 shows an example of the way fiber response pattern depends on level of shock and click stimuli. For the lowest level of shocks shown [in (d)], response latency is about 1.5 msec, which is approximately the latency of response to clicks [(b), (c)]. [The click response shows a single peak, as is always the case for high- f_c fibers (Kiang, 1965).] For higher current levels, in (e) and (f), the histograms show an additional peak at short latency. The range of latencies of the spikes which constitute this peak in the histogram is only 160 μ sec, while the latencies of spikes which constitute response to clicks are distributed over a range of about 1 msec. In the histogram of (d), no short-latency spikes occur, but in (f), shocks of twice the amplitude (6 dB higher level) evoke short-latency response every time a shock is presented.

The spikes which occur at these two latencies evidently represent two separate response components since 1) they have different thresholds and 2) they depend on stimulus level in different ways. The two components of response to shock are distinguished primarily on the basis of latency. For identification purposes, the component of response to shock which occurs at a latency of about 0.5 msec will be designated the α -component, and the remaining response will be designated the β -component [see histogram (f)].

The 1.5 msec click latency of the fiber shown in the figure is representative of the shortest latency found in auditory-nerve fibers

Figure 4.1

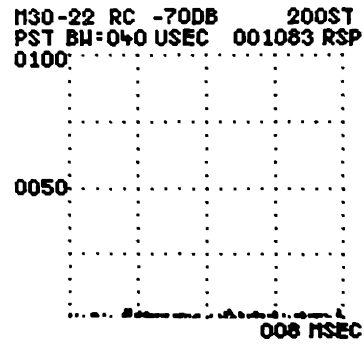
PST histograms of fiber response to clicks and shocks at three levels.

In (a), (b), and (c), histograms of response to three amplitudes of rarefaction click. Click level expressed as dB re 100 V peak into 1-inch condenser earphone. In (d), (e), and (f) response patterns are shown for three levels of shock, along with examples of spike voltage waveform. [Photographs of superimposed responses, two in (d), three in (e) and (f).] Positive voltage plotted as a downward deflection; 3-dB recording bandwidth 80 Hz-1 kHz. In (f), α and β denote response components. Negative current polarity indicates negativity of round-window electrode. Shocks and clicks at 10/sec, 100 μ sec duration. Each histogram computed from response to 200 identical stimuli. Note the difference in stimulus increments for clicks and shocks. Fiber 30-22, $f_c = 9.1$ kHz, tone threshold = 3 dB SPL, spontaneous discharge rate = 42/sec.

UNIT 30-22

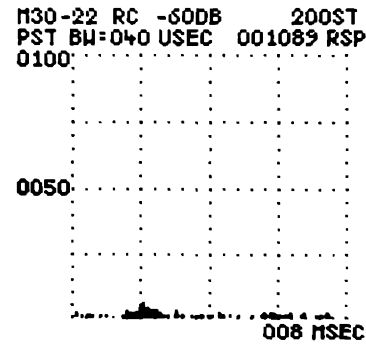
$f_c = 9.1 \text{ kHz}$

ACOUSTIC
CLICKS



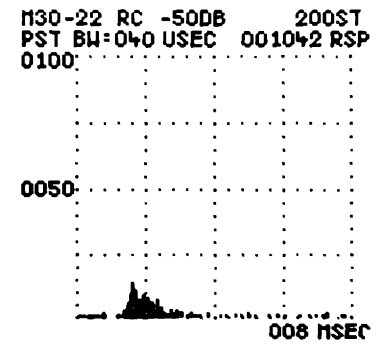
-70 dB

(a)



-60 dB

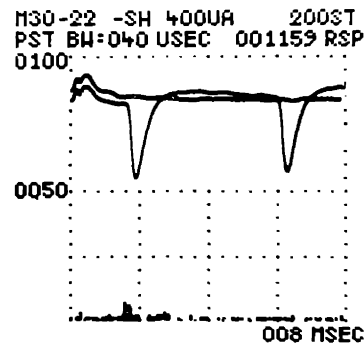
(b)



-50 dB

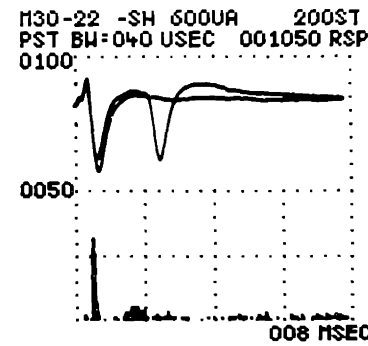
(c)

ELECTRIC
SHOCKS



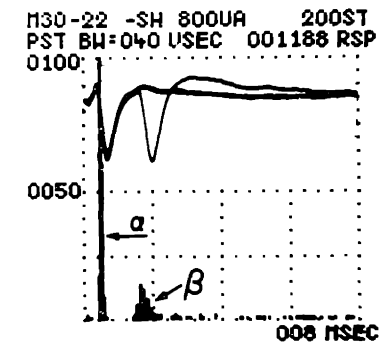
-400 μA

(d)



-600 μA

(e)



-800 μA

(f)

(Kiang, 1965); the figure shows that the click-response latency and β -component latency are about the same. The 0.5 msec α -component latency shown is typical of the shock response of all auditory-nerve fibers. This α -latency is much shorter than the latency of the click response in any fiber.

When fibers of low characteristic frequency were electrically stimulated, other similarities were found between click response and the β -components of shock response. The click responses of low- f_c (< 5 kHz) fibers show several preferred times of firing (several peaks in a PST histogram) which are spaced by about $1/f_c$ (Kiang, 1965). For clicks of equal amplitude but opposite polarity, the preferred firing times are displaced by about $\frac{1}{2} \frac{1}{f_c}$, and the peaks of PST histograms for opposite polarity are interleaved.

The β -component of response to opposite polarities of shock showed similar characteristics. An example is shown in figure 4.2. At the shock level shown, the response showed only a β -component. The peaks of the response to negative shocks in the histogram in (b) occur between the peaks of the response to positive shocks in the histogram in (a).

For comparison, the response of the fiber to a moderate-amplitude rarefaction click is shown in (c). The click response and the two shock responses, which are entirely β -component, show inter-peak intervals of about 0.6 msec, or approximately $1/f_c$. This relationship

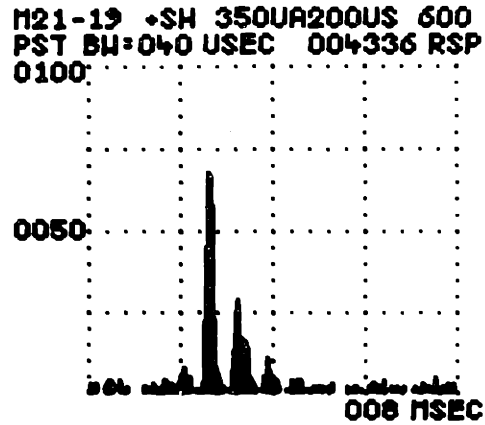
Figure 4.2

PST histograms of fiber response to shocks of opposite polarity.

In (a) and (b), response to 200 μ sec, 350 μ A shocks; in (a), round window positive, in (b) round window negative. In (c), response to rarefaction click. Clicks 100 μ sec, -65 dB re 100 V peak into 1-inch earphone. Clicks and shocks at 10/sec. Each histogram computed from response to 600 identical stimuli. Fiber 21-19, $f_c = 1.6$ kHz, tone threshold = 5 dB SPL.

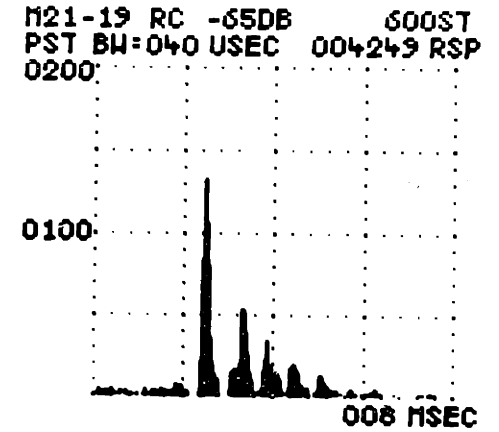
UNIT 21-19

+
SHOCK



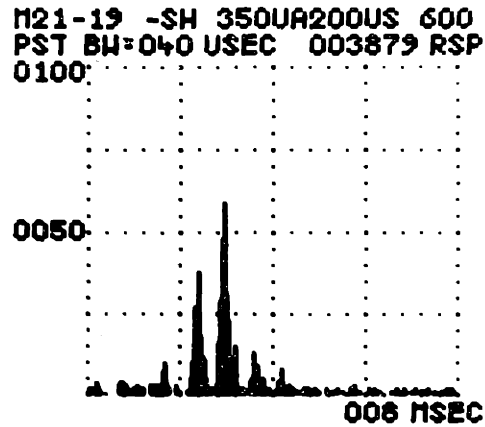
(a)

RAREFACTION
CLICK



(c)

-
SHOCK



(b)

$$f_c = 1.6 \text{ kHz}$$

which is a property of click response is also a property of the β -component of response to shock.

In many fibers, the β -component of shock response was not observed, possibly because threshold for producing detectable β -component in these fibers was too high. It was observed that fibers in which the β -component was detected were those which also showed the lowest thresholds for acoustic stimuli. It should be noted that the data shown in figures 4.1 and 4.2 were obtained from such fibers, and therefore these results represent examples of possible rather than typical response. In most fibers, the α -component showed the lower threshold, and even the highest shock amplitudes employed (2 to 3 mA) produced no discernible β -pattern.*

The α -component of shock response was found in all fibers. The plot of figure 4.3 shows α -component threshold for fibers of different characteristic frequency. These data show no systematic trend in threshold as a function of f_c . At a given frequency, different fibers in the same animal exhibit threshold differences as large as the differences observed across the range of f_c .

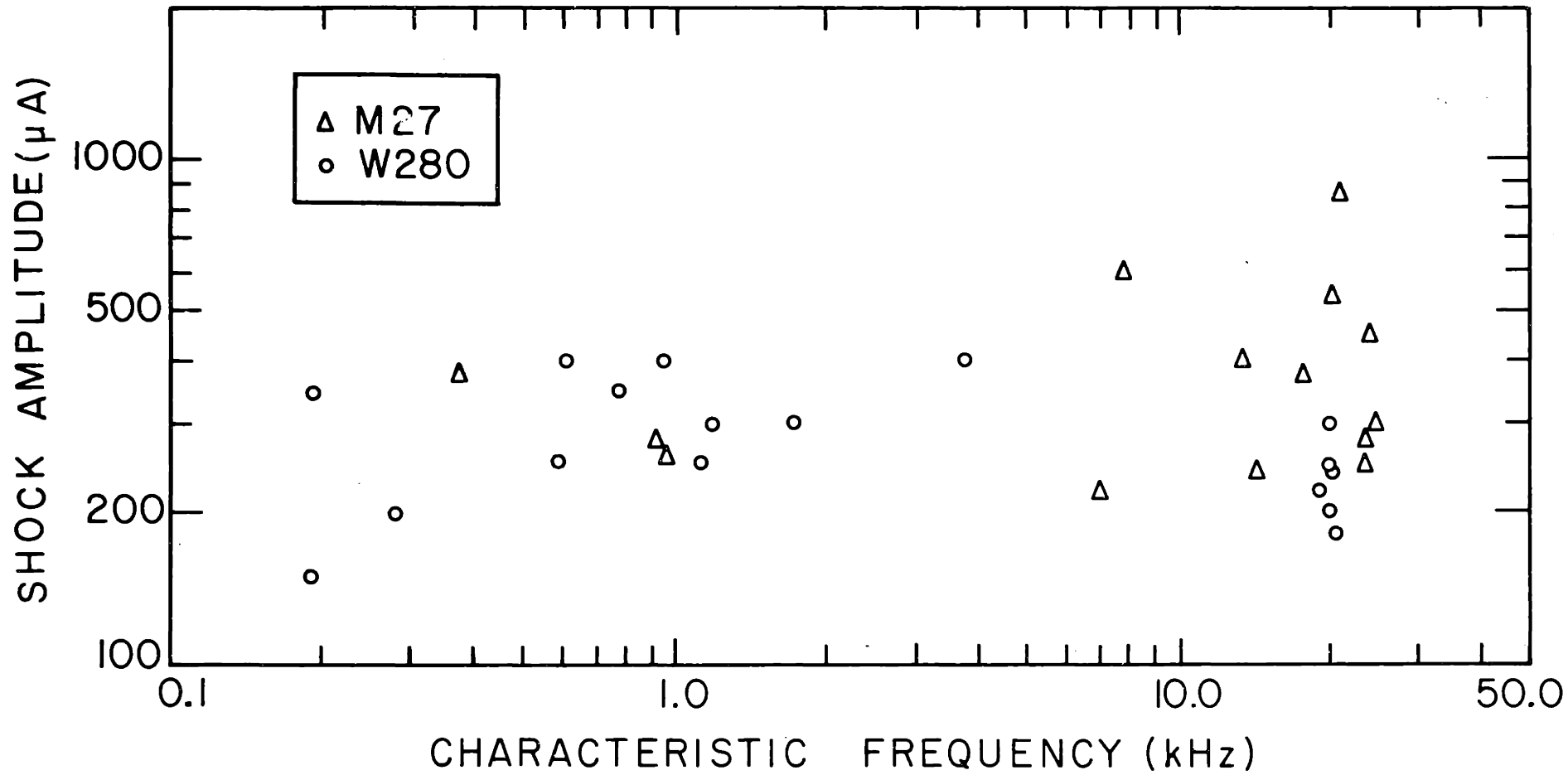
The data indicate that the α -component of response is about the same for all auditory-nerve fibers. On the other hand, the time pat-

* This upper limit on acceptable current amplitude was dictated by non-auditory responses of the preparation to the electric stimulus (see Appendix III).

Figure 4.3

Threshold for α -component of response to shock plotted against f_c for 19 fibers from 2 cats.

Threshold was defined as amplitude of electrode current which produced short-latency (α -component) response for approximately half the stimuli as judged from the oscilloscope display of the spikes. Shock duration, 100 μ sec, round window electrode negative.



terns of β -component are different in different fibers, and the similarities of β -component and responses to clicks indicate that production of β -component shares at least some of the frequency-selective processing stages of the cochlea which influence the response to acoustic stimuli.

4.1.2 Bursts of sinusoidal current and tone.

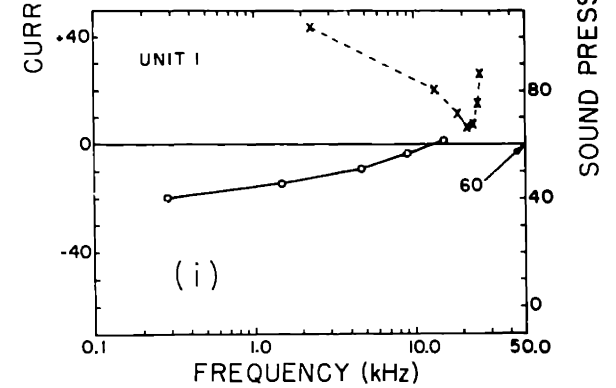
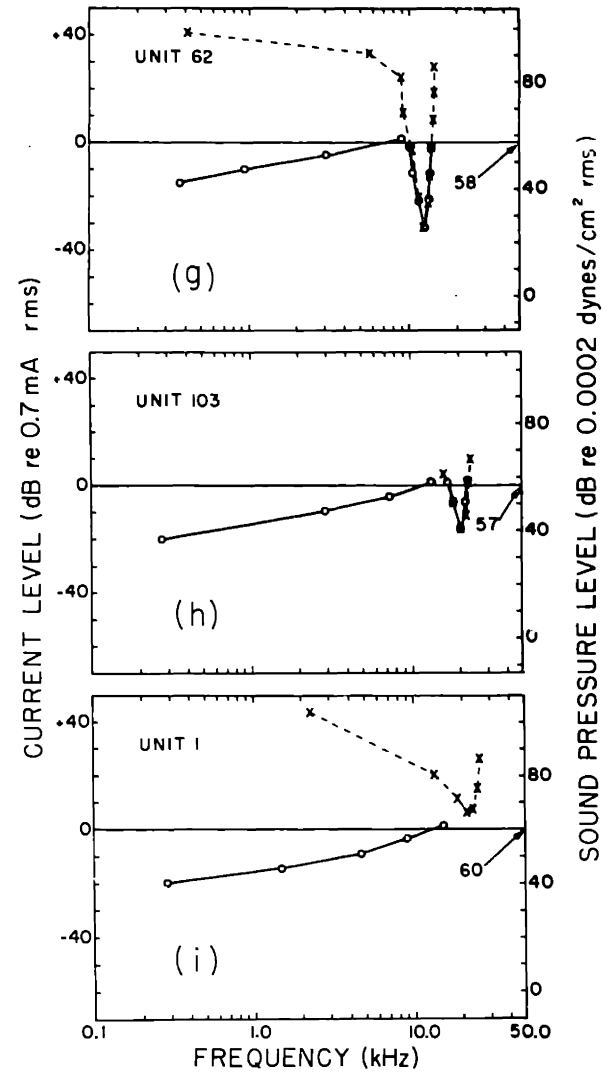
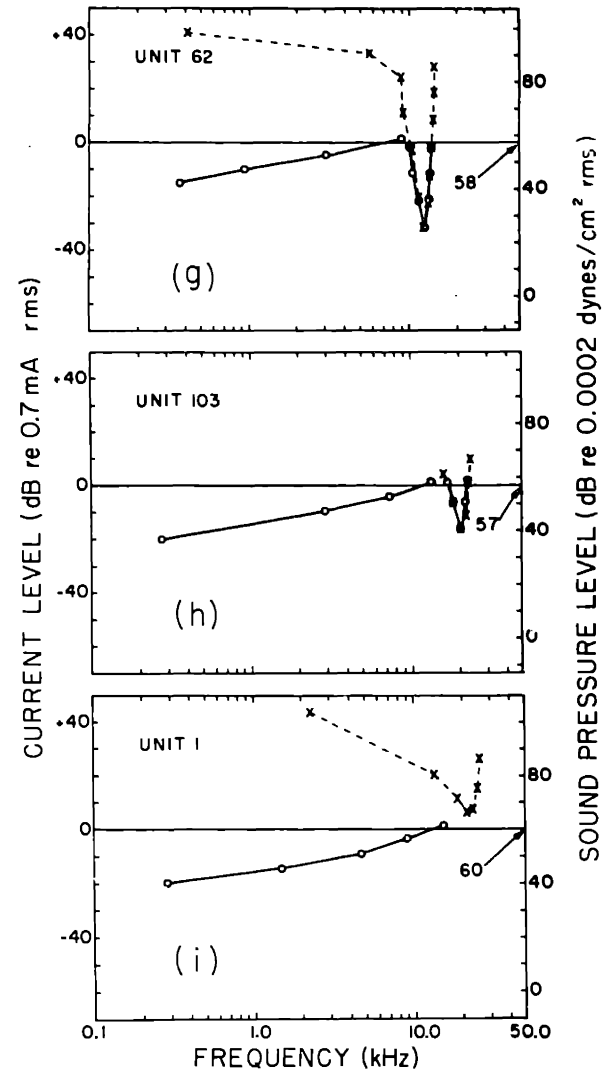
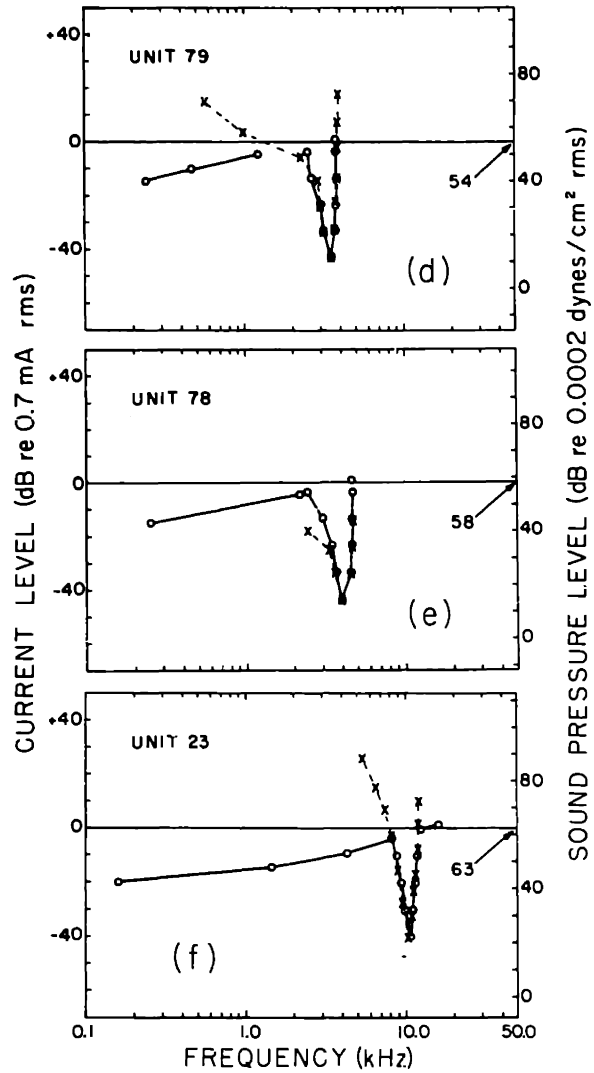
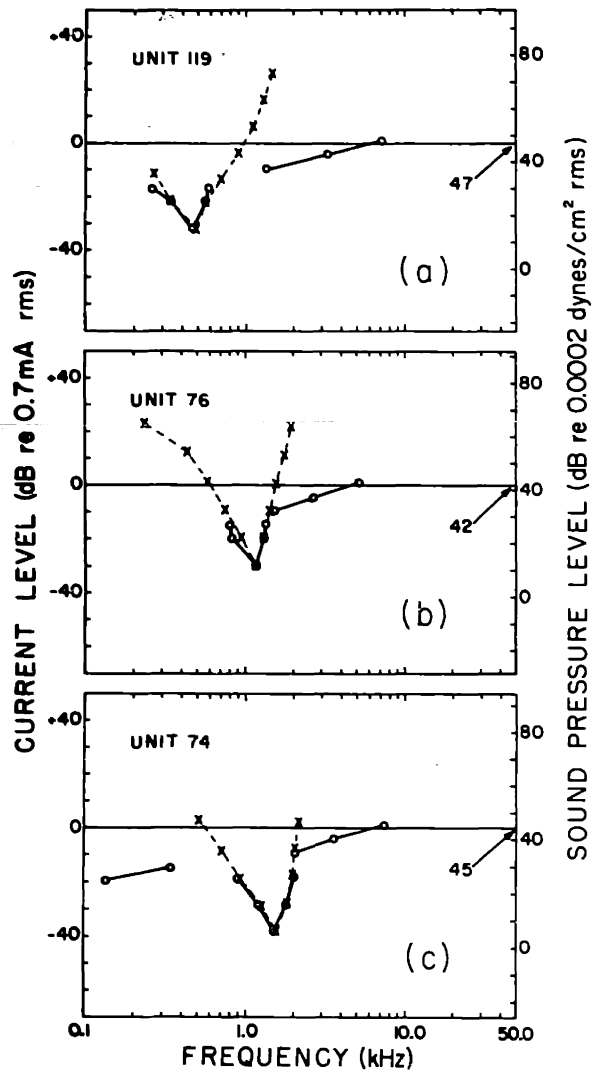
An important characteristic of auditory-nerve fiber response to tone is the unique frequency selectivity which each fiber exhibits. This frequency-selective behavior is represented in the tuning curve, a plot of response threshold as a function of frequency.

Auditory-nerve-fiber response to bursts of sinusoidal electric current was also a function of frequency and level, and tuning curves for electric stimuli could be obtained using the same procedures used to determine tuning curves for tones [Method I described by Kiang (1965, p. 86)]. Examples of nerve-fiber tuning curves for both electric and acoustic stimuli are shown in figure 4.4. The tuning curves for tone have a minimum at the characteristic frequency, f_c , and rise more sharply on the high-frequency side of f_c than the low-frequency side. For each of eight of the fibers represented, the electric tuning curve contains a V-shaped segment which is similar to a segment of the acoustic tuning curve; the similarity has been emphasized by shifting the vertical position of the two curves so that the V-shaped segments

Figure 4.4

Tuning curves for sinusoidal electric and acoustic stimuli for 9 fibers from one cat.

For both stimulus types, stimulus waveform was a 30 msec burst of sinusoid, rise-fall time 2.5 msec, presented at 10/sec. Data points were obtained by setting a level of stimulus on an attenuator and varying oscillator frequency until a "threshold" response was detected using audio-visual cues. For all but one fiber shown, a region of frequency exists for which both acoustic and electric curves show similar V-shape. V-shaped segments of curves have been superimposed by aligning scales so that minima in the two curves for each fiber coincide vertically. Numbers at the right of each set of curves indicate the intercept of the current reference level (0.7 mA) with the sound-pressure axis. The fiber in (i) shows no V-shaped segment in the electric tuning curve; in this case the vertical axes have been aligned by equating the current reference level to 60 dB on the sound pressure axis, since other fibers of $f_c > 4$ kHz show intercepts of 58 to 63 dB. Two segments of electric tuning curves can intersect to form a sharp corner, as in (f). For curves in which a data point did not describe the intersection, the sharp corner was not described; consequently no line has been drawn to connect the V-shaped segment with the other curve segment(s).



M 38

x---x TONE

o---o CURRENT

superimpose. The frequency at the minimum of the V-shaped segment of the electric tuning curve is a characteristic of response to current and will be designated the electric characteristic frequency, f_{ce} . Evidently because threshold was not explored at sufficiently high current levels, the fiber represented in (i) shows no V-shaped electric tuning-curve segment, and consequently no f_{ce} . For all the fibers, the segment(s) of the electric curves which depart from the V-shape show a threshold which rises with increasing frequency with a slope of 10 to 20 dB per decade. For identification purposes, the V-shaped segment of an electric tuning curve which resembles a portion of the acoustic tuning curve for that fiber will be designated S_I, and the remaining segment(s) of the electric tuning curve will be designated S_{II}.

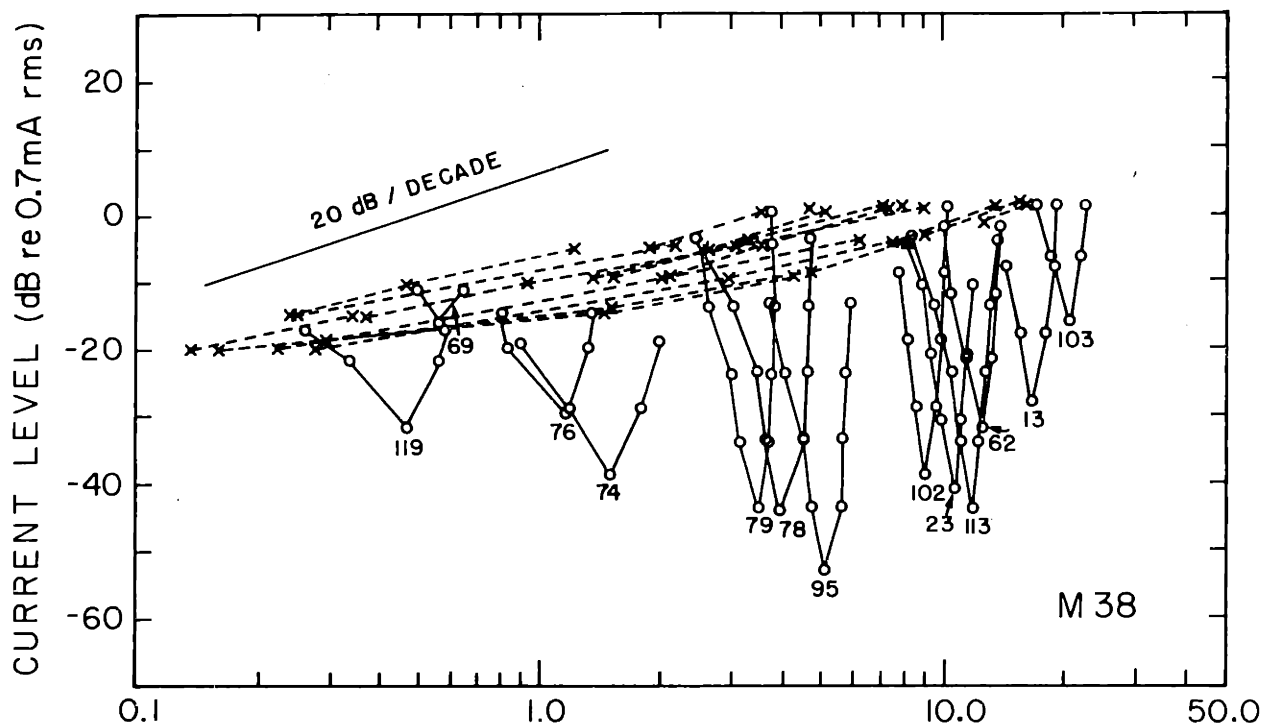
Figure 4.5 shows superimposed plots of electric tuning curves. On the basis of shape, segments of each curve have been identified and are represented by different symbols. The figure shows that the S_{II} portions fall fairly close to one another, both for different fibers within a cat and for fibers in different cats, even though the S_I portions (and the acoustic tuning curves) for these fibers are markedly different. The figure shows that the frequency dependence of S_{II} is nearly the same for all auditory-nerve fibers, and at any one frequency the absolute levels of S_{II} vary by at most 15 dB.

For sinusoidal electric stimuli at levels above the threshold indicated by their respective tuning curves, fibers responded with a dis-

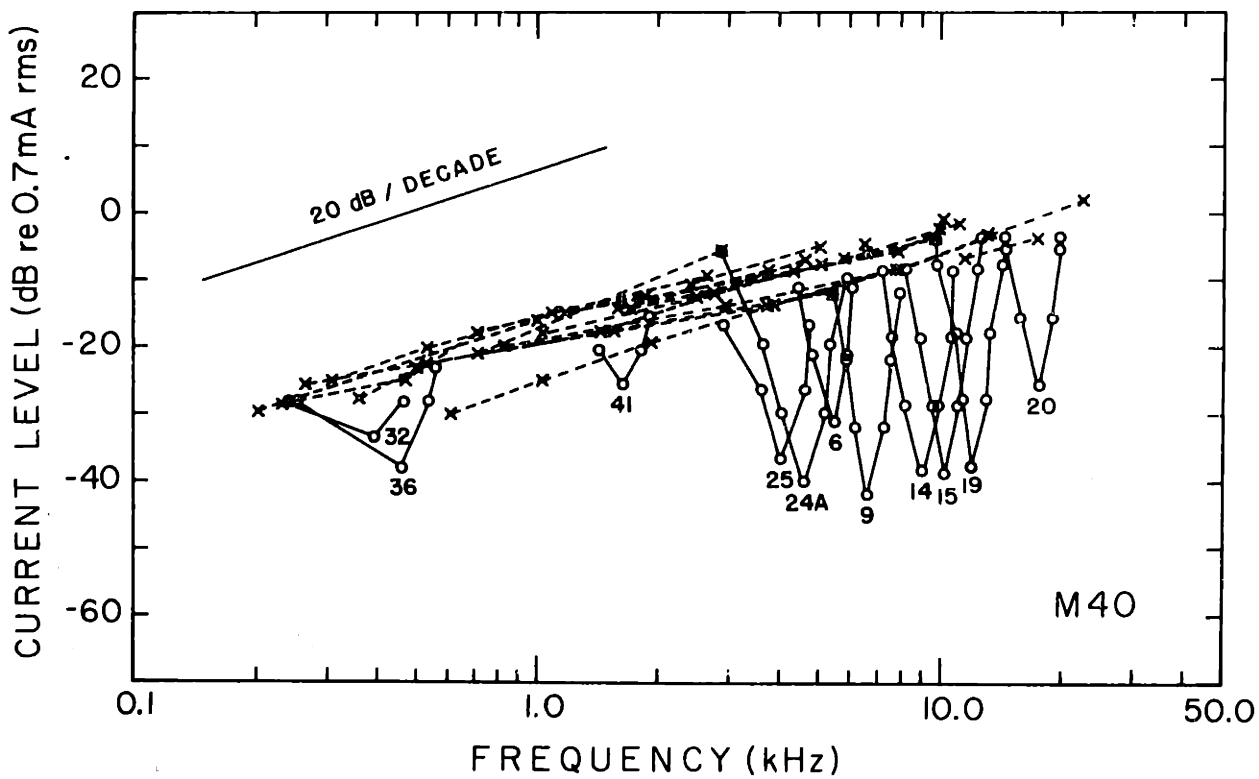
Figure 4.5

Composite plots of tuning curves for electric stimuli
for two cats.

In (a), electric tuning curves of figure 4.4 are replotted along with 4 additional curves from the same cat. In (b), 13 electric tuning curves from another cat are shown. Tuning-curve segments have been distinguished on the basis of shape. For each curve, V-shaped segment (S_I) is shown by circles and solid lines. Remaining curve segment(s) (S_{II}) are shown by crosses and dashed lines. In (b), curves for two fibers ($f_c = 24.1$ kHz and $f_c = 0.12$ kHz) have no S_I segment. A line of slope 20 dB/decade is shown for comparison with S_{II} segments. Numbers associated with each S_I segment are fiber serial numbers.



(a)



(b)

charge rate which was greater than the rate of spontaneous activity. However, the detailed characteristics of the response were different at different points in fiber response areas. In particular, the two types of tuning-curve segment distinguished on the basis of shape in figure 4.5 define the threshold boundary of two distinct regions of the response area of each fiber. These regions are associated with two distinct classes of response which can be distinguished on the basis of characteristics of discharge. These two response classes will be designated Class I and Class II responses. The remainder of this section and the following section are concerned with description of the characteristics which distinguish Class I and Class II responses.

An example of Class I response of a fiber to 30 msec bursts of both electric and acoustic stimuli is shown in figure 4.6. Both histograms show that, on the average, the fiber discharges throughout the presentation of the burst, showing a large number of initial discharges, corresponding to the onset of the stimulus. Both also show a reduced number of discharges occurring immediately after the cessation of the burst. These characteristics are typical of the response of auditory-nerve fibers to tone bursts (Kiang, 1965); the histograms show that the Class I response to the electric stimulus and the response to tone exhibit the same time patterns of discharge.

Figure 4.7 shows the way responses of this fiber depend on frequency and level of current in the two regions of the response area and

Figure 4.6

Histograms of fiber response to bursts of sinusoidal acoustic and electric stimuli (tone bursts and current bursts).

Each PST and interspike-interval histogram computed from responses to 100 identical stimuli. Stimuli in (a), bursts of tone at the frequency of maximum tone sensitivity (10.23 kHz); stimuli in (b), bursts of current at the frequency of maximum current sensitivity (10.33 kHz). Level of each stimulus was 20 dB above threshold. PST histograms are synchronized with the pulse to the electronic switch which formed the bursts, time reference approximately 2.5 msec before onset of bursts. Bursts at 10/sec, rise-fall time 2.5 msec, duration 30 msec. (Envelope of voltage waveform applied to earphone and electrode systems is shown below PST histograms.) Inset in each PST histogram is a photograph of the voltage waveform of spikes occurring during a single stimulus presentation. Downward deflection represents positive voltage at the recording electrode; 3-dB recording bandwidth 800 Hz - 2 kHz. Peak spike amplitude in (a) approximately 1 mV, in (b) approximately 3 mV. Gradual changes in recorded spike amplitude generally occur but do not affect the temporal pattern of discharge [see Kiang (1965)]. Fiber 44-71, spontaneous discharge rate approximately 50/sec.

UNIT 44-71

PST HISTOGRAMS

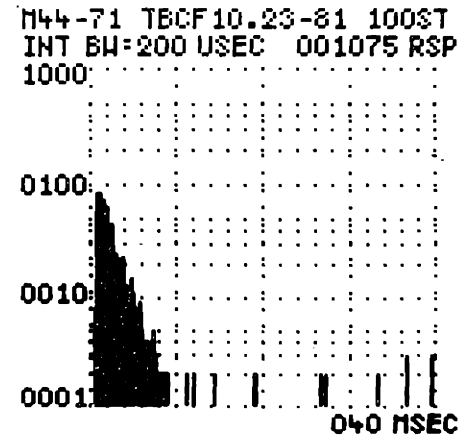
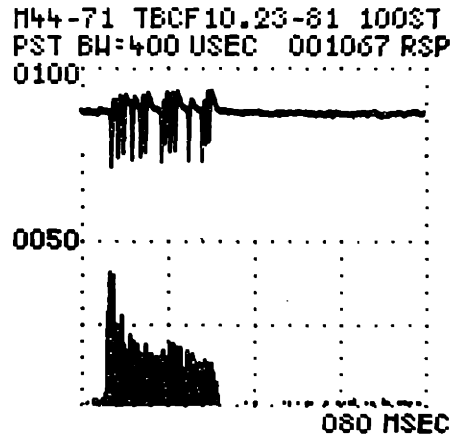
INTERVAL HISTOGRAMS

TONE BURSTS

(33 dB re 0.0002 dynes/cm² rms)

10.23 kHz (f_c)

(a)

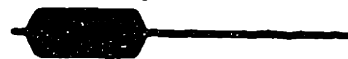
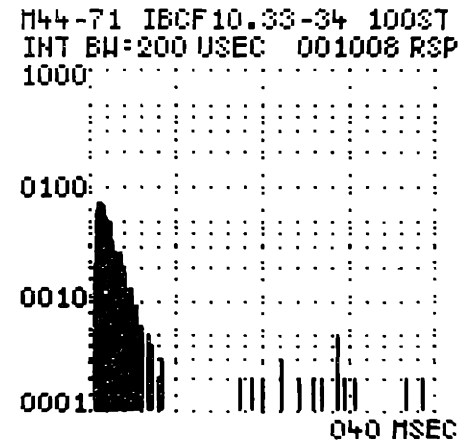
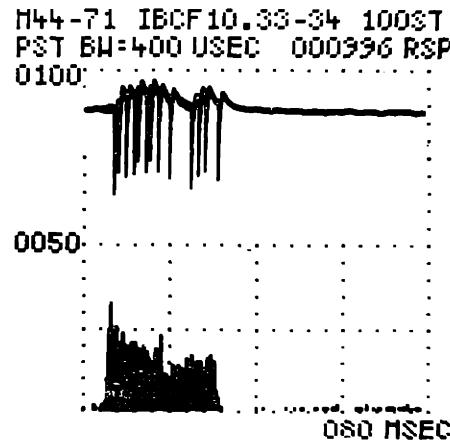


CURRENT BURSTS

(-34 dB re 0.7 mA rms)

10.33 kHz (f_{ce})

(b)



illustrates the differences between Class I and Class II responses. For comparison, responses to the analogous tone bursts are also shown. For the 10 kHz electric and acoustic stimuli [histograms in (a) and (b)] the histograms show that patterns of response are similar at three levels shown. The histograms in (b) depict Class I response; both the time pattern of discharge and the dependence of pattern on level are similar to the response to the analogous acoustic stimuli.

At 7 kHz, the electric stimuli evoke Class II response [histograms in (d)]. Comparison with the response to 7 kHz tone bursts [(c)] shows distinct differences in the Class II discharge pattern and the pattern evoked by acoustic stimuli. It is evident in the histograms of (d) that the 1 dB increments of electric stimulus produce an increase in the number of responses comparable to that produced by the 10 dB steps of acoustic stimulus [histograms of (a) and (c)]. Such rapid change of response pattern with stimulus level is never found with acoustic stimuli and is a characteristic of Class II response to electric stimuli.

At the highest 7 kHz current level shown [bottom histogram in (d)], distinct peaks are visible in the PST histogram, but there are no corresponding peaks in the histograms of tone response in (c). Multiple peaks have not been described in auditory-nerve-fiber response patterns for tone at frequencies as high as 7 kHz. Although discernible peaks do occur in PST histograms for fibers driven with low-frequency

Figure 4.7

Histograms of response to tone bursts and of Class I and Class II response to bursts of sinusoidal current.

Data are from the same fiber represented in figure 4.6. At each frequency, response was recorded at three levels for each stimulus type. At each stimulus level, PST and inter-spike interval histograms were computed. Stimuli in (a), tone at 10.23 kHz (f_c), and in (b), current at 10.33 kHz (f_{ce}). Tone in (c) and current in (d) at 7 kHz. Note stimulus level increments in (d) are 1 dB; other increments, 10 dB. Each histogram computed from response to 100 stimulus presentations. Bursts at 10/sec, 30 msec duration.

UNIT 44-71

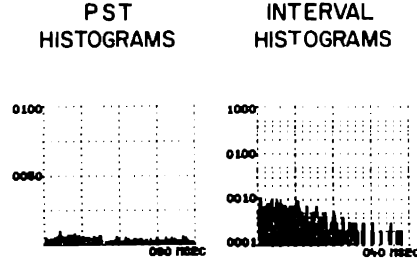
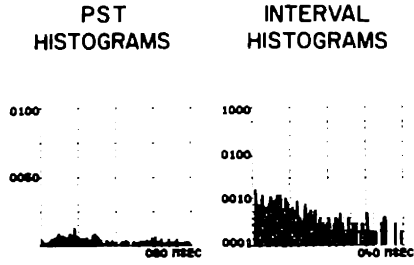
TONE BURSTS

CURRENT BURSTS

dB re 0.0002
dynes/cm² rms

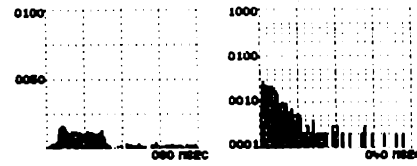
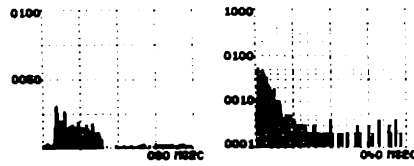
dB re
0.7 mA rms

13



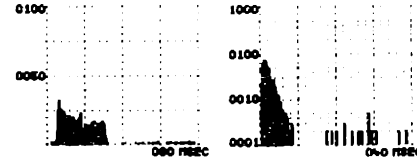
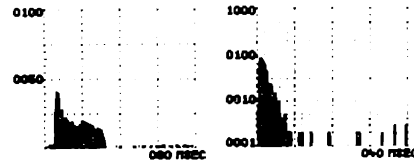
- 54

23



- 44

33



- 34

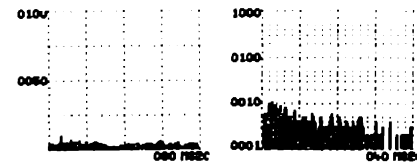
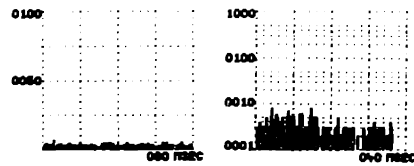
10.23 kHz (f_c)

10.33 kHz (f_{ce})

(a)

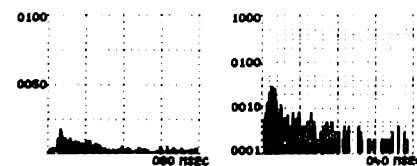
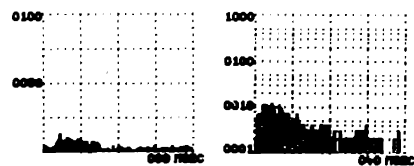
(b)

59



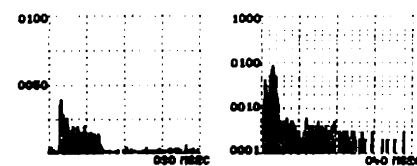
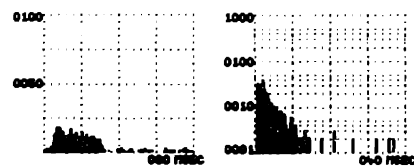
- 5

69



- 4

79



- 3

7 kHz

7 kHz

(c)

(d)

(< 5 kHz) tone, the pattern is due to synchrony of spikes with individual cycles of the tone, and the spacing of peaks is equal to the period of the stimulus. The spacings of the peaks of the Class II response pattern visible in the figure are between 2 and 5 msec, while the period of the stimulus is about 140 μ sec. The corresponding inter-spike interval histogram shows a bimodal interval distribution. The peaks in the histogram show a large number of intervals of from 2 to 4 msec, and a smaller number of intervals of about 1 msec. The fiber shows repetitive, quasi-periodic firing in response to the stimulus current, and the intervals are not simply related to the stimulus. Repetitive, quasi-periodic firing is a property of Class II response of all fibers and occurs for bursts of electric stimuli whose frequency is greater than a few kHz and whose level is a few dB above the S_{II} portion of the threshold curve.

The data of this section have illustrated typical characteristics of auditory-nerve-fiber response to short bursts of sinusoidal electric stimuli. Class I response resembles response to tone bursts in the following characteristics:

- 1) temporal distribution of discharges (indicated by PST and interval histograms)
 - 2) dependence of temporal distribution and number of discharges on stimulus level
- and
- 3) frequency-dependence of threshold (tuning curve).

Class II response is distinguished by:

- 1) repetitive, quasi-periodic firing during bursts of

- high-frequency current, with preferred intervals which do not correspond to the stimulus period
- 2) rapid change of temporal distribution and number of discharges with current level
- and
- 3) threshold that is a gradual function of frequency and is similar in all auditory-nerve fibers.

Class II response characteristics are not duplicated in response to analogous tone bursts.

4.1.3 Maintained sinusoidal current and tone.

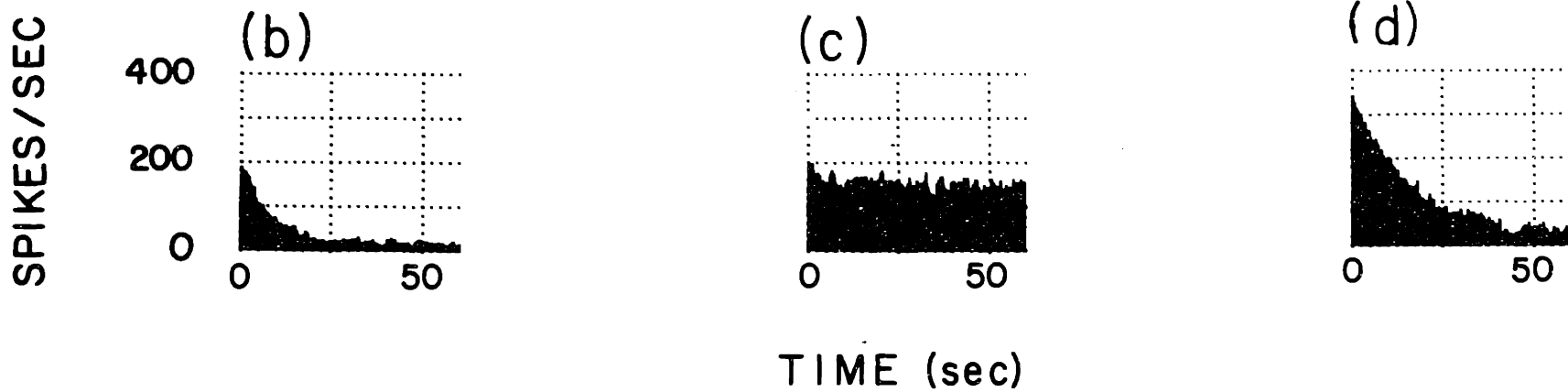
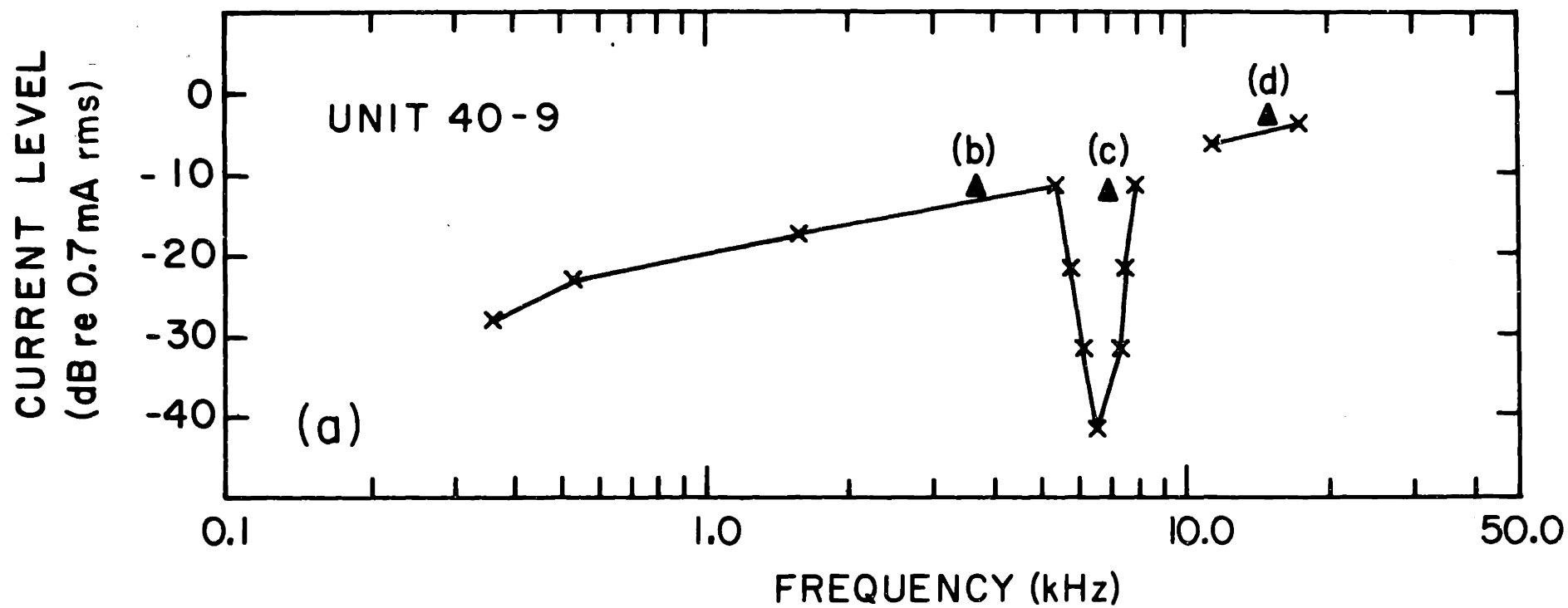
Further distinctions between Class I and II nerve-fiber responses were observed when the cochlea was stimulated with maintained sinusoidal currents (bursts of one-minute duration). An example is shown in figure 4.8. Part (a) of the figure shows the tuning curve of a fiber determined in the usual way using 30-msec bursts of sinusoidal current to determine threshold, and points b, c, and d in the response area indicate the frequency and level of three stimulus sinusoids. The histograms in (b), (c), and (d) show fiber discharge rate as a function of time during a one-minute presentation of each corresponding stimulus.

The histograms in (b) and (d) were computed from the responses to stimuli which fall just above the S_{II} portion of the tuning curve and illustrate Class II response. Discharge rate is high immediately after the stimulus is applied and declines over tens of seconds to a final rate much lower than the initial value. The stimuli which evoke the

Figure 4.8

Time course of Class I and Class II discharge rate in response to maintained sinusoidal electric current.

In (a), tuning curve of the fiber determined using bursts of sinusoidal current according to the standard procedure. In (b), (c), and (d), histograms of discharge rate plotted after the onset of 1-minute presentations of sinusoidal current. Triangles in (a) show location of stimuli in (b), (c), and (d). In (b) and (d) stimuli are a few dB above S_{II} threshold. Response in (b) and (d), Class II; in (c), Class I. Fiber 40-9, $f_c = 6.4$ kHz, spontaneous discharge rate approximately 8/sec.



high initial rate are only a few dB above threshold.* Histogram (c) shows the discharge rate evoked by the stimulus which falls within the V-shaped portion of the tuning curve and represents Class I response. The rate shows a slight decline during the first few seconds, but then shows little systematic change during the remainder of the one-minute stimulus presentation. The time course of Class I discharge rate is similar to the response to continuous tone (Kiang, 1965).

The photographs of figure 4.9 show samples of the spike trains whose rates were plotted in figure 4.8. In the photographs of (a) and (c), the change in Class II discharge rate is apparent. In both cases the later records contain many fewer spikes per unit time than the first. In (b), the Class I spike train appears unchanged throughout the one-minute sample period. The upper photograph in (a) and (c) shows the appearance of spikes during the initial period of rapid Class II discharge, and the inter-spike intervals appear to be more regular than those in (b), showing fewer very short (< 2 or 3 msec) or very long (> 10 msec) intervals. The quasi-periodic firing pattern is only evident when discharge rate is high, immediately after the onset of the current. At the lower rates attained later in the stimulus

* The decay of rate from an initial high value to a low maintained value should not be confused with the transient component of response to short burst stimuli described earlier. The latter changes over tens of msec, while the change of rate in histograms (b) and (d) occurs over tens of seconds.

Figure 4.9

Photographs of the discharges from which data of figure 4.8 were computed.

Photographs represent 200 msec of discharge sampled at 15 second intervals during each 1-minute stimulus presentation. In (a) and (c), Class II response; in (b) Class I response. Positive voltage represented by a downward deflection; 3-dB recording bandwidth 800 Hz-1 kHz. Broadening of baseline in (a) due to incomplete suppression of the 3.65 kHz stimulus waveform recorded by the microelectrode.

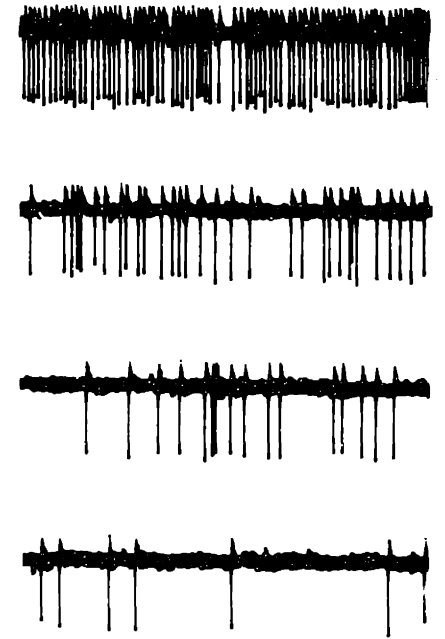
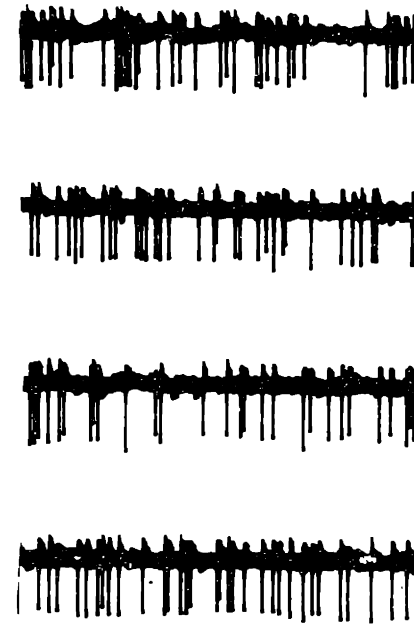
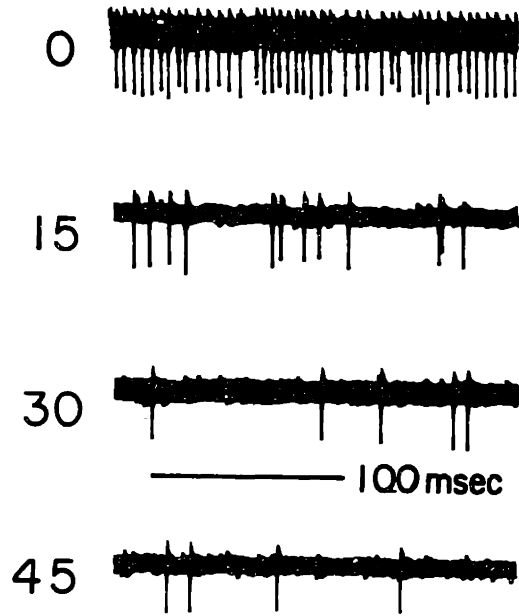
UNIT 40-9

FREQUENCY → 3.65 kHz
LEVEL → -13 dB
(re 0.7 mA rms)

6.91 kHz
-13 dB

15.06 kHz
-3 dB

TIME AFTER ONSET
OF CURRENT (seconds)



presentation [lower photographs in (a) and (c)], firing is no longer so clearly regular.

The change of firing rate (figure 4.8) and the initial quasi-periodic firing pattern (figure 4.9) are both characteristics of Class II response to maintained high-frequency sinusoidal current just above S_{II} threshold. These characteristics further distinguish Class I from Class II response.

At low stimulus frequencies, nerve-fiber response to tone characteristically shows discharges synchronized with cycles of the stimulus. Figure 4.10 shows the response patterns of a low- f_c fiber for low-frequency sinusoidal current. The two lower levels of electric stimulus [in (d) and (e)] produce Class I response; the PST and interval histograms show discharges synchronized with the stimulus sinusoid and are similar to the histograms of response to tone, shown in (a) and (b). However, an increase of current level of only 2 dB changes the pattern significantly [histograms of (f)]. Prominent, narrow peaks not present at lower levels are seen in the PST histogram; the corresponding interval histogram shows a large peak at about 3 msec, indicating spikes occurring on consecutive cycles of the current. Because the time pattern represented by the sharp peaks in the histograms of (f) is not similar to that evoked by tone, this response is classified as Class II response. The large number of additional responses evoked by the additional 2 dB of current level is a

Figure 4.10

Histograms of response pattern of a low- f_c fiber to three levels of tone and sinusoidal current.

Zero time in PST histograms is derived from positive zero crossing of the voltage applied to the earphone or stimulating electrodes. These histograms show the temporal distribution of fiber discharge within two cycles of the stimulus waveform. For reference, stimulus waveform is shown below each column of PST histograms. Interval histograms computed from the same data are shown to the right of each PST histogram. Histograms in (a), (b), and (c) computed from response to tone, and in (d), (e), and (f) from response to sinusoidal current. At each level, stimulus was continuous throughout the 20-second presentation period. In (c) and (f), additional interval histograms computed at higher resolution show distribution of shorter intervals more clearly. The stimulus level increment between (e) and (f) is 2 dB; other level increments = 5 dB. Fiber 40-35, $f_c = 340$ Hz.

UNIT 40 - 35

$f_{ce} = 0.352 \text{ kHz}$

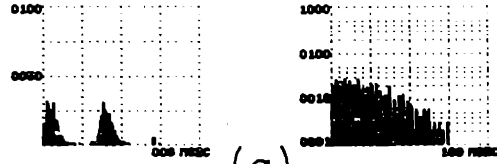
SOUND PRESSURE LEVEL AT TYMPANIC MEMBRANE
(dB re 0.0002 dynes/cm² rms)

29

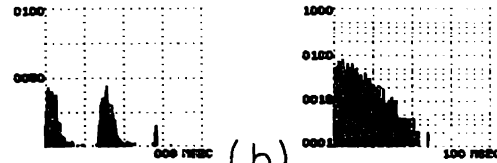
34

39

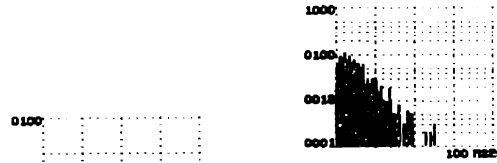
CONTINUOUS TONE
PST INTERVAL



(a)



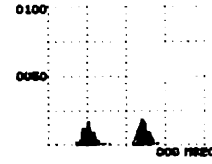
(b)



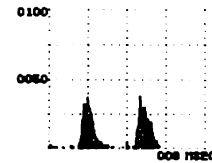
(c)



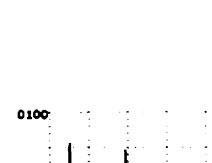
CONTINUOUS SINUSOIDAL CURRENT
PST INTERVAL



(d)



(e)



(f)



-26

-21

-19

CURRENT LEVEL (dB re 0.7 mA rms)

parallel of the Class II response behavior shown for burst stimuli in figure 4.7 (d).

In figure 4.11, examples of electric and acoustic intensity functions show explicitly the relationship between number of discharges (discharge rate) and stimulus level. For three fibers [in (d), (e), and (f)], the electric intensity function is similar to the acoustic intensity function over a 30 to 40 dB range of level. For the others, the electric curve departs from the contour described by the acoustic curve, rising to high rates for increases of only a few dB. For the two fibers with lowest f_c [in (a) and (b)], the curves rise abruptly just above threshold. In (c), the electric curve resembles the acoustic curve at low levels, but departs dramatically from it with a sharp rise at about 15 dB above threshold. *

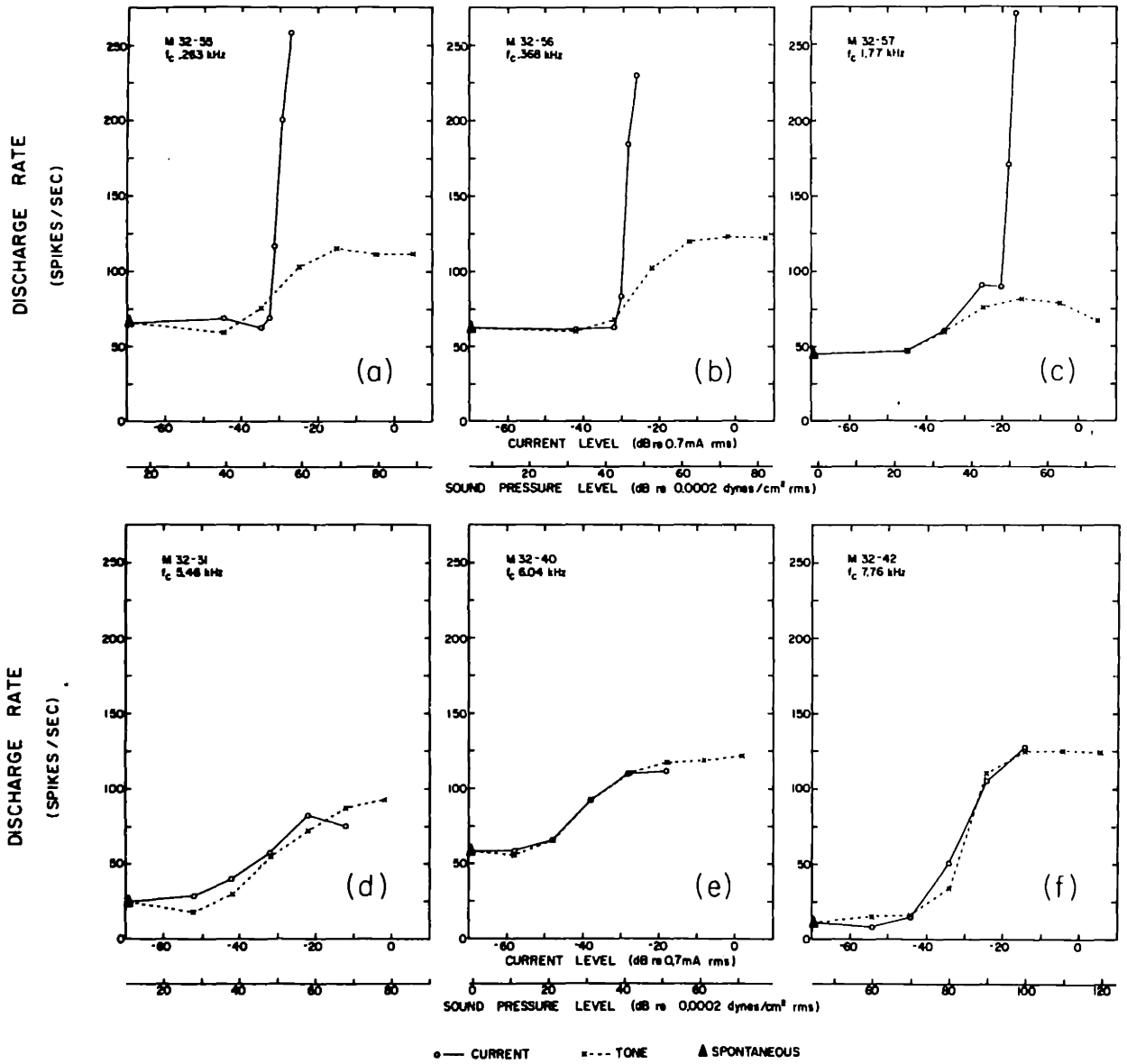
The range of level over which electric intensity functions are similar to acoustic intensity functions is at least 30 dB at high frequency [in (d), (e), and (f)], but is essentially non-existent at low frequency [in (a) and (b)]. As a function of frequency, this range corresponds approximately to the range between threshold at f_{ce} and the S_{II} threshold curves shown in figure 4.5.

* Note that the average rates plotted were formed by counting spikes over 20-second periods of continuous stimulation. At levels where the electric curves depart from the acoustic curves, the average rates may be appreciably less than the maximum instantaneous rates (see figure 4.8).

Figure 4.11

Discharge rate plotted against level of acoustic and electric stimuli.

Data for 6 fibers from one cat are represented. Each point was obtained by counting the number of spikes occurring during a 20-second presentation of sinusoidal stimulus. Horizontal stimulus-level scales were aligned for each fiber by equating the levels of tone and current at subjectively-determined threshold. Lowest stimulus level in each curve is 10 dB below threshold. For each fiber stimulus frequency was f_c .



Figures 4.10 and 4.11 show that the range of level for which Class I response at f_{ce} resembles response to tone is limited. As current is raised to a sufficiently high level, the response takes on characteristics which are not similar to the response to tone, that is, Class II response. The transition occurs at current levels which are within the range of the S_{II} thresholds of other fibers (figure 4.5).*

Thus the S_{II} curves of figure 4.5 divide the current-level current-frequency plane into two halves. In the lower half-plane, auditory-nerve fibers exhibit Class I response, which resembles the response to tone in both tuning and discharge characteristics. In the upper half-plane, all fibers show the distinctive Class II response, which is distinctly different from response to tone. The data show that at a given frequency the exact level at which this division occurs can vary by 15 dB among different fibers.

4.1.4 Simultaneous bursts of sinusoidal current and tone.

Because the responses to tone and Class I response to electric stimuli are similar, it is possible that both stimuli develop the same

* Note that the difference between threshold levels for Class I and Class II responses was generally small at extremes of characteristic frequency (> 20 kHz, < 2 kHz). For some fibers in these ranges, threshold for Class II response was evidently lower than the Class I threshold; in these fibers no Class I characteristics were observed. However, for fibers of characteristic frequency between about 2 and 20 kHz, electric stimuli always evoked Class I response.

effective stimulus at some point in the linear stages of cochlear signal processing, prior to the stage at which stimuli are encoded into nerve-fiber discharge. If so, acoustic and electric stimuli which produce equal and opposite effective stimuli should combine to produce zero net effective stimulus, and no resultant nerve-fiber response.

This hypothesis was tested experimentally by using acoustic stimuli to cancel response to electric stimuli. For fibers of different f_c , the characteristic frequency and threshold for both current and tone bursts were first determined. Current-burst level was then raised, usually to a point 10 to 20 dB above threshold, and the acoustic stimulus was applied simultaneously. By varying the level and phase of the acoustic stimulus relative to the electric stimulus, it was possible to reduce the number of nerve-fiber discharges to the point that no response pattern could be detected audio-visually.

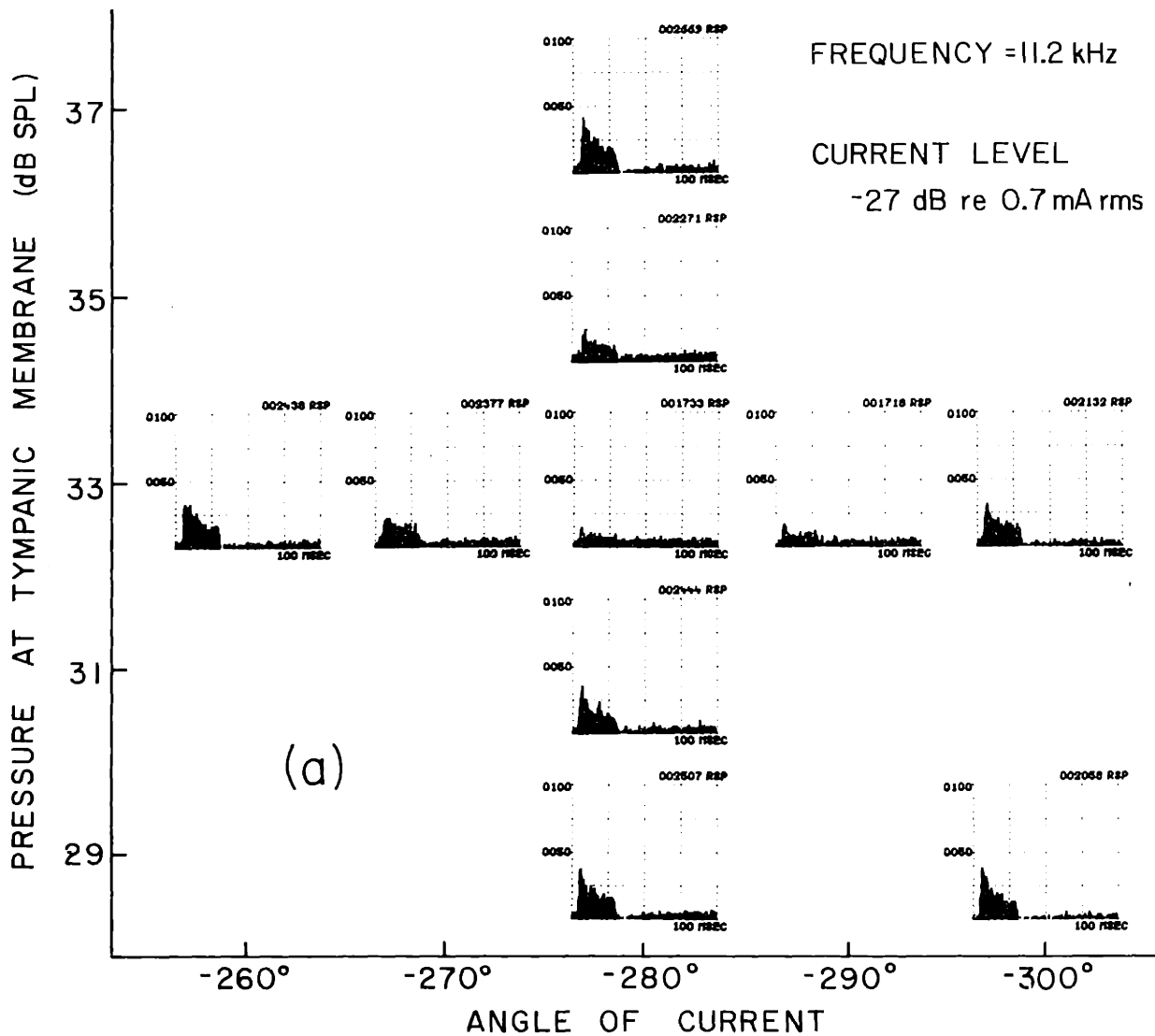
An example of the patterns of fiber response to null and near-null conditions is shown in PST histograms in figure 4.12 (a). At the null point (histogram at 33 dB SPL and -280°) there is far less response than for either tone or current alone [histograms (b) and (c)], and the pattern approaches the pattern of unstimulated (spontaneous) activity [histogram (d)]. The adjustment of level and phase for cancellation was found to be quite critical, and as indicated in part (a) of the figure, a 2 dB or 10° departure from the null point produced an appreciable response.

Figure 4.12

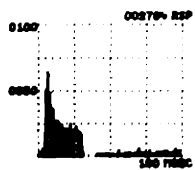
Histograms of fiber response to simultaneous bursts of sinusoidal electric and acoustic stimuli.

In (a), at 11.2 kHz (f_{ce}), bursts of current were presented at fixed level (-27 dB re 0.7 mA rms, 15 dB above threshold) and level and relative phase of simultaneously-applied tone bursts were varied. Histograms show pattern of response as a function of tone level and phase difference. Phase angle shown is angle of the round-window-electrode current referred to the sound pressure at tympanic membrane. In (b), histogram of response to tone alone at 33 dB SPL, and in (c) current alone at -27 dB; in (d) histogram of spontaneous activity. Each histogram compiled from 30 seconds of data, or approximately 300 stimulus presentations. Fiber 49-7, $f_c = 11.1$ kHz, spontaneous discharge rate = 75/sec.

UNIT 49-7
 $f_{ce} = 11.2 \text{ kHz}$
TONE + CURRENT



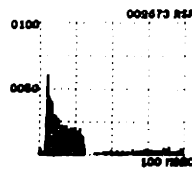
TONE ALONE



33 dB SPL

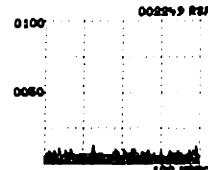
(b)

CURRENT ALONE



(c)

SPONTANEOUS



(d)

Since the response pattern in the vicinity of the null was so sensitive to level and phase, the null condition was easily detected audiovisually, and histograms were not routinely computed to determine the null point.

The relationship of absolute level of the two stimuli which produced null was studied in one experiment. Once null had been achieved, one stimulus was raised or lowered by 5 to 10 dB and the other stimulus level was adjusted to re-establish null. No significant differences were found in either the relative level or phase of the two stimuli required to maintain the null condition. This result suggests that the electric stimulus does establish an effective stimulus in linear stages of the cochlea, which in turn generates Class I nerve-fiber response.

4.1.5 Equivalence of sinusoidal acoustic and electric stimuli based on Class I nerve-fiber response.

The data presented in the preceding sections have shown that Class I response of single auditory-nerve fibers is essentially equal to the response to a suitably chosen tone. A sound pressure P_d and an electrode current I_e which produce equal responses will be defined to be equivalent stimuli. Two stimuli which have equal but opposite effect, such as in cancellation experiments, will be called anti-equivalent. A quantitative relationship between equivalent pressure and current stimuli can be derived from characteristics of auditory-nerve-

fiber response.

Since threshold stimuli produce equal, just detectable responses, one measure of the magnitude of equivalent acoustic and electric stimuli is threshold level of tone and current. In figure 4.13 (a) and (b), tone threshold at f_c is plotted at f_c for a sample of fibers from two cats. For fibers of nearly the same f_c , the thresholds all lie in a relatively narrow (≈ 20 dB) range of sound-pressure level, as described by Kiang (1968). The plots of (c) and (d) show current threshold at f_{ce} for the same fibers and these points show a comparable spread. The figure shows that the distribution of threshold as a function of frequency is somewhat different for the two stimulus types, indicating a frequency-dependent difference in the effectiveness of the two stimuli.

The difference is shown explicitly in the plots of figure 4.14. For each fiber the level (magnitude) of threshold sound-pressure $|P_d^t|$ is divided by the level of threshold current $|I_e^t|$ to form a quotient

$$|Q_f^t| \equiv \frac{|P_d^t|}{|I_e^t|}$$

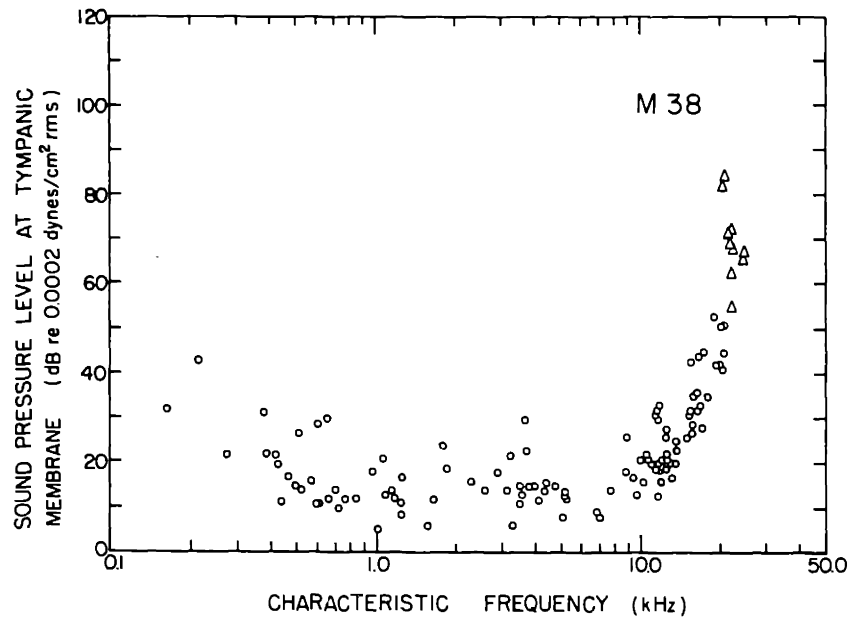
The figure shows values of $|Q_f^t|$ for each fiber plotted at f_c . The solid lines are smooth curves fitted to the data points.* These data

* Although values of $|Q_f^t|$ obtained for different fibers of comparable f_c differ by as much as 20 dB, it is possible that these differences could be due to measurement errors, rather than actual differences in the value of this function for different fibers. The threshold values $|P_d^t|$ and $|I_e^t|$ are based on subjective detection of a response signal in the presence of background activity. Since response near threshold

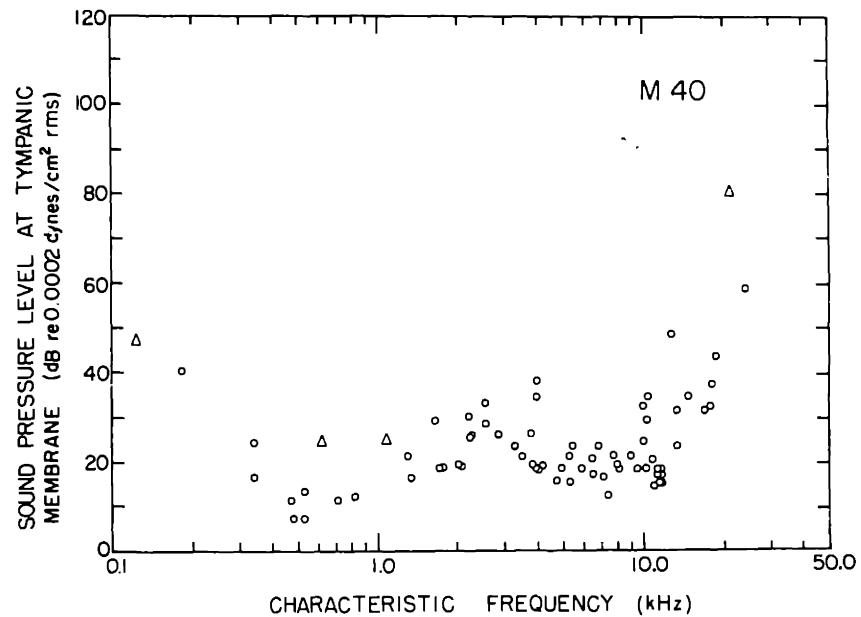
Figure 4.13

Plots of tone threshold at f_c and current threshold at f_{ce} for fibers from each of two cats.

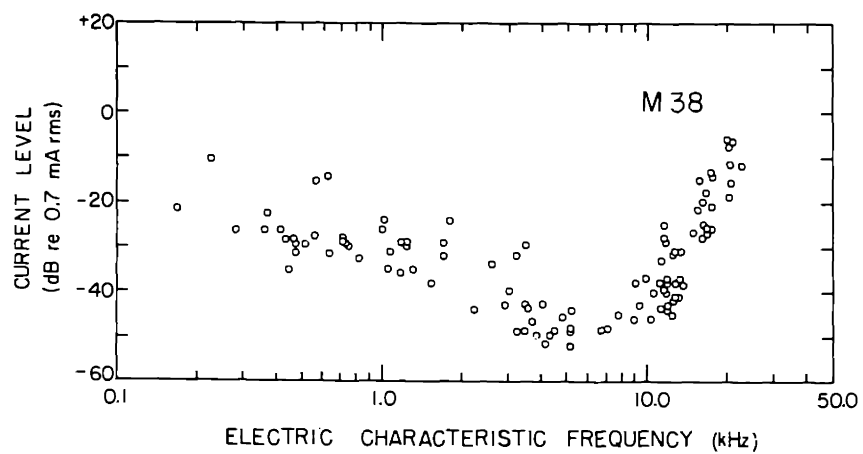
In (a) and (b), a circle represents the tone threshold at f_c for a fiber whose current threshold at f_{ce} is plotted in (c) or (d). A triangle indicates tone threshold at f_c for a fiber for which no f_{ce} could be found. For such fibers having high f_c and high tone thresholds at f_c , it may be that an f_{ce} and a current threshold at f_{ce} could have been found if higher current levels had been used. For such fibers having low f_c , only Class II response was found and consequently f_{ce} could not be determined.



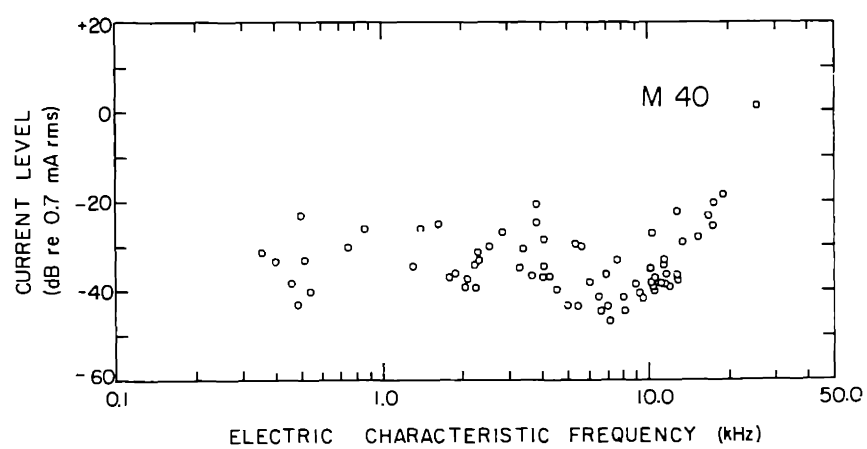
(a)



(b)



(c)

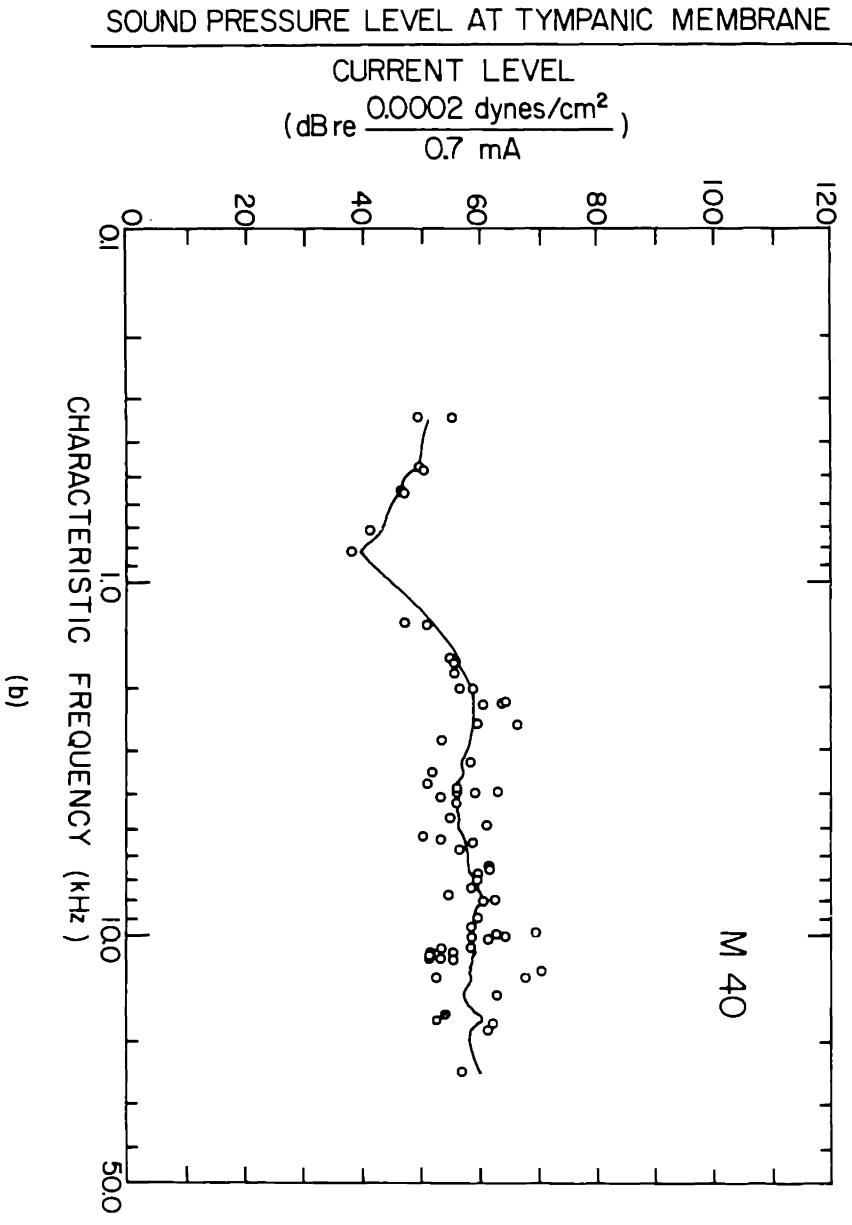
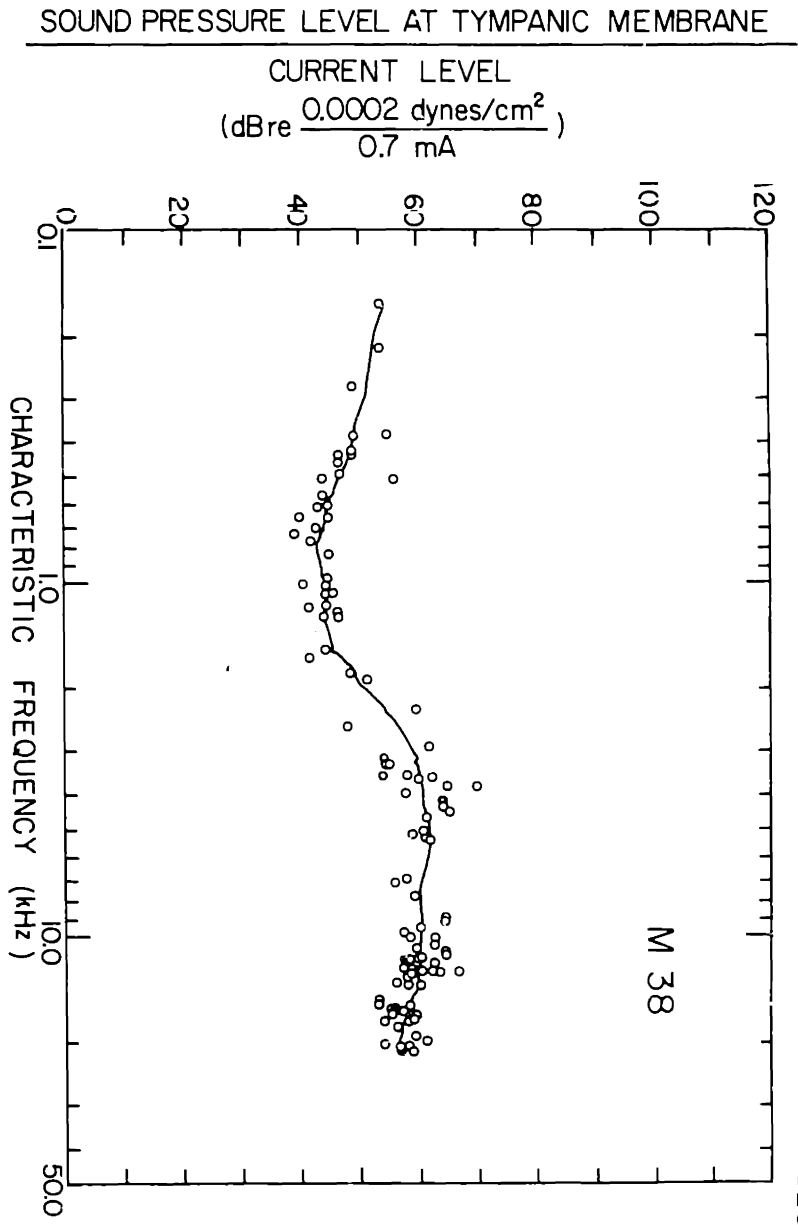


(d)

Figure 4.14

The magnitude of the ratio of equivalent stimuli $|Q_f^t|$ based on fiber threshold for tone at f_c and threshold for current at f_{ce} .

The ratio of threshold tone level to threshold current level is plotted at f_c for fibers whose thresholds are shown in figure 4.13 (circles). Solid curves were obtained from the data points by plotting at each f_c the average magnitude (in dB) of all points within an octave band centered at f_c .



indicate that the magnitude of the ratio of equivalent current and pressure is about the same in different animals.

These ratio data represent the sound-pressure level required to equal the effect of constant current level for fibers of different f_c . It should be emphasized that these ratios pertain only to Class I response, and in applying this result, the threshold of Class II response must be kept in mind. For example, the curves suggest that above 2 kHz the reference current level (0 dB re 0.7 mA rms) would be equivalent to a tone at about 60 dB SPL. However, since an actual 2 kHz current of 0.7 mA would evoke Class II response (see figure 4.5), the response of the nerve fibers to this stimulus would not duplicate the response to tone, and at this high level, the stimulus equivalence based on Class I response does not completely characterize the response of auditory-nerve fibers. However, these data do indicate that response to a 2 kHz current at -20 dB (re 0.7 mA rms) would equal response to a tone at 40 dB SPL.

Another measure of equivalent stimuli is provided by the parameters of pressure and current which combine to produce no nerve-fiber response (null). The stimulus parameters at null define complex amplitudes of anti-equivalent pressure and current; by shifting the

is not very sensitive to small increments of stimulus level, errors of several dB could occur in each measurement and, therefore, in the ratio points in figure 4.14. Thus a smooth curve describing $|Q_f^t|$ was formed by averaging the data to reduce the effects of these errors.

phase of either by 180° , anti-equivalent stimuli are converted to equivalent stimuli. Figure 4.15 shows the magnitude and angle of the complex ratio of equivalent pressure and current as determined from cancellation data,

$$Q_f^c \equiv -\left(\frac{P_d^c}{I_e^c}\right) \quad (c = \text{"at cancellation"})$$

Comparison of the plotted points with the solid curve (replotted from figure 4.14) shows that the magnitude ratios are essentially the same as the magnitude ratios based on thresholds. The data show that, above 3 kHz, current is equivalent to a constant sound-pressure level, and pressure leads current by larger angles as frequency increases.

The stimulus parameters required to produce null depended only on stimulus frequency, and not on characteristics of the responding nerve fiber. For example, figure 4.16 shows angles of equivalent sound pressure and current determined at frequencies other than f_{ce} . These angle data are not significantly different from the angles determined for other fibers at f_{ce} . Although the absolute stimulus levels at cancellation were in general different (-10 to -25 dB re 0.7 mA rms, 10 to 20 dB re threshold), the variations of angle at any given frequency are within 10 to 20 degrees. These data show that, for different fibers and different absolute stimulus levels, a given frequency required a particular phase for cancellation.

The cancellation method of specifying stimulus equivalence pro-

Figure 4.15

The complex stimulus equivalence ratio Q_f^c based on cancellation of nerve-fiber response.

Data from two cats are shown. Each point represents measurements from a different fiber. For each fiber, f_{ce} and threshold at f_{ce} were determined. Then bursts of sinusoid at f_{ce} and at fixed level, usually 15 dB above threshold, were presented simultaneously with tone bursts derived from the same signal source. Level of tone bursts and angle between tone and current sinusoid were adjusted to produce minimum fiber response, as judged by the experimenter. Each fiber gave values of stimulus quantities P_d^c and I_e^c which at f_{ce} had equal and opposite effects, or which were anti-equivalent. Equivalent stimulus quantities were formed from the anti-equivalent quantities by adding 180° to the relative phase angle (multiplying one stimulus quantity by -1). Data are magnitude and angle of ratio of equivalent stimuli

$$Q_f^c \equiv -\left(\frac{P_d^c}{I_e^c}\right)$$

for each fiber. No points are shown below about 2 kHz because low relative Class II threshold in low- f_c fibers prevented use of current level adequate to produce well-defined cancellation. Solid curve in magnitude plot is smoothed threshold-based ratio $|Q_f^t|$ of figure 4.14(a) replotted for comparison.

SOUND PRESSURE AT TYMPANIC MEMBRANE

ELECTRODE CURRENT

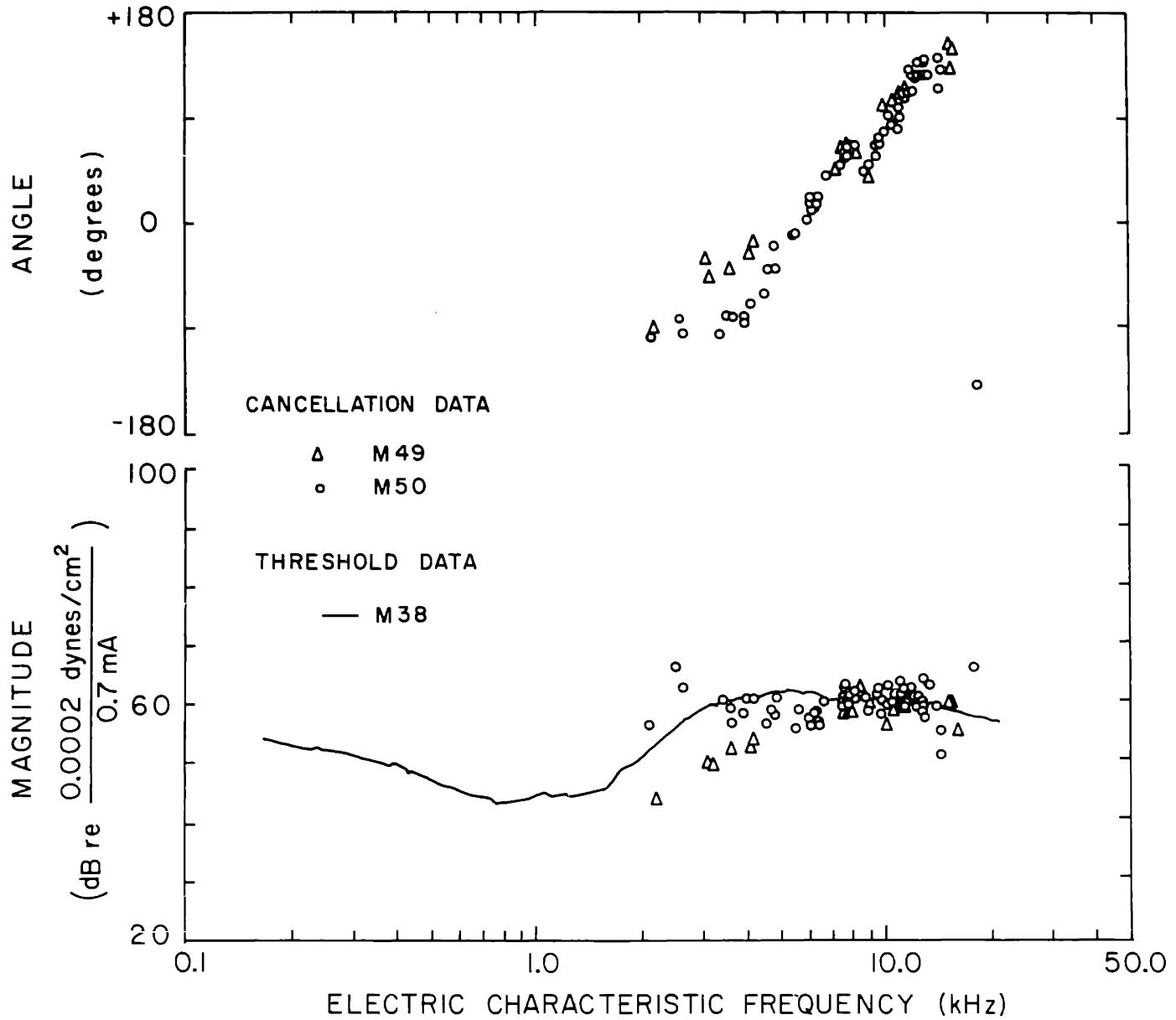
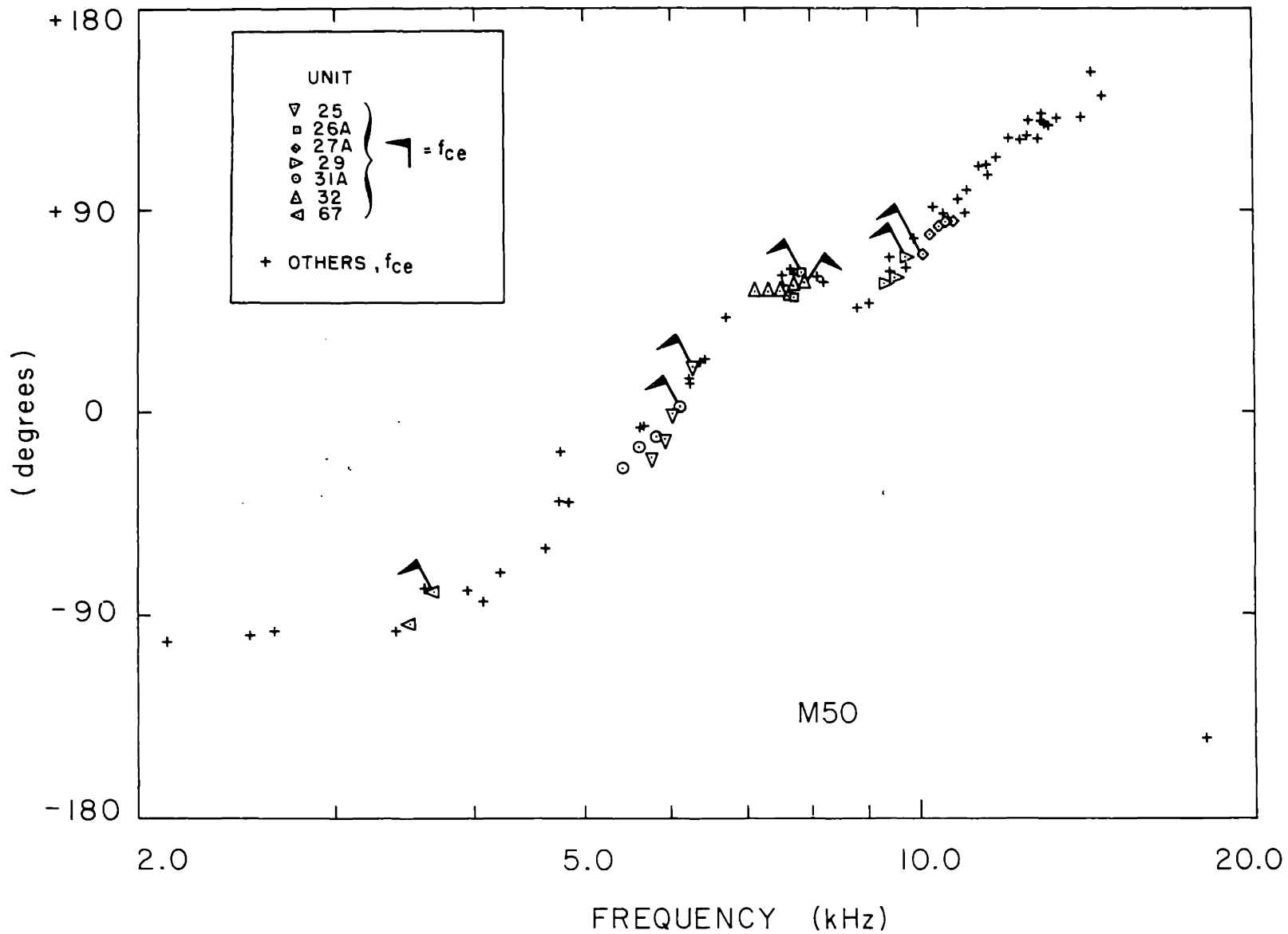


Figure 4.16

Angle of Q_f^c based on cancellation of nerve-fiber response at frequencies other than f_{ce} .

Each set of open symbols represents data from a different fiber. For these fibers, each data point at f_{ce} is indicated by the flagged symbol. Other points represent data at f_{ce} for other fibers. Data are only shown at frequencies close to f_{ce} because the cancellation method was based on Class I response which occurs only within the narrow frequency range defined by S_I of the tuning curve (figure 4.5). For some fibers shown, absolute stimulus level was adjusted at different frequencies to maintain well-defined Class I response. For example, frequencies and levels for fiber 27A were 10.2, 10.4, 10.6 kHz at -17 dB, and 10.8 kHz at -7 dB.

ANGLE OF $\left[\frac{\text{SOUND PRESSURE AT TYMPANIC MEMBRANE}}{\text{ELECTRODE CURRENT}} \right]$



vides both magnitude and phase information, but is practical only at frequencies > 2 kHz. In this range, however, the cancellation magnitude data are consistent with the threshold-based magnitude equivalence. The complex equivalence ratio Q_f is specified most completely as a function of frequency in terms of the threshold-based magnitude data (figure 4.14) and the cancellation-based phase data (figure 4.15). Thus $|Q_f|$ is specified for frequencies $0.2 \text{ kHz} < f < 20 \text{ kHz}$, and $\angle Q_f$ is given for $2 \text{ kHz} < f < 20 \text{ kHz}$.

4.2 Experimental Investigations of Origins of Responses.

The experiments described in the following sections of this chapter were intended to investigate the sites of production of the two components (α and β , in figure 4.1) of shock response and the two classes (I and II) of response generated by sinusoidal electric stimuli. To determine possible stages of the peripheral auditory system in which different responses were generated, response was studied when the operation of various stages was experimentally altered.

To determine whether responses were generated central or peripheral to the hair cell, response was studied when cochlear function was modified at the sensory-cell stage, both physiologically (by activation of the efferent COCB) and pharmacologically (by means of ototoxic drugs). The role of more peripheral stages of cochlear and middle-ear mechanics was studied in experiments in which physical con-

straints were imposed on variables at the acoustic terminals of the cochlea. Finally, a possible role of stimulating electrodes in production of response was also investigated.

4.2.1 Responses to electric and acoustic stimuli in cochleas modified at the sensory cell stage.

Figures 4.17 and 4.18 show examples of the effect of COCB activation on the pattern of fiber response to electric and acoustic stimuli. Patterns are shown for click and shock stimuli (figure 4.17) and bursts of sinusoidal stimuli (figure 4.18).

Figure 4.17 (a) and (c) shows the effect of COCB activation on the click response. With COCB activation [in (c)], the number of responses is reduced. This effect is consistent with the reduced amplitudes of click-evoked gross neural potentials which have been reported [see Wiederhold and Peake (1966)].

The shock response in 4.17 (b) shows both α - and β -components. With COCB activation, histogram (d) shows no discernible β -component, and the number of α -component discharges is reduced by perhaps 25%. For different fibers, COCB activation always reduced the β -component, but no consistent effect was observed on the α -component. Activation of the COCB sometimes increased and sometimes decreased the number of α -component discharges. Effect on the α -component showed no systematic dependence of f_c , and the average effect for 29 fibers sampled amounted to a slight (about 6%) reduction in number of

Figure 4.17

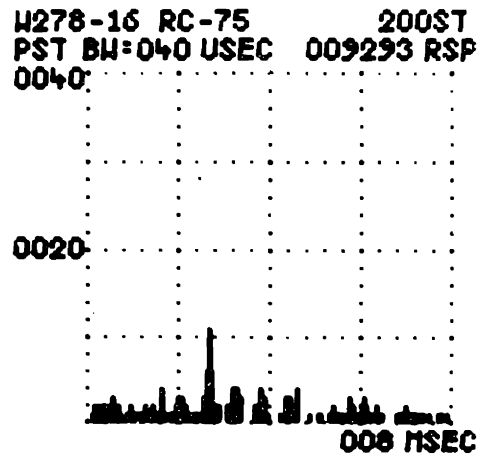
Histograms of fiber response to shocks and clicks modified by activation of the COCB.

Stimuli were presented at 2/sec, alternate stimuli preceded by an 80 msec train of stimuli to the COCB (32 biphasic pulses at 400/sec) which ended 10 msec before the zero time of the histogram. In (a) and (c), response to clicks, in (c) clicks preceded by COCB activity; (b) and (d), response to shocks, in (d) shocks preceded by COCB activity. Each histogram compiled from response to 200 stimuli. Shocks 350 μ A, 100 μ sec, round window negative; rarefaction clicks formed from 100 μ sec pulses, -75 dB re 100 V into 1-inch condenser earphone. Fiber W278-16, $f_c = 1.56$ kHz, spontaneous discharge rate ≈ 90 /sec.

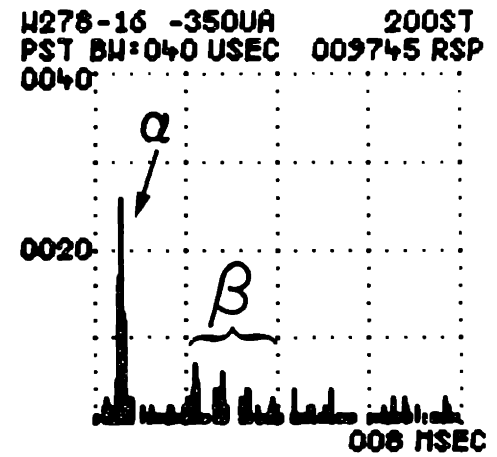
UNIT

W278-16

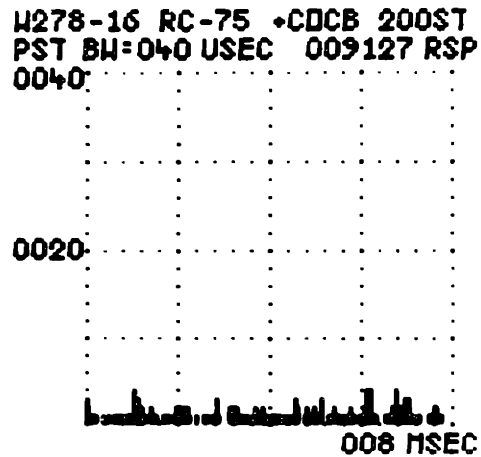
CLICKS



SHOCKS



CLICKS
+
OCB



SHOCKS
+
OCB

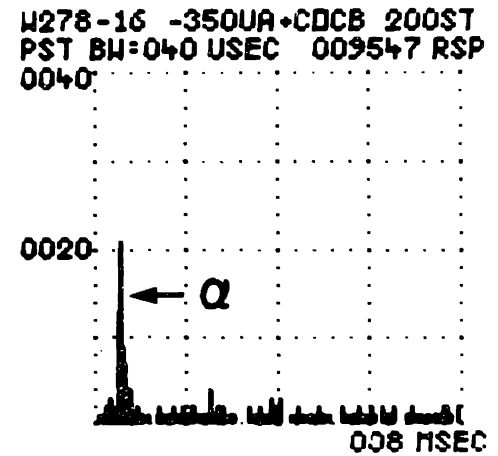


Figure 4.18

PST histograms of fiber response to bursts of tone and sinusoidal current modified by activation of the COCB.

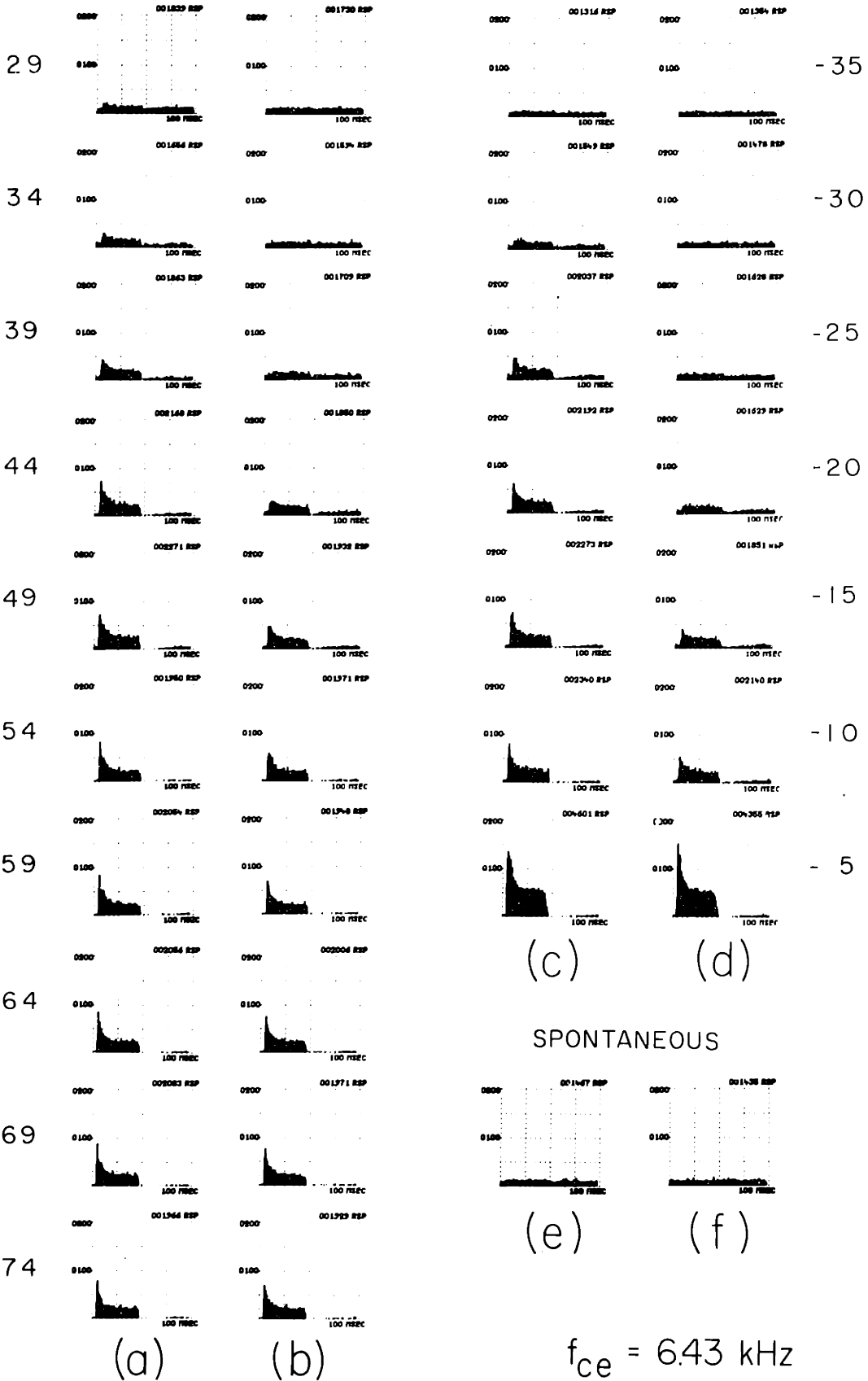
Histograms of response at 10 levels of tone burst [columns (a) and (b)] and 7 levels of current burst [columns (c) and (d)]. In (b) and (d), stimuli accompanied by 80 msec trains of COCB stimulation (32 shocks at 400/sec, occurring between 10 and 90 msec on the histogram time axis). Tone and current bursts at 6.43 kHz (f_{ce}), 10/sec, duration 40 msec. In (e) and (f), histograms computed with stimuli turned off (spontaneous activity), in (f) with COCB stimulation. Each histogram is computed from response to 200 stimulus presentations. Fiber W292-25, $f_c = 6.53$ kHz, spontaneous discharge rate ≈ 74 /sec.

TONE BURSTS
OCB

CURRENT BURSTS
OCB

SOUND PRESSURE LEVEL AT TYMPANIC MEMBRANE (dB re 0.0002 dynes/cm² rms)

CURRENT LEVEL (dB re 0.7 mA rms)



$f_{ce} = 6.43 \text{ kHz}$

α -discharges [see Chamberlain et al. (1968)].

The effect of COCB activation on response to tone bursts shown in figure 4.18 (a) and (b) is typical of the reduction in number of responses found by Wiederhold (1970). The response to bursts of sinusoidal current shown in (c) and (d) depends on stimulus level and COCB activity in nearly the same way as the response to tone bursts at all except the highest current level shown. At -10 dB and below, the response pattern indicates that this is Class I response. At the -5 dB level, however, response to current is far greater than the response to the highest-level tones, and the response is not noticeably affected by COCB activity. At this level, the response showed the repetitive firing which is characteristic of Class II response; the histograms actually show several peaks, but they are separated by only 1 or 2 bins and are hard to see in the figure.

Since the OCB is presumed to act through its endings on the sensory hair cells and on the fine terminals of the auditory nerve near the hair cells, any response which is affected by the OCB could originate at a stage peripheral to the hair cell. The data show that the β -component of shock response and Class I response to sinusoid, both of which resemble response to acoustic stimuli in other ways, are affected by the COCB in the same way as acoustic response. The responses, then, originate either at, or somewhere peripheral to the hair cell.

This conclusion is consistent with characteristics of shock response found in animals in which large numbers of hair cells were destroyed by large doses of the ototoxic drug kanamycin. In these animals, a correspondingly large number of nerve fibers showed no spontaneous activity and no response to acoustic stimuli [see Kiang, Moxon, and Levine (1970)]. However, a shock response was found in these fibers at about the same current level as in normal animals.

Figure 4.19 (a) shows an example of response to shock for a fiber in an animal with extensive ototoxically-induced hair-cell damage. The response pattern shows the 0.5 - msec latency characteristic of the α - component of shock response in normal animals, but the response of the hair-cell-deficient cochlea shows no β -component. This result indicates that production of a response indistinguishable from the α -component is not associated with the hair cell. The data also suggest that the hair cell is required for production of the β -component of response to shock. In all, more than 350 fibers which did not respond to acoustic stimuli were observed; without exception these fibers showed no β -component of shock response. As the example shown in the figure indicates, no significant latency differences were observed between α -components of responses found in hair-cell-deficient cochleas and those found in normal ears.

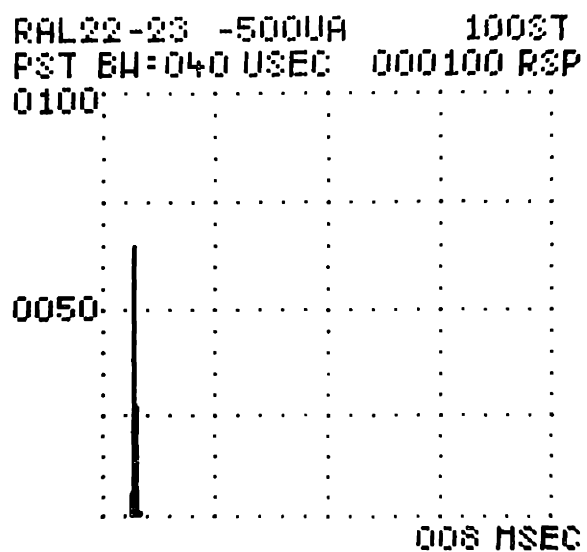
Figure 4.19

PST histograms of response to shock for a fiber in a kanamycin-treated cat and a fiber in an untreated cat.

In (a), example of response of a fiber from a kanamycin-treated cat in which 80% of the basilar membrane was devoid of hair cells. This fiber did not respond to sound and showed no spontaneous activity. In (b), response of fiber ($f_c = 9.1$ kHz) in an untreated cat (histogram replotted from figure 4.1). Histogram in (a) computed from response to 100 presentations of 1 msec, 500 μ A shocks, about 1.5 x threshold (320 μ A); in (b) 200 presentations of 100 μ sec, 800 μ A shocks, about 1.3 x α -threshold (600 μ A). For fibers in untreated animals, a 1 msec shock of given amplitude is equivalent to a 100 μ sec shock of about 2 to 3 times the amplitude; hence shocks in (a) are effectively stronger than those in (b).

KANAMYCIN-TREATED
CAT

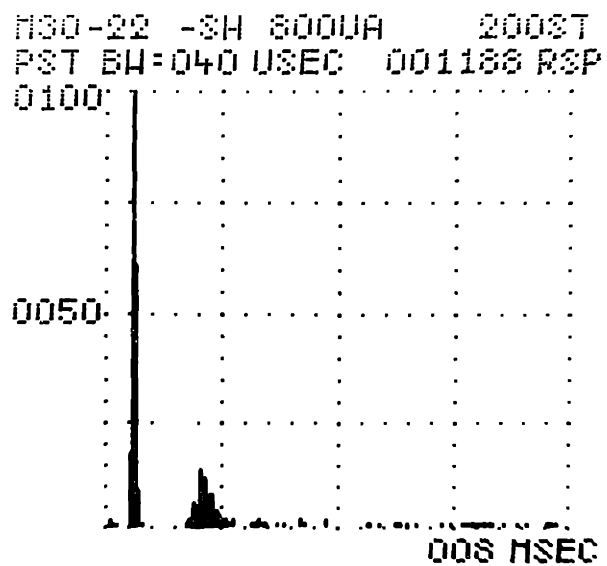
- 500 μ A SHOCK



(a)

UNTREATED CAT

- 800 μ A SHOCK



(b)

4.2.2 Effects of constraints on mechanical variables at the input terminals of the cochlea on responses to sinusoidal current and tone.

In some experiments the mechanical operation of the cochlea was modified by imposing constraints on stapes motion. In one experiment, the stapes was joined to the cochlear capsule with dental cement to reduce stapes mobility in the oval window. Judging from response to acoustic stimuli, stapes mobility was greatly reduced. After the stapes was cemented, click amplitude had to be raised by about 60 dB in order to evoke a given amplitude of gross round-window neural response, and some single auditory-nerve fibers showed tone thresholds that were 80 dB or more above the normal range. For other fibers no response to tones could be found, and the thresholds apparently fell above the highest levels of tone that the stimulus system could generate.

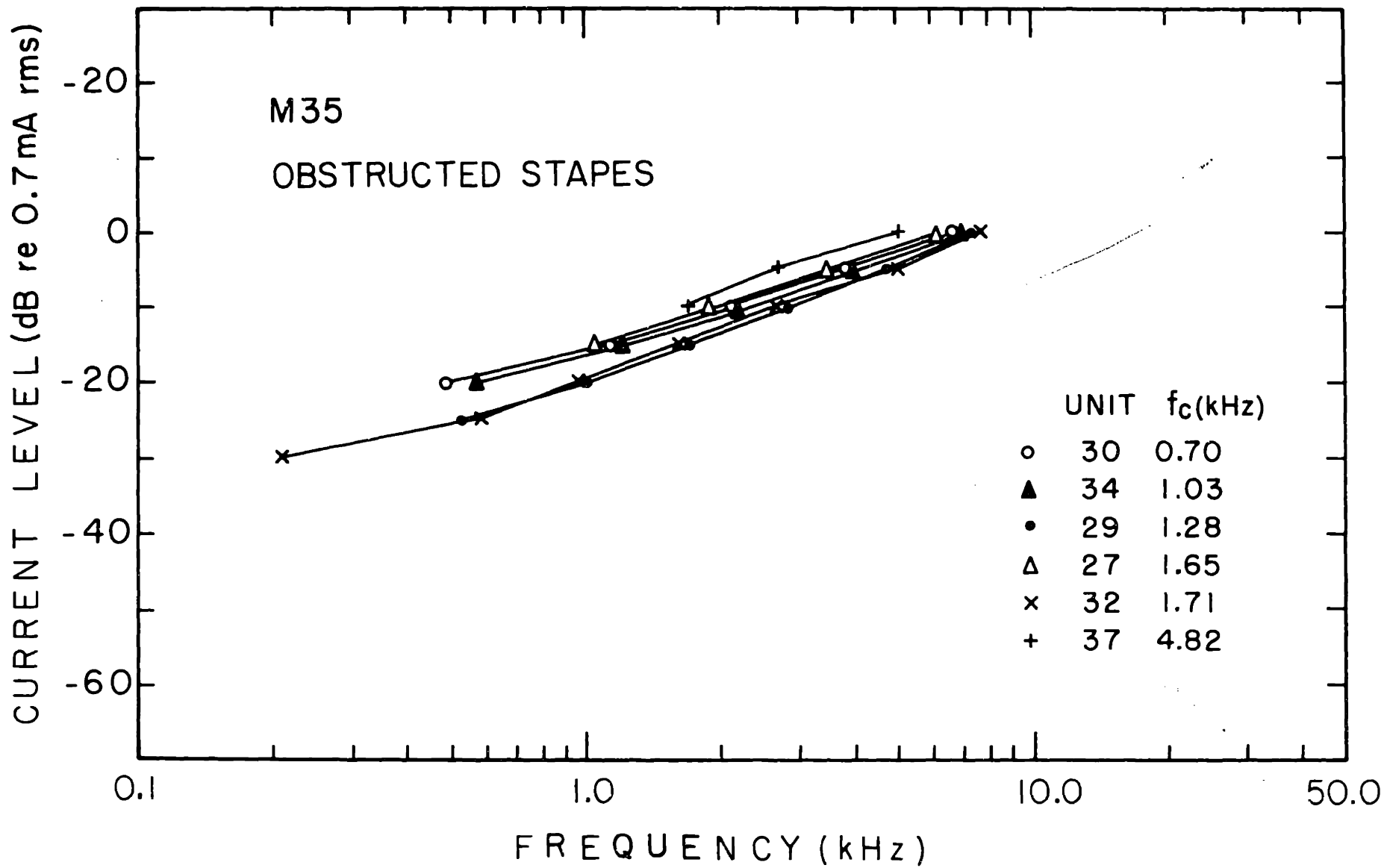
Electric stimuli did elicit response from all fibers, although response differed from the normal. The difference is apparent in the examples of electric tuning curves shown in figure 4.20. All lack the V-shaped S_I segment found in normal animals. These curves resemble the S_{II} segments of the curves shown in figure 4.5.

The data show that, in order for the response to electric stimuli to contain a component which resembles response to acoustic stimuli, the stapes must be allowed to move. Evidently Class I response is mediated by a mechanical response to electric stimuli

Figure 4.20

Tuning curves for sinusoidal electric stimuli in a cat with stapes embedded in dental cement.

Dental cement was applied to the stapes and temporal bone in the middle-ear cavity to reduce motion of the stapes relative to the cochlea. Transmission of sound to the cochlea was reduced by 60 dB, judged by the increase in click amplitude required to evoke just-detectable neural response (N_1) recorded by a gross electrode near the round window. Prior to cementing the stapes, gross electric response to clicks indicated that the overall sensitivity of the ear was within the range of sensitivities of the ears represented in figure 4.5. In some fibers, no response to tone could be detected at the highest levels generated by the earphone (> 110 dB SPL, $f < 10$ kHz; > 90 dB SPL, 10 kHz $< f < 20$ kHz). For other fibers, a response could be found, but only at extremely high levels of sound pressure at the tympanic membrane. For fibers which did respond to tone, a value of f_c could be obtained in the usual way. The electric tuning curves are shown for those units for which f_c was determined. These and 4 other electric tuning curves from this cat show no V-shaped segments.



delivered to the cochlea.

In order to determine whether electric stimuli generated mechanical signals peripheral to the cochlea, a different mechanical constraint was placed on the middle ear. First, threshold data such as those shown in figure 4.13 were obtained for tones and sinusoidal electric stimuli for fibers of f_c between 0.2 and 25 kHz. Then the lenticular process of the incus near the induco-stapedial joint was cut, to interrupt the transmission path of the middle ear. Another sampling of fiber thresholds was made for tone and sinusoidal electric stimuli for this condition of the middle ear.

The results obtained before and after interruption of the ossicular chain are shown in figure 4.21. Difference in tone thresholds [in (a) and (b)] is apparent. In (b), fiber thresholds are raised at most frequencies by more than 40 dB, indicating that sensitivity to sound pressure at the tympanic membrane is reduced.* In contrast, no difference in thresholds for Class I response to electric stimuli is apparent in the figure [parts (c) and (d)]. The figure also shows plots of the threshold-based equivalence ratio $|Q_f^t|$ for the two conditions of the middle ear in this animal. With middle ear intact [in (e)], the

* Interruption of the ossicular chain only disables the primary mechanism of sound transmission to the cochlea; the response that is found with the ossicular transmission interrupted could be the result of any of several secondary mechanisms by which sound is transmitted to the cochlea [see Wever and Lawrence (1954); Tonndorf (1966)].

Figure 4.21

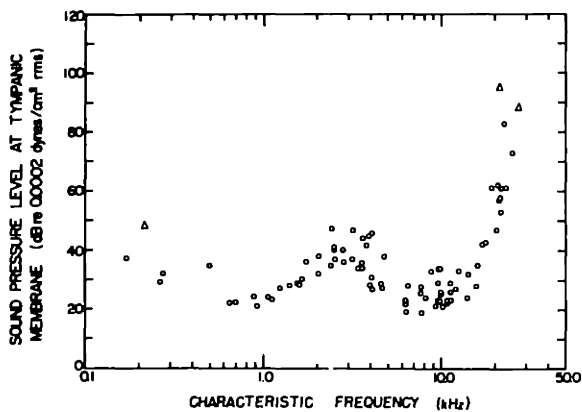
Effect of interruption of the ossicular chain on tone threshold at f_c , current threshold at f_{ce} , and magnitude of the ratio of equivalent stimuli $|Q_f^t|$.

Tone threshold at f_c and current threshold at f_{ce} were obtained while the ossicular chain was intact [data of parts (a), (c), and (e)]. The same quantities were then obtained for other fibers after the incus had been disconnected from the stapes at the incudo-stapedial joint by removing a 1/3 mm segment of the long process of the incus [data of parts (b), (d), and (f)]. In (a) and (b), triangles are plotted for fibers for which no point exists in (c) and (d). In (d), triangles are plotted for fibers for which no point exists in (b). For some of these fibers, it may be that threshold fell above the highest levels of stimuli used. For some low- f_c fibers, only Class II response to electric stimuli was found and consequently no f_{ce} could be determined. In (e) and (f), ratios of the magnitude of equivalent stimuli $|Q_f^t|$ formed as described in figure 4.14 for each condition of the ossicular chain. Solid curve in (e) is obtained from data points by plotting at each f_c the average of all points within an octave band centered at f_c and connecting the resulting points. After all single-fiber data were obtained, ossicular transmission was restored by bridging the gap between incus and stapes with a small quantity of dental cement; stimuli which restored the amplitudes of the gross neural and microphonic potentials to their original values differed only slightly (< 3 dB) from those used prior to interruption of the ossicular chain.

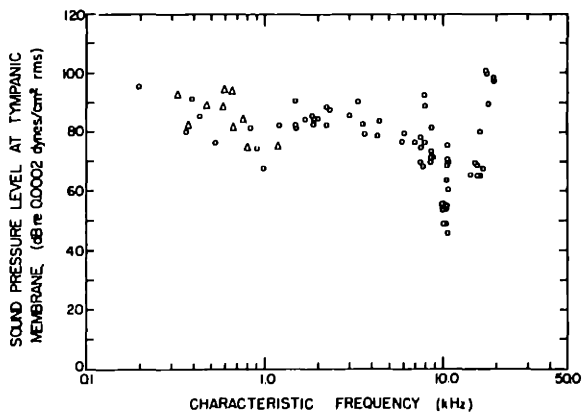
M 44

OSSICULAR CHAIN INTACT

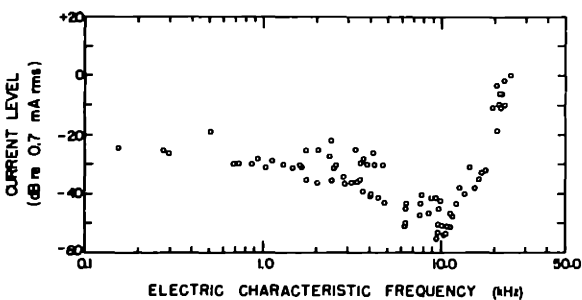
OSSICULAR CHAIN INTERRUPTED



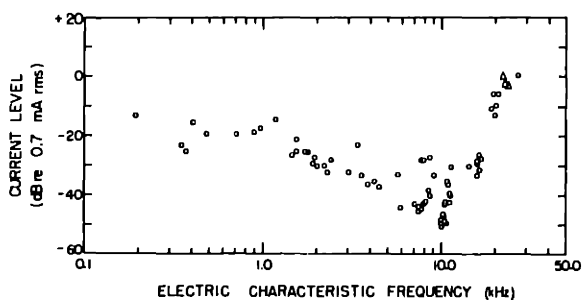
(a)



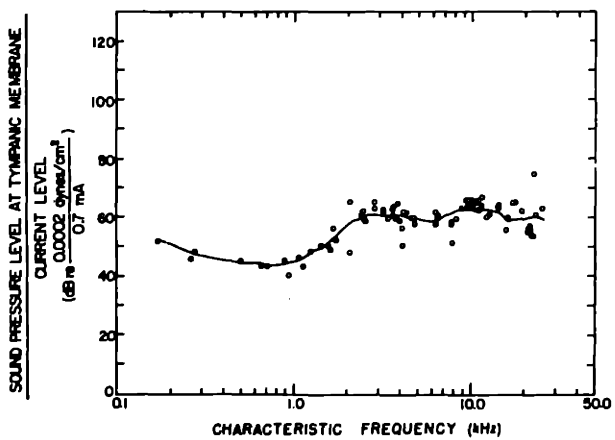
(b)



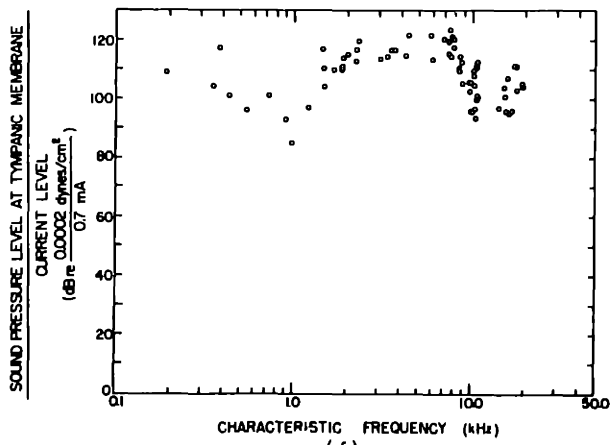
(c)



(d)



(e)



(f)

ratio is about the same as that obtained in other animals (figure 4.14). With the ossicular chain interrupted [in (f)], the ratio is considerably different, reflecting the raised sound-pressure thresholds.

These data show that the Class I response to sinusoidal current is essentially independent of the ossicular transmission path and, therefore, that it cannot be the response to an acoustic signal generated peripheral to the cochlea.

4.2.3 Influence of stimulating electrodes on response to sinusoidal current.

The data presented above suggest that Class I nerve-fiber response was produced by mechanical excitation of the cochlea. It was possible that the hypothesized mechanical signals could have originated at the points where the metal stimulating electrodes contacted the tissue. To investigate this possibility electrical connection to the cochlea was made through fluid contacts, using electrolyte-filled glass tubing. In these electrodes, the junction between metal and electrolyte occurred in a 0.2 to 0.3 cm³ volume of fluid about 2 cm from the cochlea. The stimulus equivalence ratio $|Q_f^t|$ was determined for fibers of $f_c > 3.3$ kHz, and the ratios were between 55 and 60 dB $\left(\text{re } \frac{0.0002 \text{ dynes/cm}^2}{0.7 \text{ mA}} \right)$, values which are within the range of data shown in figures 4.14 and 4.21.

In another experiment, when current was delivered with two electrodes on the periosteum on the surface of the cochlea, threshold

of Class I response for a 7 kHz fiber was about 30 dB higher than the threshold for current delivered through an electrode contacting the round-window membrane. This evidence suggests that Class I nerve-fiber response is not produced by forces developed by the stimulating electrodes themselves, but is associated with current flow into the cochlea.

4.3 Summary.

The data presented above have shown two components (α and β) of auditory-nerve-fiber response to pulses of electric current (shock). The α -component is distinguished by a well-defined short latency (≈ 0.5 msec) and by a sharp threshold which does not depend on f_c in any systematic way. The β -component resembles fiber response to clicks.

Nerve-fiber response to sinusoidal current depends on frequency and level of the stimulus. In one subdivision of fiber response area, the response shows tuning characteristics and temporal patterns of discharge which resemble the response to a tone stimulus; this behavior defined Class I response. In the remainder of the response area, response shows distinctive tuning and discharge characteristics and differs from response to acoustic stimuli; this behavior defined Class II response. Class I response can be canceled with a suitably chosen acoustic stimulus, is inhibited by activation of the efferent system,

and is found only when structures in the cochlea are allowed to move. This response is maintained when middle-ear transmission is interrupted by breaking the ossicular chain; it is therefore not a response to signals developed peripheral to the cochlea.

CHAPTER V.

MECHANICAL RESPONSES OF THE COCHLEA
TO SINUSOIDAL ACOUSTIC AND ELECTRIC STIMULI

The data of the preceding chapter suggest that electric current delivered to the cochlea causes structures in the cochlea to move, and that the resulting motion produces a response in auditory-nerve fibers which resembles the response to acoustic stimuli. In the experiments described in this chapter, a mechanical detector was used to measure motion of the round-window membrane in response to electric stimuli.

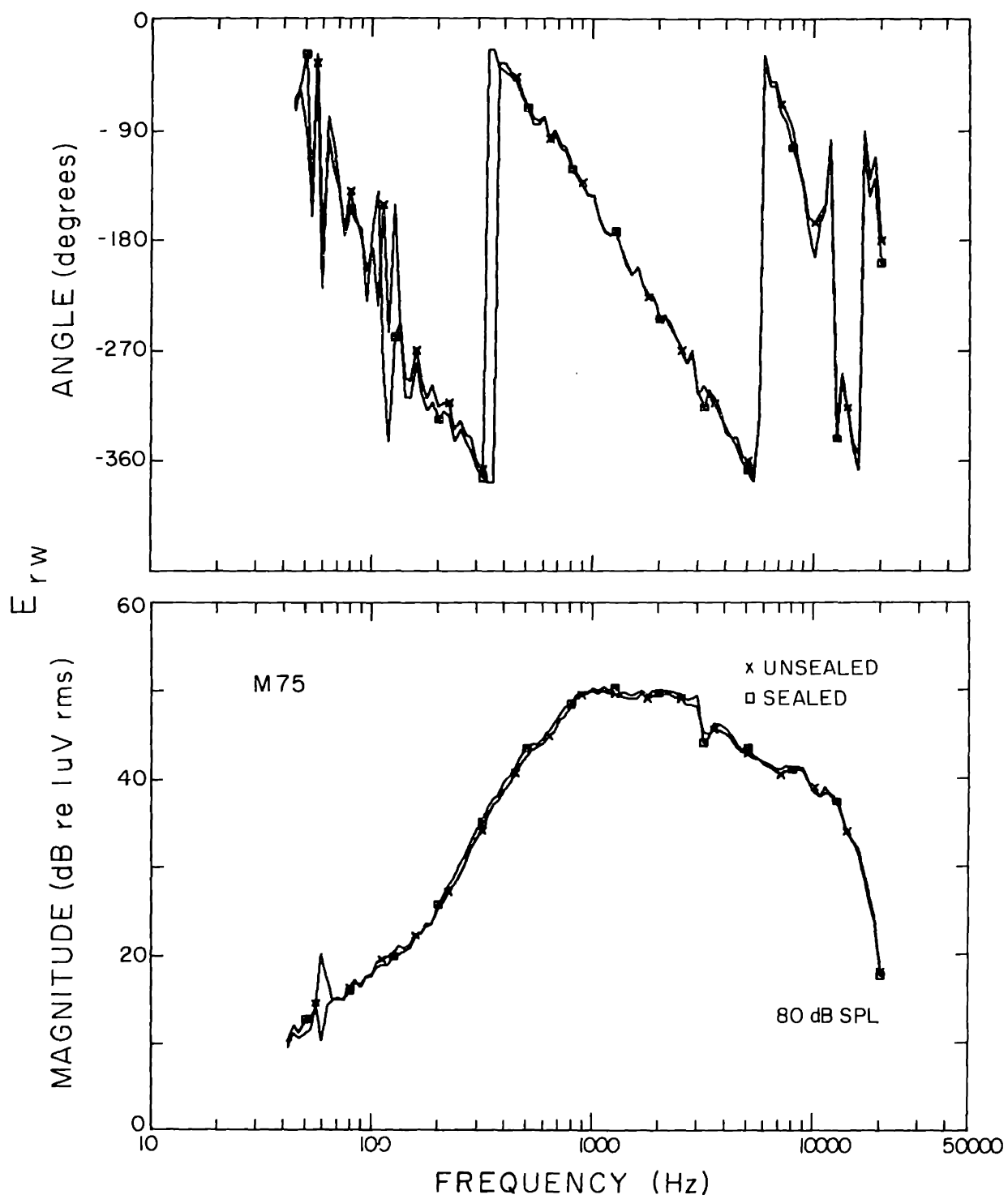
5.1 Effect of Measuring System on the Function of the Normal Cochlea.

The mechanical response was detected by a microphone and probe-tube assembly which was sealed over the round window, as described in Chapter III. To determine whether the normal motion of the round-window membrane and other cochlear structures was altered when this assembly was in position, the round-window potential, E_{RW} , (recorded by a gross electrode) was measured before and after the tube was sealed into place. It has been shown experimentally that a restriction of round-window motion is reflected in a reduction of round-window potentials (Wever and Lawrence, 1954; Tonndorf and Tabor, 1962). Typical results are shown in figure 5.1. Only slight differences exist in the two frequency responses shown. The

Figure 5.1

Round-window potential E_{RW} measured before and after sealing probe-microphone system over the round window.

Curves show the magnitude and angle of fundamental component of round-window voltage recorded in response to tones of 80 dB SPL at the tympanic membrane. Data point density, 40 points/decade. Note that plotted symbols serve to identify individual curves and do not represent all the data points. The recording electrode contacted fluid on the surface of the round-window membrane. Phase of round-window potential is referred to sound pressure at tympanic membrane. The "unsealed" curves were obtained after the cochlea had been completely prepared to receive the probe-tube assembly, but before the tube was sealed in place. The tube was then positioned over the round window and the "sealed" curves were obtained. The stimulus was at a level low enough so that cochlear microphonic potential was essentially proportional to stimulus level. The magnitude data show a difference at 60 Hz due to stray coupling between the recording system and the power line.



(a)

differences are made more apparent by forming the ratio of the responses recorded under the two conditions. Figure 5.2 shows ratios of measurements from three separate experiments.

The input impedance of the probe-tube system is high at some frequencies and low at others (see Appendix II). If the cochlea is loaded appreciably by the tube, it would be expected that E_{rw} would be reduced most at frequencies where tube impedance is highest, at 5.4, 10.8, and 16.2 kHz. No local minima in the ratio curves appear at these frequencies. In the ratios of (a) and (c), the differences in round-window voltage are less than 2 dB; in (b), the difference reaches 4 dB, but only at about 20 kHz.

These data indicate that the microphone and tube system sealed over the round window has no appreciable effect on the operation of the cochlea. The tube input impedance, even at its highest value, is evidently small compared with the acoustic impedance the cochlea exhibits at the round window. For present purposes, the round window can be considered to be a source having infinite output impedance, that is, a volume-velocity source.

5.2 Signals Recorded in the Absence of Stimuli.

When the microphone system was sealed over the round window, and in the absence of any external stimuli, a large, low-frequency signal appeared in the oscilloscope display of the microphone output.

Figure 5.2

Ratio of round-window potentials measured before and after sealing probe-microphone system over the round window.

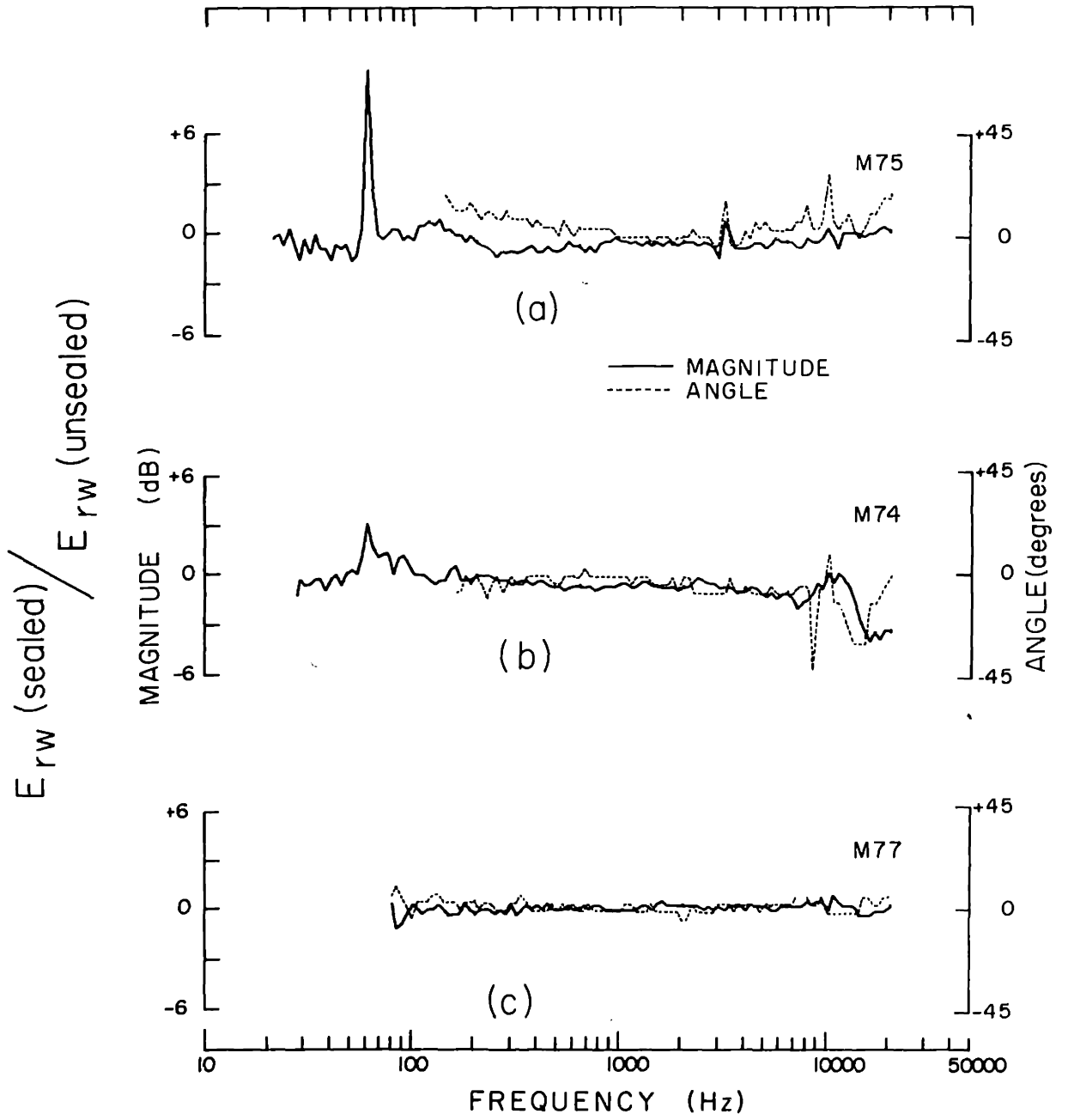
Curves in (a) represent the ratio of the two responses shown in figure 5.1; curves in (b) and (c) are ratios of data from two other similar experiments. Solid line is magnitude of ratio, dotted line is angle of ratio. At low frequency, signal-to-noise ratio becomes poor, and data are not shown below arbitrarily-determined cut-off frequencies. All responses recorded for constant 80 dB SPL at the tympanic membrane.

Elapsed time between pairs of measurements:

M75, 1 hr. 38 min.

M74, 1 hr. 24 min.

M77, 37 min.



When the waveform was reproduced through a loudspeaker, characteristics could be detected which suggested that this signal might be related to the animal's heartbeat. To investigate this possibility, an electrocardiogram (EKG) signal was simultaneously recorded from a subcutaneous electrode on the thorax. The EKG signal was used to trigger the oscilloscope display, and the microphone output was found to be synchronized with the EKG. Examples of the waveform are shown in figure 5.3. The peak amplitude in each case is of the order of 10 dynes/cm^2 , and occurs about 100 msec after the large R wave of the EKG waveform. This signal was found only when the probe-tube system was sealed; when the seal was not total, the microphone output was essentially zero, as shown in figure 5.3(e). In this case a hole in the side of the probe tube was opened, preventing appreciable low-frequency pressures from being developed in the system. The effect was the same when the seal between the end of the tube and the cochlea was not complete.

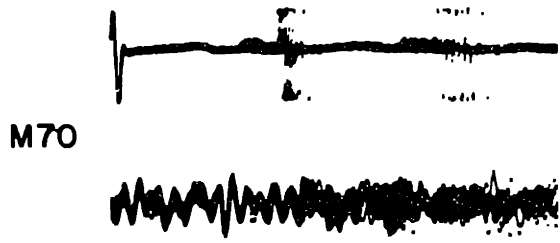
This EKG-synchronized pressure signal did not necessarily originate within the cochlea. Similar signals were found when the tube was sealed over a solid portion of the skull. Thus it is possible that these signals were caused by relative motion between the skull and probe-tube system, and not by relative motion between cochlear structures and the cochlear capsule.

The EKG-synchronized pressure signal was larger than the

Figure 5.3

Microphone pressure waveform recorded in the absence of controlled stimuli.

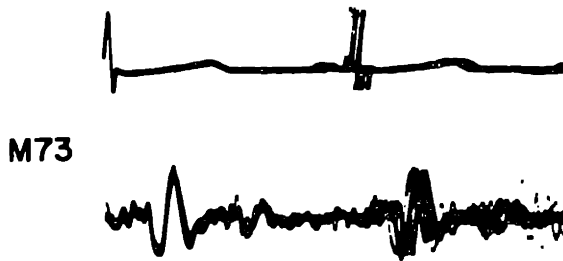
Data from four cats are represented. Upper trace of each pair is an electrocardiogram voltage recorded by a subcutaneous electrode on the chest. Lower traces are microphone output. Positive voltage and condensation pressure are plotted as an upward deflection. Oscilloscope photographs of ten superimposed traces, each trace triggered from the leading edge of the large positive component of the EKG. In (a), (b), (c), and (d), the probe-tube system was sealed in place over the round window. In (e), all conditions as in (d) except that a hole was opened in the probe tube. Microphone amplifier low-frequency 3-dB frequency ≈ 5 Hz.



(a)



(b)



(c)

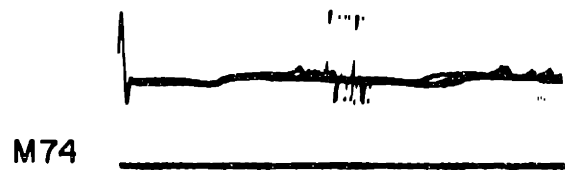
I 1 mV - EKG

I 10 dynes / cm² - MICROPHONE

0.5 sec



(d)



(UNSEALED)

(e)

signals of interest, and tended to exceed the dynamic range of some stages of the measuring apparatus. This problem was overcome by filtering the microphone output to reduce the low-frequency response of the system. For this purpose, it was convenient to use the standard frequency-response contour A available in the microphone amplifier (the A weighting network of the International Electrotechnical Commission). The round-window-microphone response routinely measured was the microphone output multiplied by the transfer function of this network, H_A . The recorded values were subsequently expressed as actual microphone output by dividing by H_A .

5.3 Responses of the Normal Cochlea.

5.3.1 Waveform of microphone output.

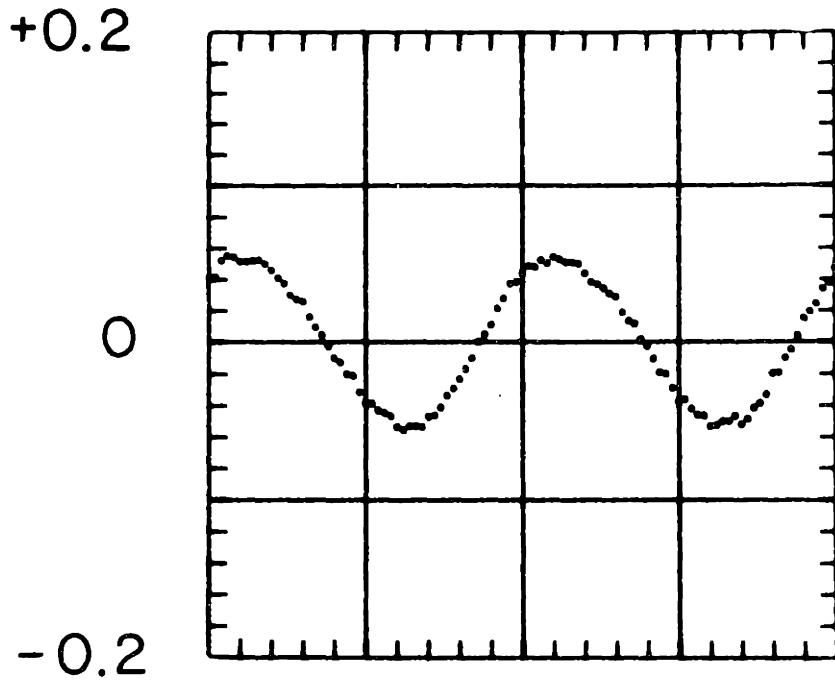
When sinusoidal current was applied to the cochlea, a response could be detected in the output of the microphone. Figure 5.4 shows an example of the averaged waveshape of the microphone response to a sinusoidal electric stimulus. Also shown is the waveshape of the current probe output. Neither waveform appears to depart significantly from a sinusoid, at the frequency shown or at several other frequencies examined. The response to acoustic stimuli was also substantially sinusoidal. Consequently, to characterize responses to electric and acoustic stimuli it was sufficient to determine magnitude and phase of the fundamental response component as a function

Figure 5.4

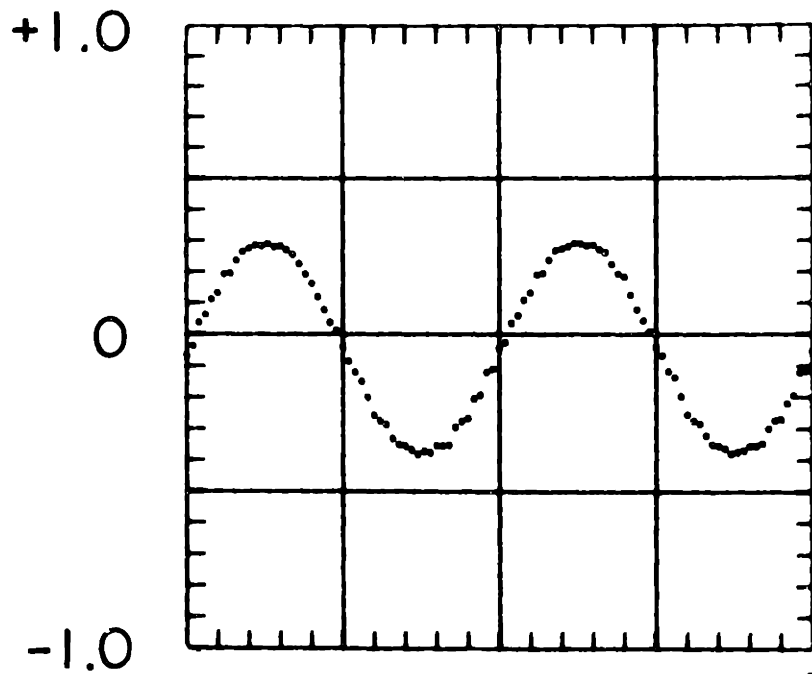
Averaged probe-microphone pressure waveform and current waveform in response to 2 kHz electric stimulus.

In (a), microphone pressure waveform; in (b), current waveform. Averages consist of 100 points, interpoint time 10 μ sec. Each point in (a) is average of 1000 individual samples, in (b), each point is average of 100 samples.

PRESSURE AT PROBE
MICROPHONE (dynes/cm²)



ROUND WINDOW ELECTRODE
CURRENT (mA)



0 0.5 1.0 msec

STIMULUS FREQUENCY = 2 kHz

of frequency.

5.3.2 Response to acoustic stimuli.

Figure 5.5 shows the magnitude and angle of the voltage developed at the output of the probe-microphone amplifier measured from 20 Hz to 20 kHz in response to a tone at 80 dB SPL. Curve (1) was measured using flat amplifier frequency response (lower 3 dB frequency \approx 5 Hz), while Curve (2) was measured using the A weighting network of the microphone amplifier. The figure also shows the spectrum of the noise level found when the microphone output was recorded using the A network and with the stimulus turned off [Curve (3)]. Curve (4) was measured under the same recording conditions post-mortem. The peaks seen in Curves (1) and (2) at about 5, 10, and 15 kHz are caused by the characteristics of the tube (see Appendix II). The rise in Curve (3) at low frequency is evidently a measure of the spectrum of the EKG-synchronized signal. When the animal was dead, the noise baseline appeared essentially flat [Curve (4)]. Signals which fall sufficiently far above the level of Curve (4) represent actual microphone output amplified and weighted by curve A. *

The reduction in the weighted output seen at low frequencies [Curve (2)] is due to the effects of the weighting network; the actual

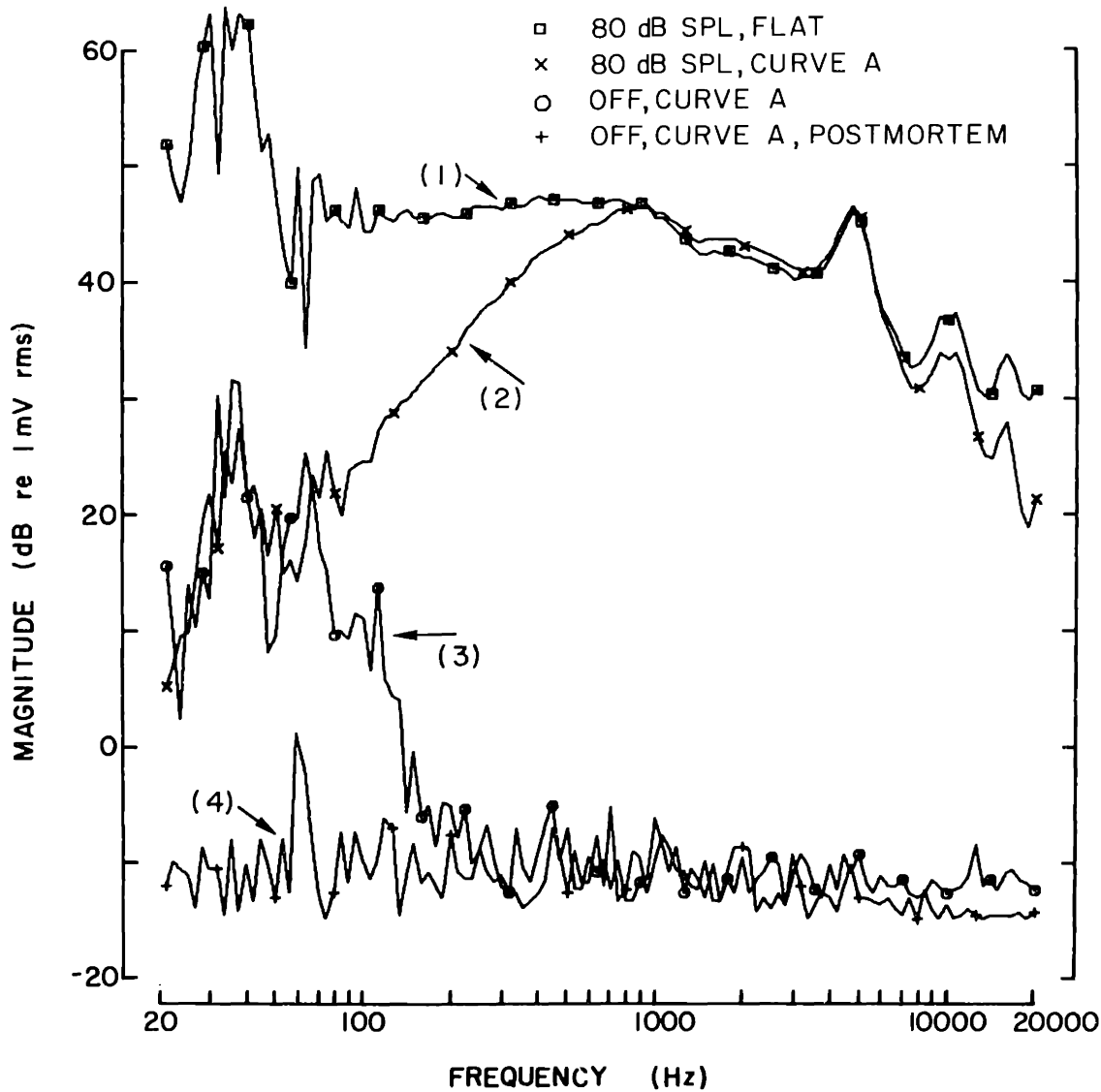
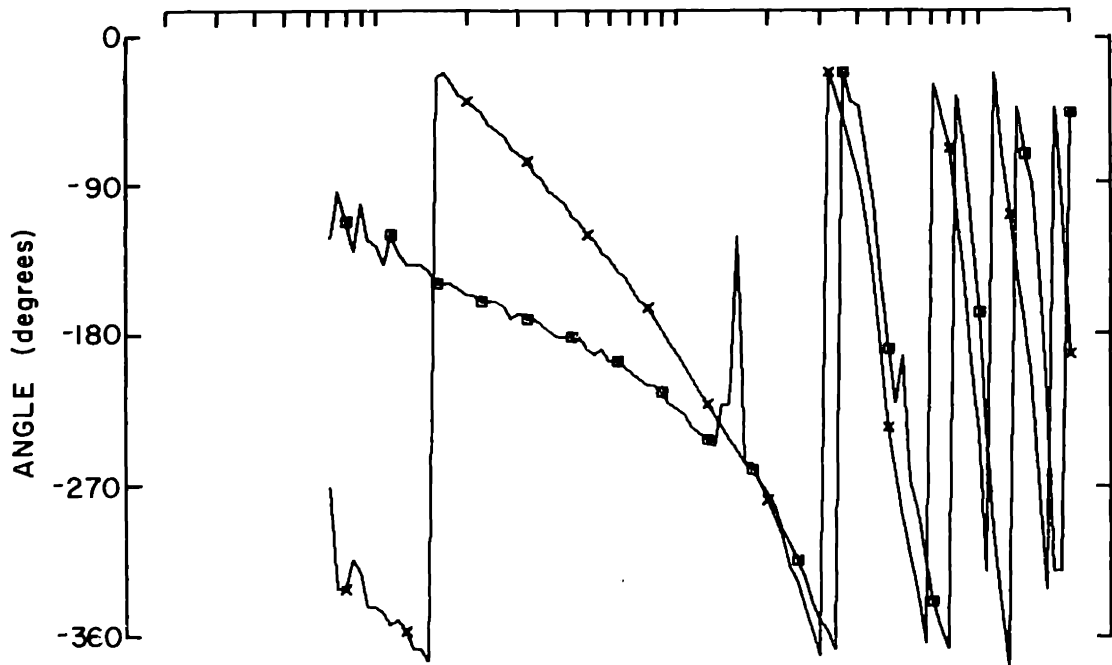
* Since Curve (4) is flat, it evidently is a measure of noise contributions which arise in the recording system at stages after the frequency response is shaped by the weighting network.

Figure 5.5

Output voltage of the probe-microphone amplifier under different recording conditions.

Curves (1) and (2) show magnitude and angle of microphone-amplifier (MA) output voltage recorded for a constant level (80 dB SPL) of sound pressure at tympanic membrane. Angle of MA output is referred to electric input to the capacitor earphone. Curve (1) was measured using flat MA frequency response (10 Hz - 200 kHz); in (2), response was remeasured with MA weighting network A switched in. For Curves (3) and (4), the A weighting network was left in and stimulus was turned off; curves show noise levels of the measuring system. Data in Curve (3) obtained while the animal was alive, data in Curve (4) obtained post-mortem. For conditions of (3) and (4), response is unrelated to the stimulus and no phase is defined. For all curves, MA midband gain was 60 dB. In (1) and (2), MA output voltage above about 70 Hz is response to the sound-pressure stimulus. The data can be expressed as sound pressure at the probe microphone by correcting for i) the transfer function of the microphone amplifier, and ii) the absolute sensitivity and frequency response of the microphone cartridge. The angle of probe-microphone sound pressure can be referred to sound pressure at the tympanic membrane by correcting for the phase characteristics of the earphone system. Plotted symbols identify individual curves (see figure 5.1). Cat M72.

VOLTAGE OUT OF MICROPHONE AMPLIFIER



microphone output is nearly flat from 80 Hz to 1 kHz [Curve (1)]. Output decreases gradually at frequencies above 1 kHz. Interpretation of this roll-off requires knowledge of the detailed transmission characteristics of the tube. It may be partially attributable to smaller round-window displacements at these frequencies.

The phase data shown represent phase of recorded voltage referred to voltage delivered to the capacitor earphone, and is influenced by the phase characteristics of both the acoustic stimulus system and the probe-tube measuring system. By correcting for the characteristics of the microphone cartridge, microphone amplifier, and acoustic stimulus system, data such as those shown in figure 5.5 can be expressed in terms of sound pressure at the probe-microphone diaphragm referred to sound pressure at the tympanic membrane.

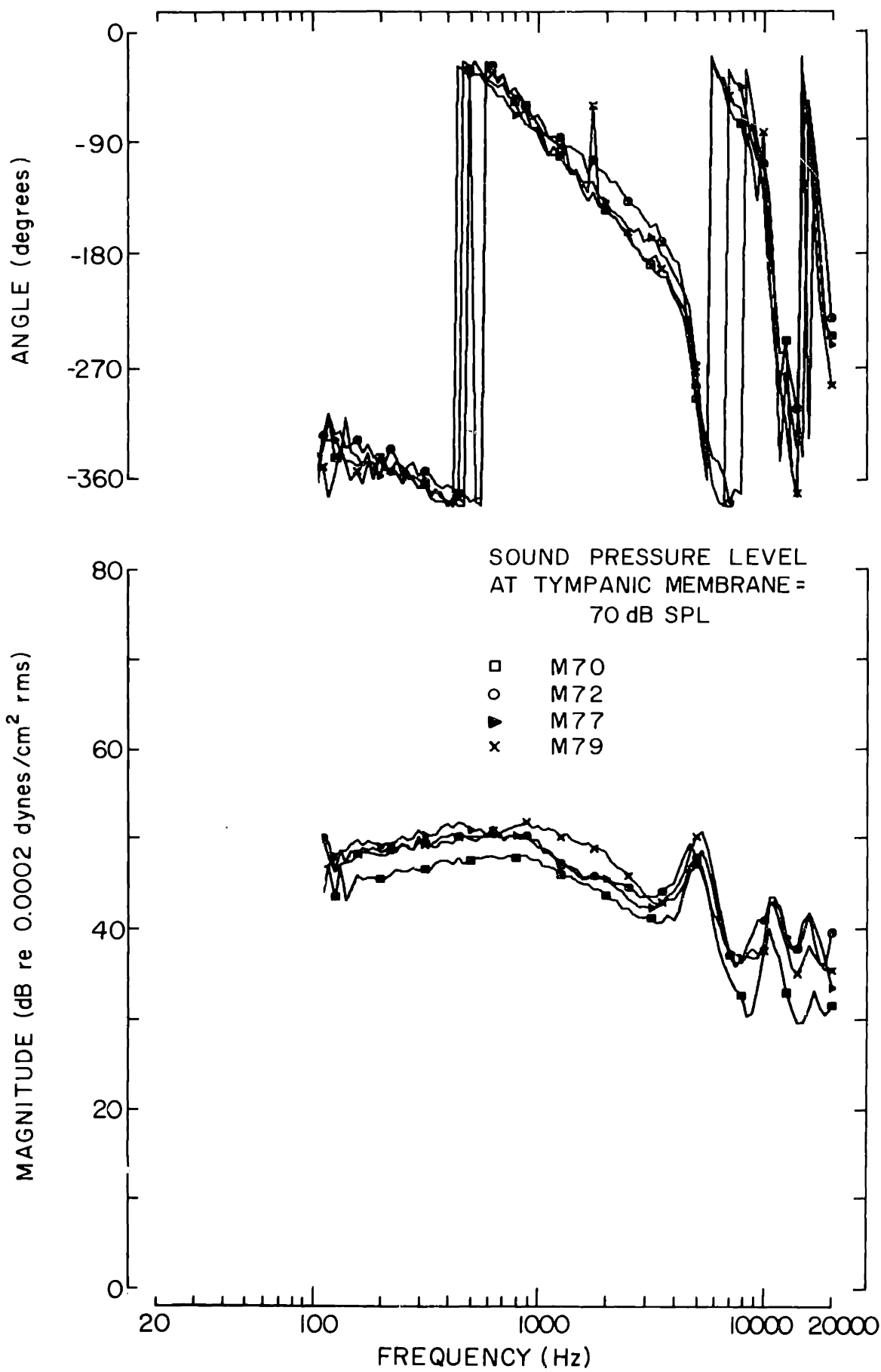
Figure 5.6 shows data from four experiments expressed in this way. The responses shown were recorded under comparable conditions and at a stimulus level of 70 dB SPL. Response magnitudes are flat within 3 dB below about 1 kHz, and general roll-off in magnitude occurs above a few kHz. Peaks at about 5, 10, and 15 kHz are evidently produced by resonances in the probe tube (see Appendix II). Although measurements are not shown at low frequencies, where signals are close to or below the noise level, the figure shows that the microphone pressure at low frequency approaches the phase of the stimulus ($0^\circ = -360^\circ$), indicating that inward motion of the tym-

Figure 5.6

Sound pressure developed at the probe microphone in response to acoustic stimulus in four experiments.

Sound pressure at tympanic membrane was a constant 70 dB SPL at all frequencies. Phase curves represent angle of probe-microphone sound pressure referred to sound pressure at tympanic membrane. Data are not shown below 100 Hz because of high noise level at low frequencies. Plotted symbols identify individual curves (see figure 5.1).

SOUND PRESSURE AT PROBE MICROPHONE



panic membrane causes the round-window membrane to deflect outward. At high frequency, probe-microphone pressure progressively lags the sound pressure at the tympanic membrane. Part of this lag may be introduced by middle-ear transmission characteristics. Also, since the probe tube is approximately a wavelength long at 10 kHz, a significant part of this lag is evidently attributable to propagation delay through the tube. The variation in response magnitudes for these four experiments is at most 8 dB, and phase variation is less than 45° . This variability is within the range of the variability in middle-ear transmission found by Guinan and Peake (1967).

For the range of frequencies for which the length of the tube is much less than a quarter wavelength, pressure distribution in the microphone system is uniform and the system behaves as a compliance. For these low frequencies, microphone output is proportional to the volume displacement of the round-window membrane. For example, below about 1000 Hz, the measurements of figure 5.6 show sound-pressure levels of about 50 dB SPL, or 0.06 dynes/cm^2 rms. The acoustic compliance of the tube system is given in Appendix II as about $5.6 \times 10^{-8} \text{ cm}^5/\text{dyne}$, and thus the round-window volume displacement for 70 dB sound-pressure level at the tympanic membrane is $3.3 \times 10^{-9} \text{ cm}^3$ rms. This value is not significantly different from the low-frequency volume displacement of the stapes footplate ($2.9 \times 10^{-9} \text{ cm}^3$ rms at 70 dB SPL) in the average data of Guinan and Peake

(1967). Since middle-ear transfer characteristics show inter-animal variation of several dB, this result is not inconsistent with the idea that the outward volume displacement of the round-window membrane is normally equal to the inward volume displacement of the stapes footplate. *

5.3.3 Response to electric stimuli.

Figure 5.7 shows the sound pressure developed at the probe microphone for four levels of electric current. At most frequencies the response magnitude increased 5 dB when the stimulus was increased 5 dB, indicating that the microphone output is proportional to the current level. At low frequency, however, a clear non-linearity is seen at the two highest current levels. Here the response increments are much greater than the stimulus increment, and the response is not proportional to the stimulus. At the low frequencies, where the response amplitude shows non-linear behavior, the phase shows rapid change with frequency, changing by 720° between 60 and 250 Hz. At high frequency (> 3 kHz), microphone pressure progres-

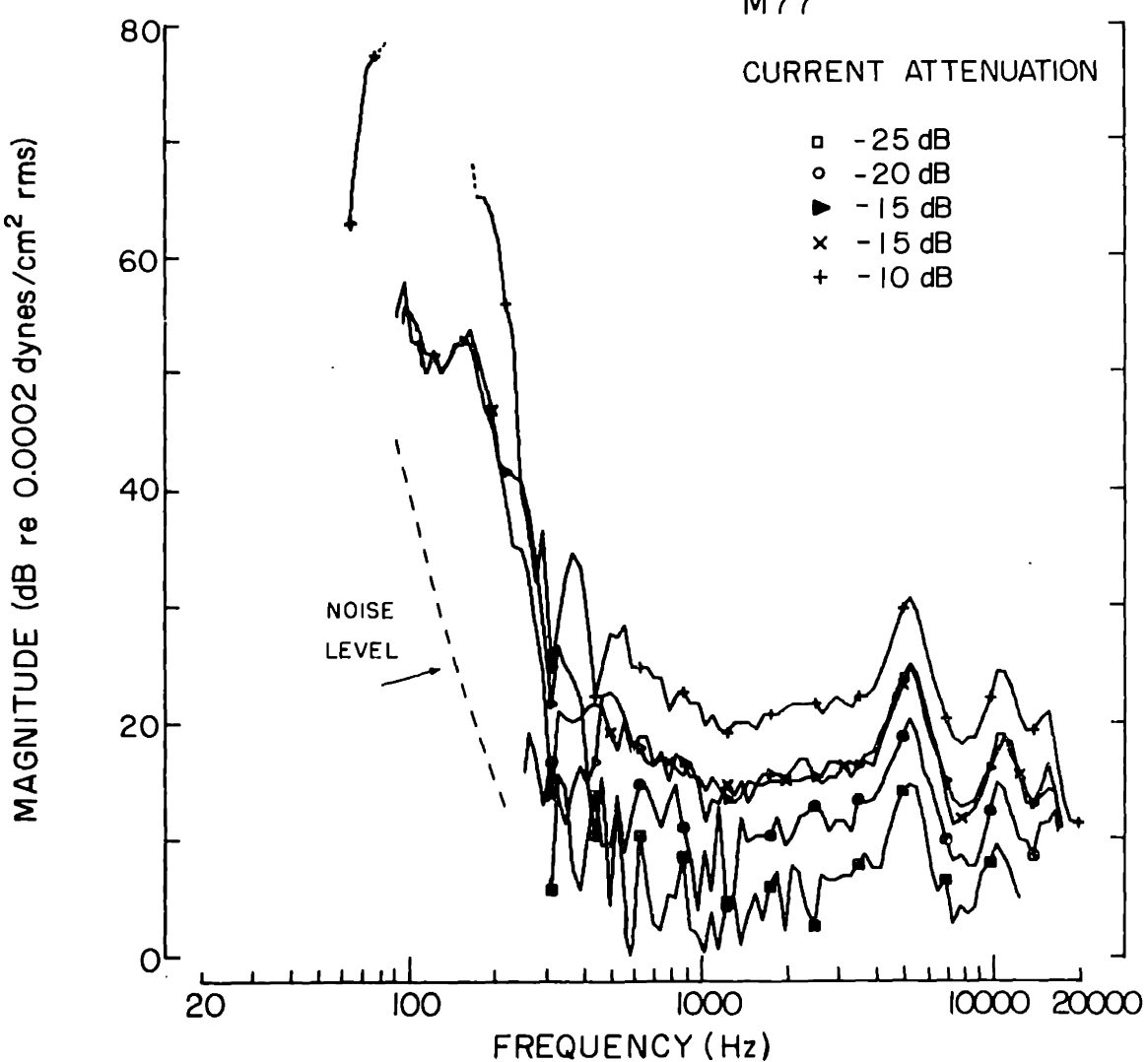
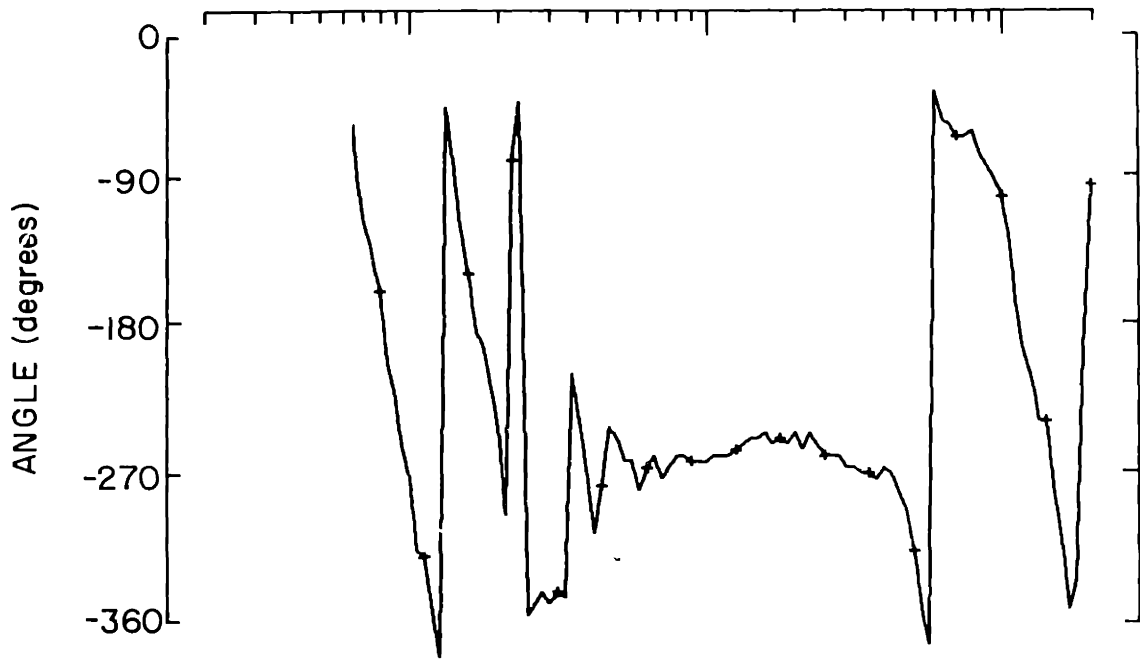
* Møller (1963) has reported measurements which show that the linear displacement of the round-window membrane and the displacement of the long process of the incus depend on frequency in the same way, and from this, he concluded that round-window motion was tightly coupled to both the stapes and the malleus. Tonndorf and Tabor (1962) have indicated that mechanical signals in the cochlea are reduced less by blockage of the round window than by blockage of the stapes, possibly because of other paths for volume velocity flow.

Figure 5.7

Sound pressure at the probe microphone in response to four levels of sinusoidal electric stimulus.

Magnitude and angle of microphone sound pressure are shown. Data are plotted only at frequencies for which response was 10 dB above the noise level. Response was measured at constant settings of the attenuator controlling the electric stimulus; current at constant attenuation varied as shown in figure A1.1. In the vicinity of 100 Hz, response at the 10 dB attenuator setting exceeded the dynamic range of the recording equipment. Response was measured twice at the 15 dB attenuator setting and the two curves are superimposed. Signal-to-noise ratio in data obtained at the lower current levels is poor; below 300 Hz responses at 15, 20, and 25 dB attenuations were below the noise level (dashed line). Angle of microphone sound pressure is referred to positive round-window electrode current; the phase curve shown was obtained at the highest (10 dB attenuation) current level. Plotted symbols identify individual curves (see figure 5.1).

SOUND PRESSURE AT PROBE MICROPHONE



sively lags stimulus current, but the phase does not change as rapidly as the response to tone shown in figure 5.6.

Figure 5.8 shows the response to electric stimulation in three ears. (Response of these ears to acoustic stimuli was shown in figure 5.6.) In each set of data shown the current evoked the low-frequency non-linear response just described. Above 300 Hz, response behaved linearly. Both the magnitudes and the angles of the linear, high-frequency responses from these three experiments are fairly close to each other. Below 18 kHz, the data show a magnitude variation of < 4 dB and a phase variation of $< 30^{\circ}$; at 20 kHz, magnitudes differ by about 8 dB.

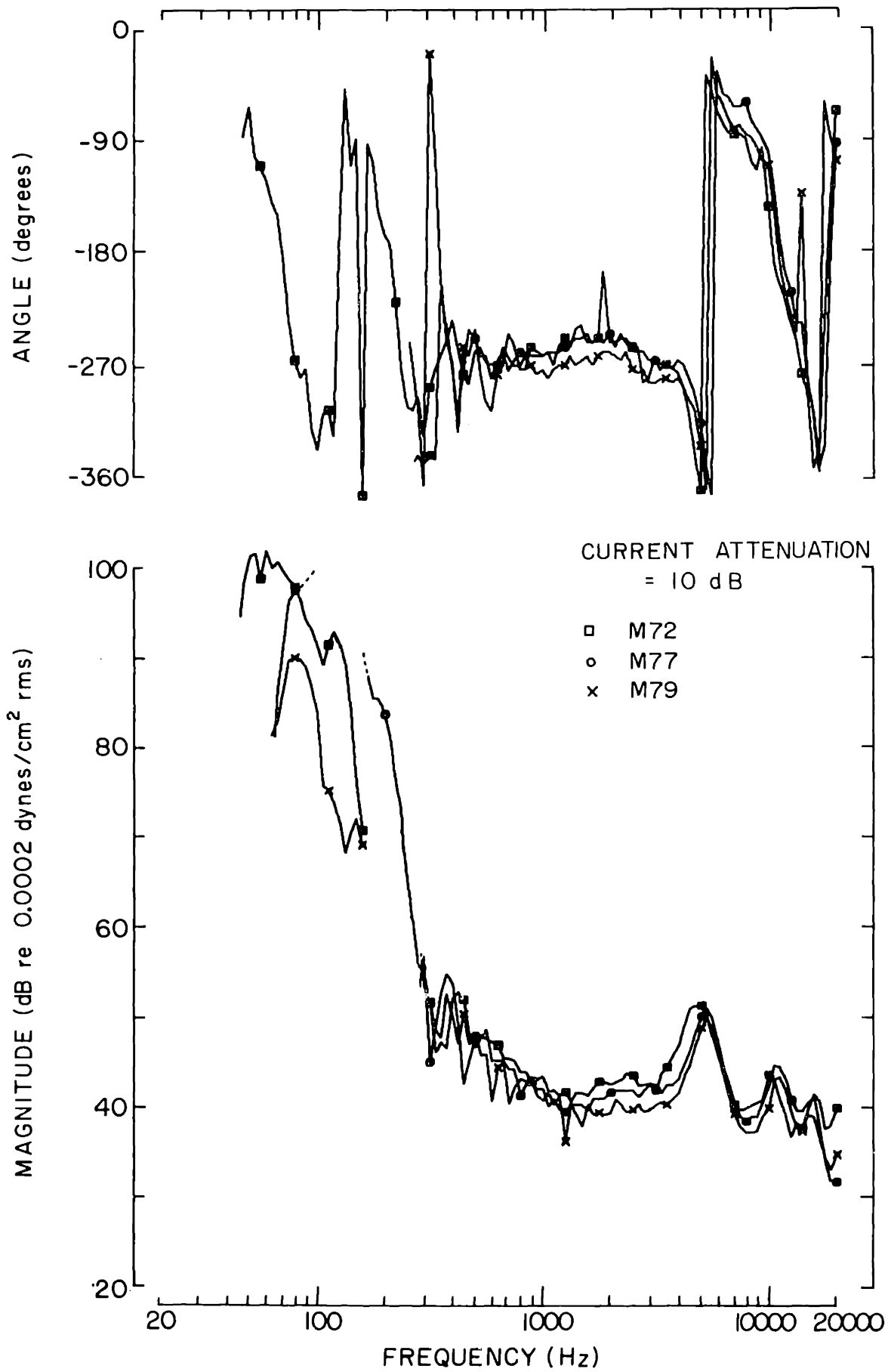
The non-linear low-frequency response magnitudes in these experiments are not nearly as close as the high-frequency responses. The non-linear response was not extensively studied as interest was primarily directed to the linear electro-mechanical phenomenon found at higher frequencies. It was observed, however, that the non-linearities did not appear in post-mortem measurements, suggesting that it may have had a physiological origin. One possibility is that low-frequency electric stimuli excited one or both middle-ear muscles, and vibrations set up by the resulting contractions were detected by the microphone. Middle-ear-muscle contraction was decoupled from the ossicular chain by cutting the tendons, but muscle-generated vibrations could appear in microphone output much as heartbeat-

Figure 5.8

Sound pressure developed at probe microphone in response to sinusoidal electric stimuli in 3 cats.

Data from three of the experiments for which response to tone was shown in figure 5.6 are superimposed. In each experiment magnitude and angle of response were measured at 10 dB settings of the attenuator controlling the electric stimulus. Current varied with frequency approximately as shown in figure A1.1; at any particular frequency currents in the three experiments all fell within a 2-dB level range. Data are shown only at frequencies where response was 10 dB above the noise level. Between 100 and 200 Hz, response in M77 exceeded the dynamic range of the recording equipment and no data are shown. Below 300 Hz, phase data are shown for only one measurement.

SOUND PRESSURE AT PROBE MICROPHONE



related vibration does. As described in Appendix III, middle-ear muscles were visually observed to respond to high-level electric stimuli.

In the range of frequency above 300 Hz, the data of figure 5.7 show a mechanical response that is linearly related to the electric stimulus. Figure 5.8 shows that this response is similar in different animals; the reproducibility of this response from animal to animal seems to be about as good as the reproducibility of the response to acoustic stimuli.

5.3.4 Equivalence of sinusoidal acoustic and electric stimuli based on round-window motion.

To compare the effects of electric and acoustic stimuli in production of round-window motion, the following procedure was used. For the range of frequency for which response was linearly related to the stimulus, it was possible to determine transfer functions relating probe microphone pressure P_m to each stimulus. If the microphone responses to the acoustic and electric stimuli are denoted P_m^a and P_m^e respectively, the transfer functions are

$$\frac{P_m^a}{P_d} = H_a$$

and

$$\frac{P_m^e}{I_e} = H_e$$

The transfer functions are useful in determining P_m for values of P_d and I_e other than those for which response was measured, and can be used to show the relationship between equivalent stimuli (stimuli which produce equal response). The equal-response condition

$$P_m^e = P_m^a$$

implies that

$$H_e I_e = H_a P_d$$

or

$$\frac{P_d}{I_e} \Big|_{P_m^e = P_m^a} = \frac{H_e}{H_a}$$

$$\equiv Q_m$$

where Q_m represents the ratio of equivalent stimuli based on round-window motion. Expressed in this form, the mechanical measurements can be compared to the stimulus equivalence based on neural responses obtained in the preceding chapter.

The stimulus equivalence ratio Q_m for a typical cat is shown in figure 5.9. The shaded area in the figure indicates the range of data from 7 ears. Above about 4 kHz, the magnitude ratios are essentially flat. A local minimum occurs at about 1.5 kHz, and below this frequency the ratio rises approximately as $1/f$. The phase angle of the ratio approaches -270° at low frequency, and the angle leads

Figure 5.9

Stimulus equivalence ratio Q_m based on measurements of the motion of the round-window membrane.

The data shown are the ratio of transfer functions

$$\frac{P_m^e / I_e}{P_m^a / P_d}$$

which, under the equal-response condition

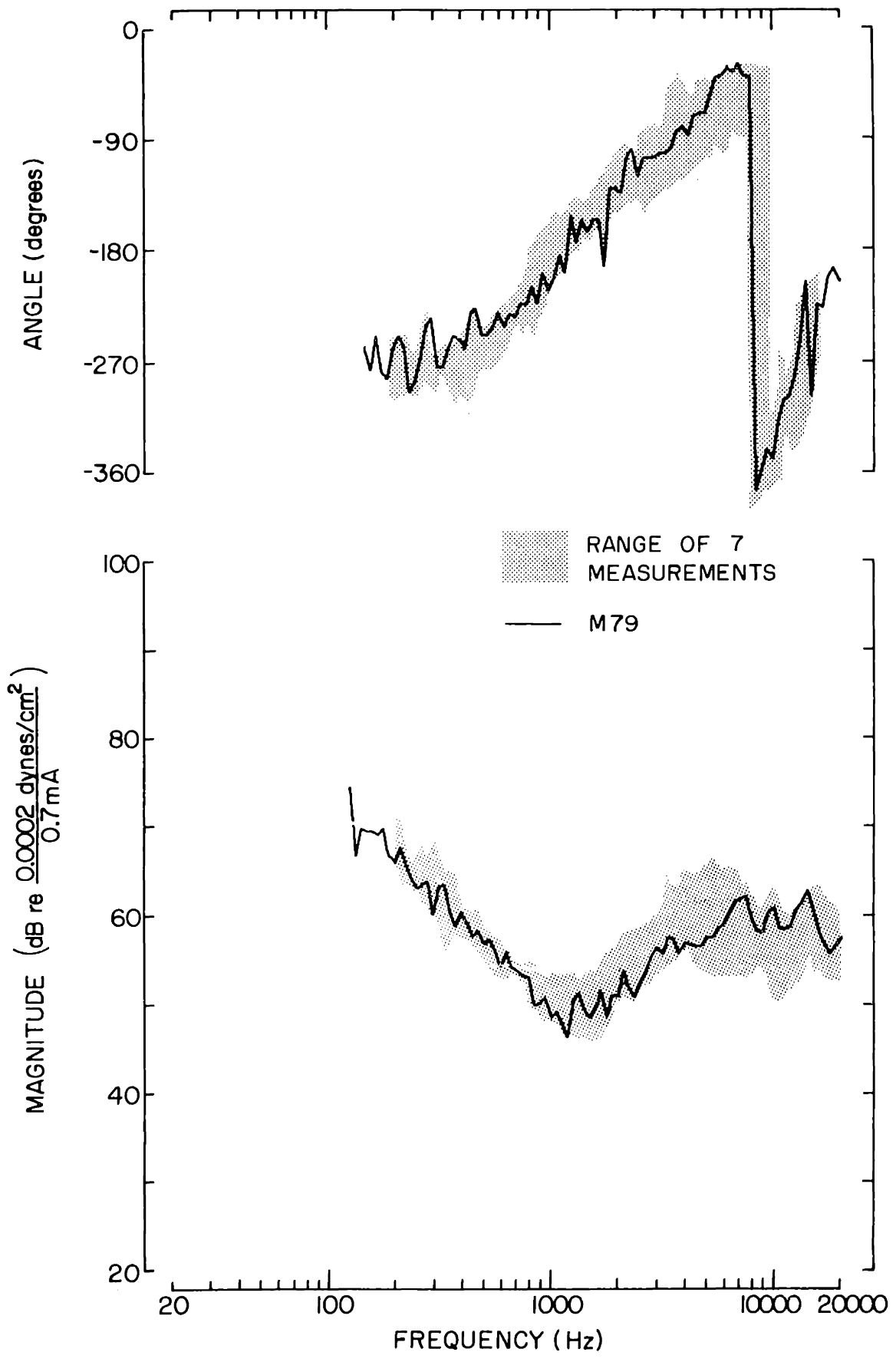
$$P_m^a = P_m^e$$

reduces to the ratio of equivalent stimuli

$$Q_m \equiv \frac{P_d}{I_e} \Big|_{P_m^a = P_m^e}$$

Solid curves show magnitude and angle of this function measured in one ear; shaded area shows the range of data from 7 ears. The measured quantities which enter into this ratio were considered valid if response was at least 10 dB above the noise level, and data are shown only at those frequencies where this condition was met.

SOUND PRESSURE AT TYMPANIC MEMBRANE
ELECTRODE CURRENT



progressively with increasing frequency.

The function Q_m shown in this figure can be compared with the corresponding functions Q_f based on nerve-fiber response in figures 4.14 and 4.21. While these functions show some general similarities, significant differences exist. A discussion of the differences between Q_f and Q_m is included in Chapter VI.

5.4 Responses in Modified Preparations.

The experiments described in this section were designed to explore possible sources or mechanisms underlying the linear electromechanical transduction phenomenon defined above.

5.4.1 Response of the normal cochlea to modified stimulus current distribution.

In one type of experiment, the effect of location of the stimulating electrodes was studied. The microphone output was measured when both stimulus electrodes were contacting the round-window membrane and when both electrodes were on the periosteum covering the cochlear capsule a few mm apart (neither one contacting the round window). In both of these cases mechanical response was below the noise level at most frequencies. Since response to the same level of current flowing into the round window was usually more than 20 dB above the noise level, these observations indicate that the reduction in mechanical response was at least 20 dB. These results are

consistent with the notion that current must flow into the cochlea in order to develop appreciable mechanical response. However, the intracochlear electric signals which result from this current flow have not been specified (see Appendix IV).

In some experiments, attempts were made to stimulate smaller portions of the cochlea with suitably placed intracochlear electrodes. However, it was not possible to introduce electrodes which could carry sufficient current (of the order of 100 μ A) without also appreciably altering characteristics of the cochlea, and the results of this type of experiment were not satisfactory.

Thus it was not possible to specify electric signals associated with possible sites of transduction or to deliver stimuli which might selectively excite hypothesized transducer mechanisms. Consequently other types of experiment were devised to explore the mechanism of the transducer in other ways.

5.4.2 Post-mortem responses.

As indicated in Chapter II, a large (100 mV) direct voltage, the endocochlear potential (EP), normally exists between scala media and the other two scalae. The experiments described in this section were conducted to determine whether cochlear electromechanical transduction depended on this bias voltage.

Since EP is diminished during anoxia and after death (Békésy,

1960, pp. 684-703), one way to investigate the dependence of the transduction on EP was to observe the post-mortem behavior of the mechanical response to electric stimuli. Figure 5.10 shows an example of the time course of the recorded magnitude and phase of the probe microphone output recorded when the animal was sacrificed. The magnitude of round-window voltage E_{rw} in response to tone is shown for comparison. At about 5 minutes, the magnitude of the response to the electric stimulus shown in (a) drops by about 3 dB; the response to the tone in (c) remains essentially constant. The phases of both responses show little change. The magnitude of E_{rw} shown in (d) diminishes by 5 dB in the first 5 minutes, and has fallen 25 dB at 8 minutes. In the two hours following the period represented in the figure, little further change occurred in microphone response to either stimulus. The figure demonstrates dramatic differences between the behavior of the mechanical response to the electric stimulus and the behavior of the cochlear microphonic potential.

The fact that response to the electric stimulus drops by only a few dB and shows no phase change indicates that the transduction is not proportional to EP, since EP is known to pass through zero and remain negative for long times after death (e. g. Békésy, 1960, pp. 684-703). Figure 5.11 shows the results of an experiment in which microphone output and EP were measured simultaneously. The figure shows large differences in the time course of mechanical response and

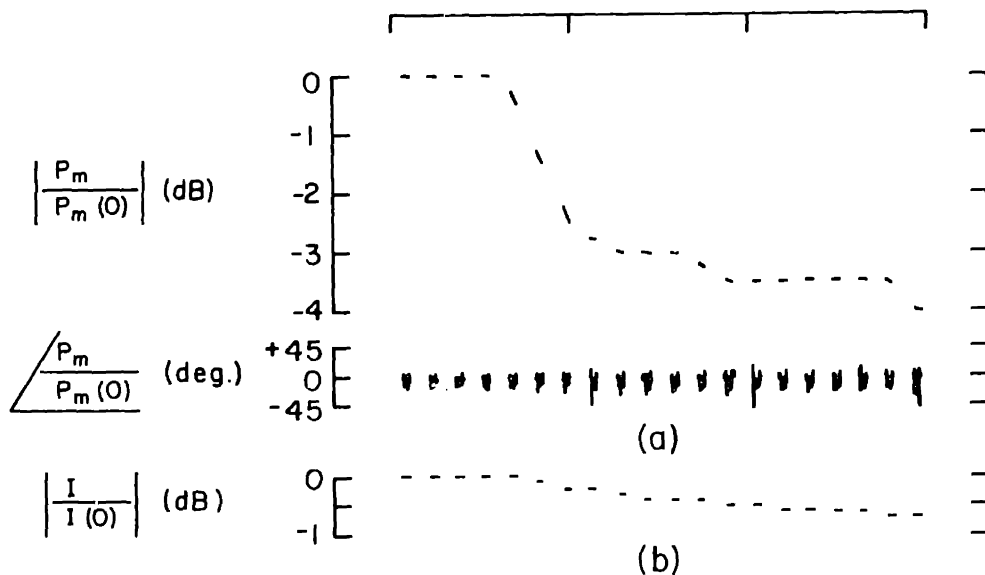
Figure 5.10

Probe-microphone response to tone and current and round-window voltage response to tone during transition from ante- to post-mortem values.

All quantities are normalized to their values at time zero. P_m , probe-microphone sound pressure; I_e , stimulus electrode current; E_{rw} , fundamental of round-window voltage. A 5 kHz stimulus sinusoid was connected alternately to the electrode and earphone systems. At zero on the time axis, 2 cc of Dial was injected near the heart. Data in (a) and (c) are magnitude and angle of normalized probe-microphone output. In (a), response to current, in (c), response to tone. In (b), normalized magnitude of electrode current from current probe output. In (d), normalized round-window voltage in response to tone. Note that vertical scale in (d) is different from other magnitude scales. For (c) and (d), sound pressure at tympanic membrane = 68 dB SPL. Initial values in (a), $|P_m(0)| = 30$ dB SPL; in (b), $|I_e(0)| = -11$ dB re 0.7 mA rms; in (c), $|P_m(0)| = 50$ dB SPL; in (d), $|E_{rw}(0)| = 28$ dB re 1 μ V rms. Phase data in (a) are noisier because of lower signal-to-noise ratio. Data shown were replotted from the original chart record onto convenient vertical scales.

M79

ELECTRIC
CURRENT
(5.0 kHz)



ACOUSTIC
TONE
(5.0 kHz)

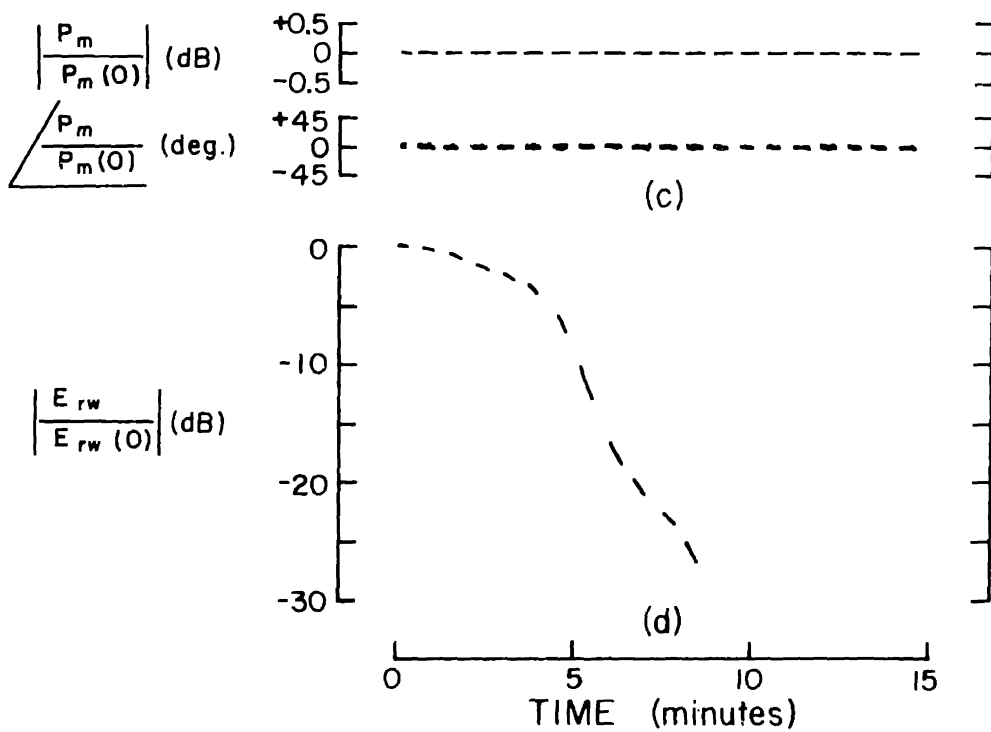
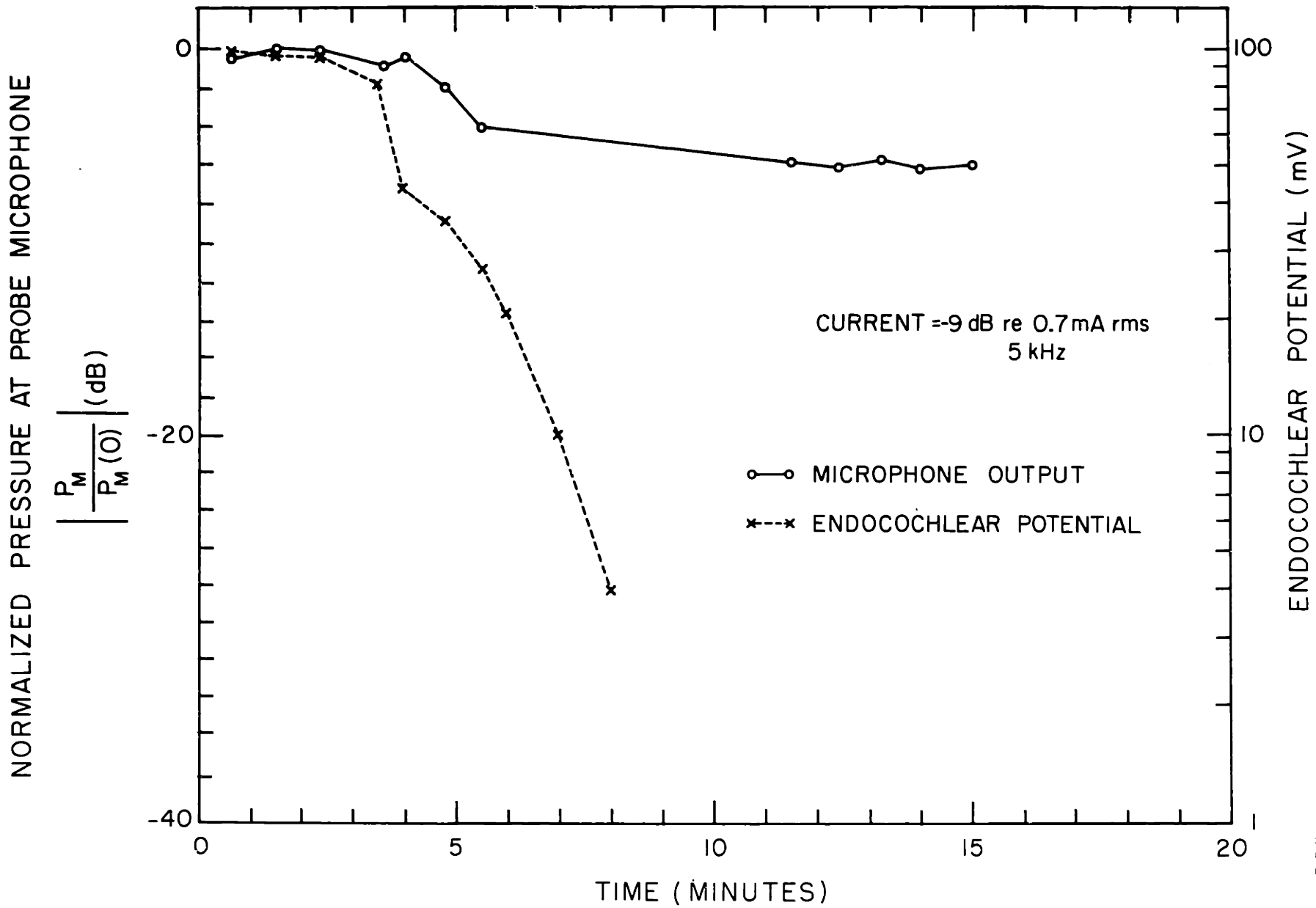


Figure 5.11

Time course of endocochlear potential and of probe-microphone response to 5 kHz current recorded during asphyxia.

Circles are endocochlear potential (EP), crosses are magnitude of microphone response $|P_m|$. EP was measured with a KCl-filled micropipette introduced through the round-window membrane and into scala media. At zero on the time scale the tracheal cannula was clamped shut. Microphone response is normalized to its value before asphyxia was begun ($|P_m(0)| = 31$ dB SPL). In the period shown, response was repeatedly measured as a function of frequency; data points are taken at times when stimulus frequency was 5 kHz. EP is plotted on a logarithmic scale for comparison with time course of microphone response. At approximately 9 minutes, EP passed through zero and became negative. Cat M64.



EP, beginning at about 3 to 4 minutes.

An example of the frequency dependence of both ante- and post-mortem response to electric stimuli is shown in figure 5.12. At frequencies above about 1.5 kHz, response magnitude post-mortem is reduced by about 3 dB, while below 1 kHz, no difference is apparent in the two magnitude curves. Ante-mortem response is shown only above about 300 Hz because of the high spectral level of the low-frequency EKG-synchronized signal described at the beginning of the chapter. Post-mortem, however, this signal is eliminated; the desired response was found as low as 30 Hz. Below 1 kHz the ante-mortem response magnitude appears to behave as $1/f$, although the data exist only for about 2 octaves. In the post-mortem response, $1/f$ behavior extends over 6 octaves. It is possible that the $1/f$ behavior of ante-mortem response would also extend to low frequency, but it has not been measured below about 300 Hz. Where both curves exist, phase of both ante- and post-mortem response is essentially the same. At low frequency, the angles of microphone output referred to positive electrode current approaches a lag of 270° .

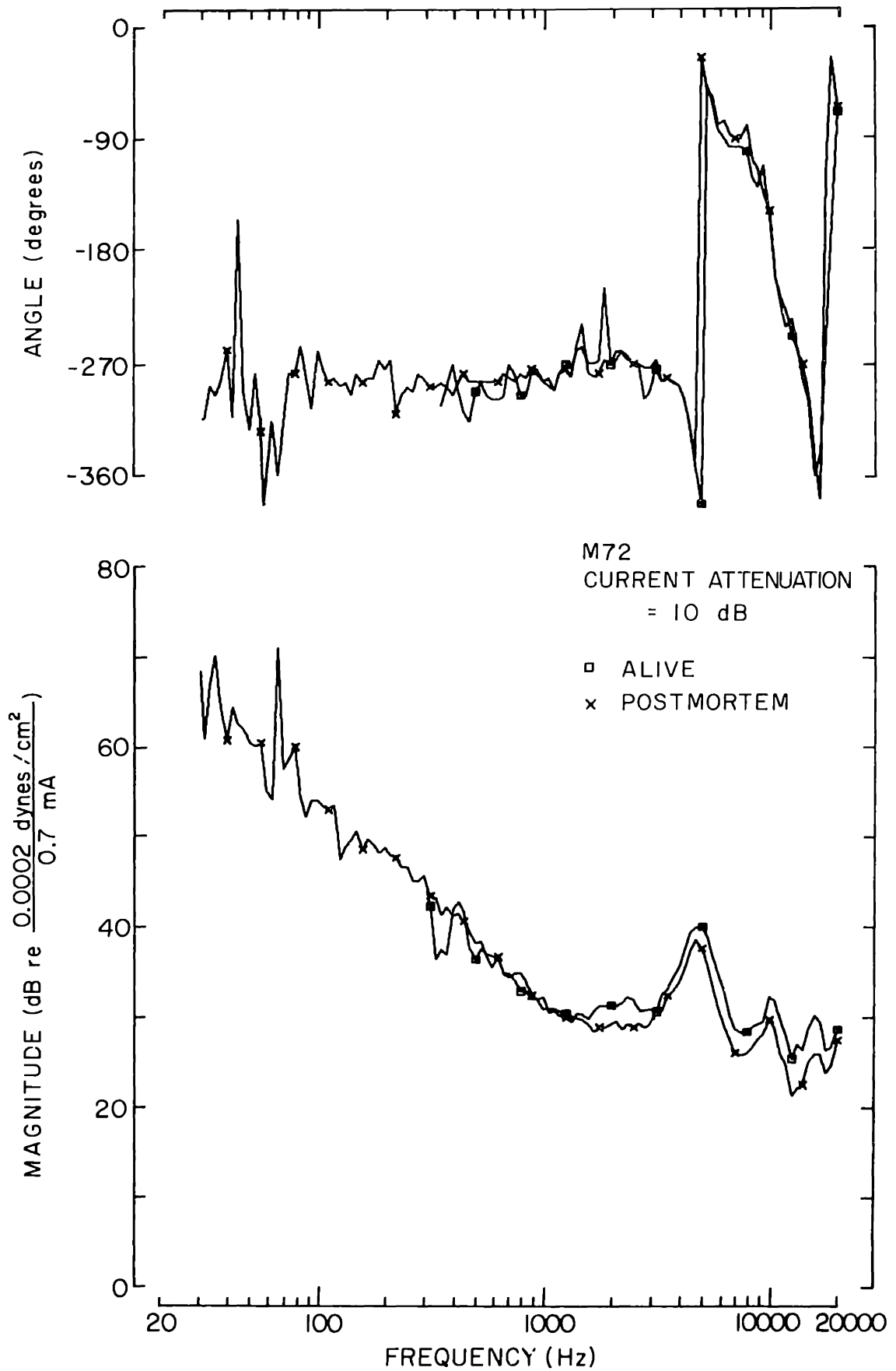
This figure shows that differences in the ante- and post-mortem responses to electric stimuli are not large at any frequency. However, figure 5.10 showed that the transition between the two values occurs rapidly, within minutes after death, and was not accompanied by significant change in mechanical response to tone. This result

Figure 5.12

The transfer function (sound pressure at probe microphone)/(electrode current) measured before and after death.

Ante-mortem data designated by squares, post-mortem by crosses. For each condition, microphone sound pressure and electrode current were measured at constant 5 dB setting of the attenuator controlling the electric stimulus. Current magnitudes differed by 3 dB at some frequencies; the ratio of microphone pressure to electrode current was formed to compensate for differences in the stimulus. Post-mortem data are shown over a wider range of frequency because low-frequency EKG-synchronized signal was eliminated. Elapsed time between ante- and post-mortem measurements, 2 hours. Plotted symbols distinguish curves from each other (see figure 5.1).

$$\frac{\text{SOUND PRESSURE AT PROBE MICROPHONE}}{\text{ELECTRODE CURRENT}}$$



suggests that a component of ante-mortem response may be attributable to a transducer mechanism which depends on vital processes. The remaining response was maintained after death, when normal cochlear mechano-electrical transduction had changed dramatically.

5.4.3 Responses in hair-cell-deficient cochleas.

To determine whether the electromechanical transduction bore any relation to the normal mechano-electrical transduction which is associated with the hair cell, the response was studied in cats having extensive ototoxically-induced hair-cell damage. In sufficient doses, the drug used (kanamycin) causes extensive degeneration of hair cells, while other cells appear to be normal and EP is maintained (Davis et al., 1958a; Engström et al., 1966).

Figure 5.13 shows the equivalence ratio Q_m from a hair-cell-deficient cochlea. The figure shows that both the magnitude and angle data from this cochlea fall within the normal range.

The extent of hair-cell damage in this cochlea is plotted in figure 5.14. Throughout the basal 18 mm of the cochlea (the entire basal turn and 2/3 of the middle turn) nearly all hair cells had degenerated. A few mm farther toward the apex, degeneration is classified as intermediate, while in the first few mm of the apical turn, hair-cell morphology appears normal. In all, hair cells in about 80% of this cochlea are missing.

Figure 5.13

Stimulus equivalence ratio Q_m in a cat having extensive ototoxically-induced hair-cell deficiency.

The solid curves show the stimulus equivalence ratio obtained as in figure 5.9. This cat had received injections of kanamycin sulfate which resulted in widespread hair-cell degeneration. The shaded area is replotted from figure 5.9 and represents the range of data from cats which received no drug and are presumed to be normal.

SOUND PRESSURE AT TYMPANIC MEMBRANE
ELECTRODE CURRENT

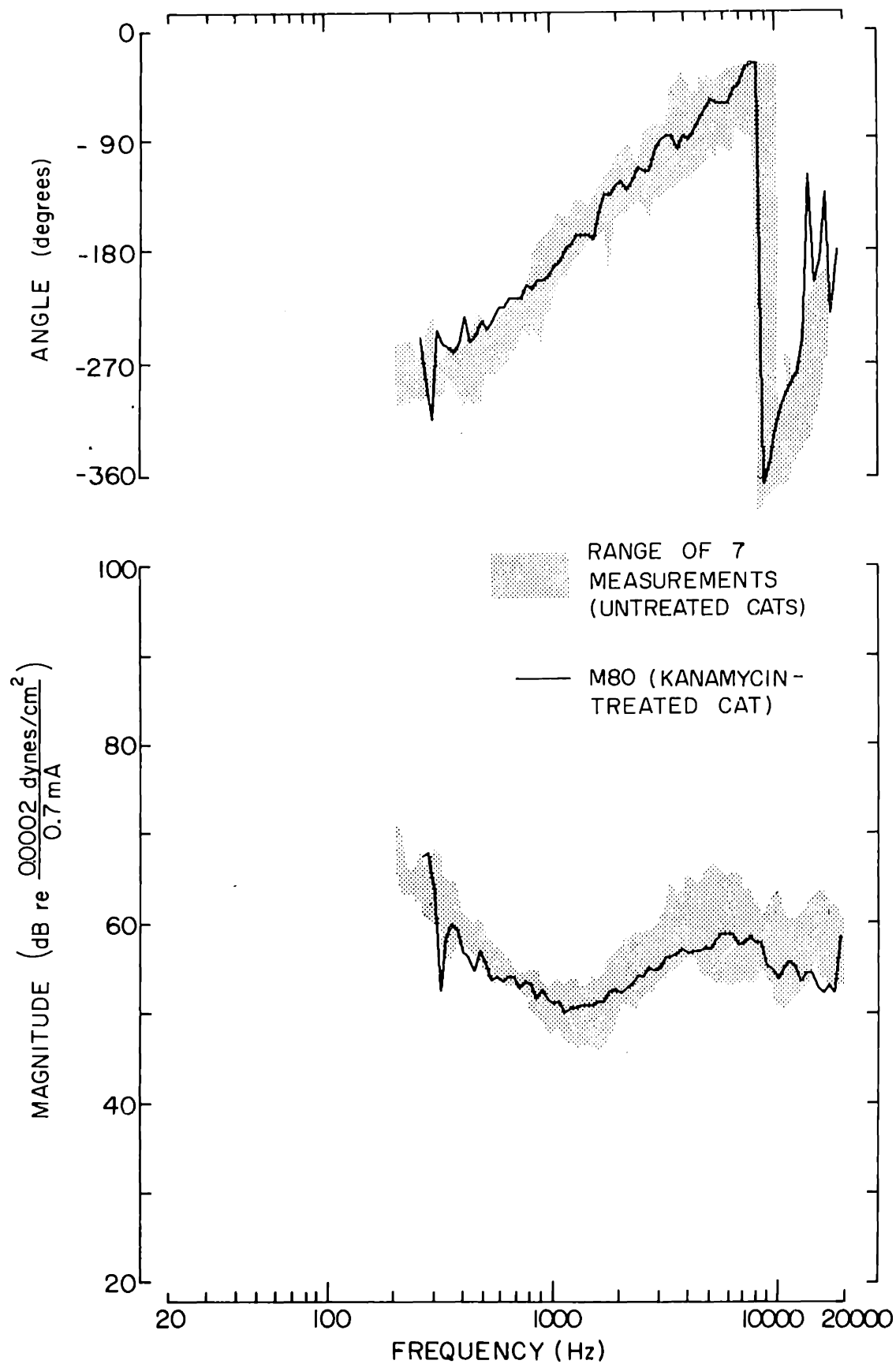


Figure 5.14

Schematic representation of hair-cell degeneration in the cochlea of the kanamycin-treated cat from which data of figure 5.13 were obtained.

The degree of degeneration in each row of hair cells was judged by viewing a surface preparation of the organ of Corti under phase-contrast. Categories of degeneration for each row are represented as a function of position along the longitudinal dimension of the cochlea; blackened area, > 90% of cells degenerated; shaded area, between 10 and 90% of cells degenerated; white area, < 10% of cells degenerated. IHC, row of inner hair cells; OHC 1, first row of outer hair cells; OHC 2, second row of outer hair cells; OHC 3, third row of outer hair cells. Kanamycin dosage, 200 mg/kg per day for 12 days, 163 days elapsed since last dose. Length of the basilar membrane in this cochlea, 24.5 mm. Approximate extent of each turn is indicated.

M80

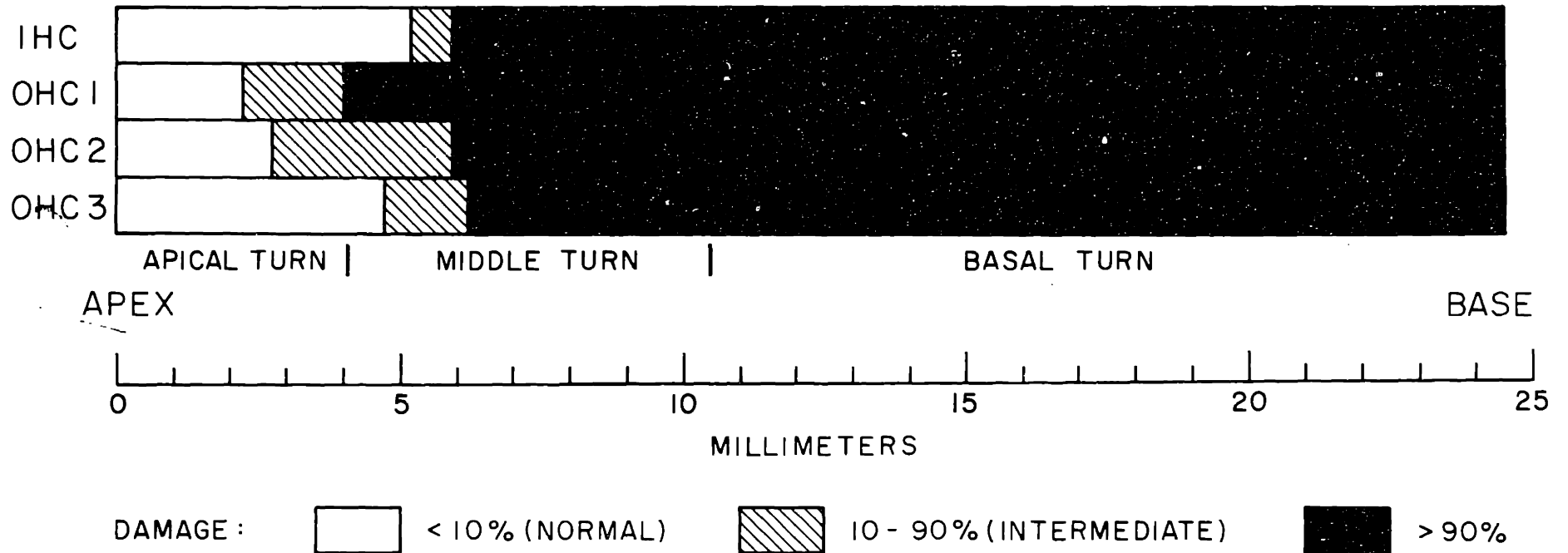


Figure 5.15 shows the round-window voltage E_{rw} in response to tone recorded in this cochlea. For comparison, the figure also shows the response recorded from an animal which had received no drug and which presumably had a normal complement of hair cells. At low frequencies the response from the kanamycin-treated animal is 10 dB below the response of the untreated ear, and above 1.5 kHz the difference is at least 50 to 60 dB. The phase of E_{rw} in the treated ear is also different from the normal response, changing by three cycles ($3 \times 360^\circ$) between 100 and 1000 Hz.

Although the cochlear mechano-electrical transduction represented by E_{rw} is distinctly abnormal in the kanamycin-treated ear, no significant departure from normal was seen in electromechanical transduction in this ear, as shown in figure 5.13. Similar results were obtained in another animal, in which hair cells throughout about 60% of the cochlea had degenerated. The electromechanical transduction appears to be maintained in the absence of large proportions of hair cells, as it is post-mortem in normal ears. In the hair-cell-deficient ears, however, the response might have differed slightly from the response that would have been recorded in that cat before administration of the drug. The experimental procedure did not permit comparison of the response before and after the hair cells degenerated, and if the degeneration resulted in a change in transduction comparable to the small change which accompanied death

Figure 5.15

Round-window potential E_{rw} in response to tone in the same kanamycin-treated cat from which data of figure 5.13 were obtained.

Magnitude and angle of fundamental component of round-window voltage recorded in response to 80 dB SPL sound pressure at tympanic membrane are shown. Solid curves, data from kanamycin-treated cat; dashed curves, data from an untreated (normal) cat. In both experiments, gross recording electrode contacted fluid on the surface of the round-window membrane. Angle of round-window voltage is referred to sound pressure at tympanic membrane. Data are shown only in the range of frequencies for which response-magnitude was 10 dB above the noise level.

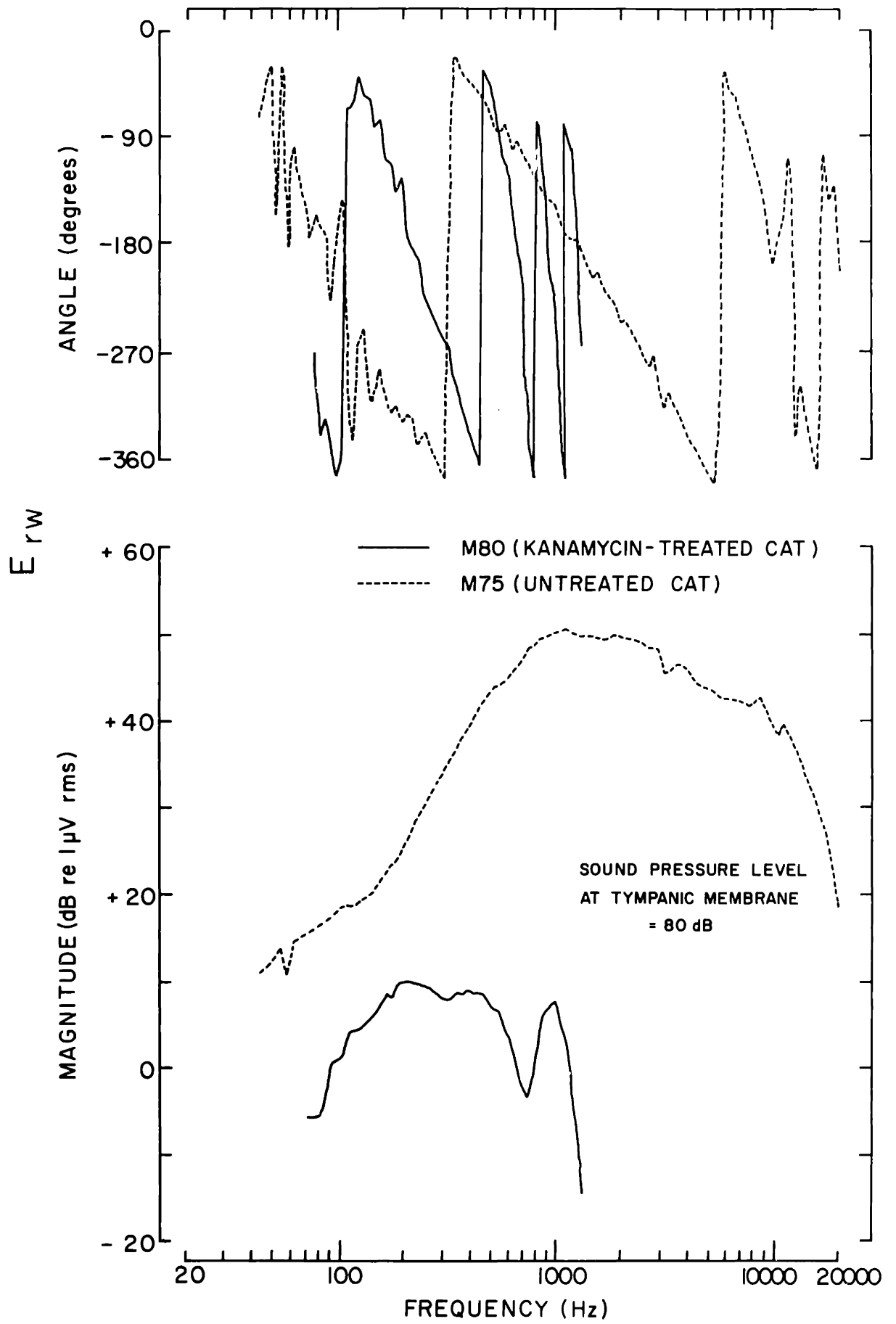


(figure 5.10), it would not have been detected. Response of the hair-cell-deficient ears was not studied post-mortem because the cochleas were fixed for histological examination immediately after the animal was sacrificed.

5.4.4 Role of electrodes in production of response.

Since the electromechanical transduction is evidently not closely associated with normal physiological transduction mechanisms, it was desirable to establish whether production of mechanical signals was associated with current flow into the cochlea or whether electro-mechanical transduction might have taken place at the point at which the metal (stainless steel) stimulating electrodes contacted tissue. This possibility could be tested by using non-metallic (fluid) electrodes to make contact with tissue.

Because of experimental problems, non-metallic electrodes were difficult to use to stimulate the living cochlea.* However, some evidence relating to the role of electrodes was obtained in another

* Low-impedance, electrolyte-filled electrodes were so large and the available space so limited that it was difficult to fit and seal both the electrodes and the probe microphone to the cochlea. With smaller, higher-impedance electrolyte-filled electrodes, it was necessary to raise stimulus voltage to produce adequate current flow. At this higher voltage level, the isolation of the stimulus and response systems was not sufficient, and signals electrically coupled into the microphone channel were larger than the response due to acoustic signals.

preparation.

Electric stimuli were applied to the temporal bone of a cat skull in which the cochlea had been filled with saline solution (0.9% NaCl). In this preparation, wider access to the cochlea was obtained, since all skin and muscle had been removed from the skull. Current was delivered through saline-soaked cotton wicks, one in contact with fluid in the internal auditory meatus, the other contacting intracochlear saline solution in the round window. No cement was applied to the cochlea, but petrolatum was used to seal the probe tube over the round window.

With this electrode configuration, the metal-tissue junction was excluded from the closed volume formed when the tube was sealed over the round window. Metal contacts with the fluid-soaked wicks were made at the point of support of the wicks, about 1 cm from the cochlea.

The mechanical response obtained in this preparation is represented in figure 5.16. Although this response is 5 to 15 dB smaller than the post-mortem response obtained using metal electrodes, this difference may be due to any of several electrical or mechanical differences in these two preparations. The significance of this result is that, in spite of these differences, an appreciable mechanical signal is developed when current is delivered through liquid contacts of the same composition as the electrolyte filling the bony labyrinth.

Figure 5.16

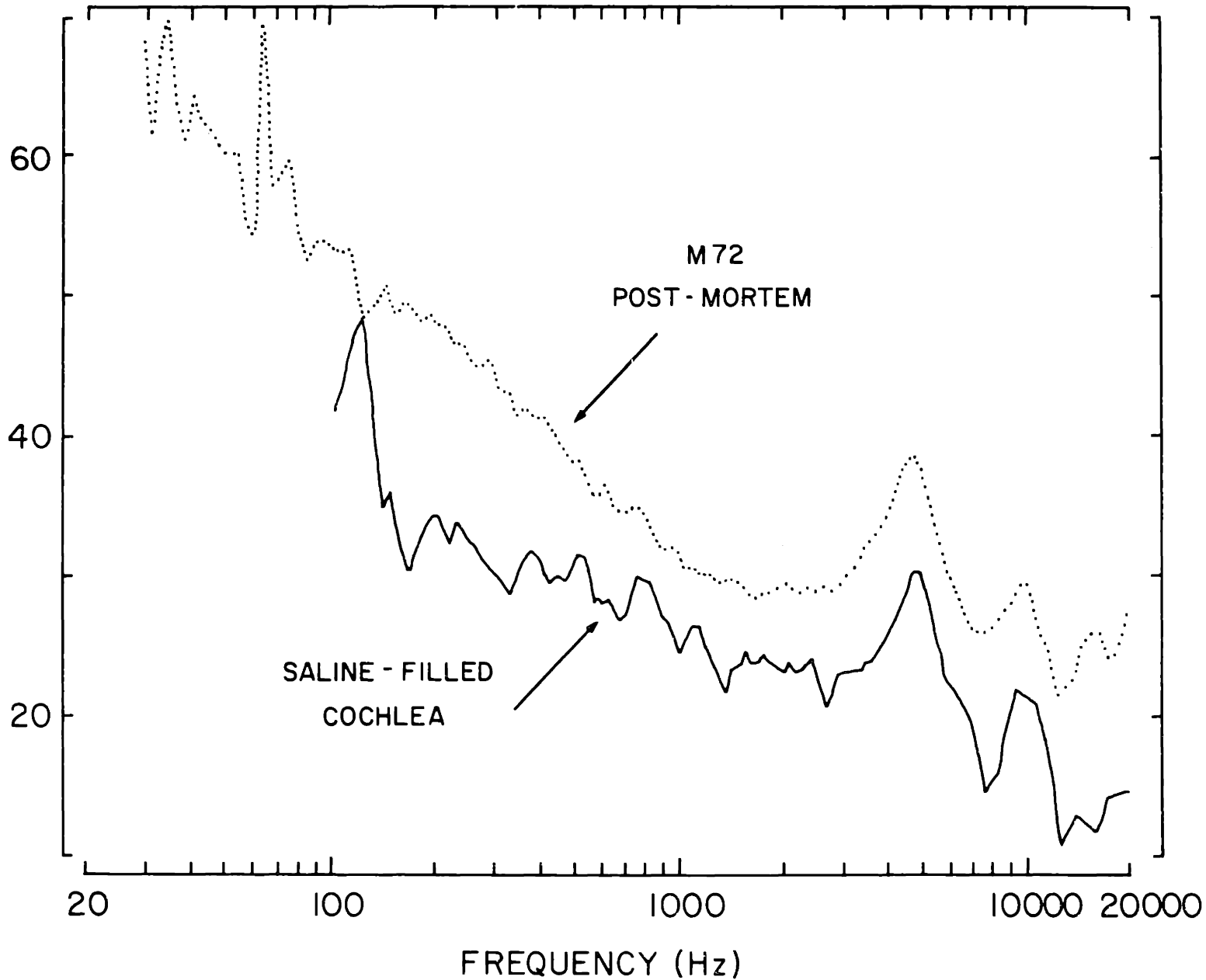
The ratio (sound pressure at probe microphone)/(electrode current) recorded from a saline-filled cochlea.

The temporal bone had been boiled to remove soft surface tissue. The stapes remained in the oval window, but the round-window membrane was absent. A saline solution (0.9% NaCl) was introduced into the cochlea through the open round window with a syringe. A combination of gravitational force and capillary action drew the solution into the cochlea. The bone was then soaked in the solution for about 1 hour. Saline-soaked cotton-wick electrodes (≈ 1 cm long) made contact with the cochlea; stainless-steel wires made contact with the wicks. Solid curve is $|P_m|/|I_e|$ for this preparation. Dashed curve is post-mortem measurement from cat M72, replotted from figure 5.12.

SOUND PRESSURE AT PROBE MICROPHONE

ELECTRODE CURRENT

MAGNITUDE (dB re $\frac{0.0002 \text{ dynes/cm}^2}{0.7 \text{ mA}}$)



According to this result, it appears that if non-metallic electrodes were used to stimulate the normal cochlea, the electromechanical transduction would still occur.

5.5 Summary.

Mechanical responses of the cochlea to sinusoidal electric and acoustic stimuli were studied using a microphone and probe system sealed over the round window. Based on the response of the mechanical detector, an equivalence ratio for acoustic and electric stimuli which is comparable to the neural-based ratio of the preceding chapter was obtained.

Behavior of electrical-to-mechanical transduction was studied post-mortem, and in cochleas having hair-cell deficiencies. In both types of experiment, the mechanical signals developed in response to electric stimuli did not differ greatly from the response in the normal, living cochlea, but transduction of acoustic signals into cochlear microphonic potential was distinctly abnormal. The results show that these two transduction phenomena are essentially independent. Finally, electrical-to-mechanical transduction was demonstrated in the saline-filled cochlea of a temporal bone which had been boiled and cleaned; this transduction occurred when contact to the cochlea was made with non-metallic electrodes and it is evidently not a phenomenon associated with the metal-tissue electrode interface. The

evidence indicates that current flow into the cochlea is required in order for the electromechanical transduction to occur.

CHAPTER VI.

DISCUSSION6.1 Origins of Neural Responses.

The data presented in Chapter IV have shown two types of auditory-nerve fiber response to electric stimulation of the cochlea. One type of response exhibited characteristics which were equivalent to response to the analogous acoustic waveforms, while other characteristics found were unique to the electric stimuli. On the basis of the data of Chapters IV and V, some conclusions can be drawn about the origins of these responses.

6.1.1 Class II response to sinusoid and α -component of response to shock.

The unique characteristics of response to electric stimuli are associated with the short-latency α -component of response to shock and with the Class II response to sinusoidal current. Characteristics of these responses suggest that these discharges are evoked by the action of the stimulus current on nerve membrane. Both of these response components exhibit 1) sharply defined threshold, 2) rapid increase of response for small increases of stimulus amplitude, and 3) adaptation of rate for supra-threshold stimuli.* These charac-

* Adaptation as a property of Class II response was illustrated in figure 4.8, and comparable adaptation of auditory-nerve response to high-rate shock was attributed to the short-latency (α) component (Moxon, 1967).

teristics are typical of nerve response to direct electric excitation [see Katz (1939); Bugnard and Hill (1935)]. Also, the frequency dependence of Class II response threshold (S_{II} tuning curve segments) is similar to results obtained by Hill et al. (1936) in a study of threshold of whole-nerve response to sinusoidal electric stimuli. Finally, the response to shock found in hair-cell-deficient cochleas was essentially the same as the α -component of response found in normal cochleas. In the absence of sensory hair cells, response is evidently the result of direct action of the electric stimulus on the remaining nerve fibers.

While the evidence is consistent with the direct action of electric stimuli on nerve membrane, a particular site of action is not indicated. As described in Appendix III, the effects of current delivered through the cochlear stimulating electrodes are not confined to the ear. Since the effect of current is so widely spread, an action potential could be initiated in an auditory-nerve fiber at almost any point.

6.1.2 Class I response to sinusoid and β -component of response to shock.

The β -component of nerve-fiber shock response and Class II response to sinusoid were similar to the response to analogous acoustic stimuli. On the basis of nerve-fiber response, and from the mechanical measurements of Chapter V, it appears that these respon-

ses can be explained in terms of mechanical signals which are generated in response to an electric stimulus.

All the similarities of nerve-fiber response to electric and acoustic stimuli are simply explained if the electric stimulus excites the cochlea mechanically. The relation of firing times of the β -component of shock response to fiber characteristic frequency and the tuning characteristics of Class I response to sinusoidal stimuli can be explained in terms of cochlear mechanics in the same way as the responses to acoustic stimuli (see section 2.1.6). Also, the inhibitory effect of OCB activity and the cancellation of electric and acoustic sinusoids are readily accounted for.

There are, however, two experimental results which are stronger evidence for the existence of an intermediate mechanical signal. First, the results of Chapter V are direct evidence that electric stimuli generate mechanical signals in the cochlea. Second, Chapter IV showed that Class I nerve-fiber response was abolished when motion of the stapes relative to the cochlear capsule was impeded by cement. On the basis of this evidence, it can be concluded that this type of nerve-fiber response is mediated by mechanical signals.

According to this conclusion, the observed Class I nerve-fiber response is apparently not produced by a purely electric interaction with cochlear systems, although there is a basis on which this kind of

interaction might have been predicted. First, according to the well-known variable-resistance model of the hair cell proposed by Davis (1960), externally applied currents might excite synaptic endings of the auditory nerve electrically to produce a frequency-independent nerve-fiber response identical to acoustically-evoked discharge. Second, some experimental studies have shown that direct and low-frequency alternating currents can interact with the cochlea electrically and modify nerve-fiber response (Tasaki and Fernandez, 1952; Konishi et al., 1970; Teas et al., 1970), possibly due to an electric effect on the sensory hair cells. However, the data of Chapter IV show no evidence of any effect which could be identified with direct electric action on hair cells. It is possible that this kind of electric mechanism might have been excited if, for example, higher current densities had been generated in the vicinity of the organ of Corti. However, the evidence indicates that the electric stimuli used in this study affect sensory cells only indirectly, by generating intermediate mechanical signals.

In summary, the two types of response found in auditory-nerve fibers when electric stimuli are delivered to the cochlea can be attributed to two distinct excitatory processes. One type is evidently the result of direct action of electric current on the nerve membrane itself. The other type of response is generated by a mechanical signal which results from the electric stimulus.

6.2 Origin of Mechanical Response to Electric Stimuli.

6.2.1 Comparison of neural and mechanical stimulus equivalence data.

Since Class I nerve-fiber response to sinusoidal electric stimuli can be attributed to mechanical signals in the cochlea, the stimulus equivalence ratios Q_f and Q_m are both measures of the mechanical response of the cochlea, as indicated by different detectors.

In figure 6.1, the neural- and mechanical-based ratios are re-plotted for comparison. At frequencies above 3 kHz the agreement between the two sets of magnitude data is good. Below 1 kHz, however, the magnitude data do not superimpose, and below 600 Hz the two sets of data are roughly parallel, increasing with decreasing frequency as $1/f$. In this range the difference between the two sets of data is about 10 dB.

The phase data from both types of measurement agree reasonably well. At frequencies greater than 4 kHz, the neural-based phase equivalence leads the mechanical-based phase equivalence, but by no more than 45° . Because neural phase data were not obtained below about 2 kHz, it is not possible to compare phases at the low frequencies, where the magnitude data disagree.

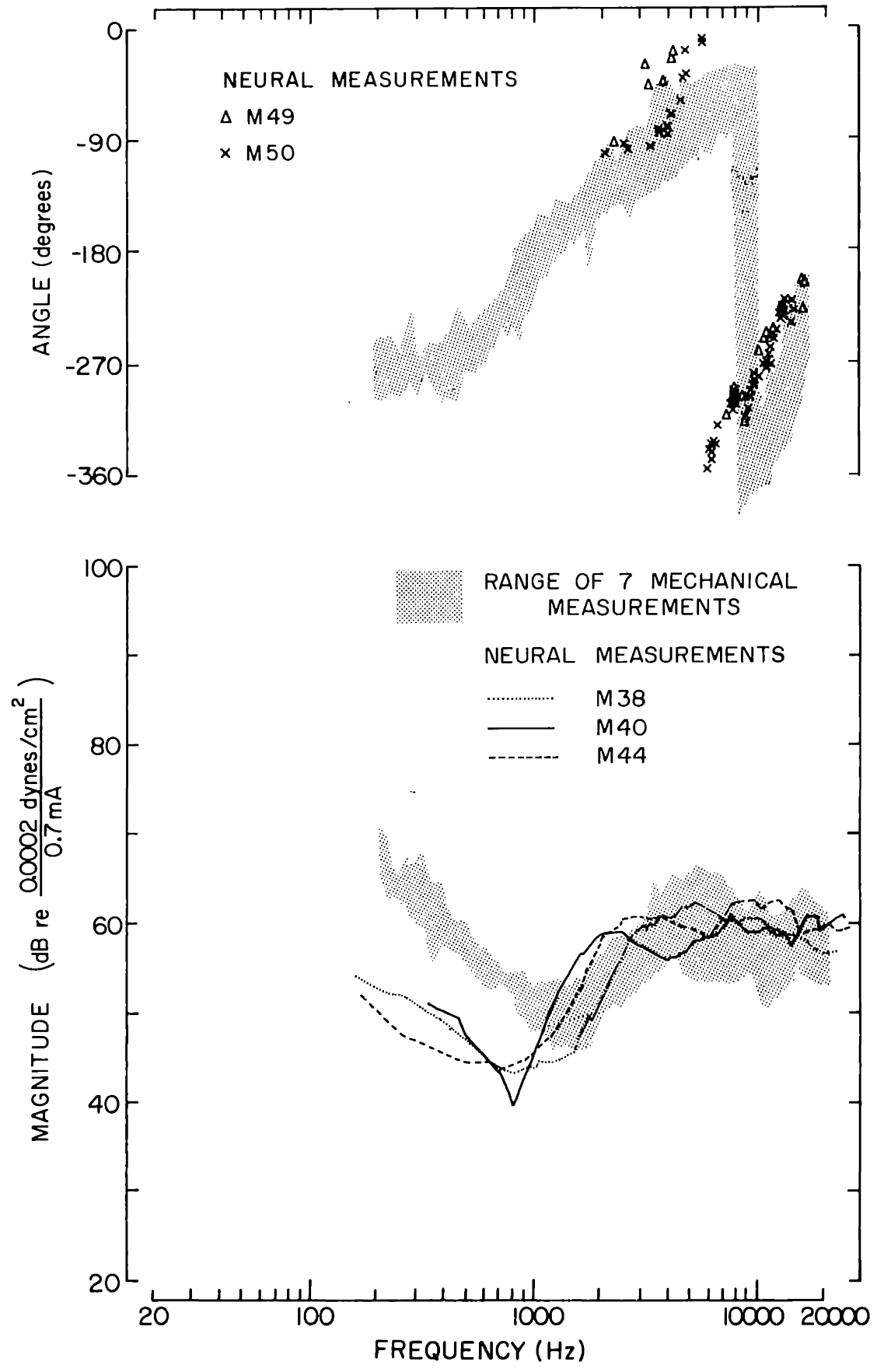
It is possible that the difference in the two measures of equivalent stimulus magnitudes which occurs below 1 kHz can be attributed to different experimental conditions in the two sets of experiments.

Figure 6.1

Comparison of the stimulus equivalence ratios Q_m and Q_f .

The shaded area shows the range of mechanical data that was shown in figure 5.9. The neural magnitude curves are the smoothed $|Q_f^t|$ replotted from figures 4.14 and 4.21 (e). Neural phase equivalence is $\angle Q_f^c$, replotted from figure 4.15.

$\frac{\text{SOUND PRESSURE AT TYMPANIC MEMBRANE}}{\text{ELECTRODE CURRENT}}$



To make the mechanical measurements, the microphone system was sealed over the round window. The microphone system was shown not to load the cochlea mechanically, but the procedures associated with installing the tube may have altered the current flow around and through the cochlea to produce a frequency-dependent difference in the effectiveness of electrode terminal current. No frequency-dependent differences were noted in measurements of electrode current. However, a difference in spatial distribution of current flow within the preparation would not necessarily have been reflected as a difference in terminal current.

The data of Chapters IV and V suggest that current flow into the cochlea is required in order to generate the response. The preparation of the cochlea in mechanical experiments probably caused a greater proportion of electrode current to flow into the cochlea, increasing the effectiveness of a given terminal current. This explanation is consistent with the results, since the equivalence ratios show that at low frequencies currents were about 10 dB more effective in producing response of the mechanical detector than in producing Class I response in nerve fibers.

There is an alternate hypothesis which could account for the difference in equivalence ratios. The neural-based equivalence Q_f represents the relative effectiveness of tone and current in generating mechanical signals which stimulate hair cells. Since equivalence Q_f

was based on fiber response at f_{ce} , the low-frequency portion of the curve represents the ratio of stimuli that produce equal basilar-membrane displacements in the apex of the cochlea, and the high-frequency portion of the curve is based on displacements produced in the base.* The mechanical-based ratio Q_m is based on displacements at yet another position, a mechanical terminal of the cochlea. Thus it is possible that the differences in Q_f and Q_m are due to the different locations in the cochlea at which the mechanical signals are sampled. If this is so, one implication is that within the cochlea, the distribution of mechanical signals (the pattern of vibration) is not the same for acoustic excitation as it is for electric excitation.** Consequently, it would be possible to conclude that the mechanical response to an electric stimulus is not equivalent to a signal acting at the cochlear terminals; this could be the case if the source of transduction were within the cochlea.

The available evidence does not indicate which of these two

* Q_f was always based on fiber response at frequencies close to f_c because Class I response occurred only over a relatively narrow frequency range (see figure 4.5).

** Single fiber data alone would not have shown such a distribution, since response of each fiber was only measured over a narrow range of frequencies close to f_c . To observe this discrepancy, Class I response of a high-frequency fiber ($f_c > 3$ kHz) would have to be observed at low frequency ($f < 1$ kHz) and compared with the response of low- f_c fibers. Because of the occurrence of Class II response, such observations were not possible.

alternative hypotheses accounts for the differences between results of Chapters IV and V. If different Q_f and Q_m were demonstrated simultaneously in the same ear, the latter possibility and the consequent conclusions concerning the site of transduction would be indicated.

6.2.2 Properties of response pertinent to mechanisms of electromechanical transduction.

Some known electrostatic mechanisms by which electric stimuli can be transduced into mechanical signals peripheral to the cochlea were described in Chapter II. These mechanisms cannot account for the transduction observed in this study for two reasons. First, unless such an electrostatic transducer is supplied with some sort of bias, its mechanical output is at twice the frequency of the electric input. However, nerve fibers showed maximum sensitivity to sinusoidal current and acoustic tone at the same frequency (see figure 4.4), and the period of the mechanical waveform recorded by the microphone system in Chapter V (figure 5.4) was the same as the stimulus period. Second, nerve-fiber response to electric stimuli was not discernibly affected by interruption of the ossicular chain which significantly reduced the transmission characteristics of the middle ear (figure 4.21). The signals generated by the electric stimuli therefore are not transmitted through the middle ear and do not originate peripheral to the cochlea.

While the data are consistent with a cochlear source of trans-

duction, the experiments of Chapter V indicate that the observed electromechanical effect is essentially independent of other known cochlear mechano-electric phenomena, since mechanical response to electric stimulation changed little after death, when normal cochlear function had ceased.

The small (< 5 dB) post-mortem reduction in mechanical response that was observed occurred concurrently with large changes in E_{rw} and EP (figures 5.10, 5.11). According to this result, a small component of the normal mechanical response may in fact be related to the specialized electromechanical sensory mechanisms of the cochlea. However, the remaining, major component of electromechanical transduction is evidently not related to normal cochlear function, and the mechanism responsible for this (larger) component may have no role in normal hearing processes. Post-mortem transduction may be attributable to the same physical mechanism which accounts for the transduction found in the preparation of temporal bone in which the cochlea was filled with saline solution. Any of a number of mechanisms may be responsible for this phenomenon. For instance, it could be based on some electro-capillary (electro-osmotic) effect [see Creeth (1951), Grodzinsky (1971)], possibly one associated with the interface between electrolyte and bone, or it might even reflect some piezoelectric property of the temporal bone itself [see Shamos et al. (1963), Shamos and Lavine (1967)]. On the basis of existing

data, however, it is not possible to specify the actual physical mechanism(s) underlying the mechanical response to electric stimulation.

6.2.3 A simple description of mechanical response.

The equivalence ratios presented in Chapters IV and V were expressed in terms of the electrode current and the sound pressure at the tympanic membrane. The results can be simplified if the acoustic stimulus is expressed in terms of stapes velocity rather than sound pressure. The stapes motion was not measured in the present experiments, but sound pressure at the tympanic membrane can be related to stapes displacement using the average middle-ear transfer function obtained by Guinan and Peake (1967).

Figure 6.2 shows the result of transforming the equivalence ratio Q_m into the ratio U_{st}/I_e , where U_{st} denotes complex amplitude of stapes volume velocity into the oval window. Data are not shown above 12 kHz, since the middle-ear transfer function has not been measured above this frequency. The figure shows that the function U_{st}/I_e can be approximated by a real constant over the entire range of data from 100 Hz to 12 kHz. The amplitude curve is flat within ± 3 dB and the phase curve is $180^\circ \pm 45^\circ$.

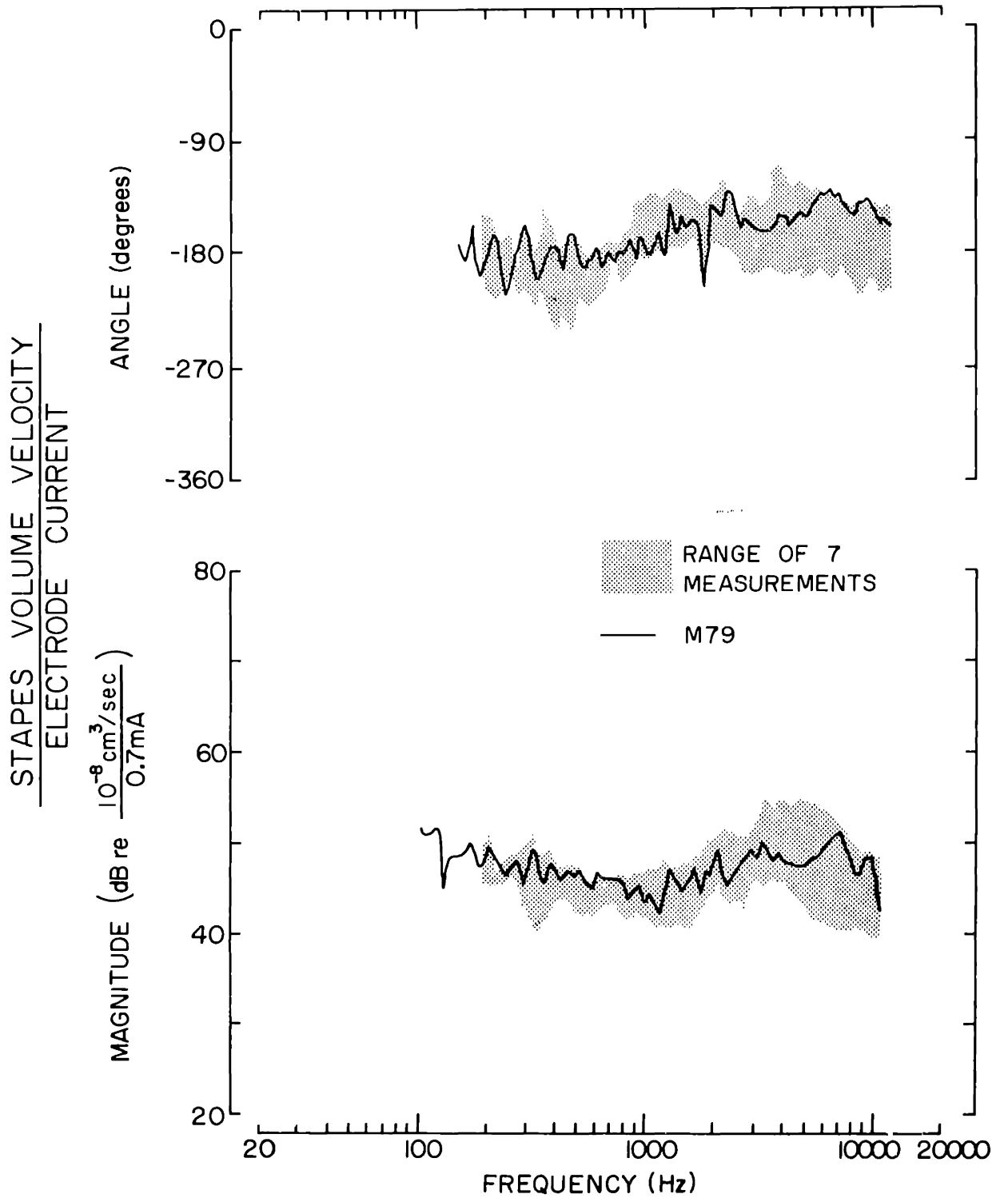
This result can be simply written as

$$\frac{U_{st}}{I_e} = -k \quad 100 \text{ Hz} < f < 12 \text{ kHz}$$

Figure 6.2

Ratio of equivalent stimuli from mechanical measurements expressed as U_{st}/I_e .

Data shown in figure 5.9 have been transformed using the middle-ear transfer function of Guinan and Peake (1967) to relate sound pressure at tympanic membrane to volume velocity of the stapes footplate into the oval window. Shaded area shows the range of 7 measurements, solid curve shows data from a single cat.



where

$$k = 2.8 \times 10^{-6} \frac{\text{cm}^3}{\text{mA} \cdot \text{sec}}$$

If it is assumed that volume velocity into the oval window produces equal volume velocity out of the round window ($U_{st} = U_{rw}$), this expression also describes the motion of the round-window membrane in response to electric stimulation,

$$U_{rw} = U_{st} = -kI_e \quad 100 \text{ Hz} < f < 12 \text{ kHz}$$

The results of the post-mortem mechanical measurements that were shown in figure 5.12 suggest that this proportionality may be valid at frequencies as low as 30 Hz.

This result can be incorporated into a simple lumped-parameter model of the acoustic terminal characteristics of the middle ear and cochlea. Figure 6.3 shows an equivalent circuit of this model. The dependent pressure source and electric terminal pair are included to account for the mechanical response to electric stimuli.

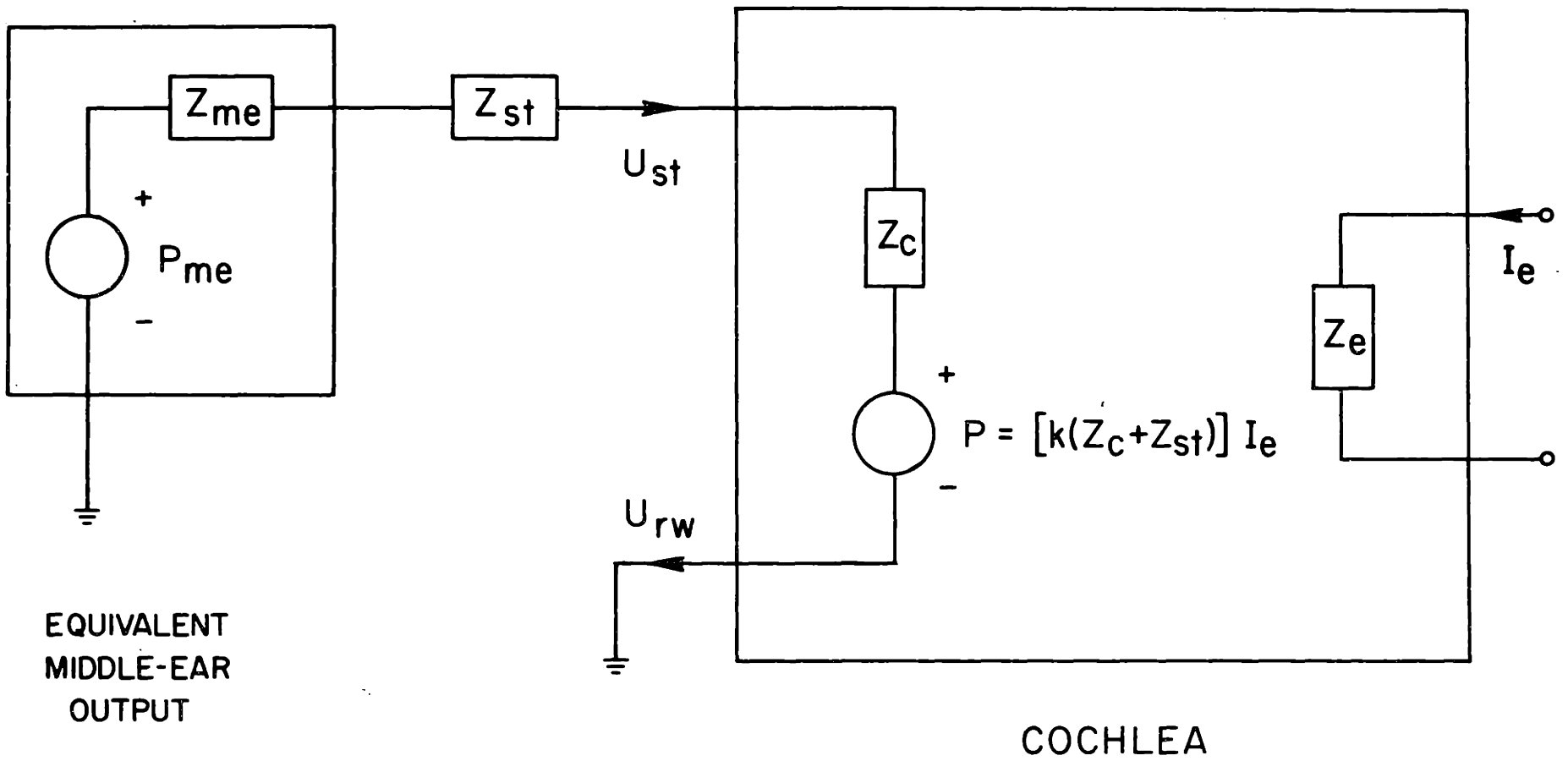
The output characteristics of the middle ear are represented by a Thévenin-equivalent acoustic network. The acoustic impedance of the stapes in the oval window (Z_{st}) has been shown separately from the rest of middle-ear impedance for convenience in interpreting results in terms of the model. *

* The probe-tube assembly used to measure round-window motion

Figure 6.3

Dependent-source model of the acoustic terminal behavior of the electrically-stimulated cochlea.

The cochlea is represented at its acoustic terminals by lumped acoustic impedance Z_c in series with current-controlled pressure source P . The pressure across Z_c with $P = 0$ is the difference between pressure on the perilymph at the oval window and pressure exerted on the round-window membrane, which is taken to be zero. The output characteristics of the middle ear are represented by Thévenin-equivalent pressure source P_{me} in series with lumped acoustic impedances Z_{me} and Z_{st} . Z_{st} , acoustic impedance of the stapes in the oval window; U_{rw} , round-window volume velocity; U_{st} , volume velocity of the stapes footplate. Electric terminal-pair represents connections of stimulating electrodes. Z_e , electrode impedance; I_e , current into round-window electrode.



In response to a stimulus current I_e

$$U_{rw} = U_{st} = -kI_e$$

$$= \frac{-P}{Z_c + Z_{st} + Z_{me}}$$

or

$$P = \left[k \cdot (Z_c + Z_{st} + Z_{me}) \right] \cdot I_e$$

This expression can be simplified somewhat by applying a result of Chapter IV. For electric stimuli, the data showed that nerve-fiber response attributed to mechanical signals in the cochlea was sensitive to conditions at the terminals of the cochlea, since response was significantly reduced when stapes mobility was artificially reduced by means of cement. However, since this response was not greatly altered when the ossicular chain was interrupted, it can be concluded that electrically generated mechanical signals are not significantly changed when $Z_{me} \rightarrow 0$, or

$$Z_{me} \ll Z_{st} + Z_c$$

According to this result, Z_{me} can be neglected, and so

$$P = k(Z_c + Z_{st}) I_e$$

introduced an impedance in series with the round-window terminal of the cochlea, but this impedance was shown to be negligibly small (see section 5.1) and it is not represented in the diagram.

Thus, to completely specify the pressure P , knowledge of the impedances Z_c and Z_{st} is required. Some mathematical models of cochlear hydrodynamics predict essentially real (resistive) Z_c (Zwislocki, 1948; Wansdronk, 1962), but some experimental data indicate that in the cat both Z_c and Z_{st} are frequency-dependent (Tonndorf et al., 1966).

For purposes of summarizing the experimental data it is not necessary to assign values to these impedances. To apply the model in general, the appropriate experimentally-determined values could be incorporated.

It should be emphasized that any equivalent circuit based only on terminal behavior does not in general describe signals within the system being modeled. In this case, however, insofar as the neural and mechanical data (figure 6.1) agree, the Thévenin equivalent configuration would approximately describe the effect of electric stimuli in generating intracochlear mechanical signals which produce Class I nerve-fiber response.

No physical mechanism is necessarily associated with this dependent source configuration. While the configuration of elements in the equivalent circuit appears to be a model of a pressure of electric origin acting at the base of the cochlea, there is no evidence to indicate whether the actual force is localized at the base or elsewhere, or whether forces are distributed throughout the cochlea. The

lumped-parameter dependent-source configuration shown represents the underlying electromechanical transducer only in terms of its effects on the terminal characteristics of the cochlea.

6.3 Relationship of Experimental Results to Human Perception.

6.3.1 Correlation of physiological and psychophysical results.

The results of Chapter IV are comparable to the experiments in which sinusoidal electric stimuli were applied to the human cochlea. In this situation, sinusoidal currents are perceived either as a pure tone at the frequency of the stimulus or as a noise of a buzzing character (Jones, Stevens, and Lurie, 1940; Salomon and Starr, 1963).

The physiological results of Chapter IV are summarized in figure 6.4. Figure 6.4 (a) is a schematic drawing of the electric stimulus plane indicating the characteristic of response which would be found throughout the whole auditory nerve, based on the single-fiber threshold data of figure 4.5. In part (b) of the figure, the contours defined in part (a) have been transformed into equivalent sound-pressure stimuli and are plotted in the acoustic stimulus plane. According to the data of Chapter IV, an electric stimulus in the portion of the plane labeled Region I (part a) establishes activity throughout the entire auditory nerve which resembles the response to tone, both in terms of the time pattern of single-fiber discharge and in terms of distribution of activity among fibers of different f_c . An electric

Figure 6.4

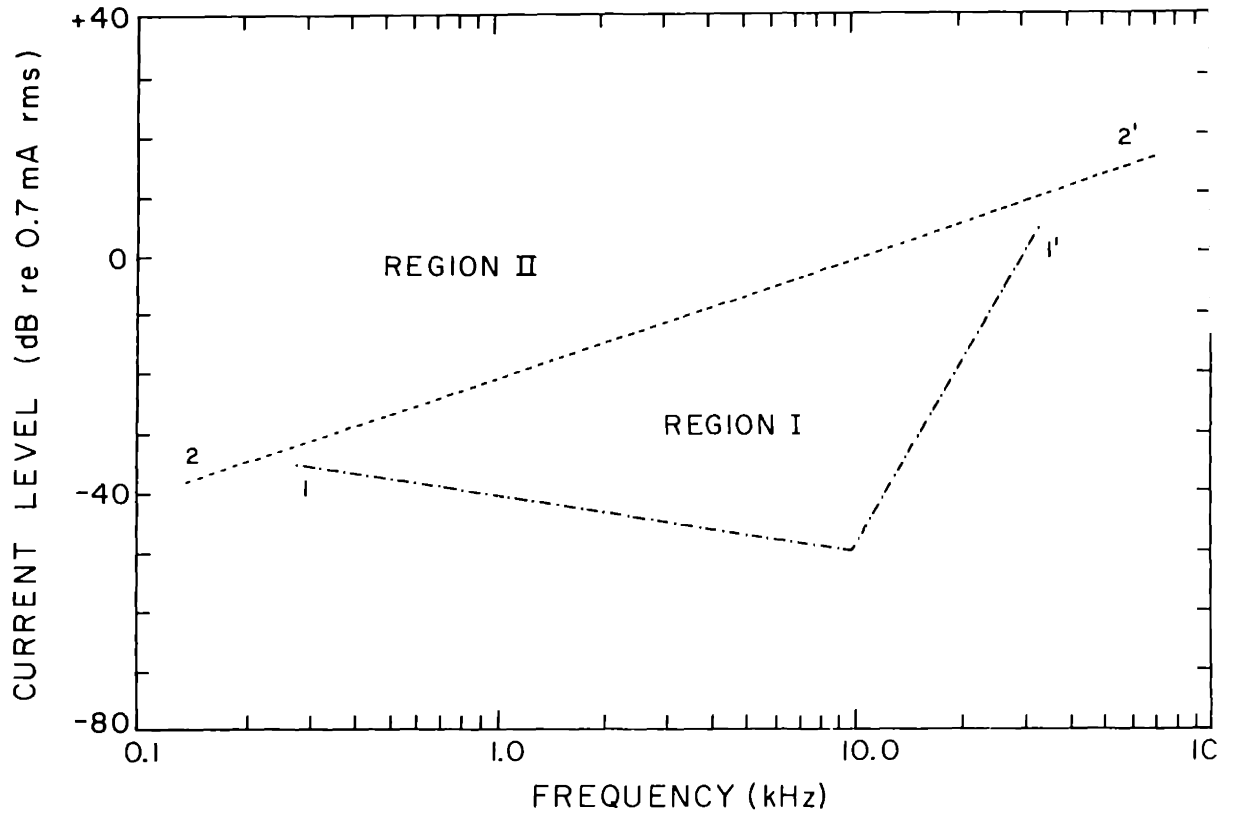
Idealized subdivision of the stimulus plane based on response characteristics of the entire auditory nerve.

In (a), curve 1-1' (lower boundary of Region I) is an idealization of the contour described by the current thresholds at f_{ce} shown in figure 4.13. Line 2-2' (lower boundary of Region II) is an idealization of a curve which would fall just below the S_{II} segments of electric tuning curves (figure 4.5). The portion of the plane below the curve 2-1-1'-2' is not labeled; stimuli in this area evoke no detectable auditory-nerve response. In (b), points from fiber threshold curves 1-1' and 2-2' defined in (a) have been mapped into equivalent sound-pressure stimuli for comparison with behavioral sound-pressure thresholds (labeled curve B) derived from data of Miller et al. (1963). All threshold values are expressed as sound-pressure level at the tympanic membrane for intact middle-ear cavities. In transforming current into equivalent sound pressure with tympanic cavities closed $P_d(\text{closed})$, it has been assumed that only the acoustic nerve-fiber thresholds would be altered, and that threshold pressure with cavities open $P_d(\text{open})$ is related to the pressure required with cavities closed by the equal-response pressure ratio [sound pressure (closed)/sound pressure (open)] presented by Guinan and Peake (1967, figure 20). From the three sets of data summarized in figure 6.1, three modified smoothed equivalence ratios $|Q_f^t|'$ were formed as

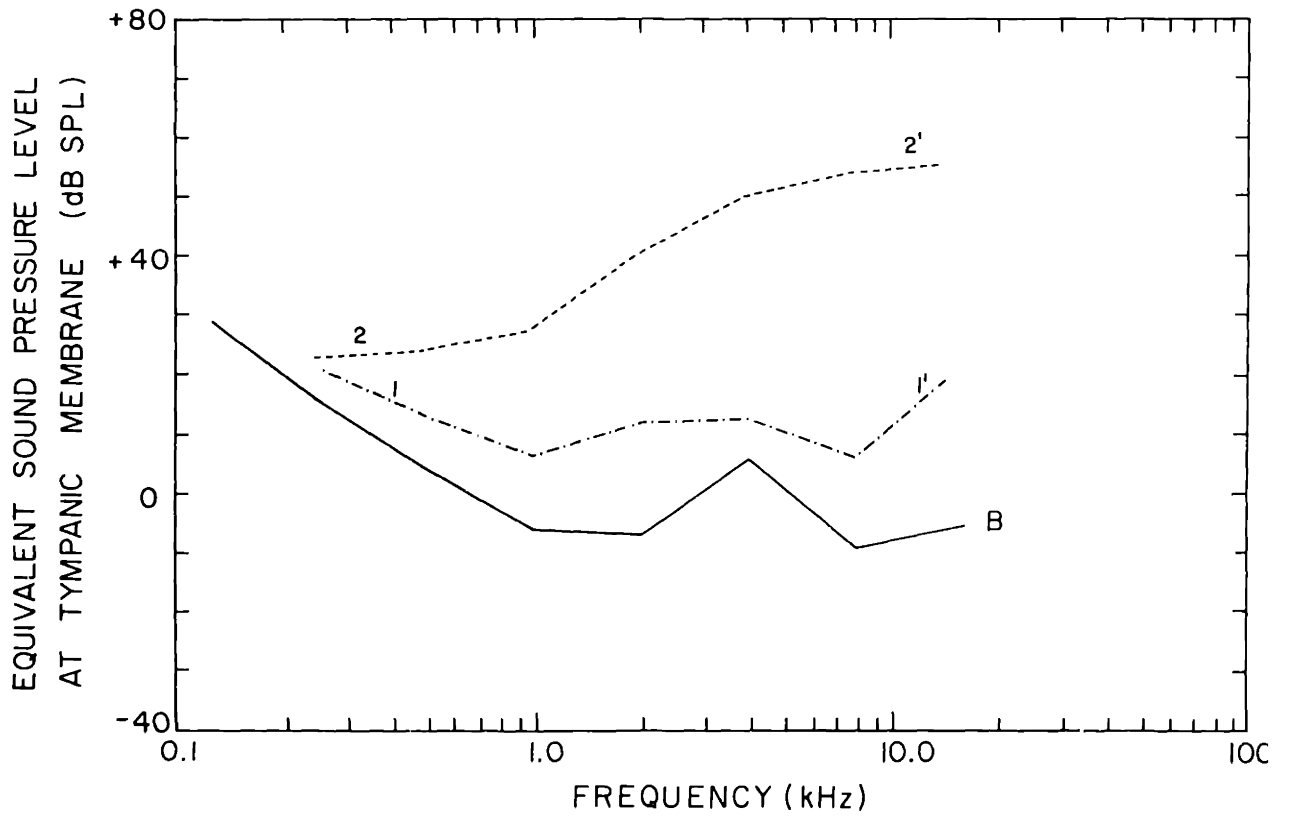
$$|Q_f^t|' = \left[\frac{\text{sound pressure (closed)}}{\text{sound pressure (open)}} \right] |Q_f^t|$$

and the average of the ratios $|Q_f^t|'$ was formed. A current level $|I_e|$ plotted in (a) was converted in (b) to sound-pressure level $|P_d|(\text{closed})$ by $|P_d|(\text{closed}) = |Q_f^t|' \cdot I_e$

Values were computed at octave frequencies from 250 Hz to 8 kHz and at 14 kHz ($|Q_f^t|$ was not obtained below about 170 Hz, and the required middle-ear data extend only to 14 kHz). The behavioral thresholds (curve B) have been converted from free-field sound pressure to sound pressure at the tympanic membrane using the data and procedure presented by Wiener, Pfeiffer, and Backus (1966).



(a)



(b)

stimulus within Region I, therefore, should be indistinguishable from a tone and consequently should give rise to perception of tone in the central nervous system.

For electric stimuli which are in Region II of the whole-nerve response area, the activity in the nerve differs considerably from the response to tone. First, these stimuli produce distinctive, Class II temporal patterns of discharge in individual fibers. Second, Class II thresholds are independent of f_c and are nearly the same for all fibers. While a moderate level of tone or Region I current excites only fibers of f_c sufficiently close to the frequency of the tone, a Region II electric stimulus can establish Class II activity in large numbers of auditory-nerve fibers without regard to fiber f_c . These response characteristics suggest that a Region II stimulus might give rise to an auditory sensation corresponding to a broad spectrum acoustic stimulus, which could be described as noise.

Other characteristics of subjective perception of noise described in the detailed study of Jones et al. (1940) can be associated with characteristics of Class II nerve-fiber response. First, some subjects heard noise only, while some heard noise for some frequencies and tone for others. In all but one subject noise was heard only for low-frequency stimuli, < 250 Hz. As shown in the data of figure 4.5 and in the schematic drawing of figure 6.4, at low frequencies the Region II boundary becomes lower and Region I vanishes. Thus, noise

is perceived at frequencies where only Class II response is found. In addition, the relatively well-defined times of discharge associated with low-frequency Class II response patterns (figure 4.10) may be a correlate of the buzzing character of the reported sensation.

Second, perceived noise showed large growth of loudness as stimulus was increased, and loudness of noise decreased with maintained stimulation; figures 4.7 and 4.11 showed that nerve-fiber discharge rates grow rapidly for small increments of current in Region II, and figure 4.9 showed a decrease in rate for maintained Region II stimulus current. Thus this discharge-rate behavior may be a correlate of perceptual loudness phenomena.

Subjective phenomena associated with electric stimuli were somewhat variable among different subjects, possibly due to different conditions of their inner ears. (Most of the subjects studied by Jones et al. had undergone radical mastoid surgery and evidently had a prior history of ear disease, although it should be noted that Jones et al. found no consistent relation between results and patients' audiograms.) In the experiments of the present study, results in cats with normal cochleas were always similar (e. g. figures 4.13, 4.14, 4.21), but the data of figure 4.20, from an ear which had an experimentally-produced conductive hearing loss resembling otosclerosis, showed no Class I response characteristics.

On the basis of these psychophysical and physiological results,

it appears that the subjective perceptions of human subjects can be identified with Class I and Class II auditory-nerve-fiber responses. Subjective sensation of tone is associated with Class I nerve-fiber response, which is found for stimuli in Region I of the whole-nerve response area, and which is attributed to a cochlear electromechanical phenomenon. Sensation of noise accompanies Class II auditory-nerve activity, which is found in Region II, and which is the result of direct electric excitation of nerve fibers.

6.3.2 Communication Possibilities.

Since response of auditory-nerve fibers to an electric sinusoid duplicates response to acoustic tone over a range of level and frequency, it might be expected that response to more complex electric waveforms would duplicate the response to the analogous sounds. This phenomenon could possibly be used for auditory communication. However, the results of previous human psychophysical experiments, as well as the results of Chapter IV, suggest that useful communication might not be achieved simply.

As described above, stimuli in Region II produce Class II nerve-fiber response, which can be associated with perceptions which do not correspond to the acoustic analog of the electric stimulus. Therefore, this region of the stimulus plane is apparently not useful for readily intelligible communication. However, an electric stimulus

waveform whose spectrum falls in Region I, below the threshold of Region II, could be perceived much the same as if the stimulus were its acoustic analog.

Figure 6.4 shows that the dynamic range of Region I is greatest at relatively high frequencies. In the range of speech frequencies, about 300 to 3000 Hz, Region I is less extensive, and at the low end of this range, where speech spectra have maximum content, the dynamic range of Region I becomes small, vanishing at about 200 Hz. In part (b) of the figure, a behavioral sound-pressure threshold for the cat derived from the data of Miller et al. (1963)(curve B) can be compared with the idealized equivalent nerve-fiber threshold curves (1-1', 2-2').* The behavioral threshold is generally lower than the 1-1' nerve-fiber threshold, by a maximum of 20 dB at 14 kHz. The lower behavioral threshold suggests that electric stimuli might generally be perceived intelligibly over a wider dynamic range than the single-nerve-fiber thresholds indicate. However, at low frequencies, the difference between these two threshold curves (1-1', B) is small, and both approach the transformed boundary of Region II (2-2'). Evidently

* The procedure for transforming data to form the contours of figure 6.4 (b) is described in detail in the caption. It should be noted that in transforming current level to equivalent sound-pressure level, an average stimulus equivalence $|\overline{Q}_f|$ has been applied in conjunction with a correction for closing the middle-ear and bulla cavities, to represent the equivalent sound-pressure level in an animal with an intact middle ear.

below about 200 Hz, there is no range of level for which a sinusoidal current would be perceived as a tone. At these frequencies, currents at or below threshold for stimulating nerve fibers directly would generate mechanical signals that are below the threshold of audibility, and which produce no detectable response.

Possibly for some other stimulating electrode configuration this would not be the case. For instance, an understanding of the electro-mechanical transducer mechanism responsible for Region I characteristics might allow simple specification of a current distribution which would excite the transducer but which would be less effective in stimulating nerve fibers directly. If such a stimulus could be presented, the difference between thresholds for Class I and Class II responses might be increased.

On the basis of the available data, it is not clear that electric stimulation of the cochlea by means of the electrode pair described would be useful for conventional speech communication, although there is no reason why electric excitation of the cochlea could not successfully communicate signals having high-frequency spectra. If spectra of speech signals were modified (filtered) so as to fall just below Region II, making maximum use of the available extent of Region I, it is possible that useful speech intelligibility might be achieved. It should be emphasized, however, that although mechanical response to electric stimuli is essentially unrelated to other

cochlear phenomena, production of the useful, Class I nerve-fiber response depends on normal cochlear mechano-electrical transducer processes; without adequate cochlear sensory function, perception would show the complex and not very useful characteristics associated with Class II response.

APPENDIX I.

CHARACTERISTICS OF THE ELECTRIC STIMULUS CIRCUIT

As indicated in the methods of Chapter III, electric stimuli were specified in terms of current at the terminals of the stimulating electrodes, and voltage across the electrodes was not routinely measured. Without a direct measurement of electrode voltage, the impedance of the electrodes and cochlea cannot be simply obtained as the ratio of electrode voltage to electrode current. However, the measured current and knowledge of other circuit constants allows the impedance to be calculated. A typical example of electrode current measured as a function of frequency is shown in figure A1.1 (a). Part (b) shows an equivalent circuit of the stimulus source connected to the stimulating electrodes. The results of the calculation of electrode impedance are shown in part (c). The impedance is fairly constant above a few hundred Hz and is about 7 k Ω . In most experiments, impedance was between 1 and 10 k Ω .

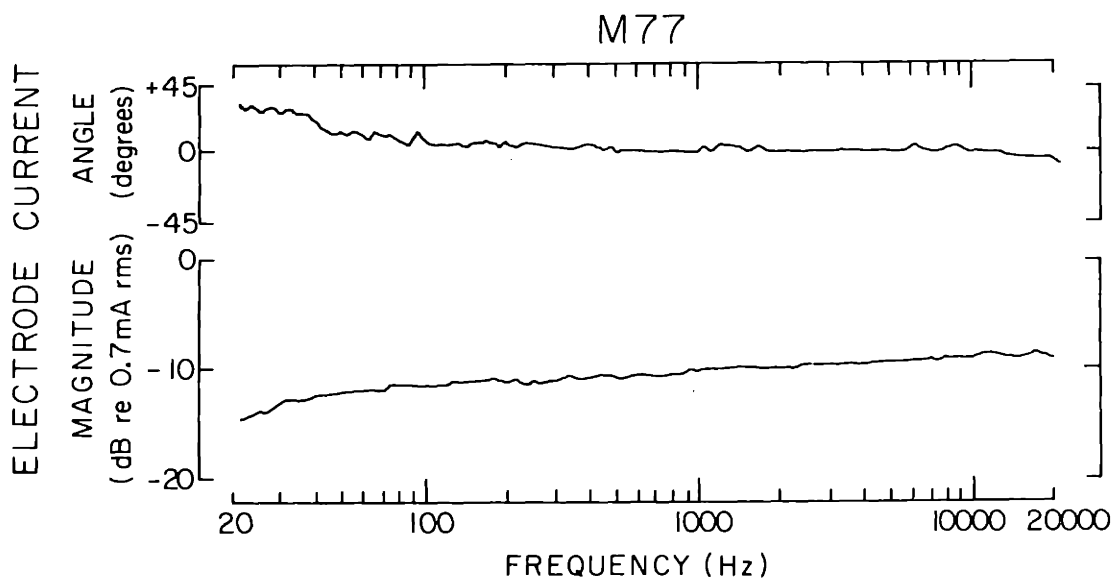
The current drawn by the electrode system at constant voltage, and hence the impedance of the electrodes and cochlea, usually was quite constant during the course of an experiment. An example of electrode current level at 1 kHz measured about every thirty minutes over a period of 17 hours is shown in figure A1.2. The total variation over this period of time was only 3 dB.

Figure A1.1

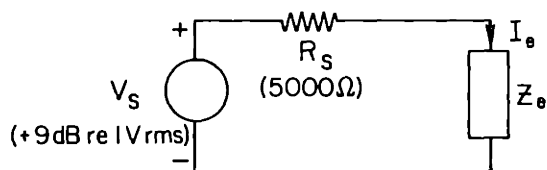
Electrical characteristics of a typical stimulating electrode pair.

Wire electrodes were in standard placement, contacting the surface of the cochlea and fluid on the surface of the round-window membrane. Curves in (a), magnitude and angle of current flow into round-window electrode at constant 10 dB setting of the attenuator controlling the electric stimulus. Angle of current referred to voltage from a low-impedance output of the source oscillator, which has the phase of the source in the equivalent circuit in (b). In (b), Thévenin equivalent of the circuit supplying the stimulating electrodes, shown loaded by the impedance between the two stimulating electrodes Z_e . Equivalent circuit parameters V_s , open-circuit voltage, and Z_s , output impedance. [Actual circuit consisted of a 500-ohm source oscillator (open-circuit output = 2.8 V rms) connected to a 500-ohm attenuator set to 10 dB and stepped up by a wide-band transformer of turns ratio $1:\sqrt{10}$.] Equivalent circuit parameters derived as $|V_s| = (2.8) \times (1/\sqrt{10}) \times (\sqrt{10}) = 2.8$ V rms, and $Z_s = (\sqrt{10})^2 \times (500 \Omega) = 5000 \Omega$. In (c), real and imaginary parts of Z_e are calculated from measured current of (a) and circuit constants of (b) according to the relation

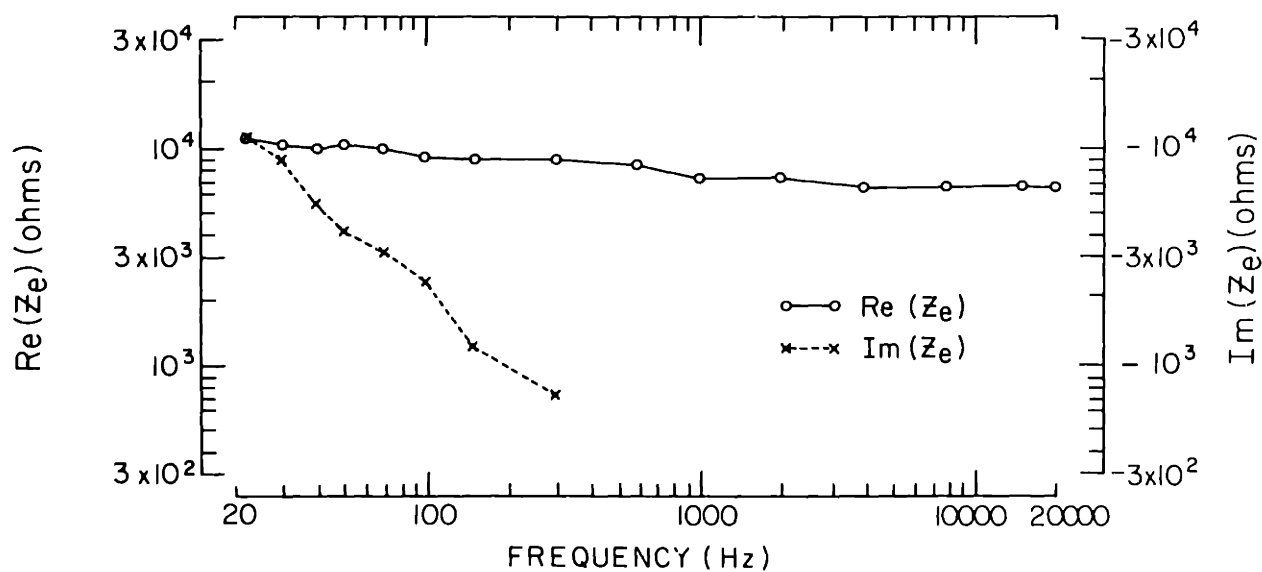
$$Z_e = \frac{V_s}{I_e} - 5000 \Omega$$



(a)



(b)

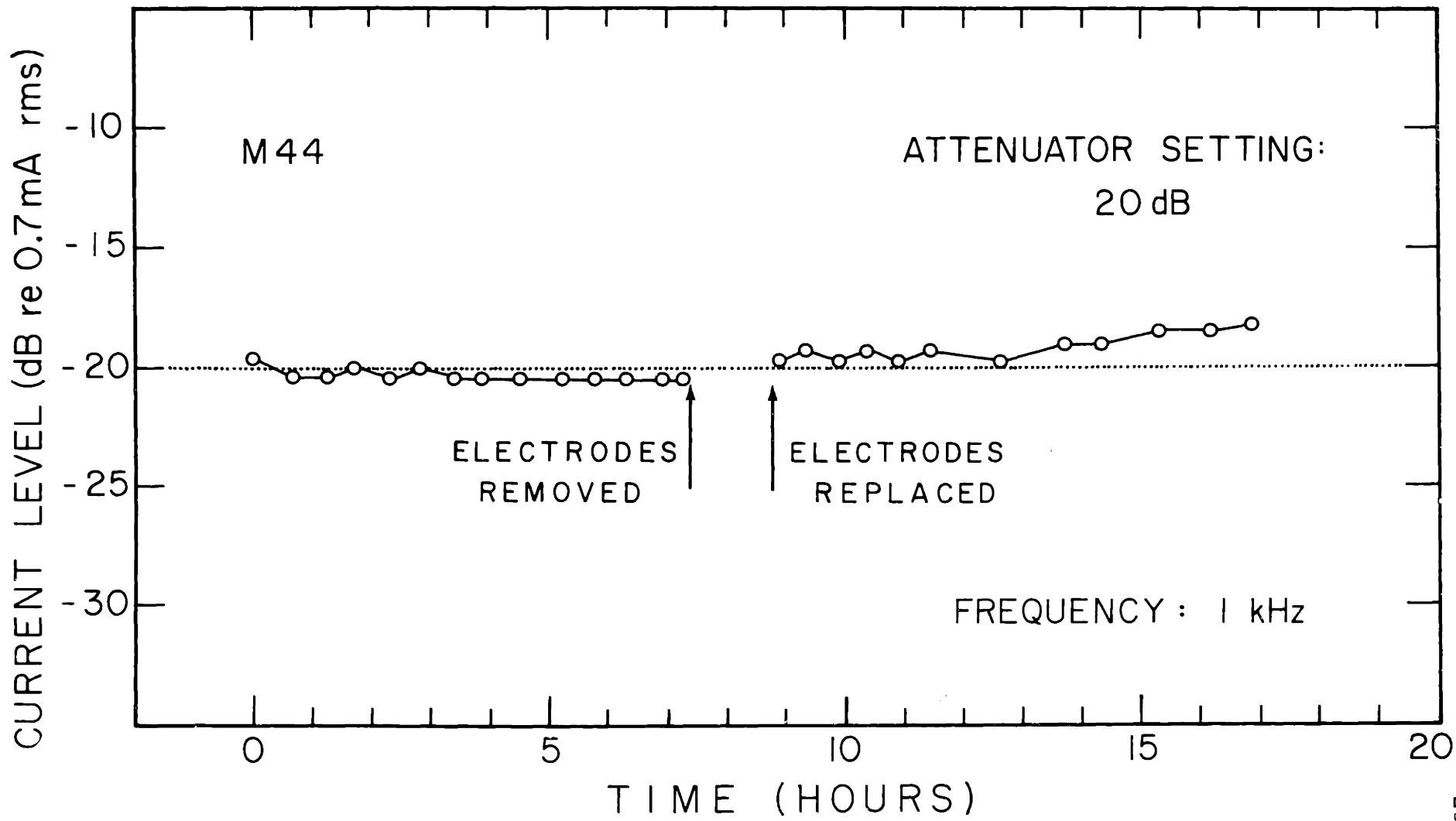


(c)

Figure A1.2

Magnitude of electrode current at constant attenuator setting plotted against time throughout the course of an experiment.

At approximately 1/2-hour intervals the electrode current at 1 kHz was measured for a 20 dB setting of the attenuator controlling the electric stimulus. After 7 hours the stimulating electrodes were removed from the cochlea and replaced about 2 hours later.



The circuit parameters of the stimulus system limited the maximum power delivered to the electrode system and cochlea. At maximum level, the equivalent open-circuit source voltage V_s was +19 dB re 1 V rms, or $\sqrt{80}$ V rms, and optimum power transfer from this source to the load would occur with a load resistance matched to the 5000-ohm source resistance R_s . Under these conditions, power delivered to the load is given by

$$\begin{aligned} P_{\max(\text{optimum})} &= \frac{1}{2} \frac{V_s^2_{\max}}{2R_s} \\ &= \frac{(\sqrt{80})^2}{(4)(5000)} \\ &= 4 \times 10^{-3} \text{ W} \end{aligned}$$

or 4 milliwatts. For a load not matched to the 5000-ohm source,

$P_{\max} < P_{\max(\text{optimum})}$. For the typical circuit parameters shown in figure A1.1,

$$\begin{aligned} P_{\max} &= I_e^2 R_e \\ &\approx (0.7 \times 10^{-3})^2 (7 \times 10^3) \\ &= 3.5 \times 10^{-3} \text{ W} \end{aligned}$$

Since P_{\max} is the total maximum power delivered to the stimulating electrodes on the surface of the cochlea, the power actually

dissipated within the cochlea would be expected to be less than the values calculated.

APPENDIX II.

CHARACTERISTICS OF THE PROBE-TUBE SYSTEM

A drawing of the probe tube, coupler, and microphone cartridge was shown in figure 3.4. The pressure transformation characteristic of this system is shown in figure A2.1, and a transmission-line analog representing the acoustic properties of the tube and its termination is shown in the inset. The first peak in the pressure transfer function occurs at about 2.7 kHz, and other peaks occur at about 7.8 and 13 kHz. The general decrease in the magnitude of the pressure transfer function at higher frequencies may be a reflection of lossy tube characteristics. No effort was made to match the tube to its terminating impedance, and the lack of damping is apparent in the pressure gain (about 18 dB) at the first resonance.

In the transmission-line analog, voltage is taken as analogous to pressure, and current is analogous to volume velocity, in accordance with the impedance-based analogy of electric and acoustic variables [see Beranek (1954)]. From transmission-line theory, the pressure transformation in a system which is the analog of a lossless line of length ℓ , characteristic impedance Z_0 , and terminated in a load impedance Z_T is

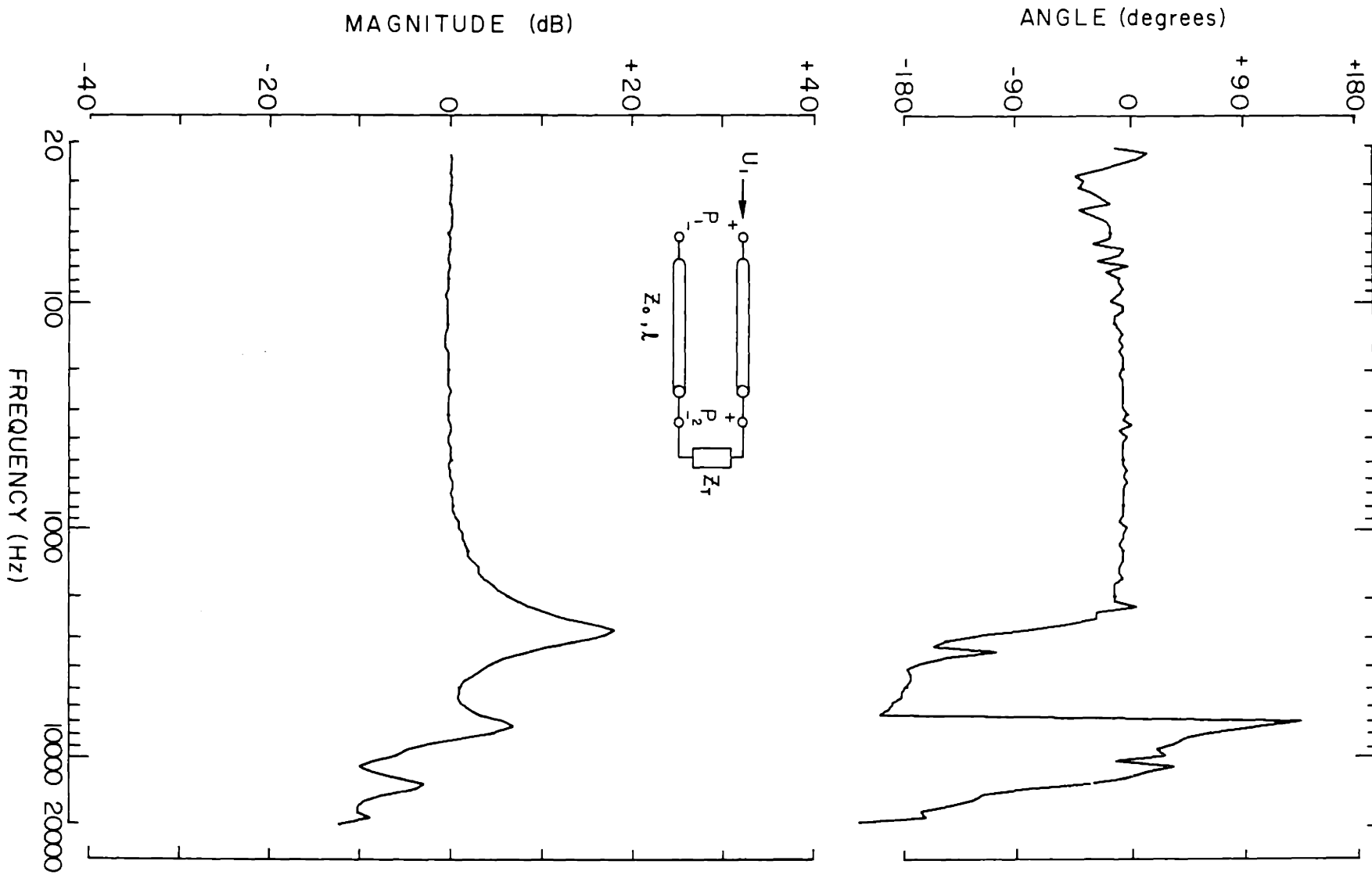
$$\frac{P_2}{P_1} = \frac{1 + \Gamma_T}{1 + \Gamma_T e^{-j2\beta\ell}}$$

Figure A2.1

Pressure transfer function of probe-microphone system.

The probe tube was inserted into a closed cavity and the sound pressure near the tube orifice was measured with a second 1/2-inch capacitor microphone (B&K 4134) as the cavity was excited by a third capacitor cartridge used as an earphone. P_1 , sound pressure at the tube entrance; P_2 , sound pressure at the probe microphone. The curves show magnitude and angle of the transfer function P_2/P_1 . The inset shows a lossless transmission-line analog of the probe tube terminated by the lumped impedance of the microphone cartridge and the small volume of air in the coupler. Z_0 , characteristic acoustic impedance of the tube; Z_T , acoustic impedance of the termination; l , length of the tube; U_1 , volume-velocity flow into tube orifice.

$$\frac{\text{SOUND PRESSURE AT PROBE MICROPHONE}}{\text{SOUND PRESSURE AT TUBE ENTRANCE}}$$



where

$$\Gamma_T = \frac{Z_T - Z_0}{Z_T + Z_0}$$

and

$$\beta = \frac{\omega}{v}$$

and v is the propagation velocity of the line. The transfer function relating pressure at the load P_2 to input volume velocity U_1 is given by

$$\frac{P_2}{U_1} = Z_0 \cdot \frac{1 + \Gamma_T}{1 - \Gamma_T e^{-j2\beta\ell}}$$

and the input impedance Z_1 is

$$Z_1 = Z_0 \cdot \frac{1 + \Gamma_T e^{-j2\beta\ell}}{1 - \Gamma_T e^{-j2\beta\ell}}$$

If it is assumed that the terminating impedance Z_T is sufficiently large (that the termination is sufficiently stiff), then the reflection coefficient $\Gamma_T \approx 1$. In this simplified model, the poles of these functions fall on the $j\omega$ axis and are easily calculated. The poles of the pressure transformation and the zeros of Z_1 occur when

$$e^{-j2\beta\ell} = -1$$

or

$$2\beta\ell = \pi(2n + 1) \qquad n = 0, 1, 2, \dots$$

The corresponding frequencies are

$$f_n = \frac{v}{4\ell} (2n + 1)$$

or if

$$f_0 = \frac{v}{4\ell}$$

then the frequencies are $f_0, 3f_0, 5f_0, \dots$. The poles of Z_1 and of transfer impedance $Z_{21} = P_2/U_1$ are found from

$$e^{-j2\beta\ell} = +1$$

which gives

$$f_m = m \frac{v}{2\ell} \quad m = 0, 1, 2, \dots$$

In terms of f_0 defined above, the (non-zero) frequencies are $2f_0, 4f_0, 6f_0, \dots$.

The lowest-frequency peak in the measured pressure transformation shows that for the probe-tube system, $f_0 = 2.7$ kHz, although the maximum pressure gain is only 18 dB, not infinity as the simplified lossless model predicts. If the tube were driven from a high-impedance (velocity) source, the peaks in measured output would occur at even multiples of f_0 , or 5.4, 10.8, 16.2, \dots kHz. The data of Chapter V suggest that the cochlea is a high-impedance source, and microphone pressure developed when the tube is sealed over the round window shows peaks at approximately these frequencies.

The maxima and minima of the input impedance Z_1 occur at

multiples of f_0 , although again, the values attained would not be expected to be 0 and ∞ as the simplified model would indicate. The impedance maxima should occur at 5.4, 10.8, 16.2, . . . kHz, the frequencies at which pressure peaks are found when the system is driven by the cochlea. At the maxima of this impedance, the tube presents the greatest acoustic load to the cochlea. Impedance minima would occur at 2.7, 8.1, 13.5, . . . kHz, and the tube loads the cochlea least at these frequencies.

At frequencies for which the length of the tube is small compared to a quarter wavelength ($l \ll \lambda/4$, or $f \ll f_0$), the system can be characterized by its compliance, which is easily calculated. From figure 3.4, the volume of air in the tube and coupler is about 0.075 cm^3 , and the equivalent volume of the microphone cartridge is about 0.003 cm^3 , giving a total equivalent volume V of 0.078 cm^3 . The acoustic compliance of an ideal gas of volume V is given as

$$C_A = \kappa V$$

where κ is the adiabatic compressibility of the gas. For air at atmospheric pressure,

$$\kappa = 0.7 \times 10^{-6} \frac{\text{cm}^5}{\text{dyne}}$$

and so

$$C_A = 5.6 \times 10^{-8} \frac{\text{cm}^5}{\text{dyne}}$$

Knowledge of the compliance specifies the approximate low-frequency value of the functions

$$\frac{P_2}{U_1} \approx \frac{P_1}{U_1} \approx \frac{1}{j2\pi f C_A} \quad f \ll 2.7 \text{ kHz.}$$

APPENDIX III.

SPURIOUS EFFECTS OF ELECTRIC STIMULI

In the experiments described in Chapters IV and V, electric stimuli were delivered with electrodes on the cochlea. However, the effects of the electric stimuli were not necessarily limited to the inner ear, or even to the auditory system. These additional effects were not studied systematically, but some observations can be reported.

Sufficiently high levels of both pulse and sinusoidal electric stimuli sometimes caused gross muscular activity, such as twitching of the animal's face and neck musculature. This was a problem in the experiments of Chapter IV, since when this occurred, it was difficult to keep a microelectrode in contact with a nerve fiber. This effect limited the level of electric stimulus which could be used successfully when recording from auditory-nerve fibers. The cause of the muscular twitch was not determined directly; however, the seventh cranial (facial) nerve, which innervates facial musculature, passes through the internal auditory meatus and the facial canal in the temporal bone, and a branch, the chorda tympani, passes through the middle-ear cavity. Also, the eleventh cranial (accessory) nerve, which sends branches to the musculature of the neck, exits from the cranium along with the ninth and tenth cranial nerves through the jugular foramen, several millimeters caudo-medial to the stimulating electrodes. It is possible

that portions of the facial and accessory nerves could have been excited by the electric stimuli delivered to the cochlea to produce the observed muscle response.

Occasionally electric stimuli at sufficiently high level seemed to disrupt normal respiration. In such a case the normal respiratory motion of the animal's chest was replaced by a more rapid, shallow motion, interspersed occasionally with a deep inhalation. This effect on the preparation also placed limits on the upper level of stimulus that could be used and the length of time a high-level stimulus could be left on. Since the vagus nerve, branches of which go to the heart and lungs, is one of those which pass through the jugular foramen, it too may have been excited electrically. The vagus is extensively distributed and innervates many organs, and possible effects of electric excitation of this nerve may have been widespread. Although there was some indication that heart function became abnormal at high current levels, EKG characteristics were not observed closely.

Often when the microelectrode was positioned anteriorly in the internal auditory meatus, it could pass through the vestibular portion of the eighth nerve. Fibers which exhibited an essentially periodic discharge waveform were recognized as vestibular-nerve fibers (Rupert, Moushegian, and Galambos, 1962). These vestibular fibers were found to respond to high-level electric stimuli, but as threshold of vestibular-nerve fibers was not routinely recorded, it is not pos-

sible to compare them with auditory-nerve-fiber thresholds.

The final spurious effect of electric stimuli to be described was found only in certain animals. In most experiments the tendons of the middle-ear muscles were cut to decouple the ossicles from any electrically-induced muscle motion. In animals in which the tendons had not been cut, an unusual response pattern was occasionally observed with electric stimuli. An example of such a pattern is shown in figure A3.1. Responses synchronized with the stimulus shock occur at latencies extremely long compared to the latency of click response. It is possible that these are responses to contractions of one or both middle-ear muscles. In some animals the middle ear was viewed through a microscope and it was easy to detect twitching of the tensor tympani at comparable stimulus levels. This muscle response could be due to electric excitation of either the motor nerves supplying the muscles or possibly of the muscle fibers themselves. This type of nerve-fiber response was never detected in animals whose middle-ear-muscle tendons had been cut.

Figure A3.1

Histograms of response of a low- f_c fiber to click and shock in a cat with intact middle-ear muscles.

Histogram in (a) shows the pattern of response to a high-level click (-30 dB re 100 V into 1-inch condenser ear-phone). Histogram in (b) shows response to a 600 μ A, 1 msec shock (round window negative). Note the multiple long-latency peaks in shock response. This cat had received a mild dose of the ototoxic drug kanamycin, but degeneration was observed only in the basal 25% of the organ of Corti. Similar patterns of response to shock were observed in cats which had not been treated with drugs, as long as the tendons of the middle-ear muscles were not severed. Fiber RAL 19-16, $f_c = 0.286$ kHz, tone threshold = 49 dB SPL, spontaneous discharge rate ≈ 2 /sec.

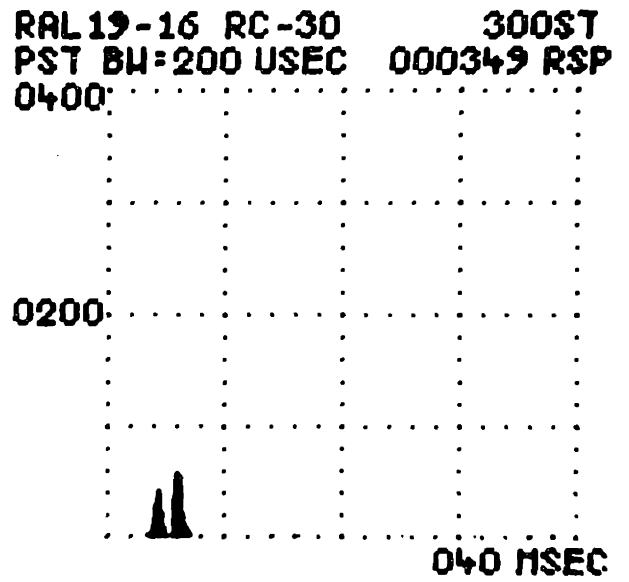
RAL 19-16

$f_c = 0.286 \text{ kHz}$

RAREFACTION
CLICK

-30 dB

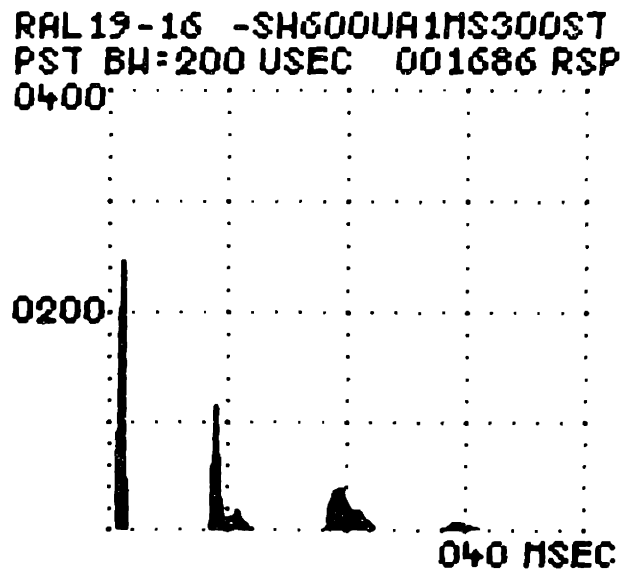
(a)



ELECTRIC
SHOCK

-600 μA

(b)



APPENDIX IV.

INTRACOCHLEAR VOLTAGE DEVELOPED
BY ELECTRIC STIMULI

In general, the intracochlear distribution of current and voltage developed by the external electric stimuli used in this study is not known, principally because variables of interest were difficult to measure. The following is an indication of the experimental problems associated with measurements of intracochlear electric variables.

In the cat the thickness of the bone makes access to scalae of upper turns difficult, and for recording spatial dependence of intracochlear electric response to sound, species with more suitable anatomical features are generally chosen (Tasaki, Davis, and Legoux, 1952). However, the basal region of the cat's cochlea is accessible through the round-window membrane, and transverse voltage distributions can be recorded with suitable microelectrodes (Sohmer, Peake, and Weiss, 1971).

Using this approach, the voltage across the basilar membrane was measured when direct current was delivered to the cochlea with stimulating electrodes in the standard configuration. Currents used ranged from 50 to 500 μ A, and throughout this range the resulting voltage was proportional to stimulus current. The constant of proportionality was approximately 80 mV/mA, or 80 ohms. A voltage trans-

fer ratio was not determined, but from the range of typical mid-band electrode impedances (1000 to 10,000 Ω), it could be estimated that between 1/10 and 1/100 of electrode voltage was developed across the basilar membrane. Since electrode impedance increases at low frequency, the actual ratios may be even smaller.

When similar measurements were made as a function of frequency, it was not certain that the recorded voltages were actually those developed at the tip of the microelectrode or whether the apparent voltage was due to stray coupling between stimulus and recording circuits. In order not to alter characteristics of the cochlea significantly, microelectrodes having small tip diameter were required. However, these electrodes exhibited high tip resistances, and the high impedance of the measuring circuit then made it susceptible at most frequencies to capacitively-coupled stray signals from the stimulus electrodes.

The recorded voltage V_r due to a capacitance C_s between a stimulus electrode (of voltage V_e) and a recording microelectrode of resistance R_μ is

$$\frac{V_r}{V_e} = \frac{j\omega R_\mu C_s}{j\omega R_\mu C_s + 1}$$

For $\left| \frac{V_r}{V_e} \right| < \frac{1}{10}$, this can be approximated as

$$\frac{V_r}{V_e} \approx j\omega R_\mu C_s$$

From this expression, a maximum allowable capacitance can be calculated by specifying a maximum stray coupling ratio. For example, if $R_{\mu} = 10 \text{ M}\Omega$ and $\left| \frac{V_r}{V_e} \right| < \frac{1}{100}$, then at 1 kHz, $C_s < 0.16 \text{ pf}$, and at 10 kHz, $C_s < 0.016 \text{ pf}$. Such small interelectrode capacitance was evidently not achieved, even with microelectrodes guarded to within a few mm of the tip. When the stimulus electrodes were energized, with $R_{\mu} = 14 \text{ M}\Omega$, the recorded voltage was approximately proportional to frequency and led the stimulus voltage by approximately 90° ,

$$\frac{V_r}{V_e} \approx j\omega \times 10^{-5} \quad 20 \text{ Hz} < \frac{\omega}{2\pi} < 5 \text{ kHz.}$$

This result could be attributed to a net effective stray coupling capacitance of the order of 1 pf. Thus it was possible that the stray signals were obscuring the signals of interest. This measurement problem was not readily solved, and consequently the intracochlear voltages developed in response to sinusoidal stimuli in the audio range were not determined.

REFERENCES

- AGIN, D., and LOWY, K. (1962). "Effect of Electrical Stimulation on Peripheral Auditory Responses," *Laryngoscope* 72, 361-366.
- ANDREEV, A. M., GERSUNI, G. V., and VOLOKHOV, A. A. (1935). "On the Electrical Excitability of the Human Ear. On the Effect of Alternating Currents on the Affected Auditory Apparatus," *J. Physiol. U. S. S. R.* 18, 250-265.
- ANDREEV, A. M., ARAPOVA, A. A., and GERSUNI, G. V. (1938). "On the Excitability of the Auditory Apparatus in Relation to its Functional State," *J. Physiol. U. S. S. R.* 25, 618-630.
- ARAPOVA, A., and GERSUNI, G. V. (1938). "On the Frequency of Alternating Current and the Pitch of the Tone during Electrical Stimulation on the Auditory Apparatus," *Tech. Phys. S. S. S. R.* 5, 447-462.
- ARAPOVA, A. A., GERSUNI, G. V., and VOLOKHOV, A. A. (1937). "A Further Analysis of the Action of Alternating Currents on the Auditory Apparatus," *J. Physiol.* 89, 122-131.
- BÁRÁNY, E. (1937). "Electrical Stimulation of the Cochlea," *Nature* 139, 633.
- BÉKÉSY, G. von (1960). Experiments in Hearing, E. G. Wever, Ed. (McGraw-Hill Book Co., Inc., New York).
- BÉKÉSY, G. von, and ROSENBLITH, W. A. (1951). "The Mechanical Properties of the Ear," in Handbook of Experimental Psychology, S. S. Stevens, Ed. (John Wiley and Sons, New York).
- BERANEK, L. L. (1954). Acoustics, (McGraw-Hill Book Co., New York).
- BUGNARD, L., and HILL, A. V. (1935). "The Effect of Frequency of Excitation on the Thermal Response of Medullated Nerve," *J. Physiol.* 83, 383-393.
- CHAMBERLAIN, S. C., MOXON, E. C., and WIEDERHOLD, M. L. (1968). "Efferent Inhibition of Electrically Stimulated Response in Cat Auditory-Nerve Fibers," *Mass. Inst. Technol., Res. Lab. Electron. Quart. Prog. Rept.* 90, 266-270.

- CHOCOLLE, R. (1950). "L'Effet Électrophonique: Son Interpretation par un Effet Électrostatique au Niveau du Revêtement Externe," *J. Physiologie* 42, 303-823.
- CHOCOLLE, R. (1954). "Aperçus Récents sur l'Effet Électrophonique," *Acta Oto-Rhino-Laryngologica Belgica* 8, 150-162.
- CLARK, G. M. (1969). "Responses of Cells in the Superior Olivary Complex of the Cat to Electrical Stimulation of the Auditory Nerve," *Exp. Neurol.* 24, 124-136.
- CLARK, W. A., BROWN, R. M., GOLDSTEIN, M. H., MOLNAR, C. E., O'BRIEN, D. F., and ZIEMAN, H. E. (1961). "The Average Response Computer (ARC): A Digital Device for Computing Averages and Amplitude and Time Histograms of Electrophysiological Response," *IRE Trans. Bio-Med. Electron.* BME-8, 46-51.
- CRAIK, K. J. W., RAWDON-SMITH, A. F., and STURDY, R. S. (1937). "Note on the Effect of A. C. on the Human Ear," *J. Physiol.* 90, 3P-5P.
- CREETH, J. M. (1951). "Electrokinetic Effects," in Electrical Phenomena at Interfaces, J. A. V. Butler, Ed. (Methuen and Co. Ltd., London).
- DALLOS, P. (1970). "Low-Frequency Auditory Characteristics: Species Dependence," *J. Acoust. Soc. Amer.* 48, 489-499.
- DAVIS, H. (1957). "Biophysics and Physiology of the Inner Ear," *Physiol. Rev.* 37, 1-49.
- DAVIS, H. (1960). "Mechanism of Excitation of Auditory Nerve Impulses," in Neural Mechanisms of the Auditory and Vestibular Systems, G. L. Rasmussen and W. F. Windle, Eds. (Charles C. Thomas, Springfield, Ill.).
- DAVIS, H. (1965). "A Model for Transducer Action in the Cochlea," in Cold Spring Harbor Symposia on Quantitative Biology 30; Sensory Receptors, L. Frisch, Ed. (Cold Spring Harbor Laboratory of Quantitative Biology, Cold Spring Harbor, L. I., New York).
- DAVIS, H., and Associates. (1953). "Acoustic Trauma in the Guinea Pig," *J. Acoust. Soc. Amer.* 25, 1180-1189.

- DAVIS, H., DEATHERAGE, B. H., ELDREDGE, D. H., and SMITH, C. A. (1958). "Summating Potentials of the Cochlea," *Am. J. Physiol.* 195, 251-261.
- DAVIS, H., DEATHERAGE, B. H., ROSENBLUT, B., FERNANDEZ, C., KIMURA, R., and SMITH, C. A. (1958a). "Modification of Cochlear Potentials Produced by Streptomycin Poisoning and by Extensive Venous Obstruction," *Laryngoscope* 68, 596-627.
- DESMEDT, J. E. (1962). "Auditory-Evoked Potentials from Cochlea to Cortex as Influenced by Activation of the Efferent Olivo-Cochlear Bundle," *J. Acoust. Soc. Amer.* 34, 1478-1496.
- DJOURNO, A., and EYRIÈS, C. (1957). "Prothèse Auditive par Excitation Électrique a Distance du Nerf Sensoriel a l'Aide d'un Bobinage Inclus a Demeure," *Presse Méd.* 65, 1417.
- DOYLE, J. H., DOYLE, J. B., and TURNBULL, F. M. (1964). "Electrical Stimulation of the Eighth Cranial Nerve," *Arch. Otolaryngol.* 80, 388-391.
- DOYLE, J. B., DOYLE, J. H., TURNBULL, F. M., and HOUSE, L. (1963). "Electrical Stimulation in Eighth Nerve Deafness," *Bull. Los Angeles Neurol. Soc.* 28, 148-150.
- EICHHORN, G. (1930). "The Electrostatic 'Radiophon'," *Radio-Craft*, 330 ff.
- EINHORN, R. N. (1967). "Army Tests Hearing Aids that Bypass the Ears," *Electronic Design* 26, 30-32.
- ENGSTROM, H., ADES, H. W., and ANDERSON, A. (1966). Structural Pattern of the Organ of Corti, (Almqvist & Wiksell, Stockholm).
- FEX, J. (1959). "Augmentation of the Cochlear Microphonics by Stimulation of Efferent Fibers to the Cochlea," *Acta Oto-Laryngol.* 50, 540-541.
- FEX, J. (1962). "Auditory Activity in Centrifugal and Centripetal Cochlear Fibers in Cat. A Study of a Feedback System," *Acta Physiol. Scand.* 55, Suppl. 189, 1-68.

- FIORI-RATTI, L., and MANFREDI, A. (1951). "Soglia di Udibilita nei Soggetti Normali per Stimolazione con Correnti a Radio-frequenza Modulate," *Clin. Otorinolar.* 3, 338-346.
- FLOTTORP, G. (1953). "Effect of Different Types of Electrodes in Electrophonic Hearing," *J. Acoust. Soc. Amer.* 25, 236-245.
- FREY, A. H. (1961). "Auditory System Response to Radio Frequency Energy," *Aerospace Med.* 32, 1140-1142.
- FREY, A. H. (1962). "Human Auditory System Response to Modulated Electromagnetic Energy," *J. Appl. Physiol.* 17, 689-692.
- FREY, A. H. (1963). "Some Effects on Human Subjects of Ultra-High-Frequency Radiation," *Am. J. Med. Electron.* 2, 28-31.
- FROMM, B., NYLÉN, C. O., and ZOTTERMAN, Y. (1935). "Studies in the Mechanism of the Wever and Bray Effect," *Acta Oto-Laryngol.* 22, 477-486.
- GACEK, R. R., and RASMUSSEN, G. L. (1961). "Fiber Analysis of the Statoacoustic Nerve of Guinea Pig, Cat, and Monkey," *Anat. Rec.* 139, 455-463.
- GERSTEIN, G. L., and KIANG, N. Y. S. (1960). "An approach to the Quantitative Analysis of Electrophysiological Data from Single Neurons," *Biophys. J.* 1, 15-28.
- GERSUNI, G. V., and VOLOKHOV, A. A. (1936). "On the Electrical Excitability of the Auditory Organ On the Effect of Alternating Currents on the Normal Auditory Apparatus," *J. Exp. Psychol.* 19, 370-382.
- GERSUNI, G. V., and VOLOKHOV, A. A. (1937). "On the Effect of Alternating Currents on the Cochlea," *J. Physiol.* 89, 113-121.
- GRAY, P. R. (1966). "A Statistical Analysis of Electrophysiological Data from Auditory Nerve Fibers in Cat," *Tech. Rep.* 451, Mass. Inst. Technol. Res. Lab. Electron., Cambridge, Mass.
- GRODZINSKY, A. J. (1971). "Elastic Electrocapillary Transduction," S. M. Thesis, Dep. of Elec. Eng., Mass. Inst. Technol., Cambridge, Mass.

- GUINAN, J. J., and PEAKE, W. T. (1967). "Middle-Ear Characteristics of Anesthetized Cats," *J. Acoust. Soc. Amer.* 41, 1237-1261.
- HALLPIKE, C. S., and HARTRIDGE, H. (1937). "On the Response of the Human Ear to Audio-Frequency Electrical Stimulation," *Proc. Roy. Soc. B* 123, 177-193.
- HARRIS, G. G., FRISHKOPF, L. S., and FLOCK, Å. (1970). "Receptor Potentials from Hair Cells of the Lateral Line," *Science* 167, 76-79.
- HARVEY, W. T., and HAMILTON, J. P. (1965). "Hearing Sensations in Amplitude Modulated Radio Frequency Fields," *Off. Tech. Serv., U.S. Dep. Commerce*, AD-608 889.
- HILL, A. V., KATZ, B., and SOLANDT, D. Y. (1936). "Nerve Excitation by Alternating Current," *Proc. Roy. Soc. B* 121, 74-133.
- INGALLS, C. E. (1964). "Sensation of Hearing in Electromagnetic Fields," *J. Acoust. Soc. Amer.* 36, 1997 (A).
- JELLINEK, S., and SCHEIBER, T. (1930). "Eine Neue Methode des Hörens," *Wien. Klin. Wochschr.* 43, 417.
- JOHNSTONE, B. M., JOHNSTONE, J. R., and PUGSLEY, I. D. (1966). "Membrane Resistance in Endolymphatic Walls of the First Turn of the Guinea Pig Cochlea," *J. Acoust. Soc. Amer.* 40, 1398-1404.
- JOHNSTONE, B. M., TAYLOR, K. J., and BOYLE, A. J. (1970). "Mechanics of the Guinea Pig Cochlea," *J. Acoust. Soc. Amer.* 47, 504-509.
- JONES, R. C., STEVENS, S. S., and LURIE, M. H. (1940). "Three Mechanisms of Hearing by Electrical Stimulation," *J. Acoust. Soc. Amer.* 12, 281-290.
- KAHLER and RUF. (1931). "Untersuchungen über das Hören durch Schwingungsanregung im Körper auf elektrostatischem Wege," *Z. Hals-Nas. Ohrenheilk.* 29, 218-230.
- KATZ, B. (1939). Electric Excitation of Nerve, (Oxford University Press, London).

- KAYSER, D., and LIBOUBAN, S. (1963). "Représentation au Niveau de l'Aire Auditive du Cobaye des Différentes Spires de la Cochlée," *J. Physiologie* 55, 155-156.
- KELLAWAY, P. (1944). "The Electrophonic Response to Phase Reversal," *J. Neurophysiol.* 7, 227-230.
- KELLAWAY, P. (1946). "The Mechanism of the Electrophonic Effect," *J. Neurophysiol.* 9, 23-32.
- KIANG, N. Y. S. (1965). Discharge Patterns of Single Fibers in the Cat's Auditory Nerve, M. I. T. Research Monograph No. 35 (M. I. T. Press, Cambridge, Mass.).
- KIANG, N. Y. S. (1968). "A Survey of Recent Developments in the Study of Auditory Physiology," *Ann. Otol. Rhinol. Laryngol.* 77, 656-675.
- KIANG, N. Y. S., BAER, T., MARR, E. M., and DEMONT, D. (1969). "Discharge Rates of Single Auditory-Nerve Fibers as Functions of Tone Level," *J. Acoust. Soc. Amer.* 46, 106 (A).
- KIANG, N. Y. S., MOXON, E. C., and LEVINE, R. A. (1970). "Auditory-Nerve Activity in Cats with Normal and Abnormal Cochleas," in Ciba Foundation Symposium on Sensorineural Hearing Loss, G. E. W. Wolstenholme and J. Knight, Eds. (J. & A. Churchill, London).
- KIANG, N. Y. S., and PEAKE, W. T. (1958). "Studies of the Auditory Nervous System by Using Combined Acoustic and Electric Stimulation," *Mass. Inst. Technol., Res. Lab. Electron. Quart. Progr. Rept.*, January, 1958.
- KIANG, N. Y. S., and PEAKE, W. T. (1960). "Components of Electrical Responses Recorded from the Cochlea," *Ann. Otol. Rhinol. Laryngol.* 69, 448-458.
- KIMURA, R. (1966). "Hairs of the Cochlear Sensory Cells and Their Attachment to the Tectorial Membrane," *Acta Oto-Laryngol.* 61, 55-72.
- KOHONEN, A. (1965). "Effect of Some Ototoxic Drugs upon the Pattern and Innervation of Cochlear Sensory Cells in the Guinea Pig," *Acta Oto-Laryngol. Suppl.* 208, 1-70.

- KONISHI, T., TEAS, D. C., and WERNICK, J. S. (1970). "Effects of Electrical Current Applied to Cochlear Partition on Discharges in Individual Auditory-Nerve Fibers. I. Prolonged Direct-Current Polarization," *J. Acoust. Soc. Amer.* 47, 1519-1526.
- LAWRENCE, M. (1965). "Dynamic Range of the Cochlear Transducer," in Cold Spring Harbor Symposia on Quantitative Biology 30; Sensory Receptors, L. Frisch, Ed. (Cold Spring Harbor Laboratory of Quantitative Biology, Cold Spring Harbor, L. I., New York).
- LYNN, P. A., and SAYERS, B. McA. (1970). "Cochlear Innervation, Signal Processing, and their Relation to Auditory Time-Intensity Effects," *J. Acoust. Soc. Amer.* 47, 525-533.
- MARTY, R., and THOMAS, J. (1963). "Réponse Électro-Corticale à la Stimulation du Nerf Cochléaire chez le Chat Nouveau-Né," *J. Physiologie* 55, 165-166.
- MEYER, M. F. (1931). "Hearing without Cochlea?" *Science* 73, 236-237.
- MICHELSON, R. P. (1970). "Electrical Stimulation of the Human Cochlea in Sensory Deafness A Preliminary Report," presented at the Meeting of the Special Scientific Program, Committee for Research in Otolaryngology. American Academy of Ophthalmology and Otolaryngology, Las Vegas, Nevada, October 3, 1970.
- MILLER, J. D., WATSON, C. S., and COVELL, W. P. (1963). "Deafening Effects of Noise on the Cat," *Acta Oto-Laryngol. Suppl.* 176, 1-91.
- MISRAHY, G. A., HILDRETH, K. M., SHINABARGER, E. W., and GANNON, W. T. (1958). "Electrical Properties of Wall of Endolymphatic Space of the Cochlea (Guinea Pig)," *Am. J. Physiol.* 194, 396-402.
- MØLLER, A. R. (1963). "Transfer Function of the Middle Ear," *J. Acoust. Soc. Amer.* 35, 1526-1534.
- MOXON, E. C. (1967). "Electric Stimulation of the Cat's Cochlea: A Study of Discharge Rates in Single Auditory Nerve Fibers," S. M. Thesis, Dep. of Elec. Eng., Mass. Inst. Technol., Cambridge, Mass.

- MOXON, E. C. (1968). "Auditory-Nerve Responses to Electric Stimuli," Mass. Inst. Technol., Res. Lab. Electron. Quart. Progr. Rept. 90, 270-275.
- PEAKE, W. T., TEAS, D. C., and CAPRANICA, R. R. (1962). "Evidence for Localized Responses to Electrical Stimulation in the Cochlea," Mass. Inst. Technol., Res. Lab. Electron. Quart. Progr. Rept. 67, 181-193.
- PERWITZCHSKY, R. (1930). "Eine neue Theorie und Methode des Hörens," Z. Hals-Nas. Ohrenheilk. 26, 477-482.
- PFALZ, R. (1966). "Zur Physiologie des zentrifugalen Hörsystems: Fehlen gegenseitiger Interaktion zwischen den Cochleae, gemessen am klickausgelösten Summenaktionspotential N_1 und N_2 bei elektrischer, supramaximaler Reizung des kontralateralen Hörnerven," Arch. Ohren-, Nasen- u. Kehlkopfheilk. ver. Z. Hals-, Nas. - u. Ohrenheilk. 185, 575-577.
- PFALZ, R. K. J., and PIRSIG, W. (1966). "Compound Afferent Action Potentials of the Cochlear Nucleus Evoked Electrically," Ann. Otol. Rhinol. Laryngol. 75, 1077-1087.
- PUHARICH, H. K., and LAWRENCE, J. L. (1964). "Electro-Stimulation Techniques of Hearing," Rome Air Development Center Final Report RADC-TDR-64-18.
- RHODE, W. S. (1970). "Measurement of the Amplitude and Phase of Vibration of the Basilar Membrane Using the Mössbauer Effect," Ph. D. Thesis, Dep. of Elec. Eng., The Univ. of Wisconsin, Madison, Wis.
- RUPERT, A., MOUSHEGIAN, G., and GALAMBOS, R. (1962). "Microelectrode Studies of Primary Vestibular Neurons in Cat," Exp. Neurol. 5, 100-109.
- SALOMON, G., and STARR, A. (1963). "Sound Sensations Arising from Direct Current Stimulation of the Cochlea in Man," Danish Med. Bull. 10, 215-216.
- SHAMOS, M. H., and LAVINE, L. S. (1967). "Piezoelectricity as a Fundamental Property of Biological Tissues," Nature 213, 267-269.

- SHAMOS, M. H., LAVINE, L. S., and SHAMOS, M. I. (1963). "Piezoelectric Effect in Bone," *Nature* 197, 81.
- SHAW, E. A. G. (1966). "Ear canal Pressure Generated by a Free Sound Field," *J. Acoust. Soc. Amer.* 39, 465-470.
- SHAW, E. A. G., and TERANISHI, R. (1968). "Sound Pressure Generated in an External-Ear Replica and Real Human Ears by a Nearby Point Source," *J. Acoust. Soc. Amer.* 44, 240-249.
- SIMMONS, F. B. (1966). "Electrical Stimulation of the Auditory Nerve in Man," *Arch. Otolaryngol.* 84, 24-76.
- SIMMONS, F. B., EPLEY, J. M., LUMMIS, R. C., GUTTMAN, N., FRISHKOPF, L. S., HARMON, L. D., and ZWICKER, E. (1965). "Auditory Nerve: Electrical Stimulation in Man," *Science* 148, 104-106.
- SIMMONS, F. B., and GLATTKE, T. J. (1970). "Some Electrophysiological Factors in Volley-Pitch Perception by Electrical Stimulation." in Ciba Foundation Symposium on Sensorineural Hearing Loss, G. E. W. Wolstenholme and J. Knight, Eds. (J. & A. Churchill, London).
- SIMMONS, F. B., MONGEON, C. J., LEWIS, W. R., and HUNTINGTON, D. A. (1964). "Electrical Stimulation of Acoustical Nerve and Inferior Colliculus Results in Man," *Arch. Otolaryngol.* 79, 559-567.
- SMITH, C. A. (1961). "Innervation Pattern of the Cochlea. The Internal Hair Cell," *Ann. Otol. Rhinol. Laryngol.*, 70, 504-527.
- SOHMER, H. S., PEAKE, W. T., and WEISS, T. F. (1971). "Intracochlear Potential Recorded with Micropipets. I. Correlations with Micropipet Location," *J. Acoust. Soc. Amer.* (in press).
- SOMMER, H. C., and VON GIERKE, H. E. (1964). "Hearing Sensations in Electric Fields," *Aerospace Med.* 35, 834-839.
- SPOENDLIN, H. H., and GACEK, R. R. (1963). "Electronmicroscopic Study of the Efferent and Afferent Innervation of the Organ of Corti in the Cat," *Ann. Otol. Rhinol. Laryngol.* 72, 660-686.

- STEVENS, S. S. (1937). "On Hearing by Electrical Stimulation," J. Acoust. Soc. Amer. 8, 191-195.
- STEVENS, S. S., and DAVIS, H. (1938). Hearing. Its Psychology and Physiology, (John Wiley and Sons, Inc., New York).
- STEVENS, S. S., and JONES, R. C. (1939). "The Mechanism of Hearing by Electrical Stimulation." J. Acoust. Soc. Amer. 10, 261-269.
- TASAKI, I., DAVIS, H., and LEGOUIX, J. P. (1952). "The Space-Time Pattern of the Cochlear Microphonics (Guinea Pig), as Recorded by Differential Electrodes," J. Acoust. Soc. Amer. 24, 502-519.
- TASAKI, I., and FERNANDEZ, C. (1952). "Modification of Cochlear Microphonics and Action Potentials by KCl Solution and by Direct Currents," J. Neurophysiol. 15, 497-512.
- TEAS, D. C., KONISHI, T., and WERNICK, J. S. (1970). "Effects of Electrical Current Applied to Cochlear Partition on Discharges in Individual Auditory-Nerve Fibers. II. Interaction of Electrical Polarization and Acoustic Stimulation." J. Acoust. Soc. Amer. 47, 1527-1537.
- TONNDORF, J. (1966). "Bone Conduction. Studies in Experimental Animals," Acta Oto-Laryngol. Suppl. 213, 1-132.
- TONNDORF, J., KHANNA, S. M., and FINGERHOOD, B. J. (1966). "The Input Impedance of the Inner Ear in Cats," Ann. Otol. Rhinol. Laryngol. 75, 752-763.
- TONNDORF, J., and TABOR, J. R. (1962). "Closure of the Cochlear Windows: Its Effect upon Air- and Bone-Conduction," Ann. Otol. Rhinol. Laryngol. 71, 5-29.
- TUHY, F. P. (1967). "An Investigation of Electrophonic Hearing," S. M. Thesis, Dep. of Elec. Eng., Mass. Inst. Technol., Cambridge, Mass.
- TUNTURI, A. (1944). "Audio Frequency Localization in the Acoustic Cortex of the Dog," Am. J. Physiol. 141, 397-403.

- TUNTURI, A. (1945). "Further Afferent Connections to the Acoustic Cortex of the Dog," *Am. J. Physiol.* 144, 389-394.
- TUNTURI, A. (1946). "A Study of the Pathway from the Medial Geniculate Body to the Acoustic Cortex in the Dog," *Am. J. Physiol.* 147, 311-319.
- VOLOKHOV, A. A., and GERSUNI, G. V. (1934). "On the Effect of Alternate Currents on the Uninjured Auditory Organ," *J. Physiol. U. S. S. R.* 17, 1257-1271.
- VOLTA, A. (1800). "On the Electricity Excited by Mere Contact of Conducting Substances of Different Kinds," *Trans. Roy. Soc. (Lond.)* 90, 402-431.
- WALLNER, Chl. (1956). "Die Adaptation bei der elektrischen Reizung des Gehörs," *Z. Laryng. Rhinol. Otol.* 35, 306-314.
- WANSDRONK, C. (1962). "On the Mechanism of Hearing," *Philips Research Reports Supplements* 1, 1-140.
- WEISS, T. F. (1966). "A Model of the Peripheral Auditory System," *Kybernetik* 3, 153-175.
- WEISS, T. F., GOLDMARK, G. M., ALTMANN, D. W., and BROWN, R. M. (1969). "Automated System to Control Stimulus and Measure Response Variables in Experiments on the Auditory System," *Mass. Inst. Technol., Res. Lab. Electron. Quart. Progr. Rept.* 95, 122-127.
- WEVER, E. G. (1966). "Electrical Potentials of the Cochlea," *Physiol. Rev.* 46, 102-127.
- WEVER, E. G., and LAWRENCE, M. (1954). Physiological Acoustics, (Princeton University Press, Princeton, N. J.).
- WIEDERHOLD, M. L. (1967). "A Study of Efferent Inhibition of Auditory Nerve Activity," *Ph.D. Thesis, Dep. of Elec. Eng., Mass. Inst. Technol., Cambridge, Mass.*
- WIEDERHOLD, M. L. (1970). "Variations in the Effects of Electric Stimulation of the Crossed Olivocochlear Bundle on Cat Single Auditory-Nerve-Fiber Responses to Tone Bursts," *J. Acoust. Soc. Amer.* 48, 966-977.

- WIEDERHOLD, M. L., and KIANG, N. Y. S. (1970). "Effects of Electric Stimulation of the Crossed Olivocochlear Bundle on Single Auditory-Nerve Fibers in the Cat," *J. Acoust. Soc. Amer.* 48, 950-965.
- WIEDERHOLD, M. L., and PEAKE, W. T. (1966). "Efferent Inhibition of Auditory-Nerve Responses: Dependence on Acoustic-Stimulus Parameters," *J. Acoust. Soc. Amer.* 40, 1427-1430.
- WIENER, F. M. (1947). "On the Diffraction of a Progressive Sound Wave by the Human Head," *J. Acoust. Soc. Amer.* 19, 143-146.
- WIENER, F. M., PFEIFFER, R. R., and BACKUS, A. S. N. (1966). "On the Sound Pressure Transformation by the Head and Auditory Meatus of the Cat," *Acta Oto-Laryngol.* 61, 255-269.
- WIENER, F. M., and ROSS, D. (1946). "The Pressure Distribution in the Auditory Canal in a Progressive Sound Field," *J. Acoust. Soc. Amer.* 18, 401-408.
- WOOLSEY, C. N., and WALZL, E. M. (1942). "Topical Projection of Nerve Fibers from Local Regions of the Cochlea to the Cerebral Cortex of the Cat," *Bull. Johns Hopkins Hosp.* 71, 315-344.
- ZÖLLNER, F., and KEIDEL, W. D. (1963). "Gehörmittlung durch elektrische Erregung des Nervus acusticus," *Arch. Ohren - Nasen - u. Kehlkopfheilk. ver. Z. Hals - Nas. - u. Ohrenheilk.* 181, 216-223.
- ZWISLOCKI, J. (1948). "Theorie der Schneckenmechanik," *Acta Oto-Laryngol. Suppl.* 72, 1-76.

BIOGRAPHICAL NOTE

Edwin Charles Moxon

Born: December 7, 1943, Manchester, New Hampshire.

Education

Entered Massachusetts Institute of Technology, September, 1961.

Received: S. B. in Electrical Engineering, June, 1965.

S. M. in Electrical Engineering, September, 1967.

Professional Experience

- | | |
|---------------|--|
| 1965-1967 | Teaching Assistant, Department of Electrical Engineering, M. I. T. |
| 1965 (Summer) | Staff Member, Division of Sponsored Research, M. I. T. |
| 1966 (Summer) | Employee of Digital Equipment Corporation, Maynard, Massachusetts. |
| 1967 | Instructor, Department of Electrical Engineering, M. I. T. |
| 1967-1971 | Trainee of the National Institute of General Medical Sciences of the National Institutes of Health, U. S. Public Health Service. |
| 1967-1971 | Research Assistant in Otolaryngology, Eaton-Peabody Laboratory, Massachusetts Eye and Ear Infirmary, Boston, Massachusetts. |

Courses Taught

Experimental Electronics (6.70)

Electronic Circuits and Signals Laboratory (6.71)

Introduction to Neuroelectric Potentials (laboratory) (6.372)

Honors and Awards

Elected to: Eta Kappa Nu, 1963
 Tau Beta Pi, 1964
 Sigma Xi (Associate member), 1965

Teaching Award, Department of Electrical Engineering,
 M. I. T. (1967).

Publications

Moxon, E. C. (1968). "Auditory-nerve Responses to Electric Stimuli," Quarterly Progress Report 90 (Research Laboratory of Electronics, M. I. T.).

Chamberlain, S. C., Moxon, E. C., and Wiederhold, M. L. (1968). "Efferent Inhibition of Electrically Stimulated Response in Cat Auditory-nerve Fibers," Quarterly Progress Report 90 (Research Laboratory of Electronics, M. I. T.).

Kiang, N. Y. S., Moxon, E. C., and Levine, R. A. (1970). "Auditory-nerve Activity in Cats with Normal and Abnormal Cochleas," in Sensorineural Hearing Loss, G. E. W. Wolstenholme and J. Knight, Eds. (J. & A. Churchill, London).

Meeting Papers

Moxon, E. C., and Kiang, N. Y. S. "Discharge Rates of Auditory-nerve Fibers in Response to Electric and Acoustic Stimuli." Seventy-fourth Meeting of the Acoustical Society of America, Miami Beach, Florida, November 17, 1967. (J. Acoust. Soc. Amer. 42, 1206 (A), 1967).

Levine, R. A., Moxon, E. C., and Kiang, N. Y. S. "Responses of Single Auditory-nerve Fibers in Cochleas Damaged by Ototoxic Drugs." Seventy-seventh Meeting of the Acoustical Society of America, Philadelphia, Pennsylvania, April 10, 1969. (J. Acoust. Soc. Amer. 46, 106 (A), 1969).